THE PHANEROZOIC BASIN-FILL HISTORY OF THE ROEBUCK BASIN

Author

Stuart A Smith

(BSc Hons. – University of Southampton)

National Centre for Petroleum Geology and Geophysics

Thesis submitted to the University of Adelaide in fulfillment of the requirement of the degree Doctor of Philosophy, September 1999.

DECLARATION OF AUTHENTICITY

This thesis contains no material which has been accepted for the award of any other degree or diploma in any university or other tertiary institution and, to the best of my knowledge and belief, contains no material previously published or written by any other person, except where due reference is made in the text.

I give consent to this copy of my thesis, when deposited in the University Library, being available for loan and photocopying.

Stuart Andrew Smith

September, 1999

This thesis is dedicated to Ted Moorcroft who always did like the odd rhyme!

From
EPISTLE TO J. LAPRAIK,
AN OLD SCOTCH BARD

Burn's Apologia for his Poetry

I am nae *Poet*, in a sense,
But just a *Rhymer* like by chance,
An' hae to Learning nae pretence,
Yet, what the matter?
Whene'er my Muse does on me glance,
I jingle at her.

Your Critic-folk may cock their nose,
And say, How can you e'er propose,
'You wha ken hardly *verse* frae *prose*,
To mak a *sang?*
But by your leaves, my learned foes,
Ye're maybe wrang.

What's a' jargon o' your Schools,
Your Latin names for horns an' stools;
If honest Nature made you *fools,*
What sairs your Grammars?
Ye'd better taen up *spades* and *shools,*
Or *knappin-hammers.*

A set o' dull, conceited Hashes,
Confuse their brains in *Colledge-classes!*
They *gang* in Stirks, and *come out* Asses,
Plain truth to speak;
An' syne they think to climb Parnassus
By dint o' Greek!

Gie me ae spark o' Nature's fire,
That's a' the learning I desire;
Then tho' I drudge thro' dub an' mire
At pleugh or cart,
My Muse, tho' hamely in attire,
May touch the heart.

ACKNOWLEDGEMENTS

I have had an enlightening and enjoyable time whilst undertaking this study. Not only was I offered the opportunity to develop academically but have also had the pleasure of meeting new friends, experiencing new cultures and undertaking new recreational pursuits. As an individual these experiences will always remain with me and are just as important as the academic enlightenment. This opportunity has been made possible through the encouragement and support of several people and their respective organisations. I would like to acknowledge them here.

Generous financial support was supplied by the Australian Geological Survey Organisation, and I would like to thank Geoff O'Brien whom (on the recommendation of Chris von der Borsch) I first approached at the survey and who championed my application for funding. I would also like to sincerely thank my supervisor at the survey, Howard Stagg, who did a fantastic job in organising data donations from JNOC and supplying data from the survey database – I'm sure that he will suggest that I owe him a curry or two! Additional equipment and computer support were supplied by the Australian Petroleum Cooperative Research Centre and National Centre for Petroleum Geology and Geophysics (NCPGG). Basic data was donated from a number of contracting companies including, Wiltshire Geological Services (petrophysical well data), Morgan Palaeo Associates (palynological data and a very useful "whale-o-gram"), and JNOC for the Roebuck Basin regional seismic data set.

My initial supervisors at the NCPGG were Bill Stuart and Chris von der Borsch. Bill regretfully passed away mid-way through this study after a long battle with cancer. I gratefully acknowledge his early support in this project and admire his courage and determination during this time. Chris retired from academic life mid-way during the study but contributed to the early part of the study, especially with obtaining funding.

The NCPGG and the University of Adelaide were extremely lucky at the time of Bill's death, that Professor Cedric Griffiths was prepared to "pick-up the pieces" during a very difficult period when the future direction of the NCPGG was very uncertain. I am sure that the NCPGG would not exist today if it were not for the effort that Cedric put in during this time. In addition, Cedric also undertook the supervision of this study at this time. He has been a sensational and enlightening mentor who encourages independent thought and analysis in a fun working environment. I owe a great deal to him and look forward to rewarding future interaction with him and his students – "I haven't stopped listening yet!!" Additional supervision, advice and training was supplied by Andy Mitchell who gave his time generously, especially during the seismic interpretation and mapping phase of this study – "Andy, I apologise that my UNIX, Vi and Ludwig skills are so poor!" Nick Lemon supplied structural geological advice and a bit of culinary inspiration. Peter Tingate helped with the thermal modelling and reviewed the manuscript and was always more than willing to share a decent bottle of red. Maureen "travel-agent" Sutton, Nick and Barbara, are thanked for admin and technical support and goading poor students into running lunch-time BBQ's, Ted and Jan Moorcroft for being the best of social secretaries – "that 707 is still one of the best." I'd also like to thank the Barossa set - Johnny, Hamish, $(Chris)^3$, Sharon, Bridget and Chainsaw – for many entertaining Friday evenings.

Many of the other students have also become good friends and have energised me during my period at the NCPGG, they include - Simon (for getting me going!), Paul, Alex, Lyndon, Lousie, Gharzi, Tony and three years of honours students. I would also like to thank my wife Jacinta and parents for support (quite often financial as well as emotional) through this study. In the end I hope that I have given a little back.

SAS

ABSTRACT

The Roebuck Basin is the least understood of four major sedimentary basins that makeup Australia's North West Shelf. During this study the key aim was to provide a structural and stratigraphic framework for the evolution of the basin and to evaluate its future petroleum potential.

Regional mapping has enabled accurate delineation of the structural features in the Roebuck Basin which were only crudely defined in older studies. Of note is the Oobagooma High, a newly identified Palaeozoic structure that separates the Oobagooma Sub-basin from the Rowley Sub-basin at the Palaeozoic level. Both the Oobagooma and Bedout Highs appear structurally related and are interpreted to have formed due to compressional forces over a major crustal detachment possibly related to an accommodation zone formed during earlier NE extension. Structuring along the margins of the basin are complex and changes from asymmetrical half-graben extension onshore to symmetrical graben extension in the near offshore to thin-skinned detachment in the outer offshore area. Style of extension appears to be controlled by the location of the more rigid elements of the basin, with normal faults developing near the stable bounding Kimberley Craton and Leveque Platform to the NE and the Broome Platform to the SW. These structural provinces were used to divide the Oobagooma Sub-basin at the Palaeozoic level into three compartments separated by hardlinked transfer zones.

More detailed interpretation was conducted in conjunction with sequence stratigraphic analysis of available well data. This proved problematic in the upper part of the section which is carbonate-dominated. For carbonate-rich sediments wire-line methods have not been well documented. To resolve this, a new method of log interpretation was utilised for the upper part of the section. Using this and clastic wireline log interpretation methods, sixty-four boundaries were identified that could be partially correlated throughout the basin and used to date the section and divide the basin-fill.

Structurally, the Roebuck Basin is interpreted to have developed as a result of a multiphase rift history under four main stress regimes: NE-SW extension resulting in an intra-cratonic fracture sequence associated with the separation of the Chinese blocks from Gondwanaland during the Cambrian to Silurian; a transitional phase from NE-SW to NNW-SSE extension associated with the separation of the China-Burma-Malaya-Sumatra (SIBUMASU) blocks during the Late Carboniferous to Late Permian with development of both NW-SE and ENE-WSW structures; a NNE-SSW post Late Permian extensional phase resulting in formation of the Westralian Superbasin sequence (separation of Argoland and India); and a NE-SW compression phase during collision with Asia during the Middle Miocene to Recent. Each extensional basin phase is strongly related to the development of five break-up events that have effected the northwestern margin of Australia, four of which have been previously identified. A possible fifth break-up event which developed during the Early Jurassic has been identified during this study (previously identified as rift onset for the Middle Jurassic breakup episode).

Large scale differences in structuring between the Roebuck Basin (subtle) and its adjacent basins (pronounced) suggest that either the crustal composition or stress regime was different in this area. In contrast to the other basins, the Roebuck Basin has undergone NE extension prior to NNW extension which may have altered the crustal composition. Annealling of the upper crust by period heating and cooling during early rifting may strengthen it.

Major Triassic thermal sag and marine transgression has been punctuated by a series of NW-SE transpressional events that occurred along the margins of each sub-basin, known as the Fitzroy Movement. A theoretical model for progressive rift development around a pole or hinge point, that helps

explain the formation of transpressional features during rifting, has been developed for the North West Shelf. The model demonstrates that as rifting progresses from NE to SE, transtensional/transpressional stresses will be developed due to differential rotational movement between adjacent blocks. During this study the Fitzroy Movement has been sub-divided into three tectonic episodes. Of these events Fitzroy Movement III appears associated with rift shoulder development on the margin during lower crustal/upper mantle thinning through pure shear processes during rifting in the unidentified rift event described above.

Due to limited availability of data, dating of events has been extremely difficult in the Roebuck Basin. Other authors identify similar surfaces in adjacent basins but with slightly different timing. This is interpreted to be a result of slight diachronous formation of sequence boundaries in response to different sediment budgets and tectonic regimes in each basin.

Forward sedimentary modelling using SEDPAK was employed directly as a tool for palaeogeographic and lithology prediction as well as hypothesis testing. Such predictions were used to directly develop hydrocarbon exploration play concepts and play element distribution and fairway maps in the area.

Six sea-level curves were used to derive sea-level during modelling. Simulations using locally derived Roebuck Basin sea-level curves, the Haq second and third order eustatic sea-level curves, produce similar overall geometries and internal characters which matched well with observed geometries in wells and seismic data. All offered reasonable and possible solutions. Simulations using the Roebuck Basin, Haq second and third order sea-level curve, although of differing frequencies and amplitudes, produced similar results. It appears that sediment supply rate is more important in controlling sediment geometries than higher order sea-level curve frequency and magnitude. Results from this study suggest that the curves derived by Haq et al. (1987) are reasonable approximations of the high-frequency relative sea-level oscillations that have occurred in the Roebuck Basin and could potentially be used as a first approximation to simulate basin-fill at other locations globally.

Failure to find commercial hydrocarbons in the basin is attributed to lack of source rock, seal potential and timing of maturation. During this study, source rocks were identified and their distribution predicted using a number of techniques, including; sequence stratigraphic correlation, seismic mapping, forward sedimentary modelling and geochemical analysis. Using the above methods, ten source rock intervals were identified. These can be sub-divided into four groups of units depending on their tectono-depositional setting. Tr1 and Tr2 were deposited during rapid thermal sag, J1 to J5 were deposited during gentle thermal sag and infill, K1 and K2 were deposited during rift and post-rift sedimentation, and K3 was deposited during passive margin conditions. During maturity analysis vitrinite data suggests a thermal maturity lower than modelled maturities using present thermal conditions. The difference in modelled versus measured vitrinite reflectance is likely to be the result of vitrinite suppression which has been observed elsewhere on the North West Shelf. There is a general correlation between marine sequences and increased suppression in the Roebuck wells examined so far.

Sedimentary modelling of the Jurassic has been used to simulate the basin fill. Four marine incursions, each of which are followed by the development of a progradational wedge, are clearly identifiable. Thickest delta front development occurred in the inner Rowley Sub-basin to the north-west of the Bedout High and may offer many attractive stratigraphic exploration targets such as isolated channel systems, coastal sand deposits and barrier-bar systems. These reservoir-trap systems are potentially sourced/sealed by high-quality source rich, pro-delta, shale systems.

TABLE OF CONTENTS

LIST OF FIGURES

LIST OF TABLES

CHAPTER 1

INTRODUCTION

"The point of philosophy is to start with something so simple as not to seem worth stating and to end with something so paradoxical that no one will believe it!"

"The Philosophy of Logical Atomism"
Bertrand Russell

1.1 Introduction

The Roebuck Basin (commonly referred to as the "offshore" Canning Basin) is one of four major sedimentary basins, the Northern Carnarvon, Roebuck, Browse and Bonaparte (Fig. 1.1), that makeup Australia's North West Shelf. The basin covers an area of approximately 160,000 km^2 and consists of a series of linked northwest and northeast trending depocentres. Although the basin is situated in the middle of Australia's rich hydrocarbon province, only sub-economic gas discoveries at Phoenix-1 and 2 have been made in wells around the basin to-date. Poor early exploration results have led to a down-grading of the basin's prospectivity and a decline in interest in the area from Australia's petroleum industry.

Lack of interest has resulted in a stagnation of our knowledge of the Roebuck Basin, to the point where it is a frontier area, within a rapidly maturing hydrocarbon province. To address this imbalance the Australian Geological Survey Organization (AGSO) began a regional study of the Roebuck Basin in 1993. The study was primarily based upon the acquisition of some 4087.25 line km of regional deep (16 s TWT) seismic reflection data as part of the North West Shelf Deep Seismic Data Program. Whilst interpretation of this regional data set has helped define the major basinal elements, structural events and basin-fill episodes, it was not of sufficient coverage to allow detailed regional mapping. In addition to in-house structural studies at AGSO, this PhD study was also commissioned to conduct more detailed regional work using in-fill seismic and well data. In 1995, at the beginning of this PhD, an exciting opportunity existed to reappraise the area using new concepts and a more systematic approach to basin evaluation which had developed since exploration interest ceased.

Recently, exploration interest in the basin has been rekindled by oil discoveries at Gywdion-1 (1995) and Cornea-1 (1997) in the Browse Basin to the northeast, and at Nebo-1 (1993) in the Beagle Sub-basin to the southwest. Renewed interest prompted the Western Australian Government to announce a new round of gazettals in March 1998 for much of the acreage covering the Roebuck Basin, including outboard areas previously never explored.

1.2 Location and Basin Definition

The Roebuck Basin formed as part of Australia's north-western continental margin. This margin evolved as a result of the development of a number of rift systems from Cambrian to Cretaceous age during the breakup of Gondwanaland and the formation of the Tethyan Seaway. This rifting resulted in four major northeast trending sedimentary basins (northern Carnarvon, Roebuck, Browse and northern Bonaparte Basins) that have been jointly termed the Westralian Superbasin by Yeates et al. (1987).

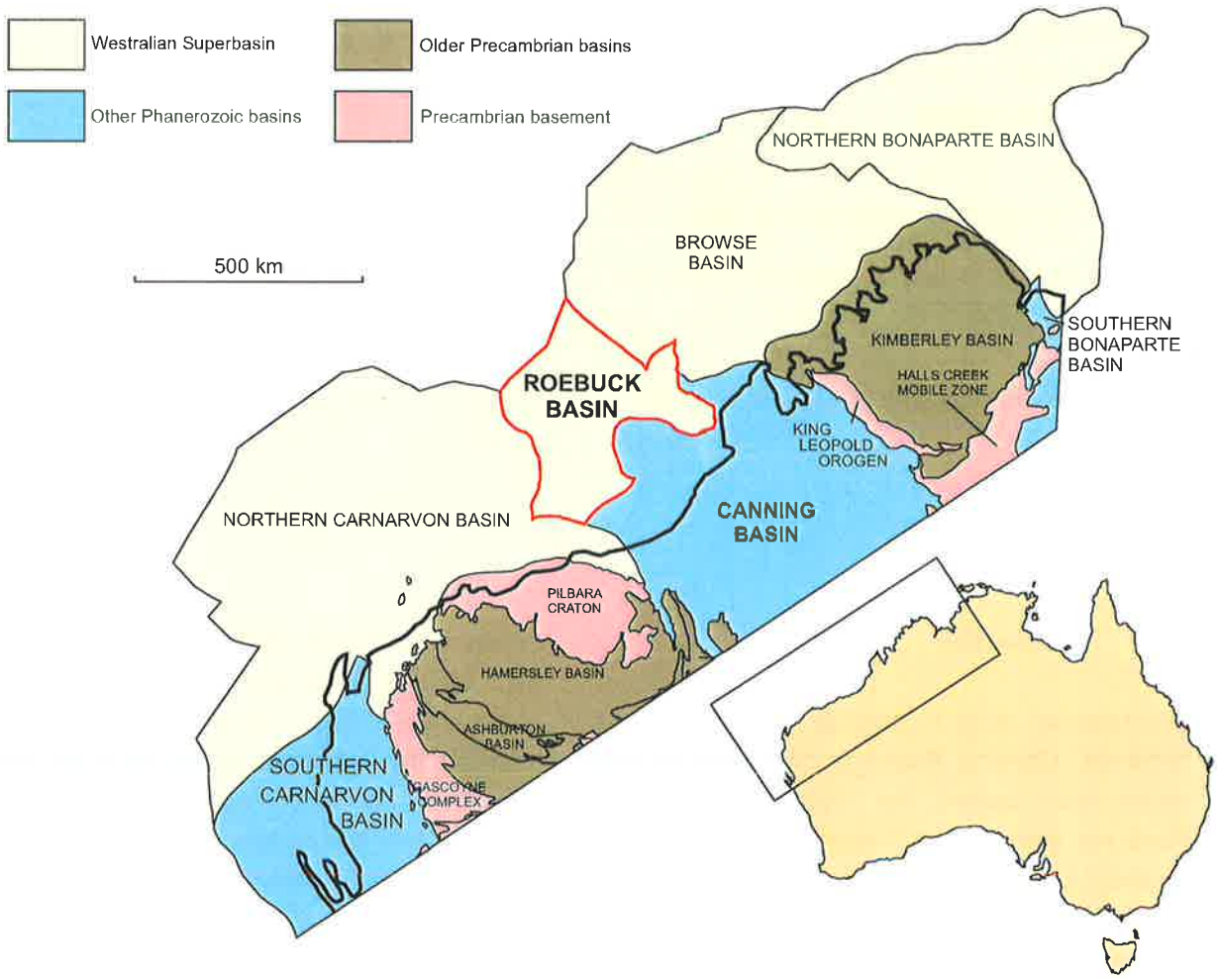

Figure 1.1 Location diagram of the Roebuck Basin in relation to the North West Shelf structural framework (from Hocking et al. (1994)).

Geographically, the Roebuck Basin lies offshore from the intra-cratonic Canning Basin and Lambert Shelf which forms the basin's south and southwestern limit (Fig 1.1 and Chapter 2 Figure 2.11). Oceanic crust of the Argo Abyssal Plain forms the northwestern limit. The basin is separated from the Beagle Sub-basin to the southwest along the North Turtle Hinge Zone, a basement ridge extending north from the Pilbara Block and Lambert Shelf. To the northeast - in the inner offshore area – the basin is separated from the Browse Basin along the southern margin of the Leveque Platform. However, there is little distinction between the outer Roebuck Basin and either the Browse or Beagle Sub-basins to the north and south. Internally the basin consists of three major depositional centres; the Oobagooma (previously known as the "offshore" Fitzroy Trough), Bedout and Rowley Sub-basins which are divided by three Palaeozoic highs. A more detailed description of each of these tectonic elements is given in Section 2.6.2.

1.3 Report Structure

This report has been divided into seven chapters including introduction, structural interpretation, stratigraphic assessment, forward sedimentary modelling, petroleum potential, conclusions and recommendations for further work. As the study covers several varied topics incorporating different elements of basin analysis, the methodology and discussion of each stage of the work have been included in each relevant chapter. To avoid repetition, previous literature has also been included in the relevant sections rather than as a formal chapter.

1.4 Scope of Study and Products

Most studies of the Roebuck Basin to date, have focused on broadly defining the litho-stratigraphic

and tectono-stratigraphic evolution of the area (see Forman and Wales, 1981, Horstmann and Purcell, 1988, Lipski, 1993, 1994 and Colwell and Stagg, 1994). During this higher resolution study, the key aim was to provide a structural and stratigraphic framework for the evolution of the basin based on sequence stratigraphic concepts. This framework was then used as the basis for understanding, and ultimately predicting the timing, distribution and nature of petroleum systems in the basin.

Emphasis was placed initially on the identification of regionally significant tectonic events that form an overall tectonic framework of the basin. These major tectonic events were used to divide the basin-fill into megasequence cycles that have controlled the basin's gross accommodation history. Seismic correlation of these events throughout the study area has enabled the definition of the major tectonic elements that make up the basin.

After megasequence definition, higher-order events were determined using bio-stratigraphically controlled wire-line log correlations and high resolution seismic mapping. The interaction of lower and higher order events have controlled the distribution of petroleum play elements throughout the Roebuck Basin.

The project largely used seismic reflection data tied to wells. Forward sedimentary modelling was used to predict and test hypotheses relating to the nature of the basin-fill history. Palaeogeographic maps of the Roebuck Basin have been produced on the basis of seismic interpretation and forward modelling.

A summary of the methodology used during the study, which is also discussed in more detail during subsequent chapters, is shown in Fig. 1.2

1.5 Materials

In total, information from 19 wells was utilized during the study. A listing of these wells and the types of data available is shown in Table 1.1. Unfortunately, little or no conventional core exists within these wells. The only significant coring program conducted was that of the Late and Middle Triassic reservoir units in Phoenix-1 and 2, where massive uniform sandstones were recovered. All cores were examined and logged at the Bureau of Resources Sciences Laboratory in Canberra, but on a regional basis little useful information could be obtained from them. Key palaeontological data supplied from third parties is proprietary and permission was not granted for its reproduction.

In addition to well information, six seismic surveys were utilized during the study – Carnot81, W81, HB85, JNOC87, JNOC88 and BMR120. The coverage of these surveys and their well ties is shown in Fig. 1.3.

Other published or open-file material including interpretive reports and academic papers were also incorporated into the study.

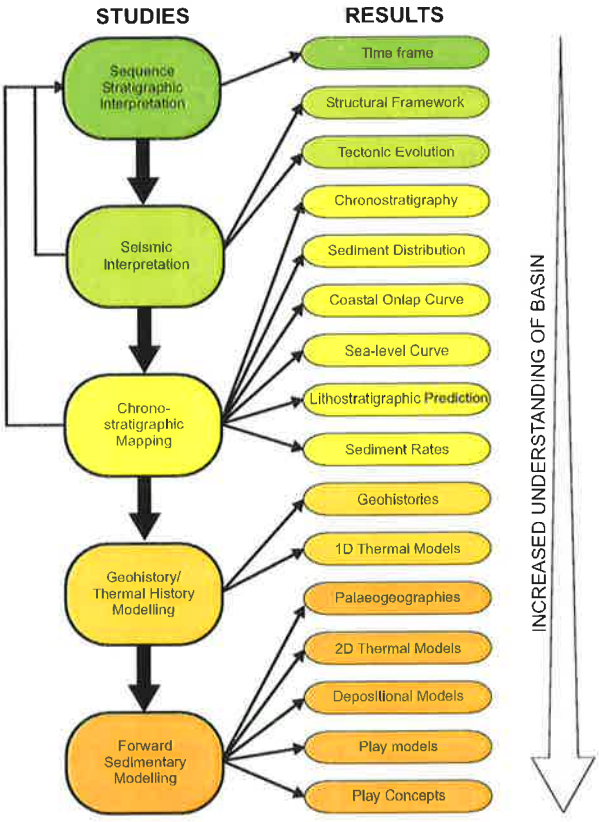

Figure 1.2 Work-flow diagram.

Well Name	*Wireline Logs*	*Well Completion Report*	*Morgan Palynology*	*AGSO Stratdat*	*Velocity Survey*
Barcoo-1	✓	×	✓	✓	×
Bedout-1	✓	✓	✓	✓	✓
Depuch-1	✓	✓	✓	✓	×
East Mermaid-1	✓	✓	✓	✓	✓
Jarman-1	✓	✓	✓	✓	×
Kambara-1	✓	✓	✓	✓	×
Keraudren-1	✓	✓	✓	✓	✓
Lacepede-1	✓	✓	✓	✓	✓
La Grange-1	✓	✓	✓	✓	✓
Lyhner-1	✓	✓	✓	✓	×
Minilya-1	✓	✓	✓	✓	×
Minjin-1	✓	✓	✓	✓	✓
Nebo-1	✓	×	×	×	×
North Turtle-1	✓	✓	✓	✓	×
Perindi-1	✓	✓	✓	✓	✓
Phoenix-1	✓	✓	✓	✓	✓
Phoenix-2	✓	✓	✓	✓	✓
Poissonnier-1	✓	✓	✓	✓	✓
Wamac-1	✓	✓	✓	✓	✓

Table 1.1 Availability of well data, wireline log information from Wiltshire Geological Services, palynology from Morgon Palyo Associates, biostratigraphy from the AGSO StratDat database, for all wells used during the study.

1.6 Roebuck or "offshore" Canning Basin

Due to its close location to the Canning Basin the Roebuck Basin was previously labelled the "offshore Canning Basin," a term developed when early exploration revealed that many of the onshore structures extended into the offshore area (Horstman & Purcell, 1988). This name implied a structure and stratigraphy which recent exploration has shown is not characteristic of the basin. In such a sense, the name "offshore Canning Basin" was more geographically, rather than geologically, appropriate (Lipski, 1994). The name Roebuck Basin, after Roebuck Bay near Broome was suggested by Horstman and Purcell (1988) and has since been adopted by the Geological Survey of Western Australia (Hocking et al., 1994). Although officially called the Roebuck Basin, the term "offshore" Canning Basin is still in common usage, especially by the Australian petroleum industry. Note that the term 'basin' here is used in the European and North American sense rather than the usual Australian sense of 'megasequence' (such as the Cooper

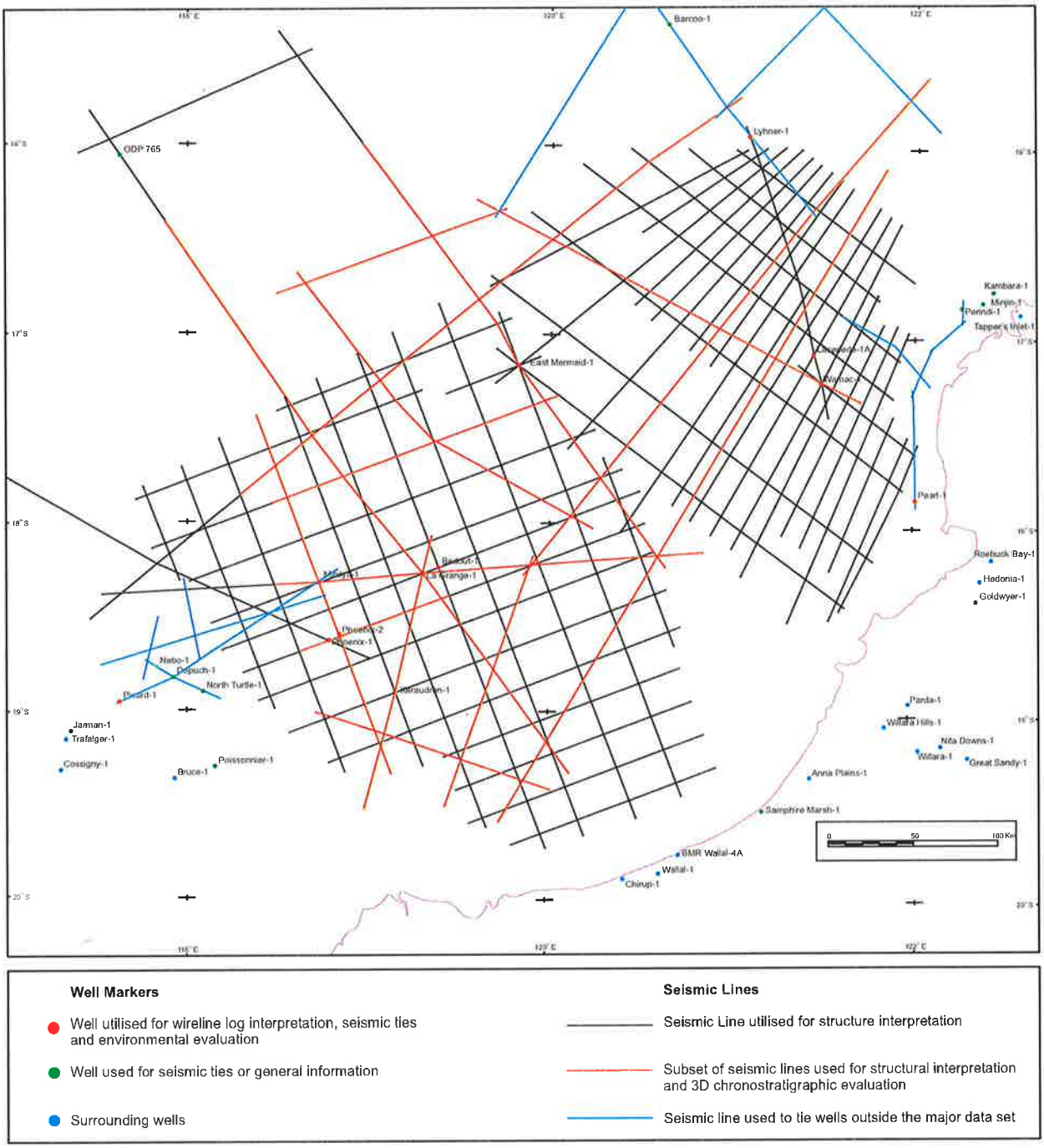

Figure 1.3 Available well and seismic data coverage.

and Eromanga Basins), thus the Roebuck Basin is a geographical location rather than a chronostratigraphic unit.

1.7 Exploration History

The Roebuck Basin has been sparsely explored. Prior to drilling its prospectivity was rated highly (Challinor, 1970) when gravity and seismic data were interpreted to show the Rankin Platform extending into the area. It has since been labelled one of the least prospective basins of the North West Shelf (Horstman & Purcell, 1988).

To date, thirteen wells have been drilled in two rounds of activity; the early 70's and early 80's (Fig. 1.3). Of these wells, four have been drilled in the Bedout Sub-basin and one in the Rowley Sub-basin; eight wells have been drilled in the fault zones and pre-Mesozoic highs that bound the sub-basins (Lipski, 1994). None of these wells encountered significant hydrocarbon discoveries. The only wells to provide encouragement to exploration were Phoenix-1 in the Bedout Sub-

basin (minor gas shows in Triassic sandstones) and Perindi-1 in the offshore Fitzroy Trough (minor oil shows in Permian sandstones) (Colwell and Stagg, 1994).

Since the drilling of the last well in 1984, the only exploration until 1993 has been the acquisition of 11 000 km of regional seismic data by the Japan National Oil Corporation (JNOC) (1987, 1988) in 1986-7 under a Special Prospecting License granted by WA Department of Mines. In 1993 AGSO, as part of a program of acquiring a grid of regional deep-seismic data over the North West Shelf, recorded 4025 line km of high quality data on 14 lines in the Roebuck Basin (Colwell & Stagg, 1994). In total, approximately 80,000 km of multi-channel seismic data have been recorded in the basin.

Several scientific seismic and sampling programs, including outer margin dredging (von Rad & Exon, 1983) and ODP well 765 have contributed information on the geology and structural history of the basin.

The most recent company activity has been undertaken by Esso, Hadsen and Stirling, who in the early 90's, were awarded exploration permits covering the southern Rowley Sub-basin, the eastern Beagle and Bedout Sub-basin's. Interest was focused on a possible Triassic play involving onlap onto the Palaeozoic sequence in the Bedout Sub-basin (Lipski and Beattie, 1992). Such a play has not been tested.

With the drilling of Nebo-1, the first sub-economic oil discovery (Middle Jurassic fluvial sands) in the neighbouring Beagle Sub-basin (Osborne, 1994), new interest, especially in the western sector of the basin, has been generated.

The 1999 acreage release by the Western Australia Government has led to the acquisition of a further 8000 km of new 2D seismic data and reprocessing of 75,000 km of old seismic data by Seismic Australia. These data sets were unavailable for this study.

Several areas are unavailable for petroleum exploration, especially in the Rowley Shoals region, a present day reef area (Mermaid, Clerke and Imperieuse Reefs) over which a marine park has been proposed.

CHAPTER 2

REGIONAL SEISMIC MAPPING AND STRUCTURAL FRAMEWORK

"By means of a secret charm, to draw
All creatures living beneath the sun,
That creep or swim or fly or run,
After me so as you never saw!
And I chiefly use my charm
On creatures that do people harm,
The mole and toad and newt and viper;
And people call me the Pied Piper."

The Pied Piper of Hamelin
Robert Browning (1812-1889)

2.1 Introduction

To evaluate the basin's tectonic evolution and structural framework, a 2D seismic interpretation incorporating the highest quality regional seismic data available was conducted in the study area. Seismic interpretation was performed in conjunction with chronostratigraphic construction. The horizon nomenclature used here is consistent with the stratigraphic framework defined in Chapter 3 (Chapter 3 Fig. 3.21).

This chapter details the methodology used during the seismic interpretation, describes the major structural elements that make up the basin and also discusses the major potential rift mechanisms that formed the basin. A more detailed description of basin development is given in Chapter 3.

2.2 Interpretation Methodology

The interpretation was conducted using Sierra 2DI seismic interpretation software running on a Sun Sparc 10 workstation. A mis-tie tolerance of 30 ms was permitted during the horizon and fault interpretation. Time-structure and isochron maps were created using 2DI but were exported to an external drawing package for hand contouring and final presentation. A full 3D depth conversion was not conducted on the data set as a whole. Individual seismic lines were depth converted to ascertain parameters required for high resolution chronostratigraphic and forward sedimentary modelling studies addressed in Chapters 3 and 4. The structural interpretation was based on TWT structure maps alone.

2.2.1 Seismic Cover

In total, approximately 15,000 km of digital seismic data from three surveys; JNOC JN87, JNOC JN88 and AGSO BMR120 were interpreted (Chapter 1 Fig. 1.3). The general acquisition and display parameters for each of these surveys are shown in Table 2.1. Although the average tie spacing of the combined data set was in the order of 20 to 30 km, suitable coverage was available to define the regional structures of the basin.

Data from four other surveys were also utilized during the interpretation to tie wells that were located on the margins of the basin (Chapter 1 Fig. 1.3). These surveys were obtained in sepia format and were interpreted by hand. They were then tied to the digital database at their calculated intersection points. These surveys include; Carnot 81 in the Oobagooma Sub-basin (used to tie Pearl-1), BMR119 in the Browse (used to tie Barcoo-1) and W81 and HB86 in the Beagle Sub-basin (used to tie North Turtle-1, Picard-1 and Nebo-1). In total an additional 1,050 km of paper seismic was interpreted.

	AGSO BMR120 (1994)	*JNOC JN87 (1987)*	*JNOC JN88 (1988)*
Shot Interval	50m	30m	25m
Group Interval	25m	12.5m	12.5m
Record Length	16s	7s	6s
Record Polarity	SEG Normal	SEG Normal	SEG Normal
CDP Interval	12.5m	12.5m	12.5m
Nominal Fold	40	60	60
Designature	Minimum Phase	Minimum Phase	Minimum Phase

Table 2.1 Acquisition and display parameters for the AGSO and JNOC regional seismic surveys.

2.2.2 Data Quality

The AGSO deep seismic ranged in quality from data that imaged the major structures of the basin, but contained multiple and side-swipe problems that obscured some of the fine stratigraphic detail (Appendix 1 Fig. A1.4 between 0 and 40 km below 2 S TWT) to high quality data (Appendix 1 Fig. A1.7). Seismic event continuity and strength does deteriorate over the shallower sections (Appendix 1 Fig. A1.6). Intra-crustal reflectors, where imaged, are seen quite clearly down to a depth of around 10 s TWT (Appendix 1 Fig. A1.2).

The JNOC data quality ranged from very poor (Appendix 1 Fig. A1.9) to moderate (Appendix 1 Fig. A1.10). Most sections are badly affected by sea-floor multiples which can clearly be identified in the upper section. The AGSO data set, when directly compared to the JNOC data, provides clearer images of faults and reflectors. However, at the conclusion of this study the JNOC data had just been reprocessed by Seismic Australia. These data are of a high quality (Mr Peter Purcell, pers. com., 1998) but, due to time constraints could not be incorporated into this study.

Neither survey images the Oobagooma Sub-basin section adequately below the Late Permian Unit VIII Event (Appendix 1 Fig. A1.6 between 270 and 360 km). This section is highly faulted and volcanically intruded, resulting in strong sideswipe, multiple and penetration problems.

2.2.3 Well Ties

Seventeen wells were used to tie the stratigraphy to the seismic grid (Chapter 1 Fig. 1.3 and Figs. 2.1, 2.2 and 2.3). The most important stratigraphic events were found to correspond to well documented tectonic episodes that have occurred on the North West Shelf (see AGSO, 1994) and these were chosen for regional mapping. Detailed timing of each event in the Roebuck Basin was determined during the stratigraphic interpretation (outlined in detail in Chapter 3).

Velocity surveys were available for ten of the seventeen wells. These surveys were used to depth convert all the wire-line log data from each well to TWT, using an adjusted sonic log method. In addition, synthetic seismograms were generated using minimum and zero phase Ricker wavelets, with peak frequencies of 30, 35, 40 and 50 Hz. Distinctive reflectors occurring in both the section and synthetic were then matched. For most wells, when tied to the seismic section, a good match in both frequency and amplitude content was obtained over much of the section with only minimal shifting of the well required, especially where reasonably spaced check shot data had been acquired (Fig. 2.2). However, the top zone of interest proved more problematic to match. The time converted wire-line log curves and synthetics were found to tie high in the section. In this zone, checkshots and sonic logs were not recorded in any of the wells thus

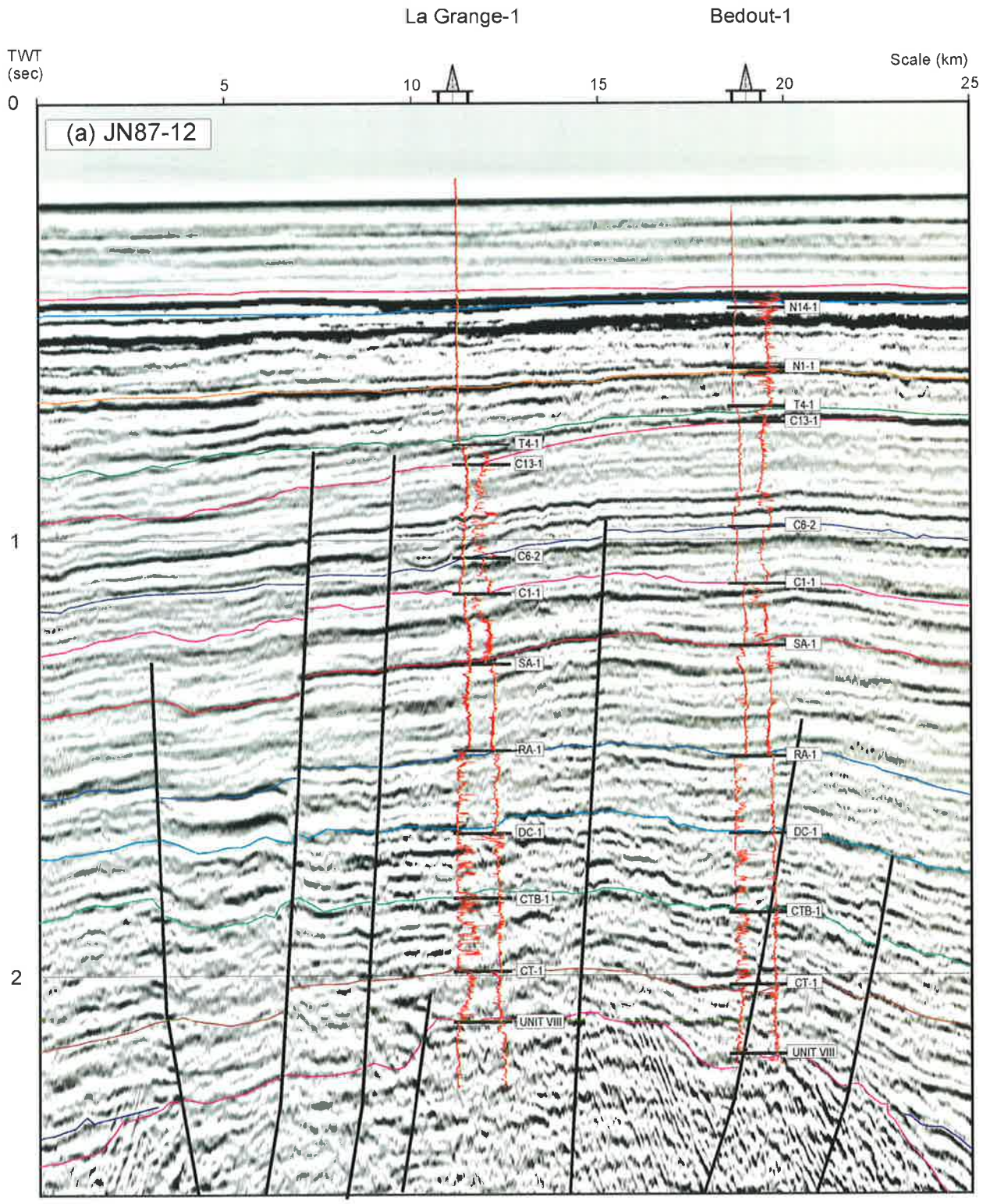

Figure 2.1 Representative well-ties across the Bedout High showing time converted gamma (left) and sonic (right) wireline logs and horizon picks. Good seismic facies changes occur across the *Unit VIII*, *DC-1*, *RA-1*, *T4-1* and *N17-2* (above *N14-1*) boundaries. A strong sea-bed multiple is evident close to the *N14-1* boundary in this area.

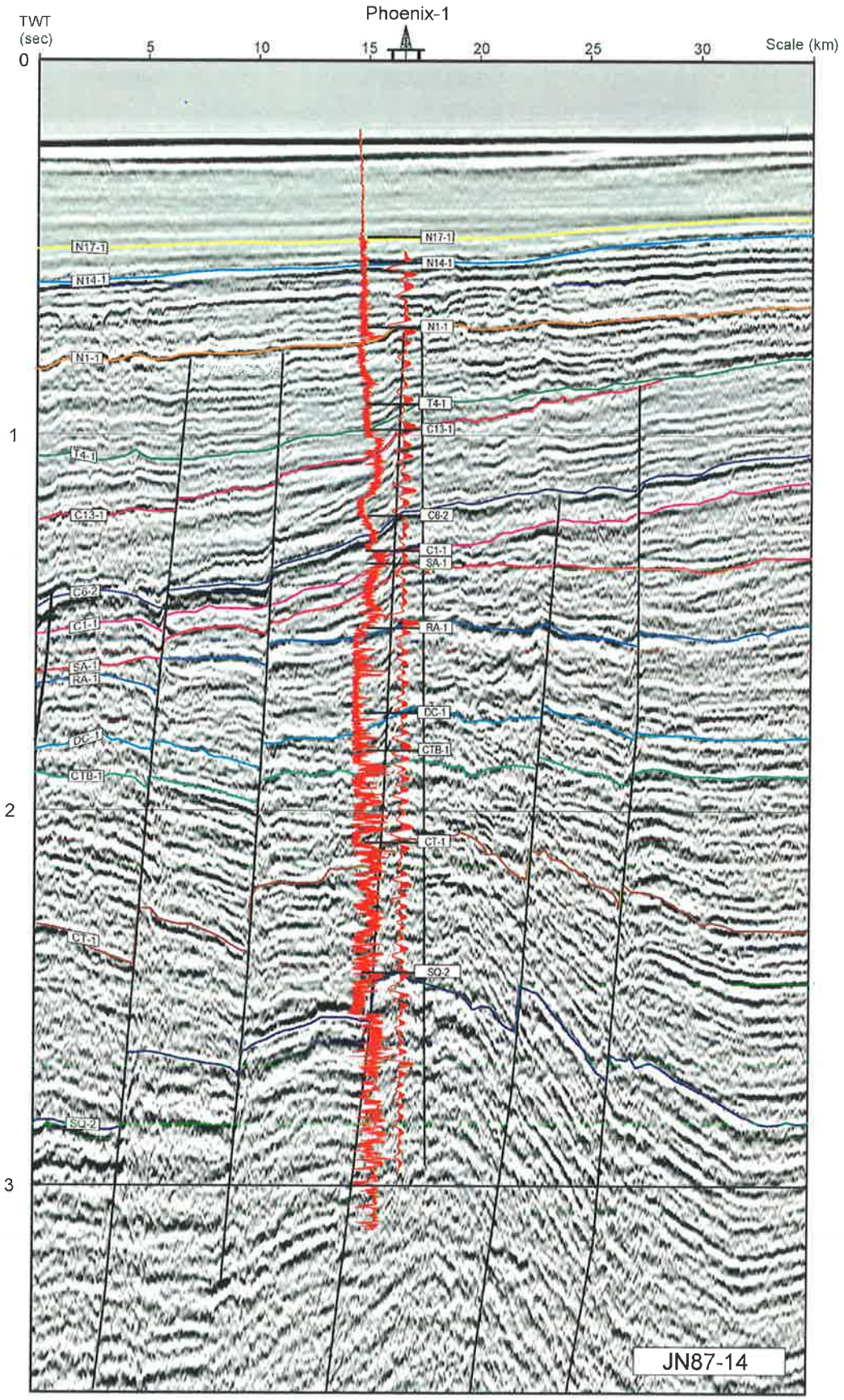

Figure 2.2 Pheonix-1 well-tie to seismic line JN87-14 in the Bedout Sub-basin showing time converted gamma (left) and minimum phase 40 Hz synthetic (right). The best hydrocarbon shows to-date have been intersected in this well (the SQ-2 event and below).

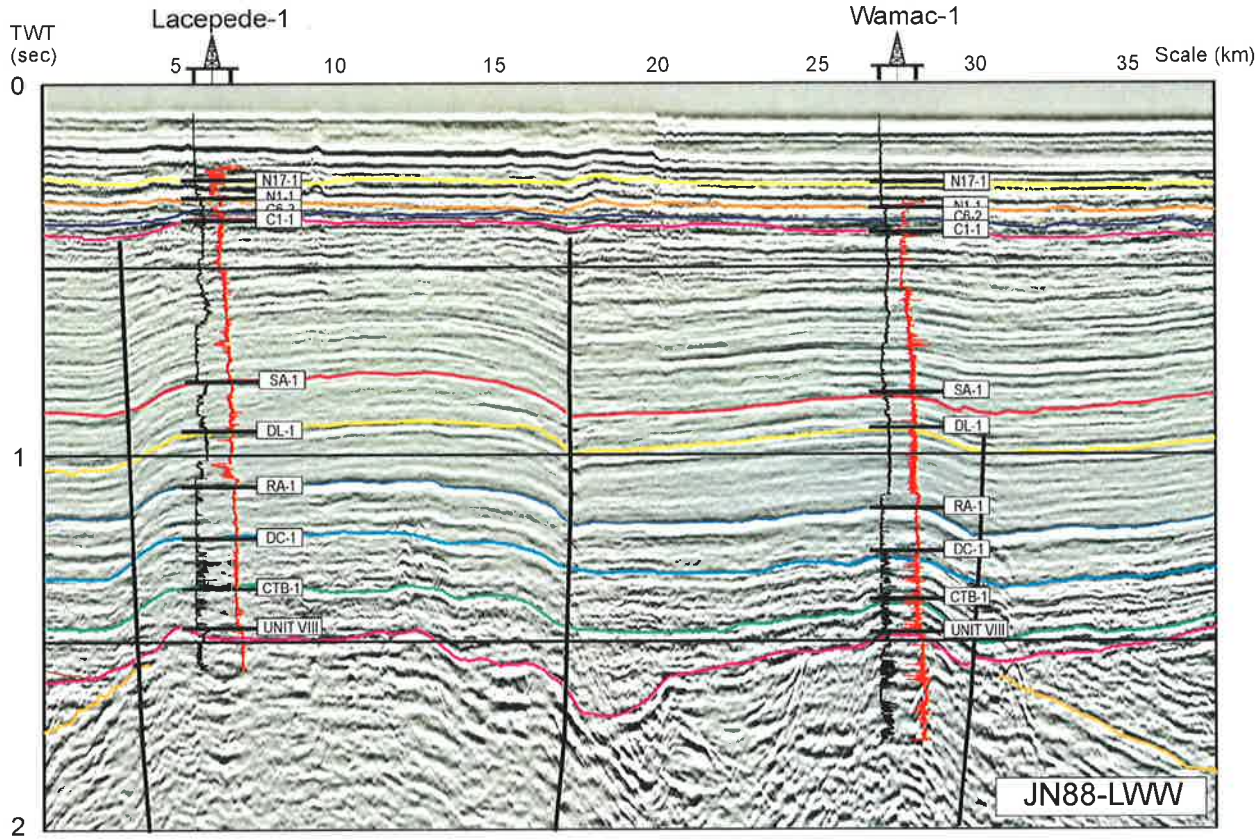

Figure 2.3 Representative well-ties across the Oobagooma Sub-basin showing time converted gamma (left) and sonic (right) wireline logs and horizon picks. Good seismic facies changes occur across the *Unit VIII*, *DC-1*, and *RA-1*. Post break-up deposition (above RA-1) is dominated by lowstand wedge and forced regression geometries. Strong sea-bed multiples and composite sequence boundaries obscure the post Aptian sequence.

explaining the poor well to seismic section ties. A linear interpolation between the highest checkshot and the seismic datum did not take into account the distinctive velocity profile of the upper-section which includes a fast well-cemented carbonate layer overlain by a slow layer of sea-water. To correct for this, a pseudo checkshot was calculated at the seafloor level using a water replacement velocity of 1500 ms^{-1} and the depth-conversion was repeated once again using the adjusted sonic log method. The result was a greatly improved depth-time tie in the upper section.

Where checkshot data was unavailable, alternative sources of information were used to tie well-data to the sections. Well-tie information for the Browse Basin and Beagle Sub-basins were supplied by AGSO's Browse and Beagle Study Groups (Symonds and Blevin pers. com.) and TWT picks for Nebo-1 were estimated from Osborne (1994). Horizon depths and TWT's of Mesozoic events are given for key wells in Table 2.2.

2.2.4 Interpreted Horizons

In total, twenty horizons and all major intra-crustal reflectors were also mapped (Chapter 3 Fig. 3.21). General seismic characteristics for each horizon and its internal lower seismic package are summarized in Table 2.3. The exact ages of each horizon are given in Fig. 3.6 (Chapter 3). Well control was available for all events except *Basement*.

2.2.4.1 Horizon Character

Basement, although not intersected in the offshore section, has a distinctive seismic character and could be tied from onshore seismic lines. No single seismic event could be picked for the horizon, which was picked at the base of, or close to, a series of high amplitude chaotic reflectors dipping at high angles (Fig. 2.4). Based on evidence from the Browse Basin and the geology of the Kimberley and Lambert Shelfs, these reflectors are believed to have resulted from highly intruded section sitting over high-grade

metamorphic and crystalline basement (Elliot 1990).

The Late Devonian *Dev* event was tied from Pearl-1 using the Carnot 81 survey. The event is interpreted to have developed in the Oobagooma Sub-basin where it has a distinctive negative acoustic impedance. This impedance contrast may be generated by well-cemented Late Devonian carbonates overlying highly weathered mid- Devonian reef complexes although acoustically fast volcanic intrusions/sills may also be partially responsible. Large amounts of relief can be observed on the horizon due partially to the reefal nature of the underlying sediments and partially due to strong faulting. The internal seismic package below the event is characterized by chaotic, high amplitude, isolated, dipping reflectors resulting from both, igneous intrusions and karst topography (Appendix 1 Fig. A1.5 between 420 to 480 km and Fig A1.10).

The Late Carboniferous *Stage 1* event was also tied from Pearl-1, although the underlying sequence has been sampled in both Wamac-1 and Lacepede-1. The event is widespread and can be seen in the Oobagooma, Rowley and Bedout Sub-basins. Although no tie exists in the Bedout Sub-basin the event has been recorded in onshore wells and is represented by a prominent reflector on onshore seismic. In the Oobagooma Sub-basin the event has a strong negative acoustic impedance contrast, resulting from Late Carboniferous coarse-grained glauconitic sandstones overlying more silty Early Carboniferous sandstones. Elsewhere, the event was picked on a change of internal character, which consists of moderate-to-strong amplitude chaotic and wavy reflectors below and a seismically quiet zone above (Fig. 2.4).

The Early Permian *Stage 3* event is only preserved in the southern most part of the Oobagooma Sub-basin where it was tied from Pearl-1 (Appendix 1 Fig A1.10). Elsewhere, it has been eroded out by the Late Permian *Unit VIII* event. The event is conformable with reflectors above and below but has a strong positive impedance contrast.

Event	*Bedout-1*	*E Mermaid-1*	*Keraudren-1*	*Minilya-1*	*Phoenix-1*	*Wamac-1*
N17-2	[-]	[-]	350/0.351	551/0.498	424/0.473	[-]
N14-1	462/0.468	730/0.807	(-)	634/0.569	543/0.534	[-]
N1-1	643/0.617	1265/1.151	560/0.472	1049/0.870	810/0.708	[-]
T4-1	772/0.690	1627/1.366	570/0.482	1660/1.240	1097/0.905	[-]
C13-1	815/0.716	(-)	(-)	1685/1.259	1163/0.992	[-]
C6-2	1112/0.972	1764/1.456	837/0.672	1884/1.399	1470/1.211	[-]
C1-1	1260/1.102	1999/1.643	1065/0.883	1968/1.452	1550/1.307	406/0.401
SA-1	1423/1.242	2381/1.908	1217/1.016	2011/1.487	1608/1.331	927/0.884
RA-1	1798/1.504	2886/2.193	1545/1.249	2040/1.575	1901/1.512	1387/1.150
DC-1	2081/1.679	3373/2.449	1890/1.451	{-}	2298/1.733	1590/1.277
CTB-1	2417/1.869	3875/2.691	2103/1.562	{-}	2523/1.835	1790/1.400
CT-1	2722/2.107	{-}	2303/1.673	{-}	2913/2.087	(-)
SQ-2	(-)	{-}	2802/1.966	{-}	3645/2.435	(-)
Unit VIII	3020/2.290	{-}	{-}	{-}	{-}	1967/1.492

Table 2.2 Depths in metres and two-way-times in seconds for the major Mesozoic and Cainozoic events throughout the Roebuck Basin. Bracketed values are either not penetrated {-}, not sampled [-] or eroded out (-).

Horizon	*Signature (SEGY-Normal)*	*Angular Relationship*	*Internal Relationship Below Reflector*	*Overall Confidence*
N17-2	Strong peak	Truncation landward below, channeling/slope failure at the shelf-break, onlap above	Parallel and continuous	High
N14-1	Strong peak	Truncation towards the coast below, channeling/slope failure at the shelf-break, onlap above	Well developed, sigmoidial prograding and aggrading wedge	High
N1-1	Strong peak	Truncation towards coast below, downlap above	Gently dipping sigmoidial prograding wedge	High
T4-1	Strong peak	Truncation towards coast below, downlap above	Chaotic karst style topography directly below	Moderate
C13-1	Moderate peak	Parallel below, downlap basinward, onlap landward	Parallel Continuous	Moderate
C6-2	Strong trough	Well channeled, downlap basinward, onlap landward	Parallel discontinuous	High
C1-1	Weak peak	Strong localized channelling	Parallel discontinuous	Low
SA-1	Weak peak	Strong localized channelling	Parallel discontinuous	Low
DL-2	Weak peak	Parallel below, downlap above in Oobagooma Sub-basin	Quiet to parallel discontinuous	Moderate
RA-1	Moderate peak	Truncation below, downlap above especially on margin edge	Parallel to slightly wavy discontinuous landward, parallel basinward	Moderate
DC-1	Moderate peak	Gentle downlap above, parallel below	Chaotic (especially in the Oobagooma Sub-basin) to parallel discontinuous	Moderate
CTB-1	Moderate peak	Parallel above and below	Chaotic (especially in the Oobagooma Sub-basin) to parallel	Moderate
CT-1	Strong trough	Truncation below, downlap above especially out on margin	Strong parallel continuous in the Bedout Sub-basin, weaker in the Rowley Sub-basin	High
SQ-2	Strong peak	Gentle downlap above, parallel below	Strong parallel in the Bedout Sub-basin, weaker in the Rowley Sub-basin	High
Unit VIII	Strong peak	Strong truncation below, onlap above	Quiet basinward, stronger parallel landward	High
Stage 3	Strong peak	Parallel above and below	Parallel continuous	Moderate
Stage 1	Strong trough	Parallel above and below	Weak chaotic	Moderate
Dev	Strong trough	Truncation below	Karst style high relief topography, intruded	Moderate
Basement	Variable	Onlap	Chaotic high amplitude high angle	Low

Table 2.3 General horizon characteristics for seismic events picked during the structural interpretation.

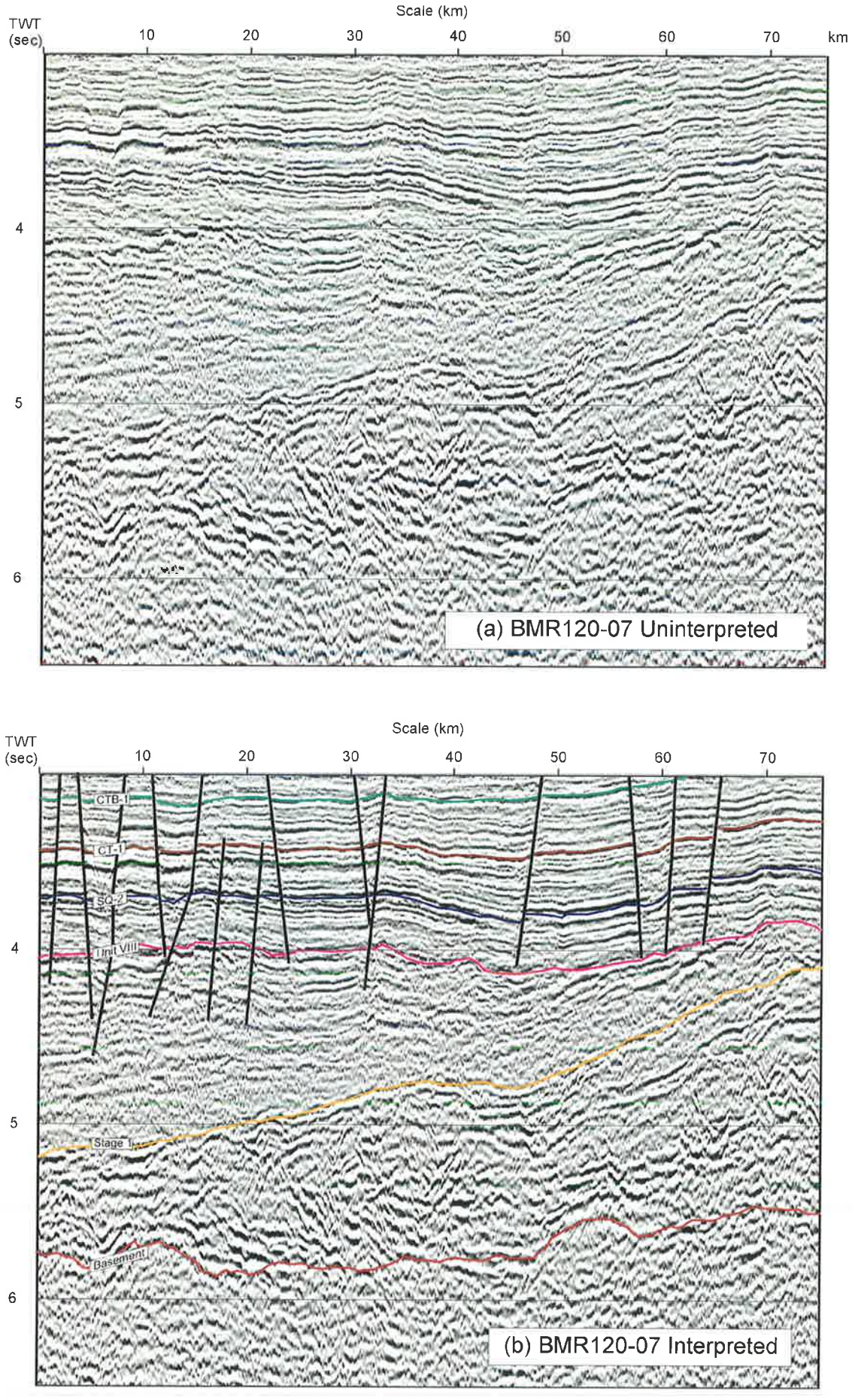

Figure 2.4 Seismic character of the *Basement* to Early Jurassic *CT-1* section in the eastern Inner Rowley Sub-basin.

The Late Permian *Unit VIII* event was tied by four wells in the study area. It has a strong positive impedance contrast throughout most of the Roebuck Basin (Fig. 2.5). Landward of the Rowley Sub-basin strong truncation occurs below the event, the result of uplift, volcanism and erosion during the Bedout Movement. No wells tie the horizon in the deeper part of the basin where it was picked on a strongly truncated surface of high amplitude alternating peaks and troughs, situated on the flanks of the major basinal highs (Fig. 2.4 best seen from 50 to 60 km). Sediments above strongly onlap the event over the whole study area.

The Middle Triassic *SQ-2* event was tied in four wells and marks the termination of a well developed marine incursion, and deposition of a thin, contemporaneous oolitic carbonate member (*Cossigny Formation*). On synthetic seismograms the event appears as a weak trough. However, on seismic, a strong trough was developed at this interval over much of the basin (Fig. 2.4). Although based on a lithostratigraphic pick the event forms a regional seismic marker and all well evidence (from the Bedout and Beagle Sub-basins), suggests that it has been contemporaneously deposited. The event was imaged well on the AGSO deep seismic data and was crucial in tying the deeper structure of the highly faulted western Rowley Sub-basin (Appendix 1 Fig. A1.5). Below the event the sequence consists of moderate to high amplitude continuous parallel reflectors. Gentle basinward downlap occurs above the event.

The Early Jurassic *CT-1* event was tied in five wells. It consists of a strong peak-trough signal on seismic, the result of Early Jurassic braided fluvial sandstones overlying Late Triassic fine grain fluvial red-bed clays (Fig. 2.4). On the margin the event is marked by truncation below and strongly developed downlap above (Fig. 2.6). Elsewhere in the basin the event consists of a parallel unconformity with minor downlap development on its upper surface. The event has traditionally been associated with rift onset during the Fitzroy Movement.

The mid-Jurassic *CTB-1* and *DC-1* events were not initially picked during the first pass interpretation. Nevertheless, the change in seismic character across these events suggested that they marked significant changes in sedimentological or tectonic regimes. A fairly strong peak-trough signature, especially in the Oobagooma Sub-basin, marks each horizon (Figs. 2.1, 2.3 and 2.5). Internally, their character is of moderate amplitude and quite chaotic in nature. This character is clearly divided by *CTB-1*. Above *DC-1*, slight downlap and a more continuous character occurs. Wire-line log interpretation reveals that the *CTB-1* event coincides closely with a sedimentological change from a braided to a more channel-dominated fluvial system. A sedimentological change was not evident for *DC-1* but evidence from fault analysis suggests that areas of structuring cease at this time indicating that *DC-1* is tectonically influenced (Fig. 2.7).

The mid-Jurassic *RA-1* event marks the final breakup along the northern margin of the Roebuck Basin. The event is marked by a moderately developed peak resulting from the deposition of fine-grain marine sediments over fluvial sandstones. On the margin, strong truncation below the event, followed by downlap above the event, formed due to uplift and erosion during rifting and subsequent thermal subsidence (Fig. 2.6). Landward, the event consists of a parallel unconformity but is marked by a change in seismic character from slightly wavy to continuous.

The Early Cretaceous *DL-1* event was only picked in detail in the Oobagooma Sub-basin where it is marked by a downlap surface at the base of a strongly developed axially fed delta system (Fig. 2.8).

Both the Early Cretaceous *SA-1* and *C1-1* events represent significant erosive episodes in the stratigraphic record, related to plate separation and the drift phase of India from Australia along the western margin. In the Bedout and Rowley Sub-basins their appearance on seismic was indistinct (Fig. 2.1 and 2.2). Synthetics suggest

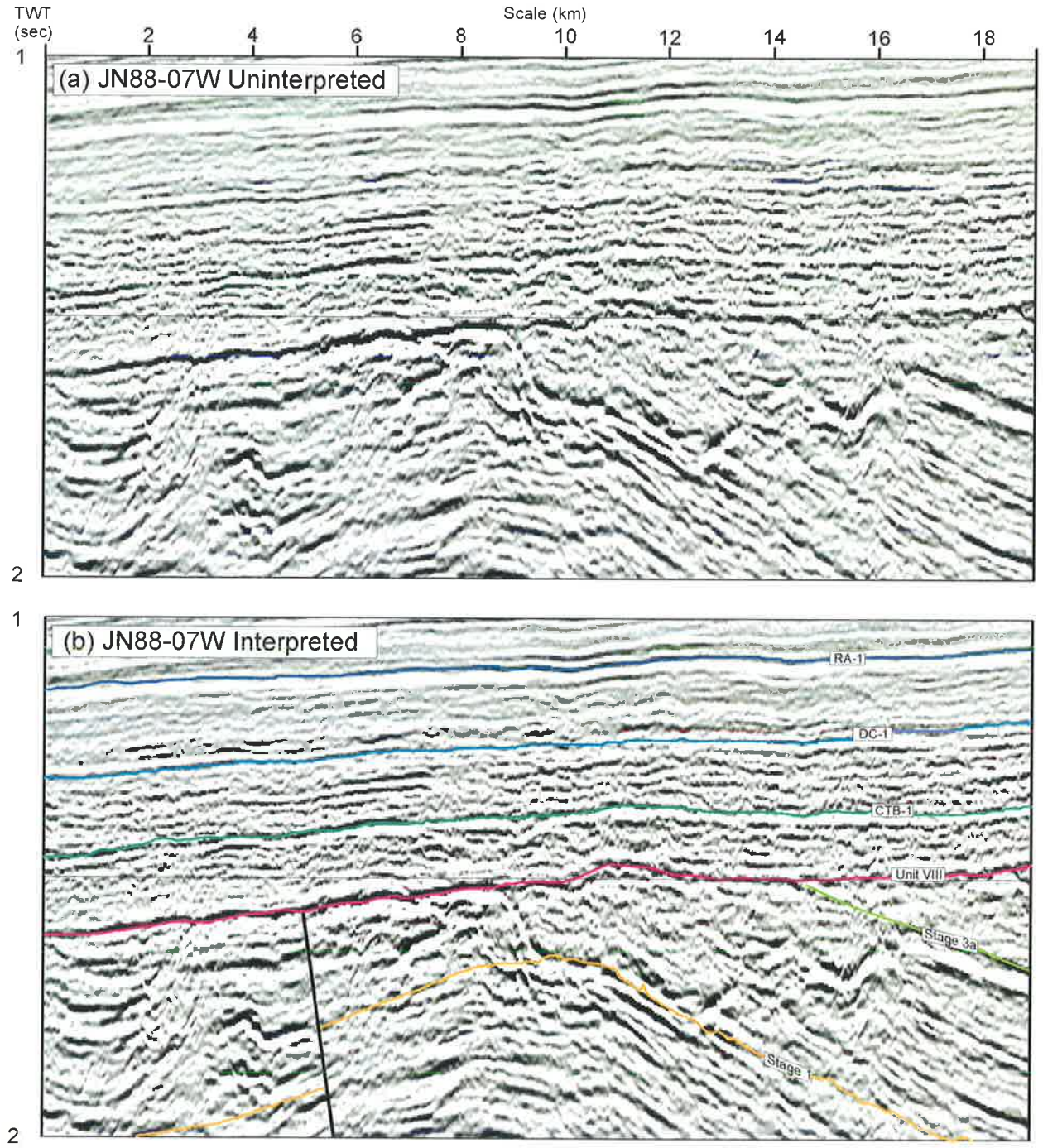

Figure 2.5 Seismic character of the Oobagooma Sub-basin highlighting the dramatic nature of the Late Permian *Unit VIII* unconformity and seismic facies change at the Middle Jurassic *DC-1* event.

that only poorly developed peaks should be present for both horizons (Fig. 2.2). Channelling was initiated at the *C1-1* event at the boundary of the Oobagooma and Rowley Sub-basins (Fig. 2.9), however, on the shelf the events are seen as parallel unconformities. In the Oobagooma Sub-basin the *SA-1* event becomes a little more coherent, marking the top of a well-developed prograding package that represents an increase in sedimentation rates across the study area (Fig 2.8), however, the *C1-1* event is eroded out by a series of composite sequence boundaries in this area (Fig. 2.3). Although considered sound in the Oobagooma Sub-basin, pick confidence of these events was generally low elsewhere.

The Late Cretaceous *C6-2* event marks the base of a well developed carbonate member and appears on seismic as a broad trough (Fig. 2.1). Regionally, truncation is developed below the horizon and downlap is visible above (Fig. 2.2). The event is associated with initiation of Antarctic-

Australian plate separation.

Five more significant unconformities were identified on seismic and due to their shallow nature were mappable throughout the area. They were the base Tertiary *C13-1* event, the Early Tertiary *T4-1* event which displays strong karst type topography, the mid Tertiary *N1-1* event, and the late Tertiary *N14-1* and *N17-2* events. All events show strong truncation below in the more landward sections (Fig. 2.1 and 2.2). The latter two events result from Miocene uplift and reactivation associated with the collision of Australia and Indonesia (AGSO, 1994). Although easily traceable throughout most of the study area, these events became difficult to pick in the Oobagooma Sub-basin due to strong sea-bottom multiples that obscured the upper section.

2.3 Regional Cross-sections

In total, nine regional cross-sections, predominantly from the AGSO seismic data set, have been presented (Appendix 1 Figs. A1.2 to A1.10). These lines demonstrate the general appearance and nature of the major structural elements of the basin. As well as structural and horizon interpretation, each megasequence has also been shaded in accordance with the colour scheme presented in the chronostratigraphic basin summary (Chapter 3 Fig. 3.21). The location of each cross-section is shown in Fig. 2.10 and

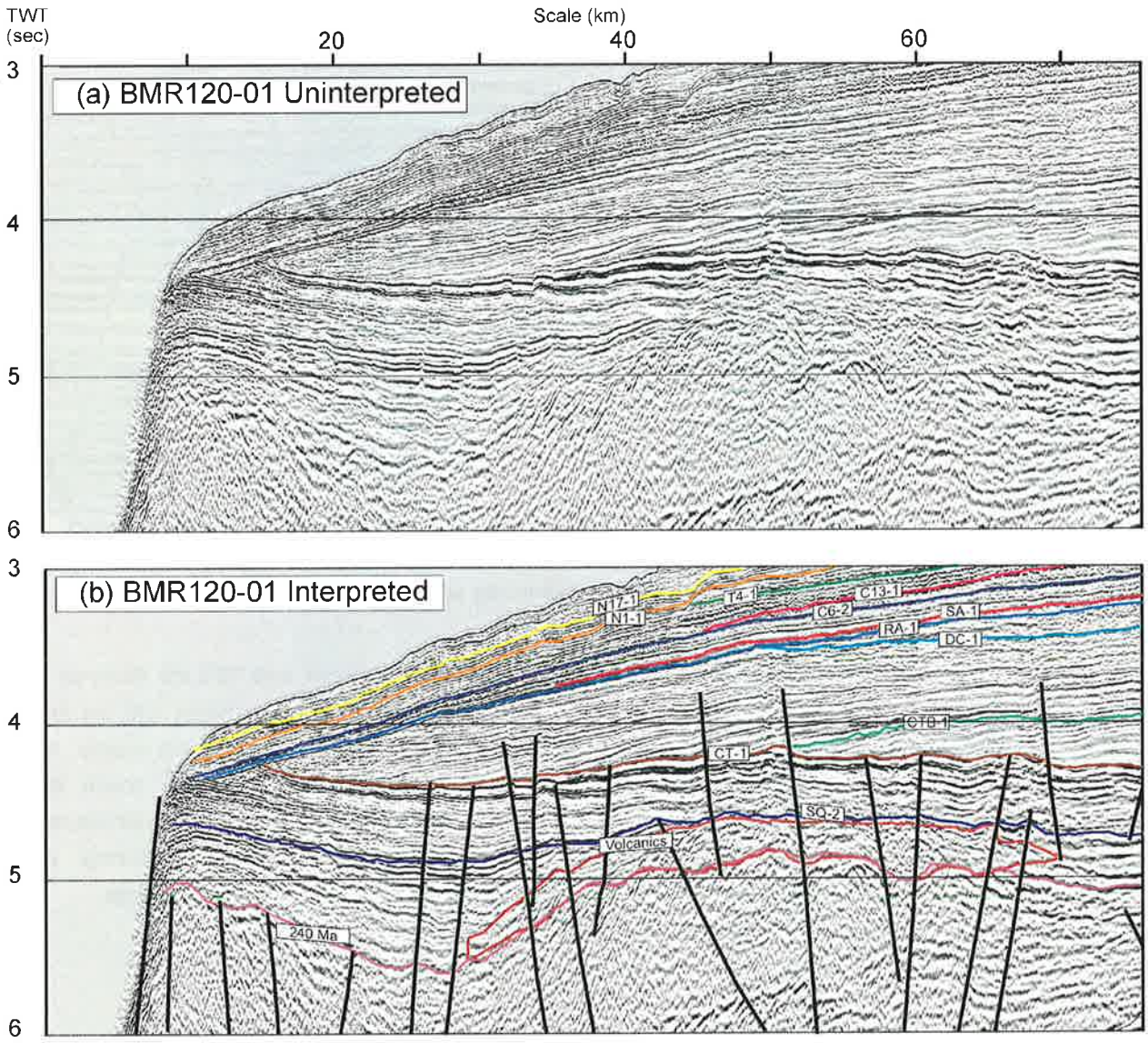

Figure 2.6 Seismic character of the outer Rowley Sub-basin. Significant truncation occurs below and downlap occurs above the Early and Middle Jurassic *CT-1* and *RA-1* events.

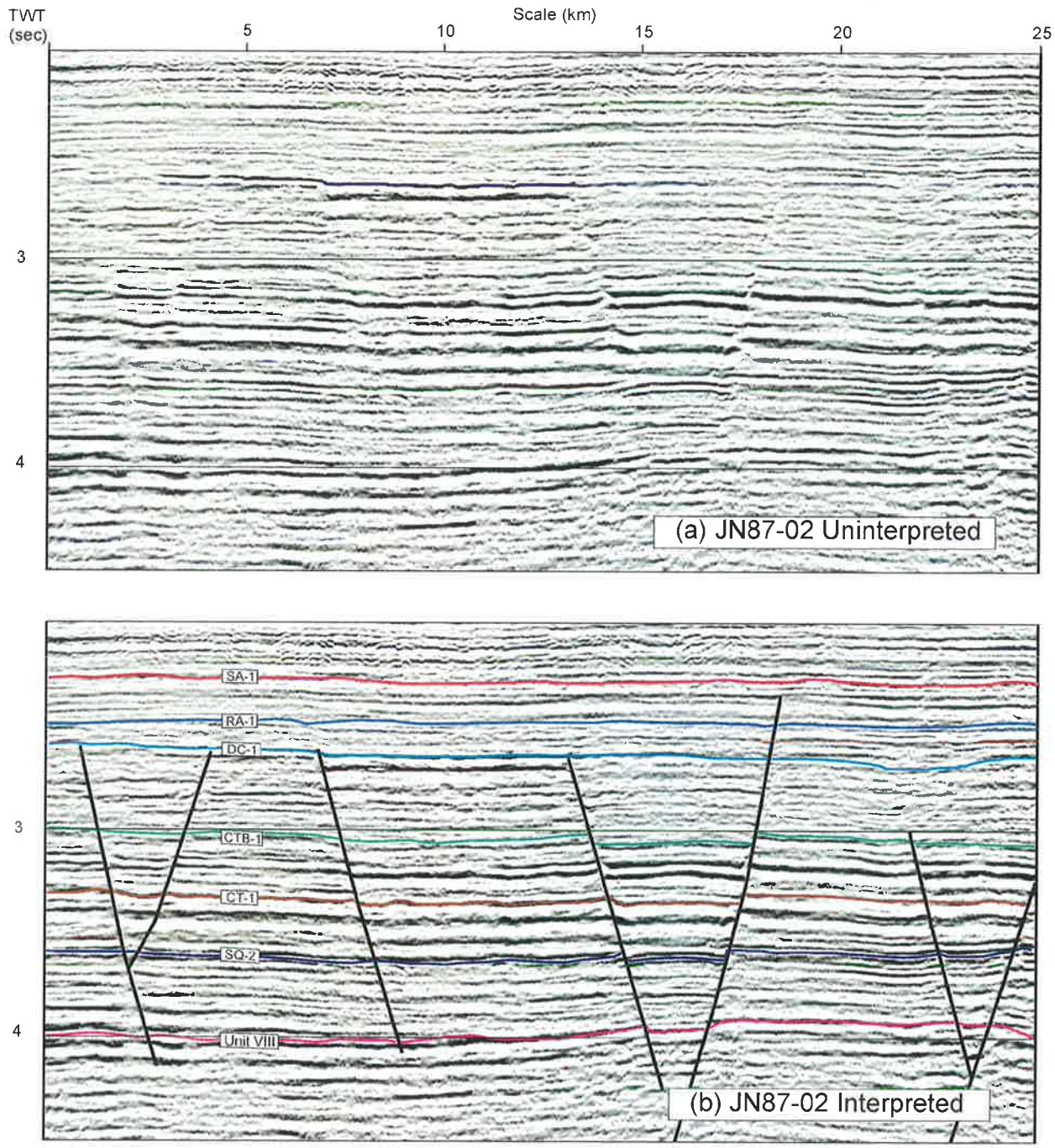

Figure 2.7 Structural character of the inner Rowley Sub-basin exhibiting possible hydrocarbon related brightening in association with rotated fault-blocks at the Middle Jurassic *DC-1* level.

Fig. A1.1 (Appendix 1).

2.4 Two-way-time Structure and Isopach Maps

TWT structure maps were produced for all major horizons (Appendix 2 Figs. A2.1 to A2.15). and isopach maps were generated for major intervals in the Mesozoic and Cainozoic (Appendix 3 Figs. A3.1 to A3.12)

Maps were contoured at 200 ms intervals below the Middle Jurassic and 100 ms intervals above. Isopachs were all contoured at 100 ms intervals. Although contouring intervals are coarse, with the seismic grid spacing available, these intervals accurately reflect the overall time-structure of the basin without introducing contouring artifacts along the sparsely distributed line data.

2.5 Fault Movement Maps

Simple fault analysis was conducted to determine timing, sense and spatial distribution of fault

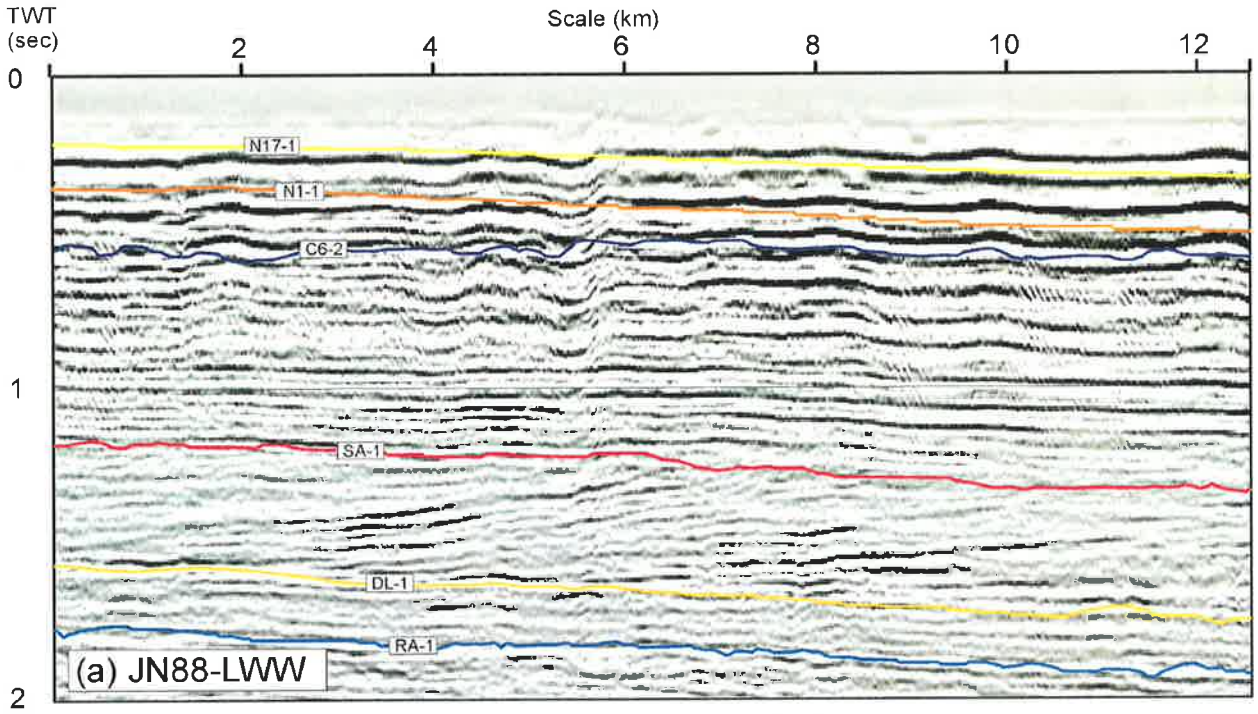

Figure 2.8 Seismic character of the upper section of the Oobagooma Sub-basin. Regional uplift associated with the Indian plate separation from Australia resulted in renewed sediment input into the Oobagooma and Bedout Sub-basins. Delta development above the Early Cretaceous *DL-1* event is best preserved here in the Oobagooma Sub-basin.

movement. Fault movement maps along with periods of volcanism (shown in red and yellow) were created at each major seismic boundary (Appendix 4 Fig A4.1 to A4.6).

2.6 Regional Mapping Results

Regional mapping has been used to analyse the major structural styles observed in the study area. This enabled determination of the overall basin geometry, description of the major tectonic elements, and discussion of potential mechanisms for the formation of the basin.

2.6.1 Structural Style of the Roebuck Basin

Five major structural styles were identified during this study in the Roebuck Basin. These included; normal basin margin faulting, fault inversion, uplift/compression associated with volcanism, normal faulting on detachments and strike-slip:

1) Normal basin margin faulting is associated with the development of large graben and half-graben features that formed the major depocentres of the basin. Faults display throws of up to 2 s TWT (Appendix 1 Fig. A1.6 between 280 and 360 km) and are especially

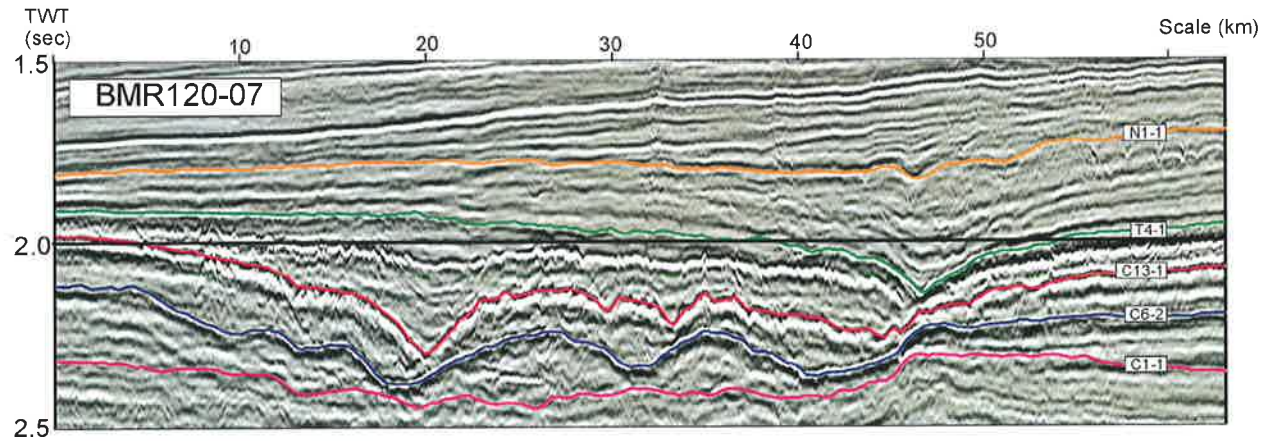

Figure 2.9 Late Cretaceous/Early Tertiary channel focused along the Oobagooma Sub-basin depositional axis.

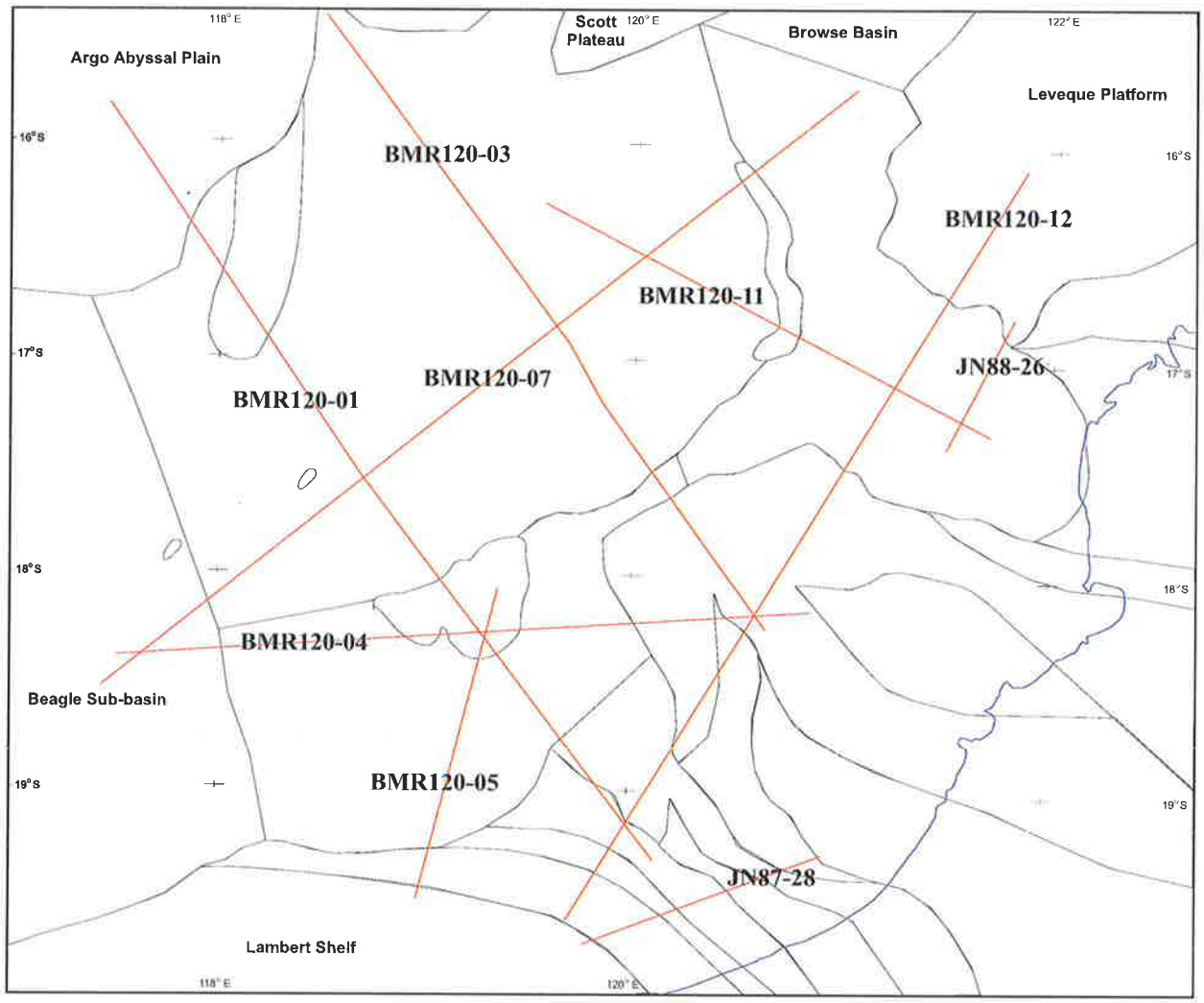

Figure 2.10 Location of regional seismic cross-sections presented in Appendix 1. Also marked are the major structural elements mapped during the study (see Figure 2.8 for details of the structural elements).

common along the margins of the older Palaeozoic depocentres which developed during NE-SW extension associated with the formation of the Canning Basin during the Cambrian to Late Permian.

2) Fault inversion is predominantly associated with basin margins, where normal Type 1 faulting described above has been re-activated during tectonic events, probably as a result of transpressional wrenching which was initiated during the Carboniferous and reactivated periodically to the Present day. Figure A1.10 (Appendix 1) demonstrates how reactivation has potentially occurred at several stages in the basin's history. Based on *en echelon* anticline development and fault patterns identified by Forman and Wales (1981) in the Canning Basin, wrenching is believed to have resulted from dextral movement along the failed rift systems of the Canning Basin (this concept is developed further in Section 3.8.4).

3) Uplift/compression associated with volcanism has resulted in the development of some of the basin's major structural highs including the Bedout and Oobagooma Highs during the Palaeozoic (Appendix 1 Fig. A1.2 between 290 and 340 km and Fig. A1.8 between 110 and 140 km). During fault analysis volcanism was marked in red and yellow (Appendix 4 Figs. A4.1 to A4.6).

4) Normal faulting on detachments has lead to the development of high frequency (4-5 km spaced) 'bookshelf or domino' style faulting (described in Wernicke and Burchfiel, 1982)

over much of the western half of the basin (Appendix 1 Fig. A1.4 between 0 to 120 km). Development of this style of faulting appears restricted to the Triassic to Tertiary section.

5) Strike-slip movement has occurred during the formation of many of the above fault styles and has often resulted in the reactivation of older structures usually as dextral transpression described in Type 2 faulting above. Nevertheless, recent sinistral trans-tensional wrenching is interpreted to have occurred in the Rowley Sub-basin based on the comparison of Miocene structures (reactivation of E-W oriented Carboniferous half-grabens (Appendix 1 A1.3 between 230 and 240 km) and inversion of N-S oriented faults (Appendix 1 Fig. A1.5 between 440 and 460 km and seen in plan view in Fig. A4.6 (Appendix 4)), with the results of clay modelling work by Christie-Blick and Biddle (1985) and with strain ellipsoid diagrams in Harding and Lowell (1979).

The examination of the distribution and timing of these fault styles has been used to broadly define the structural style of the basin through time. Three main stages: pre-Late Permian, Late Permian to mid-Cretaceous, and post mid-Cretaceous were identified.

Initial structuring of the basin occurred on a series of NW oriented normal faults that formed along the margins of the Oobagooma Sub-basin and the Willara Sub-basin and Samphire Graben during formation of these large depocentres (Fig 2.11, Appendix 4 Fig. A4.1 and Appendix 2 Fig. A2.1). These features developed under the same stress regime, NE-SW intra-cratonic extension, as the onshore Canning Basin. Each depocentre is strongly characterized by horst- and graben-like topographies formed by Type 1 normal faulting described above (Appendix 1 Fig. A1.9).

By the beginning of the Late Carboniferous large half grabens oriented NE-SW started to develop contemporaneously but orthogonal to the initial structural trends (Appendix 1 Fig. A1.3 between 240 to 280 km). However, Late Carboniferous to Late Permian structuring was generally more subtle than earlier structuring. The major depocentres that formed prior to the Carboniferous were rapidly filled in the early stages of the basin's history, and by the Late Carboniferous consisted of slowly subsiding downwarps controlled by isostatic loading and thermal sag (Appendix 2 Fig. A2.2). Normal basin margin faulting ceased sometime during the Carboniferous, and evidence suggests that Type 2 style basin inversion was first initiated on several of the NW oriented normal faults, especially in the Oobagooma Sub-basin (Appendix 4 Fig. A4.2), during this period (truncation below Unit VIII in Fig. A1.10 (Appendix 1)). Volcanism, uplift and compression at the Bedout and Oobagooma Highs, characterized by Type 3 structuring, is also interpreted to have been initiated at this time (marked in brown and yellow in Fig. A4.2 (Appendix 4)).

By the Late Permian, structuring associated with NE oriented intra-cratonic extension ceased along the Bedout and Oobagooma Sub-basins. However, these failed rift trends remained evident as broad downwarping troughs dominated by thermal sag and isostatic loading until the Tertiary (Appendix 2 Fig. A2.3). Type 2 fault inversion resulting from periodic tectonism became most prominent along the eastern margin of the Oobagooma Sub-basin at the edge of the Leveque Platform, where reactivation is observed up until the Late Cretaceous.

Rapid thermal sag in the western Rowley and Bedout Sub-basins during the Early Triassic led to detachment style type 4 faulting possibly due to a gravity-driven response to increased sediment loading in this area (Appendix 3 Fig. A3.1). From TWT and isopach map interpretation, the Triassic is interpreted to mark the beginning of restriction of sedimentation to the Rowley Sub-basin and along the slowly subsiding failed rift arms of the Oobagooma and Bedout Sub-basins (Appendix 2 Figs. A2.5, A2.6 and A2.7 and Appendix 3 Figs. A3.2, A3.3 and A3.4).

Rift breakup along the northern margin of the basin during the Callovian resulted in the development of massive down-to-the-northwest faulting, (shown in the NW corner in Appendix 2 Fig A2.2 and Appendix 4 Fig. A4.4), with the failed rift arm to this rift system running from the north towards the Lambert Shelf (Fig. 2.11 and Appendix 2 Figs. A2.6 and A2.7 at 118 °E, 17.7 °S and Appendix 3 Fig. A3.5).

Structuring after breakup was characterized by broad basinward downwarp associated with drift phase tectonics and slow sediment rates (Appendix 2 Figs. A2.10-A2.13 and Appendix 3 Figs. A3.6-A3.10). Minor reactivation occurred during separation of India from Western Australia (Appendix 4 Fig. A4.5).

By the Late Tertiary virtually all remnant structuring relating to early differential subsidence had been filled (Appendix 2 Fig. A2.14). Sediment processes were dominated by the development of a shelf-wide carbonate prograding wedge system which stretched from the Western Carnarvon to the Browse Basin (Appendix 2 Fig. A2.15 and Appendix 3 Fig. A3.12). Little structuring developed in the basin until the collision with SE Asia during the Middle Miocene. This led to the development of NE-SW oriented wrenching along old Palaeozoic half-graben structures in the Inner Rowley Sub-basin, (Appendix 1 Fig. A1.3 between 240 and 250 km), and to fault inversion on the most northern outer edge of the Leveque Platform (Appendix 4 Fig. A4.6).

2.6.2 Structural Framework

Examination of structuring and major fill distribution has enabled the sub-division and description of the major structural elements of the Roebuck Basin. These are shown in Figure 2.11 and have been named based upon the terminology of Hocking et al. (1994).

2.6.2.1 Major Basin Elements

Extension in the Roebuck Basin occurred during three major phases - NE intra-cratonic extension, associated with the formation of the southern Carnarvon, Canning and southern Bonaparte Basins prior to the Carboniferous; a transition from NE to NNW extension sometime during the Carboniferous to Late Permian (timing poorly constrained); and NNW (Westralian) extension, associated with the breakup from Gondwanaland of the SIMUBASU continental sliver (Sengor, 1987). For further details see Section 3.7.1.

The area now occupied by the Roebuck Basin can, therefore, be seen as a series of stacked basins, (in the Australian sense of the term) consisting of:

- older Palaeozoic sediments deposited during NE intra-cratonic and transitional extension prior to the Late Permian (associated with the predominantly onshore Canning Basin sequence),

- and younger Mesozoic and Cainozoic sediments of the Roebuck Basin which were deposited during NNW Westralian extension after the Late Permian.

The nature and location of sediments within these stacked basins led to the division of the basin into three sub-basins; the Oobagooma Sub-basin (previously known as the offshore extension of the Fitzroy Trough), the Bedout Sub-basin and the Rowley Sub-basin (Hocking et al., 1994). Dividing these sub-basins are three intra-basinal highs – the Bedout High which separates the Bedout and Rowley Sub-basins, the Broome Platform which separates the Oobagooma Sub-basin from the Bedout and Rowley Sub-basins, and the Oobagooma High which separates the southern end of the Oobagooma Sub-basin from the Rowley Sub-basin.

It is evident from initial descriptions that the area occupied by the Roebuck Basin was formed by a complicated series of temporally and spatially variable tectonic elements. The remainder of this chapter is dedicated to the description of these major tectonic elements and a discussion of the structural mechanisms that formed them.

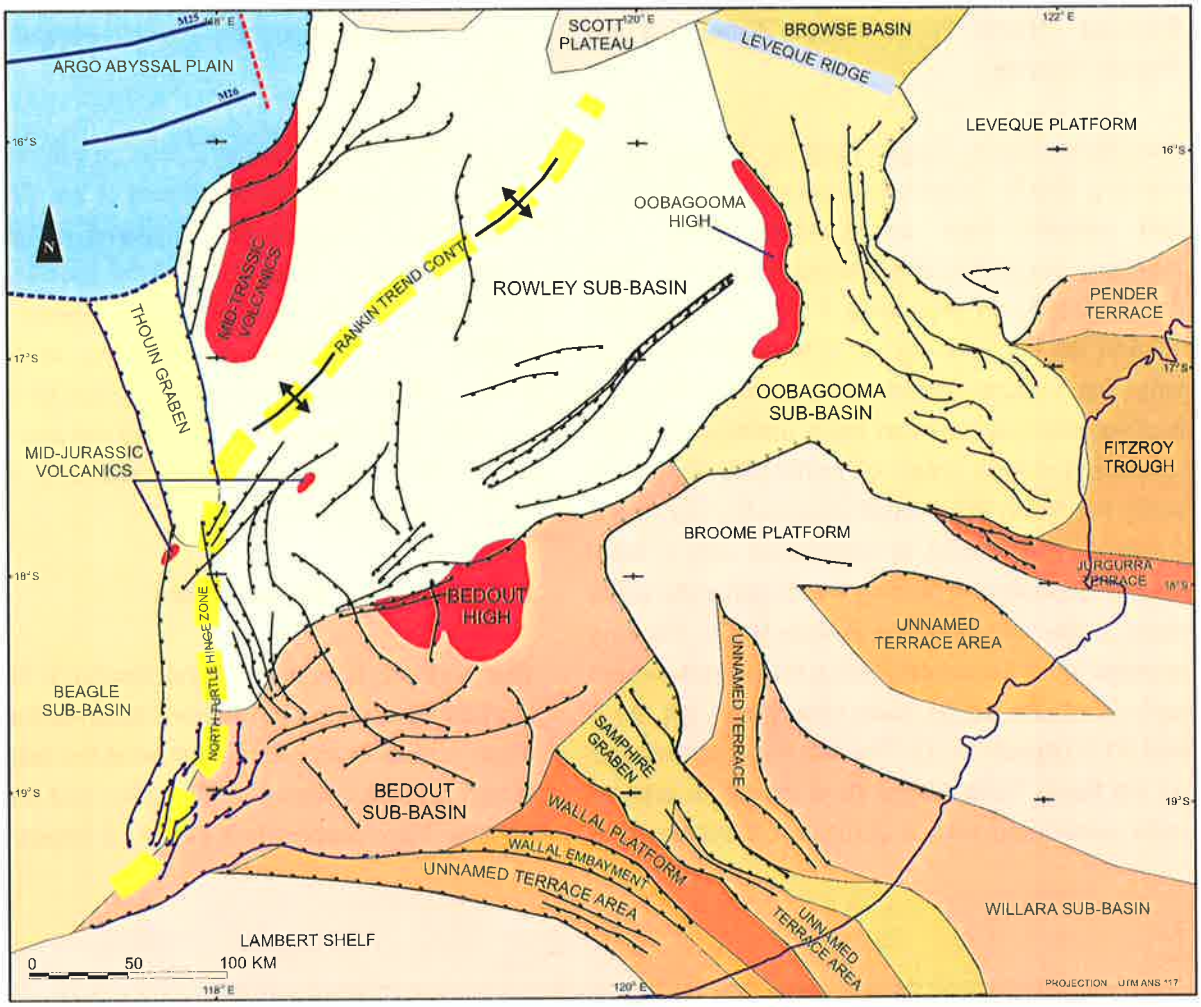

Figure 2.11 Structural elements of the Roebuck Basin defined during this study. Nomenclature after Hocking et al. (1994), faults in the Beagle Sub-basin (in blue) from Blevin et al., (1994), surrounding elements from Stagg (1993).

2.6.2.2 Basin Boundaries

2.6.2.2.1 Leveque Platform and Ridge

The Leveque Platform is the offshore extension of the Precambrian Kimberly Block and separates the Oobagooma Sub-basin from the Browse Basin. It consists of crystalline basement overlain by a thin veneer of Jurassic and younger sediments (Appendix 1 Fig. A1.6 between 360 to 440 km and Fig. A1.10 between 50 to 70 km).

To the north of the Leveque Platform, a northwest-southeast trending intra-basinal high called the Leveque Ridge separates the Rowley Sub-basin from the Browse Basin (Lipski, 1994). The feature has not been drilled, but can be tied from East Mermaid and Barcoo-1 and has been interpreted to consist of Permian sediments sub-cropping the Cretaceous (Lipski, 1994). Although not mapped during this study, Lipski (1994) describes the feature as having experienced several stages of uplift from Late Permian through to the Late Jurassic, prior to being truncated and transgressed by Neocomian marine sediments.

2.6.2.2.2 Lambert Shelf

The Lambert Shelf is the offshore extension of the Precambrian Pilbara Block (Appendix 1 Fig. A1.7 between 0 to 15 km and Fig. A1.9 between 0 to 30 km). It consists of crystalline basement overlain by a thin veneer of Palaeozoic sediments that is onlapped by Middle Jurassic and younger sequences. The edge of the shelf is marked by a series of down-to-basin normal faults at the Palaeozoic level.

2.6.2.2.3 North Turtle Hinge Zone and the Thouin Graben

The North Turtle Hinge Zone is a north-south trending Middle Triassic transpressional structure that extends from the Lambert Shelf. The structure separates the Bedout Sub-basin from the Beagle Basin (Appendix 1 Fig. A1.4 between 15 and 40 km and Fig. A1.5 between 25 to 70 km). The feature consists of a zone of complex faulting which appears to have undergone major wrenching during times of NNW-SSE extension along the North West Shelf especially prior to the Jurassic. The feature is associated with a large degree of bookshelf faulting which generally steps down to the west into the Beagle Basin. Faulting appears to be associated with a major detachment surface which can be seen clearly on Figs. A1.4 and A1.5 (Appendix 1). The last major movement on the North Turtle Hinge Zone marks an area of uplift associated with a Jurassic rift system that formed opposite to the Rankin-Picard Trend (Lipski, 1993).

The North Turtle Hinge Zone trends into the Thouin Graben, the failed rift arm of the Callovian triple junction located at the basins present-day break-up margin (Fig. 2.11). The southern-most expression of this feature is just covered by the seismic data set utilised during this study (Fig. 2.12). The graben has been the focus for density currents up to the present day and the sea-floor in this area is highly channelled resulting in poor imaging below this feature.

2.6.2.2.4 Argo Abyssal Plain

The northern boundary of the Roebuck Basin is marked by a series of massive down-to-the-north major normal faults which formed at the continent-ocean boundary between the basin and the Argo Abyssal Plain (Appendix 1 Fig. A1.2 between 0 to

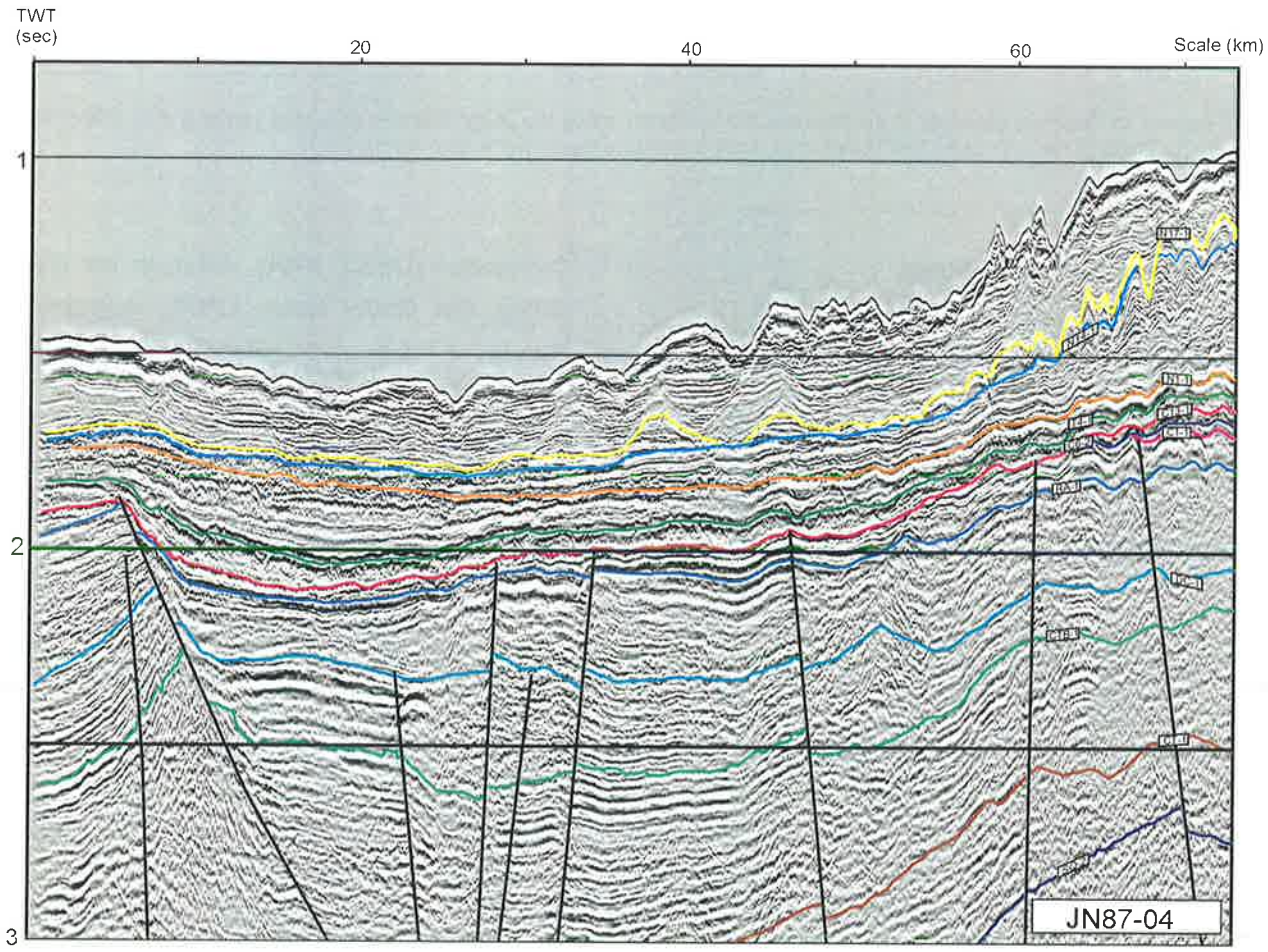

Figure 2.12 Southern-most expression of the Thouin Graben.

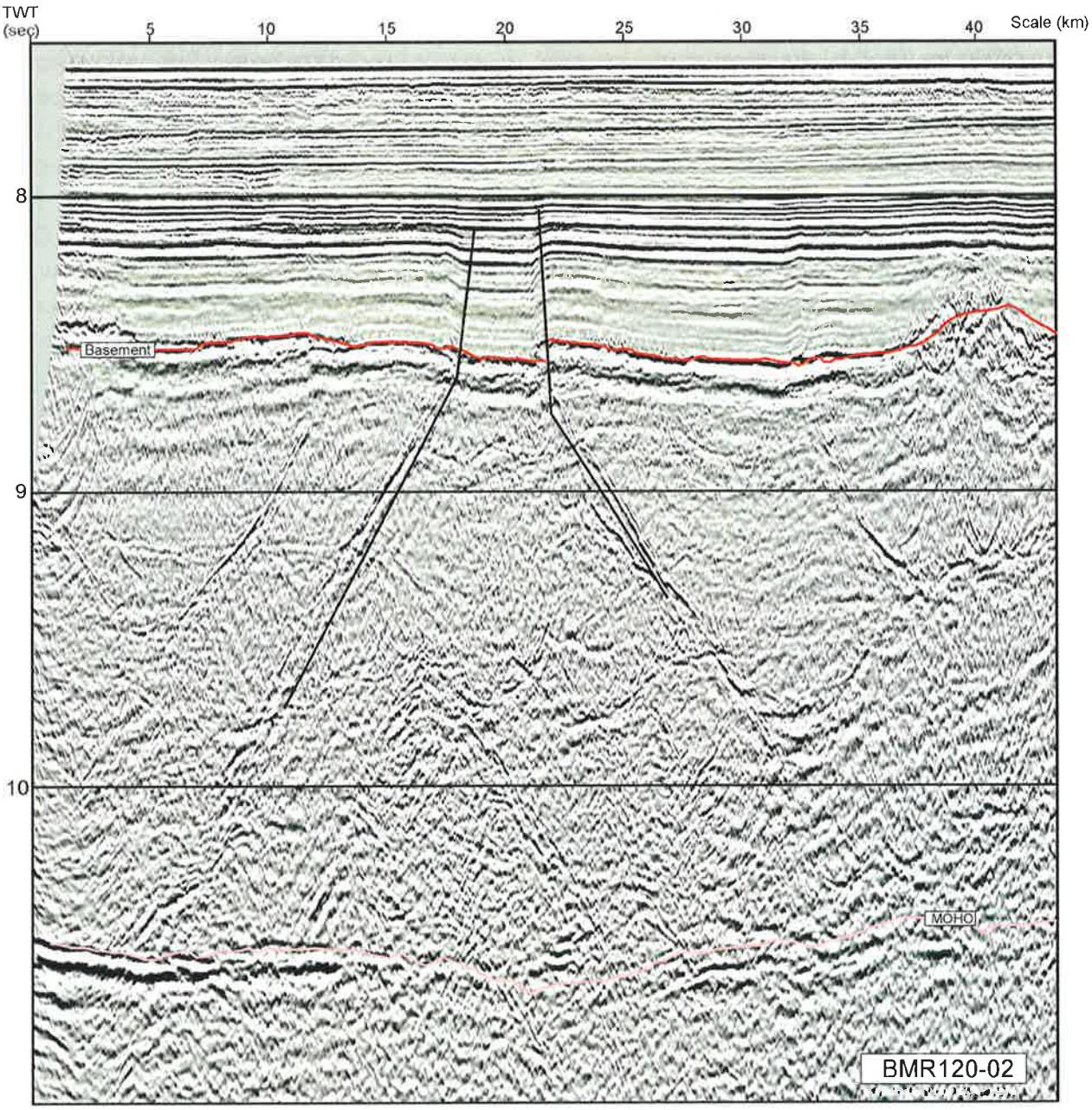

Figure 2.13 Crustal structure of the Argo Abyssal Plain showing ?Late Cretaceous compressional features in the upper crust. The origin of these features is unknown. They may be related to differential thermal contraction of the crust.

90 km and Fig. 2.13). The plain sits at a depth of approximately 5.7 km (7.5 s TWT) below sea-level and is underlain by some of the oldest oceanic crust known in the Indian Ocean. During the Cainozoic the plain has undergone subduction at the convergent margin between Australia and the Sunda-Banda Arc (Gradstein, 1992).

Major normal faulting and initial oceanic crust emplacement is interpreted to have occurred during the last episode of major rifting adjacent to the Roebuck Basin and has been dated at 155.3 +/- 3.4 Ma (Ludden, 1992). Oceanic crust is overlain by thin distal Tithonian turbidites (Gradstein, 1992). The Moho has been clearly imaged using deep seismic data (Appendix 1 Fig. A1.2 at 10.7 s TWT and Fig. 2.13).

Compressional features are observed on seismic in the oceanic crust (Fig. 2.13). The origin of these features is unknown. At depth they express high amplitude reflectors similar to intrusive dykes but are clearly compressive in nature at the basement/sediment interface. Here it is speculated that they may be related to differential thermal cooling of the crust. The upper crust cools

rapidly after formation whilst the lower crust is thermally insulated by the upper crust and cools at a slower rate. As the lower crust cools it contracts and, as it is in contact with the upper crust, places a compressive force on the shallower section, resulting in minor thrust development (analogue to molten to solid cooling of a slag on a furnace). No analogues were identified in the current literature that document the existence or formation of these features. Other mechanisms for formation could included Miocene compression, however, there is little disturbance of sediments in the shallow section suggesting that these features were formed earlier than onset of collision.

2.6.2.2.5 Onshore Canning Basin

The onshore Canning Basin marks the southern boundary of the Roebuck Basin, where seaward-thickening Mesozoic to recent sediments thin by onlap on to older north-west trending elements of the Palaeozoic Canning Basin that extend into the present day offshore area (Appendix 1 Fig. A1.2 between 420 to 480 km and Fig. A1.6 between 0 to 95 km).

As Palaeozoic sediments have been deposited under most of the Roebuck Basin succession, the division is based on the seaward extension of onshore structures rather than the timing of sediment distribution. The division is therefore more geographically rather than geologically significant. In the near offshore, the Palaeozoic trends appear to be abruptly terminated by the ENE trending Jurassic fault systems associated with the rifting and breakup of Gondwanaland and the formation of the Australian continental margin (Passmore, 1991; Horstman and Purcell, 1988). It is uncertain whether these trends are truly terminated or have not been imaged by currently available seismic data.

2.6.2.3 Major Depocentres

2.6.2.3.1 Wallal Embayment, Samphire Graben and the Willara Sub-basin

Of the Palaeozoic depocentres that extend offshore under the Bedout Sub-basin succession, the most prominent are the Wallal Embayment, Samphire Graben and Willara Sub-basin. These features were initiated during intra-cratonic downwarp and faulting associated with NE-SW extension during the formation of the Canning Basin in the Ordovician. The major structural features are quite distinct in the onshore and nearshore area where they consist of asymmetric grabens and half-grabens (Appendix 1 Fig. A1.9). They can be traced up to 50 km offshore where they become less distinct. It appears that the Samphire Graben then widens into a broad asymmetrical sedimentary downwarp approximately 80 km wide (Appendix 1 Fig. A1.6). The graben is bound on its eastern flank by the relatively stable Broome Platform and on its south-western margin by the Lambert Shelf. Although the Samphire Graben becomes dominant in the offshore section, the other Palaeozoic structural fault trends can be mapped up to 30 km basinward of the present day coastline.

Samphire Marsh-1 was drilled on a basinal high in the Samphire Graben and intersected an Early Permian to Upper Carboniferous and an Ordovician section. On seismic in the nearshore area, three packages can be seen. These are interpreted to represent Permian to Upper Carboniferous, Middle Carboniferous and older undifferentiated and Ordovician (which is only seen in the deepest graben structures in the offshore section). The Middle Carboniferous is interpreted to have been eroded out in the onshore section and hence is not seen in the Samphire Marsh-1 exploration well.

2.6.2.3.2 Oobagooma Sub-basin (Fitzroy Trough)

The Oobagooma Sub-basin consists of a major NW-SE trending intra-cratonic depocentre of Palaeozoic and Mesozoic to Recent age that occupies the northeastern half of the Roebuck Basin. The depocentre was previously known as the 'offshore' Fitzroy Trough, and is now called the Oobagooma Sub-basin (Hocking et al., 1994). The

name change was implemented to reflect the increased thickness of Mesozoic deposition that occurred in the present day offshore area in contrast to the present day onshore. During the Palaeozoic, development of the Fitzroy Trough occurred over both the onshore and offshore areas.

The sub-basin is approximately 190 km in length and 100 km in width, and contains approximately 5.5 km (3 s TWT) of Palaeozoic section and 4.5 km (2.7 s TWT) of Mesozoic and Cainozoic sediments. The sub-basin is bound to the NE by the Leveque Platform and to the SW by the Broome Platform. The northern and southern limits of the sub-basin have been controlled by different elements throughout time. During the Palaeozoic, the area existed as the offshore extension of the Fitzroy Trough, with the southeastern limit occurring in the Canning Basin (landward of the study area). During this time, the northwestern limit was partially controlled by a newly identified feature termed the Oobagooma High. During the Mesozoic to Present, the northwestern limit of the sub-basin has been defined by an arbitrary line along the Oobagooma High that divides it from the Rowley Sub-basin. This subdivision is geographically based on the older Palaeozoic structure rather than a geomorphological divide during the Mesozoic. To the south, the division between the 'onshore' Canning Basin (Fitzroy Trough) and the Oobagooma Sub-basin has been defined at the onlap extent of the Middle Jurassic sequence onto the older Palaeozoic section which had undergone major Late Permian uplift during the Bedout Movement.

The Oobagooma Sub-basin is believed to have formed initially in the Ordovician during early intra-cratonic extension as part of the Fitzroy Trough. Development of the Fitzroy Trough occurred up until the Late Permian, with the majority of fill being deposited during repeated periods of rejuvenation from the Late Devonian to Late Permian (Brown et al., 1984, Veevers, 1988).

Onshore, the structural development of the Fitzroy Trough has been described by Drummond et al. (1988, 1991), who believe that subsidence occurred on a NW-SE trending series of half-grabens which formed along the northeastern margin of the Canning Basin. Drummond et al., (1991) describe the trough as structurally asymmetric, with the northeastern margin acting as hinge and the southwestern margin faulted down on a shallow dipping detachment identified as the Fenton Fault. Colwell & Stagg (1994) suggested that in its offshore extremities the trough does not show asymmetry and does not appear to be the product of classic half-graben extension as suggested by Drummond et al. (1991). They believe that the trough results from SW and NE dipping detachment surfaces interpreted on deep seismic data. During this study indications of detachment surfaces were only observed in the outer part of the basin as the trough opens up around the Broome Platform – an old Ordovician high that bounds the troughs SW margin. However, in the southern part of the study area where the trough is only 100 km wide it is bound by a series of well-developed normal faults on both margins (Appendix 1 A1.6 between 270 to 360 km). Combining the observations from both the onshore and offshore areas, it is suggested that the style of faulting is complex along the margin and changes from asymmetrical half-graben extension onshore to symmetrical graben extension in the near offshore to thin-skinned detachment in the outer offshore area. The style of extension appears to be controlled by the location of the more rigid elements of the basin, with normal faults developing near the stable bounding Kimberley Craton and Leveque Platform to the NE and the Broome Platform to the SW. The width of the fracture zone also appears important, with narrow sections of the trough developing as a result of graben formation.

A distinct change in orientation from NW-SE to N-S occurs in the Palaeozoic section of the sub-basins at around 17° S. Orthogonal to the major rift orientation a weakly developed arm also extends to the WSW forming a small triple junction (Appendix 2 Fig. A2.1). The change in orientation is marked the Oobagooma High which

is fault bound on its southern flank and dips to the north (Appendix 1 Fig. A1.5 between 415 to 445 km and Fig. A1.8 between 110 and 145 km). Very little pre-Devonian extension sedimentation is seen to the northwest of this feature and sedimentation is believed to have been restricted to the N-S trending arm next to the Leveque Platform. The northern extent of the N-S arm occurs outside of seismic coverage.

2.6.2.3.3 Bedout Sub-basin

The Bedout Sub-basin consists of an ENE-WSW trending depocentre that occupies an area of approximately 38,000 km^2. In its thickest section the sub-basin contains approximately 2.5 km (1.4 s TWT) of Palaeozoic sediments and 6.9 km (7 s TWT) of Mesozoic section. Palaeozoic sediments are believed to have been deposited under NE-SW and NNW-SSE intra-cratonic extension before the development of a major Mesozoic depocentre which formed in response to rapid regional sag. The Mesozoic sequence gradually thins in an easterly direction and progressively onlaps the Late Permian unconformity that divides the Mesozoic section from the Palaeozoic section (Appendix 1 Fig. A1.2 between 340 and 480 km and Fig. A1.7). To date, four wells have been drilled in the sub-basin, and the oldest rocks penetrated are Middle Triassic.

The sub-basin's southern margin is defined by the Lambert Shelf and the offshore extensions of the Willara Sub-basin and Samphire Graben. To the west, the Bedout Sub-basin is separated from the Beagle Sub-basin by the North Turtle Hinge Zone. To the north, it is separated from the Rowley Sub-basin by the Bedout High, and to the east it is separated from the Oobagooma Sub-basin by the Broome Platform.

The most striking structural feature of the sub-basin is a strong well-developed detachment surface that can be seen dipping in a northwesterly direction below the western half of the sub-basin (Appendix 1 A1.4 between 0 to 80 km at 7 s TWT). Overlying the detachment are a series of high angle 'bookshelf' style faults that step down into the Beagle Sub-basin. Structural movement on the detachment is interpreted to have occurred during a series of multi-phase rift episodes. Faulting can be observed up to the *C13-1* event. Structuring becomes more subdued in the eastern Bedout Sub-basin and is predominantly restricted to the Palaeozoic section.

2.6.2.3.4 Rowley Sub-basin

The Rowley Sub-basin is situated on the outer margin and is the major depocentre of the Roebuck Basin, occupying an area of some 85,000 km^2. Only one well has been drilled in this sub-basin, terminating in Lower Jurassic sediments below 4,000 m. The Rowley Sub-basin is separated from the Beagle Sub-basin to the southwest by the outer North Turtle Hinge Zone, from the Bedout Sub-basin by the Bedout High; from the Oobagooma Sub-basin to the southeast by the Oobagooma High, and from the Browse Basin to the northeast by the Leveque Platform and Leveque Ridge. The northwestern boundary is delineated by the present continental slope.

The Rowley Sub-basin has previously been divided into an inner and outer section based on the interpretation of the continuation of the Rankin Trend through the Roebuck Basin area (Colwell and Stagg, 1994). Due to lack of seismic data over the outer part of the basin the correlation of a structural feature similar to the Rankin Trend is difficult to access. Anticlinal features are best seen in Fig A1.2 and Fig. A1.3 (Appendix 1), but major horst and graben style features seen at the continent ocean boundary on Fig. A1.3 could also represent the extension of such trends into the Roebuck area.

Major accommodation generation in the basin is interpreted to have formed in response to post Carboniferous, NNW-SSE extension during both transitional and Westralian phases. Sediments consist of a seaward thickening wedge of both Palaeozoic and Early Mesozoic sequence which are terminated at the current continent-ocean-boundary by massive down-to-the-north faults. An Early Jurassic unconformity forms the upper

surface of the wedge, which is overlain by a prograding clastic system of Lower to Middle Jurassic sediments. Late Jurassic to Late Cretaceous sediments grade into thick Late Cretaceous to Recent prograding carbonates (Appendix 1 Fig. A1.2). Up to 9 km (5 s TWT) of Palaeozoic section and 6 km (4 s TWT) of Mesozoic to Recent section has been deposited in the Rowley Sub-basin.

Structuring in the sub-basin is generally mild except for intense 'book-shelf' faulting of sediments located above a major detachment which extends from the Bedout Sub-basin into the Rowley Sub-basin. Tertiary sediments are generally undisturbed throughout the area.

2.6.2.4 Major Intra-basinal Highs

2.6.2.4.1 Broome Platform

The Broome Platform consists of a WNW trending, largely unfaulted, intra-basin basement high which extends both onshore and offshore (Colwell & Stagg, 1994). Offshore the platform acts to separate the Oobagooma Sub-basin to the northeast from the Willara and Bedout Sub-basins to the southwest (Appendix 1 Fig. A1.6 between 100 to 260 km). The NW flank of the platform is over-printed by northeast oriented fault trends developed during Westralian Superbasin extension (Colwell & Stagg, 1994). Correlation with onshore wells suggest that the Broome Platform consists of Ordovician and Permian sediments that dip to the southwest below the Mesozoic Bedout Sub-basin (Lipski, 1993, 1994).

To the north of this feature a distinct change in orientation of major faulting can be observed. Small E-W striking, asymmetric half-graben troughs are interpreted to have developed during Late Carboniferous to Late Permian NNE extension. They are hinged at the south and faulted along their northern margins and can be seen in Fig. A1.3 between 240 to 280 km (Appendix 1). Features interpreted at the NW end of Fig. A1.3 are highly speculative.

2.6.2.4.2 Oobagooma High

The Oobagooma High is a newly identified 25 km wide elongate feature that has currently been mapped for 70 km in a north-south orientation. The high has approximately 3 km (2 s TWT) relief and separates the Oobagooma Sub-basin from the Rowley Sub-basin at the Palaeozoic level. This feature consists of an asymmetric northeastward dipping structure which is fault bound on its southern flank (Appendix 1 Fig. A1.8 between 110 and 145 km and Fig. 2.14).

An examination of the Basement TWT structure map (Appendix 2 Fig. A2.1) shows that this feature is developed from the Oobagooma Sub-basin across the front of the Broome Platform and to the Bedout High. The structural mechanism of formation for this feature and the Bedout High are probably similar and to reflect their close association, it has been informally termed the Oobagooma High during this study. The exact timing of formation of each structure is difficult to constrain but it appears that the Oobagooma High formed before the Bedout High.

The Bedout High appears to have first developed during the Early to Middle Carboniferous, when sediments of that age are observed to onlap the feature. The structure appears to have also been reactivated during major tectonic events throughout the Late Carboniferous to Late Permian. However, major erosion at the Late Permian event and lack of seismic data prevents the delineation of any finer tectonic history for the structure.

Two earlier observations support the identification of this structural trend:

- of primary significance is the identification of a large N-S trending magnetic anomaly that is located in the same position and with the same orientation as the southern portion of the Oobagooma High. This anomaly was first identified by JNOC during their 1987 study, however, due to the poor quality of the seismic data, the association of this anomaly

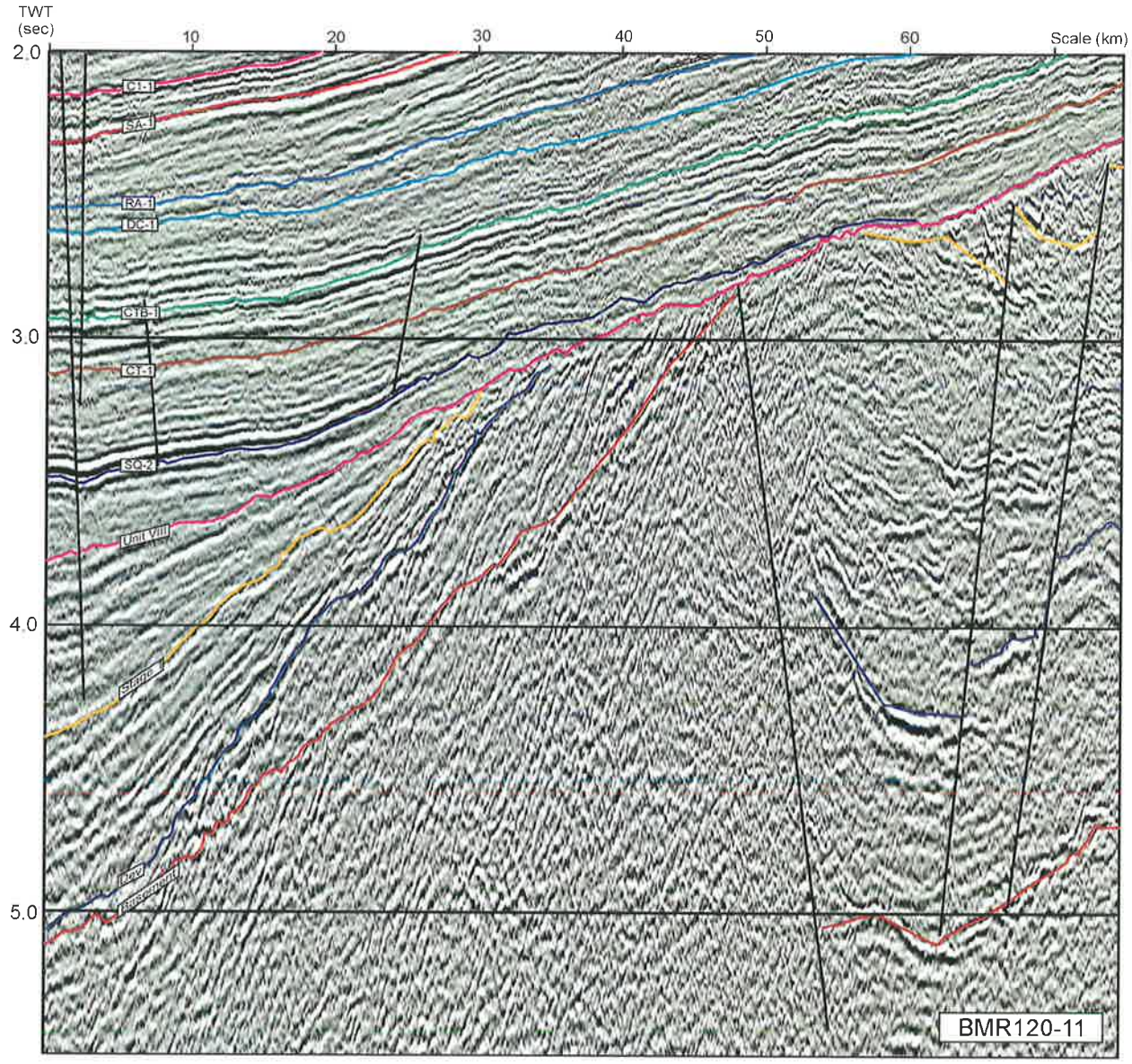

Figure 2.14 Close-up of the Oobagooma High.

to the seismic feature was never made and consequently the trend was not mapped across the basin.

- The AGSO study group (1994) have speculated that a major basin forming trend (their North West Shelf Mega-shear) runs through the Roebuck Basin. Although speculatively placed (pers. com. Howard Stagg, AGSO August 1997), AGSO's initial trend corresponds well with this new feature.

The AGSO regional deep seismic data set images the feature well (Appendix 1 Fig. A1.8 between 110 and 145 km and Fig. A1.5 between 415 and 450 km). Internally the feature consists of chaotic, high angle reflectors which when combined with the presence of a magnetic anomaly and structural association with the Bedout High suggest that the feature is highly intruded. However, several inversion features that have been interpreted as salt-related have been identified in the Oobagooma Sub-basin (Appendix 1 Fig. A1.10) and the Oobagooma High may also be a partially salt controlled feature.

2.6.2.4.3 Bedout High

The Bedout High separates the Bedout Sub-basin in the south from the Rowley Sub-basin in the north. It is a deep Palaeozoic, faulted structure that formed during the Bedout Movement in the

Late Permian (Appendix 1 Fig. A1.2 between 290 to 340 km and Fig. A1.4 between 150 to 200 km). Both Late Carboniferous and Early Permian sediments have been uplifted and peneplained during the growth of the structure, resulting in 6 km of relief in the north to 2 km to the south above the surrounding major basin depocentre lows (Appendix 2 Fig. A2.3 and A2.4). The feature is overlain by approximately 3 km (2 s TWT) of Mesozoic compaction and drape which onlap in halo fashion from all directions.

Geographically, the Bedout High is separated from the Broome Platform by a 70 km wide corridor which joins the Bedout Sub-basin to the Rowley Sub-basin (Appendix 1 Fig. A1.4 between 200 to 270 km). The high has previously been mapped (JNOC 1987) and described as a large 40 by 50 km equi-dimensional inverted structure. However the feature appears to be more reminiscent in shape of a triangle with apices to the SSE, NE and WSW (Appendix 2 Fig. A2.3 and Appendix 4 A4.2). Mapping during this study reveals that the feature is compartmentalized into two main sections, a smaller 20 by 20 km western high and a larger 40 by 40 km eastern high (Fig. 2.15). The two compartments are separated by a 10 km wide N-S trending half-graben which is faulted down along its western margin (Appendix 1 Fig. A1.4). The eastern larger compartment stands structurally higher than the western compartment by some 500 m (400 ms TWT).

The Bedout High was first discovered in the late 1960's when, prior to drilling, seismic interpretation suggested that a major horst feature similar to those found along the Rankin Trend extended into the Roebuck Basin (Horstman & Purcell, 1988). In 1971, Bedout-1 was drilled to test the potential of the high as a large horst style structure, but after penetrating 52 m of igneous rock, drilling was terminated. The igneous rocks were quite weathered, but interpreted to be intrusive, probably a sill intruding into Middle to Upper Triassic sediments. The potential of the Bedout High below the sill was therefore still considered to be untested, and additional seismic was acquired over the feature (Lipski, 1993). The

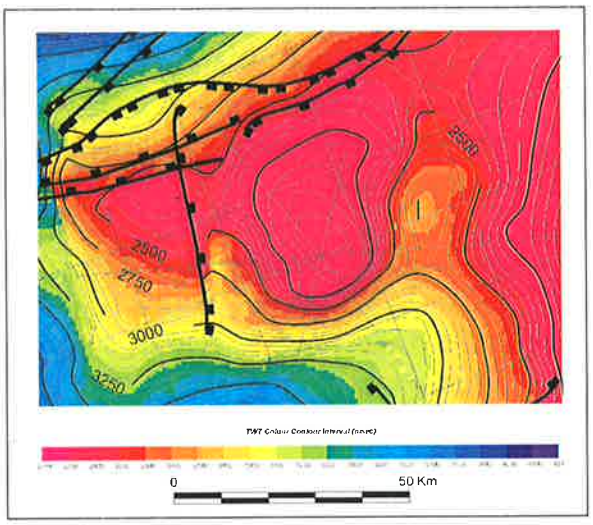

Figure 2.15 Close-up of the Bedout High showing the shape and compartmentalization of the feature.

fact that seismic interval velocities over the structure did not correspond to the typical signature of an igneous intrusion, led the BP consortium to drill Lagrange-1 on the crest of Bedout High in 1982 (BP, 1982). The objectives were Triassic sandstones below an apparently thin igneous sill, however, the well was terminated after penetrating 391 m of igneous rocks. The petrographic analysis of these rocks indicated that they were generally highly weathered basalt flows. K/Ar dating of one basalt sample from Lagrange-1 was found to have a minimum age of 253+/-5 Ma (BP, 1982). Lithological observation and sonic log analysis indicated that individual flows had experienced variable levels of weathering and exhibited anomalously high porosity. For this reason the Bedout High appears to be sedimentary in nature on seismic data (Lipski, 1994).

Formation of both the Bedout and Oobagooma Highs are discussed further in Section 2.7.2.

2.7 Discussion

2.7.1 Structural Style and Implications for Basin Development

Observations made during this study suggest that the basins that make up the North West Shelf can broadly be sub-divided into two groups based on their age, locations and mechanisms of formation:

- the Roebuck, Bonaparte and Southern Carnarvon Basins, which formed as part of or adjacent to major Palaeozoic intra-cratonic rifts which underwent later Mesozoic NNW extension; and,

- the Northern Carnarvon and Browse Basins which formed adjacent to rigid crustal blocks (the Kimberley and Pilbara) during Mesozoic NNW extension.

The processes which have led to the development of the Roebuck Basin have strongly controlled the distribution of petroleum play elements within the basin. Here, the structural development of the basin has been described in terms of major crustal rift processes of which there are three main models:

- pure shear models in which stretching of the crust and lithosphere is uniform and symmetrical (e.g. McKenzie, 1978).

- simple shear models which employ low angle detachments which cut through the crust and lithosphere resulting in asymmetric upper and lower plate geometries (e.g. Wernicke, 1985; Lister et al. 1986).

- flexural cantilever models which combine both pure shear and simple shear processes at different depths (e.g. Kusznir et al., 1991).

Examination of regional cross-sections (Appendix 1) reveals that the Roebuck Basin is only strongly structured during the development of the Oobagooma Sub-basin and Willara and Samphire Grabens, whereas, only gentle structuring of the Mesozoic fill is evident. In particular, the lack of large rotated fault blocks and isolated depocentres, which characterize other North West Shelf basins and the general absence of crustal structuring on deep seismic make it difficult to choose an overall extensional model for the late formation of the basin.

In the Roebuck Basin both NE and NNW extensional stress structures are evident. During Palaeozoic NE extension at least three basin-forming structural styles were identified along the margins of the Oobagooma Sub-basin including: asymmetric half-graben development in the present day onshore area, symmetrical graben development in the nearshore area and thin-skinned detachment in the offshore area (see Section 2.6.2.3.2). Models developed to explain the manner in which the transition between adjacent rift segments occur fall into two broad categories; hard-link basement involved models where transition occurs across narrow transfer zones consisting of sub-vertical strike-slip faults (Gibbs, 1984), and soft-linked basement detached models where transition occurs over a broad zone of ramp and flat features. The changes in structural style observed in the study area have been used to subdivide the Oobagooma Sub-basin/Fitzroy Trough into three structural compartments. Insufficient data currently exists to accurately define the location of each compartment, however, approximations can be made as to their location and rift style (Fig. 2.16). Similar compartmentalisation has been observed in the Petrel Sub-basin to the NE (O'Brien et al. (1996), which also formed in response to intra-cratonic rifting of the North West Shelf during or slightly before the formation of the Canning Basin.

Present day onshore half-graben structures are separated from offshore graben features by a hard-link (vertical basement-related transfer faults which take-up differential movement between each compartment) which extends from the NW extent of the Jurgurra Terrace to the western tip of the Pender Terrace. The shape and location relative to the Kimberley Block of the onshore compartment mirrors the Barnett Compartment described in the Petrel Sub-basin by O'Brien et al. (1996). Further offshore, the basin has been sub-divided by another hard-link which divides the Oobagooma Sub-basin from the Rowley Sub-basin, and is marked by a reduction in faulting on the margins basinward of the Broome and Leveque Platforms. This hard-link is believed to accommodate major differential movement during NE Palaeozoic intra-cratonic extension and to have controlled the formation of the Bedout and

Oobagooma Highs. This structural trend is discussed in more detail in Section 2.7.2.

Each compartment displays evidence for differing rift processes. Although not assessed in detail during this study, Drummond et al.'s (1988) structural interpretation of the onshore area suggests that a combination of asymmetrical simple shear, plus deeper (unimaged) pure shear has taken place onshore (similar to the Kusznir et al. (1991) 'flexural-cantilever' model). In the near offshore compartment symmetrical simple shear plus deeper unimaged pure shear is interpreted (analogue to a mixture of McKenzie (1978) and Kusznir et al. (1991) type models. Finally, the far offshore compartment is interpreted to have undergone rifting on shallow asymmetric detachments (similar to a Wernicke (1985) type model).

From the above description it appears that the intra-cratonic rift style in the Roebuck Basin area is complex and that changes in structural style in each compartment will strongly affect the hydrocarbon potential in each area. Palaeozoic hydrocarbon trapping configurations can be expected to alter in each compartment and distribution of source rocks during Palaeozoic NE extension are most likely restricted to the deeper depocentres. Structural indications from the Oobagooma Sub-basin suggest that in the nearshore and onshore area, half-graben development along the NE margin of the sub-basin may offer more favourable restricted conditions for source rock preservation. The NE margin of the Oobagooma Sub-basin represents the most prospective Palaeozoic play fairway for this reason. Structuring in the offshore area becomes more subtle and development of restricted depocentres less likely, down-grading prospective in terms of source potential resulting from NE extension.

The second phase of extension, the transition of from NE intra-cratonic to NNW Westralian extension during the Carboniferous to Late Permian, is marked by the development of gentle thermal sag throughout the study area probably

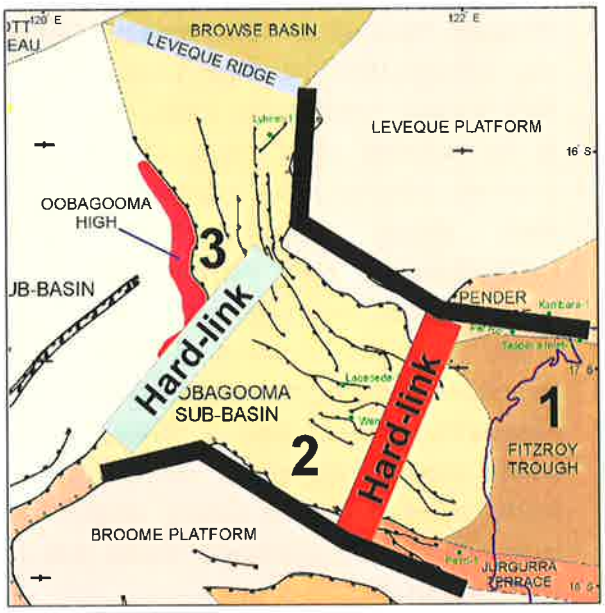

Figure 2.16 Hard and softlink locations and compartmentalization in the Oobagooma Sub-basin.

due to lower crustal thinning. However, some evidence of upper crustal simple shear (i.e. extensional faulting) does exist on seismic profiles over the eastern Rowley Sub-basin where half-graben development can be observed (Appendix 1 Fig. A1.3). Similar features have been observed in the adjacent Browse Basin by Struckmeyer et al. (1998) and may represent the continuation of these features across both basins, although lack of seismic data makes this assumption difficult to confirm.

Renewed NNW extension in the Triassic and Jurassic led to the development of two major structural provinces in the Roebuck Basin; 'book-shelf' faulting on a major detachment system to the west and another to the east with relatively gentle structuring. However, faulting is not interpreted to have contributed significantly to upper crustal extension due to its sub-vertical nature. Lack of data on the outer margin makes it impossible to say whether the difference in these structural styles is controlled by hard-link compartmentalization, or whether upper plate/lower plate geometries have switched in this area.

Based on the differences in structural observations in the adjacent basins by Symonds et al. (1994) (Browse), Struckmeyer et al. (1998)

(Browse), Blevin et al. (1994) (Beagle) and Stagg and Colwell (1994) (Northern Carnarvon), major large-scale accommodation zones are interpreted to lie between each basin. In the Browse, extension occurred in two episodes but under one main stress regime, NNW extension. Carboniferous to Early Permian extension was accommodated on large-scale upper crustal simple shear normal faults which compartmentalized the basin into distinct depocentres. Reactivation of these Palaeozoic trends occurred during the Jurassic as upper crustal simple shear on several smaller scale faults and as lower crust/upper mantle pure shear producing an element of sag.

The Northern Carnarvon Basin is interpreted to have formed in response to major lower crustal/upper mantle thinning through pure shear processes. Little evidence for upper crustal extension is evident in the basin (similar to the Roebuck Basin) except along the Rankin Fault System (Stagg and Colwell, 1994). Upper crustal extension is interpreted to have occurred in the conjugate passive margin that rifted away at break-up. The Rankin Fault System consists of a failed simple shear rift system that formed landward of the Rankin Platform and Alpha Arch. This fault system has been important in controlling the distribution of Mesozoic depocentres in the Northern Carnarvon Basin. In the Beagle Sub-basin this system is terminated to the NE by a series of NNE oriented wrenched fault blocks which form an accommodation zone that transferred rifting stresses along the outer margin of the Roebuck Basin. The trend is therefore very subdued in the study area.

Large scale differences in structure between the Roebuck Basin and its adjacent basins such as the absence of large Jurassic rotated fault blocks suggest that either the crustal composition or stress regime was different in this area. One difference is that the Roebuck Basin has undergone NE extension prior to NNW extension. It is possible that this initial rift has altered the crustal composition. Heating followed by cooling may have annealed the upper crust making it stronger and less likely to deform (a process called strain hardening by Kusznir and Park (1987)). Strain hardening has also potentially occurred in the Petrel and Southern Carnarvon Basins which have also undergone multiple rift phases like the Roebuck Basin.

It is difficult to form a conclusive model that explains the mechanism controlling NNW extension. It appears, however, that deep thinning at the base of the crust/upper mantle occurred through pure shear mechanisms which have thinned the crust to the point of complete failure at the present day continental-ocean boundary. Crustal extension is expressed in the upper crust as mild reactivation on a number of older Palaeozoic detachments formed to accommodate differential movement during NE extension (best seen at the Bedout High (Appendix 1 Fig. A1.2)). Ocean bottom refraction profiling indicates that crustal thickness thin towards the outer margin from 15 to 5 km thick (Bradshaw et al., 1998), supporting the above conclusion.

In the Roebuck Basin evidence for detachment reactivation also occurs below the Rankin Trend continuation suggesting that a series of high angle simple shears were reactivated along zones of pre-existing Palaeozoic deformation. A schematic showing the potential rift structuring of the basin after NNW-SSE extension, based on the concepts of the flexural cantilever model is presented in Fig. 2.17.

Although NNW extension related compartmentalization is less obvious across the Roebuck Basin, several general conclusions regarding petroleum potential can be made. The formation of a restricted depocentre is more likely closer to the rift axis in the rapidly sagging Rowley Sub-basin. Source rock potential is interpreted to improve towards the N and be unfavourable in the nearshore area where deposits have been reworked.

2.7.2 Nature and Development of the Bedout and Oobagooma Highs

Three main development scenarios for the Bedout High have been suggested by previous workers:-

- Lipski (1994) suggested that the feature consisted of a pre-Triassic fault bound high, capped by extruded volcanics which formed a large volcanic island situated over a mantle hotspot.

- More recent examination of deep seismic data has led Colwell & Stagg (1994) to interpret the high as consisting of a faulted core of 'basement' rocks, overlain by a sequence of Carboniferous or older Palaeozoic to Permian sediments. The high is interpreted to be underlain by major upwelling of the lower crust and is topped by extrusive volcanics which form an eroded anticline. Colwell & Stagg (1994) suggest that the mechanism of formation of the core may be partially thrust controlled.

- Gorter (1996) speculated that the Bedout High was the uplifted core of a circular feature, formed by the impact of a large extraterrestrial body with the earth near the end of the Permian.

These three hypotheses, although different, all appear to describe valid tectonic mechanisms for the formation of the Bedout High that would result

A) Flexural Cantilever Model (From Kusznir et al., 1991)

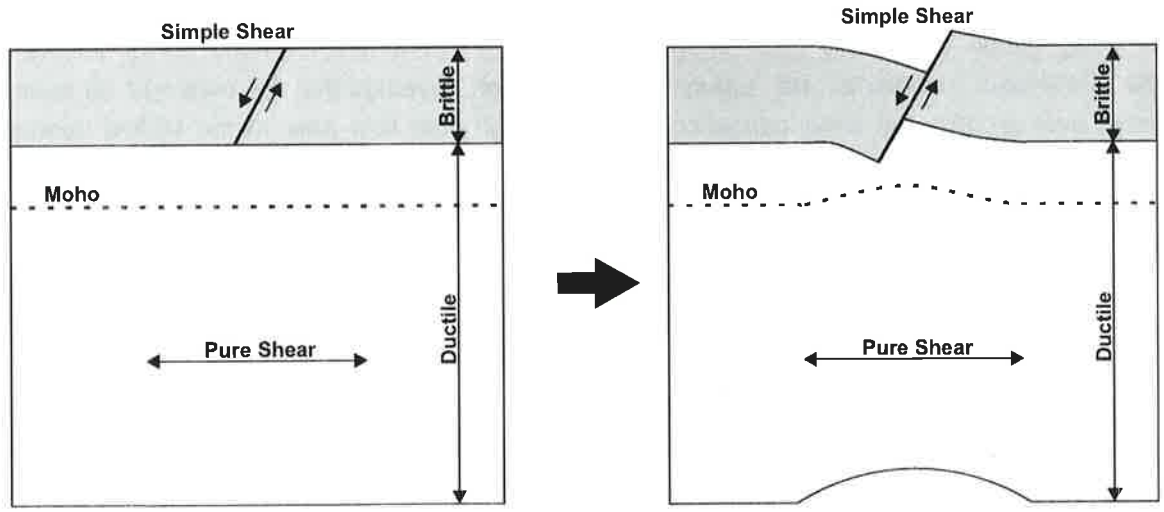

B) Simple rift model for Westralian extension in the Roebuck Basin (not to scale)

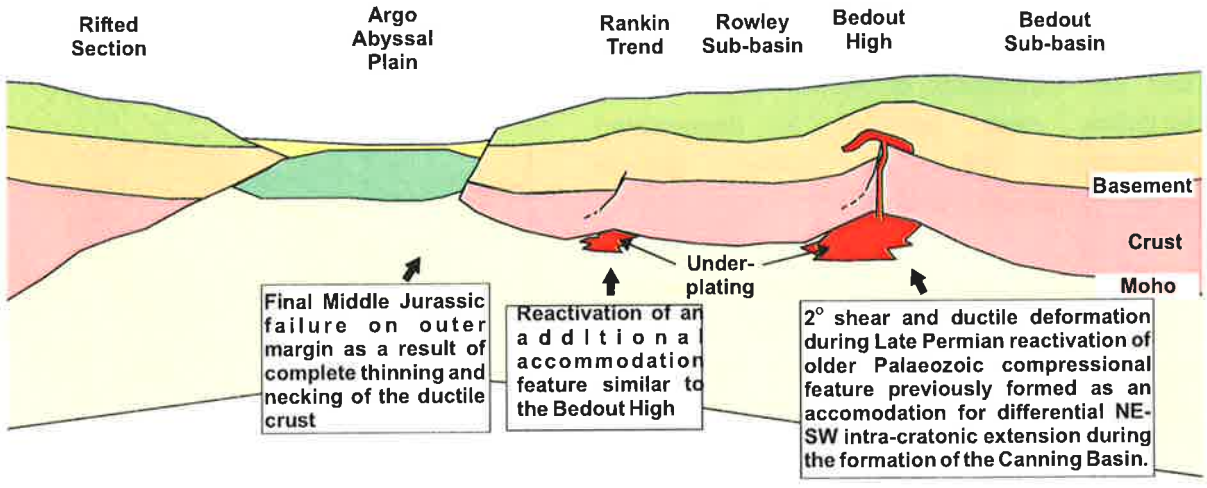

Figure 2.17 Rift geometries in the Roebuck Basin (a) the flexural cantilever model of Kusznir et al. (1991) compared to (b) a schematic of the deep structure of the Roebuck Basin.

in the currently observed features. Conclusions from this study support the concepts presented by Lipski (1994) and Colwell & Stagg (1994) to a greater extent than the astrobleme hypothesis of Gorter (1996). However, a more detailed evaluation of the feature that addresses spatial shape, structure and regional setting suggests a more complex formation mechanism than previously presented.

The Bedout High consists of a triangular to linear feature that is oriented ENE-WSW (Fig. 2.15). In addition to outline shape the structural style of the northern and southern bounding fault systems appears to change in nature from east to west along the feature. To the east, over the larger of the two compartments, deep seismic data crosses both the northern and southern flanks of the high. Here only minor faults have been imaged and older Paleozoic sediments are upturned and eroded over an upwelled lower crustal core. The northern flank of the Bedout High is underlain by a northwestward dipping detachment which can be imaged down to 12 s TWT. This detachment can be mapped areally from its Permian surface expression at the Bedout High in a northwestward direction where it plunges under the western Rowley Sub-basin (Fig. 2.18). A series of antithetic faults have developed along the northern margin of the Bedout High to this major basin detachment. The magnitude of throw on both the basin detachment and its associated antithetic fault system is not significant enough to explain the degree of uplift seen at the Bedout High. However, the identification of this major detachment does suggest that the Bedout High was an expression of major basin forming tectonics, most probably a deep-seated detachment with an earlier tectonic history/compressional origin.

In contrast, to the west, towards the smaller compartment, although not imaged with deep seismic data, the high becomes clearly fault controlled especially along its southern margin, by a series of down-to-the-south normal faults with a throw of approximately 2 s TWT (Fig. 2.19).

The two different styles of extension have resulted in the shape seen today. The smaller compartment of the Bedout High consists of a narrow more focused high with faulted margins that converge towards an apex in the WNW, and appears to have been formed by brittle failure of the upper crust above upwelling lower crust. The larger compartment consists of uplifted and warped sediments again over a lower crustal upwelling, but appears to be more diapiric in nature. The crest of the structure has been peneplained during uplift and less faulting is evident due to regional flexure of the upper crust. The volcanic cap appears to have been extruded after sediment deformation and erosional truncation.

Geohistory and thermal maturity analysis (Section 5.4), conducted for wells drilled on the Bedout High, revealed that the area had an anomalously high heat flow prior to the Middle Jurassic. The Bedout High can probably be seen as a long term thermally active area. Differential compaction and drape across the feature from Middle Jurassic have accentuated the structure to the present day

During regional mapping of the Bedout High subtle disturbances in sedimentation were observed trending from the tip of the high towards the east (Fig. 2.20). After careful mapping these features could be correlated to the Oobagooma High forming a structural lineament across the Roebuck Basin, effectively marking the hinge line

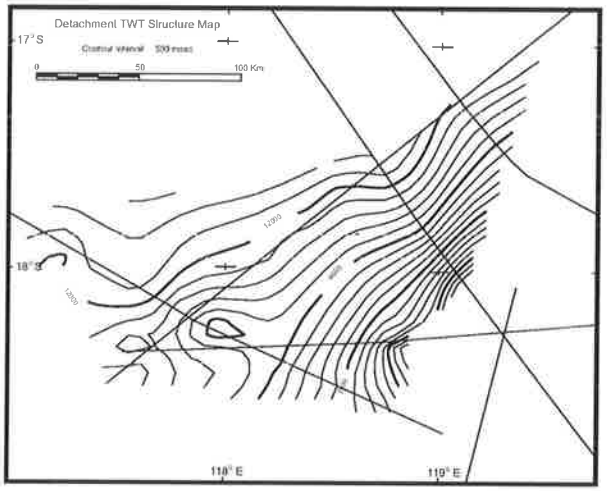

Figure 2.18 TWT structure map of the major detachment over the western half of the Bedout and Rowley Sub-basins.

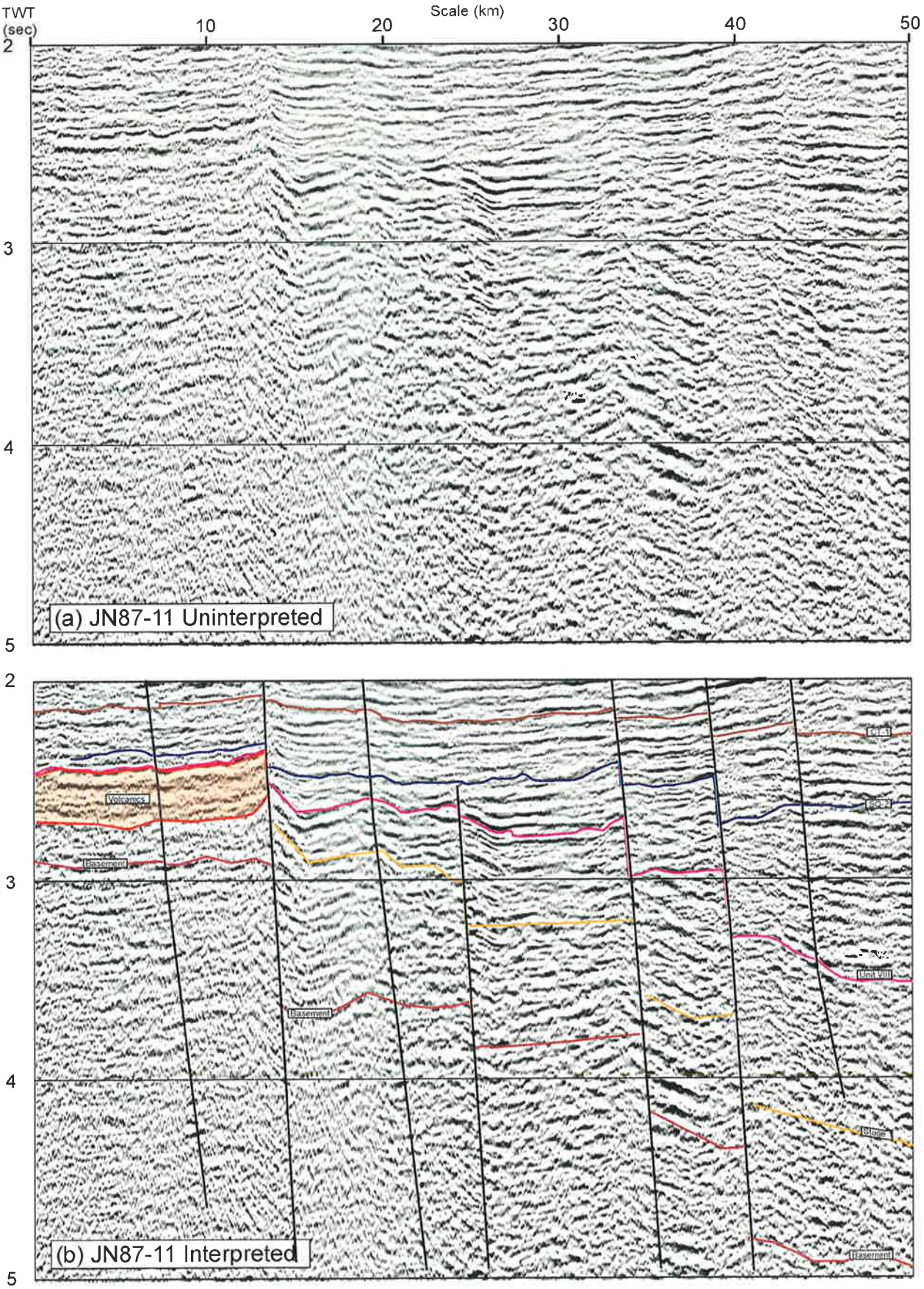

Figure 2.19 Southern flank of the smaller compartment of the Bedout High showing distinct down to the south faulting.

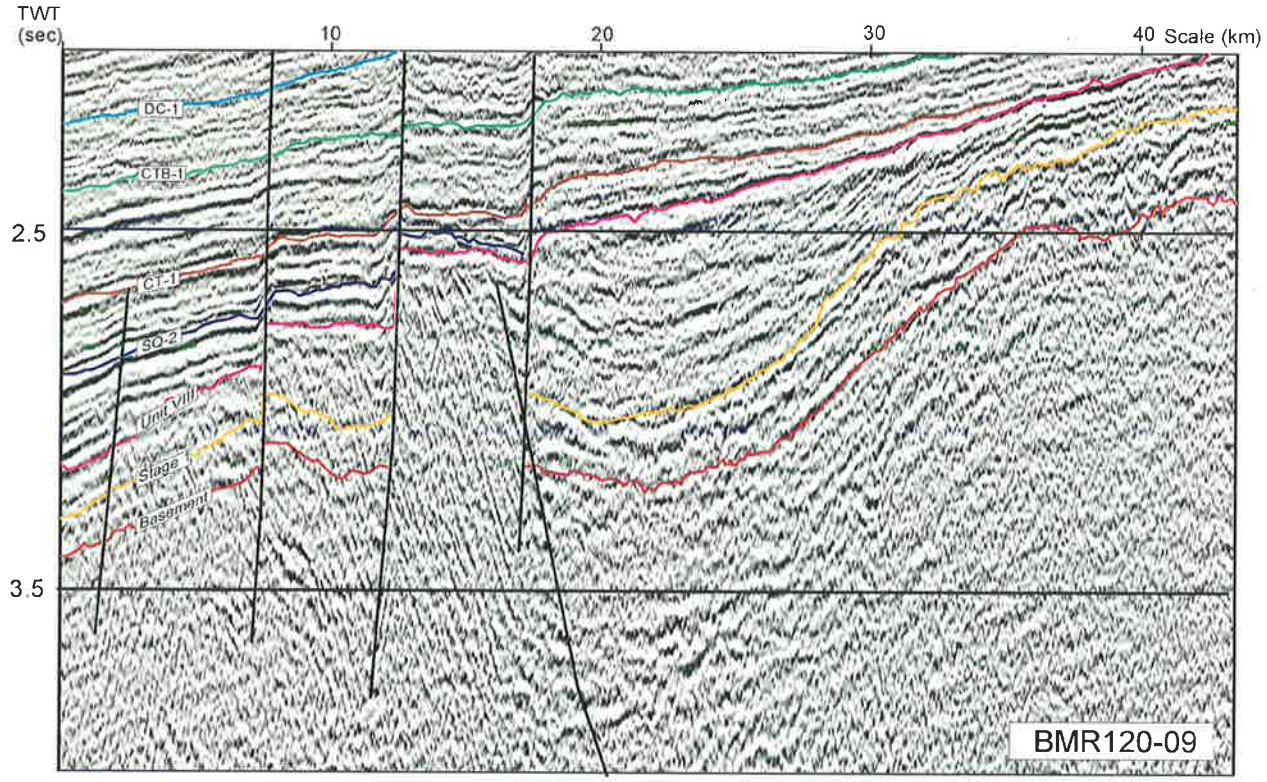

Figure 2.20 Example of structuring along the 'mega-shear' feature that runs between the Bedout and Oobagooma Highs.

between the Oobagooma and Bedout Sub-basins with the Rowley Sub-basin and terminating older NW-SE trending Palaeozoic structures of the onshore Canning Basin.

Although the Oobagooma High is believed to have initially formed earlier than the Bedout High, both features are interpreted to have formed over a shelf-wide accommodation zone developed due to differential NE oriented, Palaeozoic intra-cratonic extension (the North West Shelf Mega-shear of AGSO (1994)). Both features appear to lie in areas of major charge in orientation of this mega-shear, the Oobagooma High at transition from inner Rowley Sub-basin to outer Browse Basin and the Bedout High at inner Rowley Sub-basin to inboard Beagle Sub-basin. These zones represent areas of transpression along the mega-shear.

Based on observations at the Bedout High it appears that minor reactivation has occurred on the Palaeozoic detachment system during Mesozoic NNW extension. Deep crustal reflector patterns also suggests that crustal thinning has occurred below the Bedout High, through pure shear removal of the lower crust and through simple shear mechanisms (reactivation of the deep-seated Palaeozoic detachment). Removal of the lower crust has led to a raising of the lithospheric/asthenospheric boundary and an increased thermal gradient resulting in underplating and localized volcanism. Reactivation of the detachment system will have provided conduits for magma flow to the surface.

Evidence for underplating is suggested from basaltic rocks encountered in Lagrange-1 and Bedout-1. Thin section examination conducted by JNOC (1988) indicated that cuttings from Lagrange-1 were augite andesite or basaltic andesite showing intergranular textures. Andesitic basalts are commonly associated with the extension of continental land masses.

In summary, the Oobagooma and Bedout Highs are interpreted as localized surface expressions formed at major lateral reorientations of major Palaeozoic crustal blocks oblique to and accommodating differential movement during NE extension. The Bedout High has subsequently been reactivated during Mesozoic NNW Westralian related extension.

CHAPTER 3

CHRONOSTRATIGRAPHY

"But, when the twelvemonth passed away,
Jack found his goddess made of clay;
Found half the charms that decked her face
Arose from powder, shreds or lace;
But still the worst remained behind,
That very face had robbed her mind."

The Double Transformation
Oliver Goldsmith (1730-74)

3.1 Introduction

There are no published chronostratigraphic schemes based on modern sequence and seismic stratigraphic techniques for the Roebuck Basin. A coarse lithostratigraphy exists (the best is probably detailed in Colwell and Stagg (1994)) but it is incomplete, has picks based on diachronous boundaries and has a misleading nomenclature when compared to other basins on the North West Shelf. Some form of high resolution stratigraphy is useful; in basin-analysis it allows highly detailed correlations of sedimentation controlled by relative sea-level throughout the basin, and in its' more developed stage, is a powerful tool for predicting facies distribution. The sequence stratigraphic sub-division presented here forms the foundation for the other basin-analysis techniques undertaken during this study and was picked on the basis of wire-line log interpretation and seismic correlation.

3.2 Basic Sequence Stratigraphic Concepts

The initial techniques of sequence stratigraphy were first developed by Exxon during the 1970's and 1980's. The first major publication occurred in 1977 with the release of AAPG Memoir 26 (Mitchum, 1977) based on seismic stratigraphy. These early concepts were consolidated into what is known as the "Exxon model" in SEPM Special Publication 42 (Wilgus et al., 1988). The model has been refined since 1988 and other sequence stratigraphies have been defined (Hubbard et al., 1985, Galloway, 1989, Embry, 1995). These models all use the same stratal surfaces and genetically related sediment packages, but assign differing emphasis to each surface.

Sequence stratigraphy is not without its skeptics and the past decade has seen a heated literary debate concerning the validity of certain stratigraphic concepts, especially the forcing mechanisms (Miall, 1986, 1992; Hubbard, 1988). However, the basic observations that are made using the method are less controversial and have been widely accepted in the geoscience community.

It is not the intention here to describe in detail the sequence stratigraphic model. Instead, a brief discussion of how the method was applied during this study and how some modifications were made to adapt the method for use in the upper carbonate rich section of the Roebuck Basin are presented.

Basins can be considered to be filled by a series of sedimentation cycles that result from shoreline transgression and regression (T-R cycles). Transgression and regression can result from a number of forcing mechanisms, including eustasy, tectonics and sediment supply. For a good

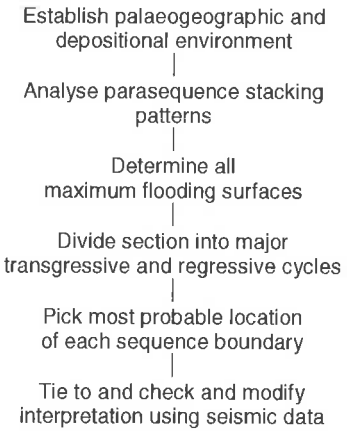

Figure 3.1 Approach taken during identification and selection of major stratal surfaces during stratigraphic interpretation.

description of the possible interactions between these forcing components see Posamentier et al. (1992). Correlation of major T-R cycles across the basin can be used to stratigraphically divide the section.

T-R cycles occur at variety of scales. On wire-line logs the smallest readily identifiable unit is the parasequence which is usually a coarsening-upward unit, the top of which is marked by a more local flooding event and an increase in accommodation space (Van Wagoner et al., 1988). Parasequence formation can result from either autocyclic processes related to sedimentation, such as lobe switching, or allocyclic processes external to sedimentation, such as tectonics and eustasy.

Parasequences stack into larger scale T-R cycles that are related to longer term variations in relative sea-level. These are often 10's to 100's of metres thick. These larger scale T-R cycles are divided by two surfaces; the maximum flooding surface and an erosive sequence boundary, and are termed sequences (Van Wagoner et al., 1988). Sequence scale units were the smallest used for subdivision of the section in this study. At this early stage of exploration in the Roebuck Basin and with the current data availability, it would probably not be possible to subdivide the section further with confidence without increased well-control. A flow chart of the method used to pick boundaries is given in Fig. 3.1.

3.2.1 Boundary Identification

The gamma, sonic, neutron and caliper log were environmentally corrected for mud type and temperature using standard Schlumberger correction formula in Mincom's Geolog 6 wire-line log software. They were then printed out at 1:2000 scale along with palaeontological data supplied by AGSO (from their STRATDAT database) and Morgan and Associates (quick-look re-evaluation palynology sheets). Palaeobathymetric and cuttings information obtained from Morgan and Associates and well completion reports were also annotated onto the logs.

From this information the palaeogeographic location with respect to the shoreline, of each well through time, was determined. Sediments were subdivided into non-marine, marginal marine, intermediate marine and oceanic, using the palaeontological water depth indictor provided. Where sediments were unsampled, water depth environmental indicators were determined, using wire-line log character in conjunction with the nearest palaeontological indicators within the well. Log signatures used during this study were modified from lithostratigraphic signatures identified by Miller (1997), which were tied to palaeontological environmental indicators supplied by Morgan and Associates to produce environmental log characters (Fig. 3.2). Wells were also placed in their shelfal context using adjacent well information. Unfortunately, little core exists to calibrate these interpretations.

Correct identification of a section's depositional environment was found to be critical when dividing each section into its major T-R cycles as maximum flooding surfaces (MFS) and sequence boundaries (SB) display different characteristics in each environment. The interpretation methods used in clastic deposits for non-marine, near-shore marine and deep marine are shown and summarized in Figs. 3.3 and 3.4.

Palaeontological data were first examined for obvious unconformities and care was taken to

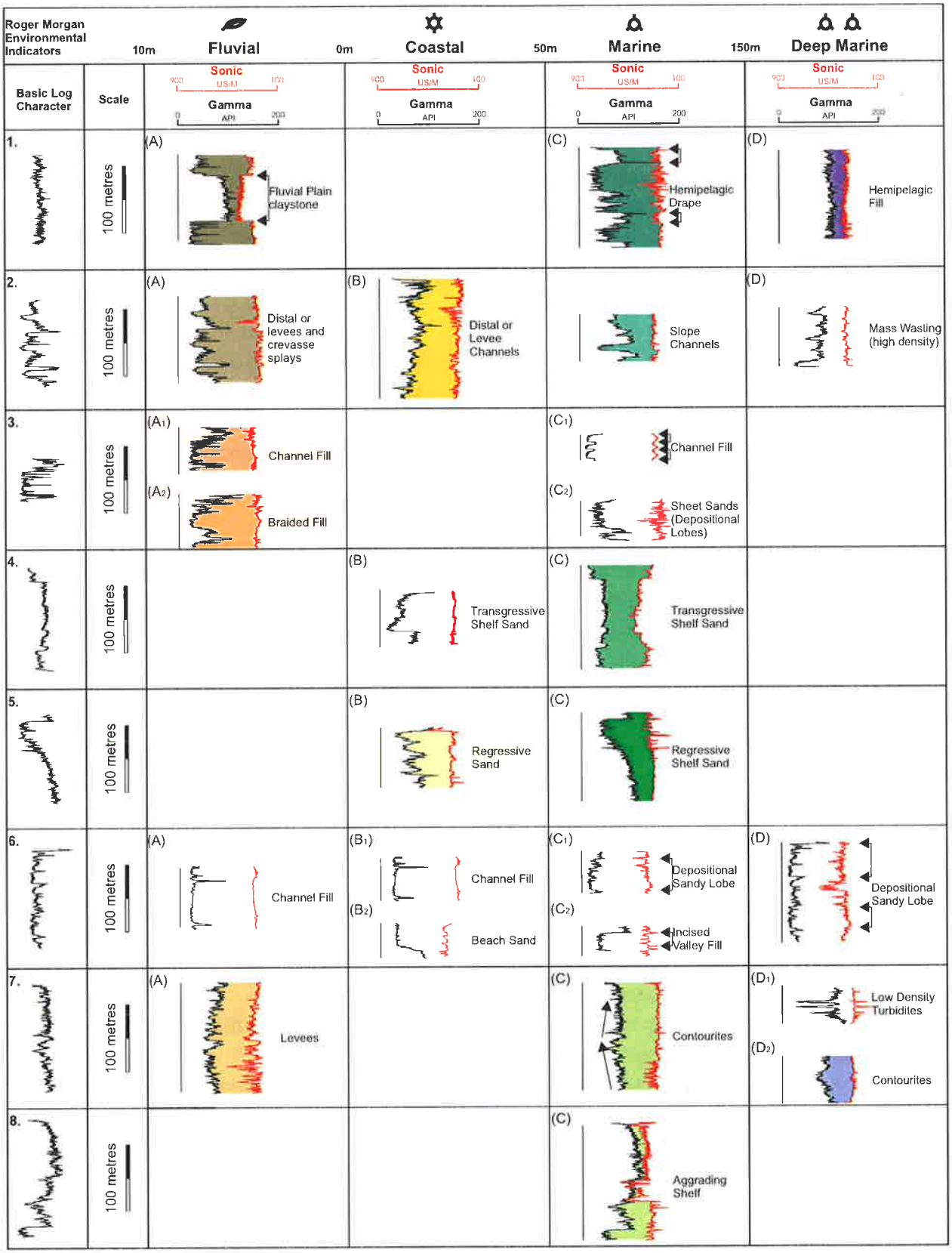

Figure 3.2 Environmental interpretation of wireline log characters based on log shape in conjunction with biostratigraphic environmental indictors.

identify all condensed zones. Maximum flooding surfaces (MFS) were then used to divide the section into basic T-R cycles. Only T-R cycles that could be confidently correlated between wells using seismic and well data were used to breakdown the stratigraphy. Sequence boundaries were then picked in accordance with the methods outlined in Figs. 3.3 and 3.4. All sequence boundaries were correlated and, where possible, their nature confirmed using seismic data.

For carbonate rich sediments wire-line methods have not been well documented. The mid-Cretaceous to Recent section of the Roebuck Basin has traditionally been overlooked during biostratigraphic sampling due to its perceived lack of hydrocarbon potential and, as a result, prediction of the timing of events is problematic. Sequence stratigraphic studies in carbonate-dominated systems have traditionally adopted the use of outcrop and seismic studies rather than wire-line log methods (Calvert and Pedersen, 1990; Reijmer et al., 1991). During this study a simple sequence stratigraphic model was developed in conjunction with Hull for the interpretation of carbonate dominated wire-line characteristics on the North West Shelf. The method and results have been published in detail in Smith et al. (1997) and Hull et al. (1998) and are summarized here.

During carbonate production, lowstand systems tracts are characterized by an increase in gamma and irregular sonic readings associated with increased clastic input and reduction in area available for carbonate production. During transgression the gamma log 'cleans-up' due to predominantly carbonate deposition as siliciclastic deposition is relocated in a landward direction and an increased proportion of the shelfal area becomes flooded and available for carbonate production. The maximum flooding surface is represented at the lowest gamma reading at the top of the distinctive cleaning up transgressive package. The subsequent highstand systems tract shows constant gamma and sonic values up until the following sequence boundary where fine grained siliciclastic input causes a sharp increase in gamma and sonic. The pick methodology using this model is shown diagrammatically in Fig 3.5.

3.2.2 Sequence Stratigraphic Chart

In total, 64 boundaries were identified that could be partially correlated through the basin and used to date the section. These events are shown in Fig 3.6. Each event was assigned an exact date. However, even having used all available biostratigraphic well data, certain events could only be very approximately dated. Error bars highlighting the scope of uncertainty of dating have been included in the event summary. Each event has been initialed and numbered according to the biozone during which it developed and its development order in that zone (e.g. *CT-1* is the first recorded sequence boundary in the *C. torosa* biozone, *C1-2* is the second sequence boundary in the C1 biozone).

A correlation panel across the Bedout, Inner Rowley and Beagle Sub-basins, which demonstrates the pick density, is shown in Fig. 3.7. The panel includes environment interpretation based on biostratigraphic and log indicators presented in Fig. 3.2. Unfortunately, permission was not granted for reproduction of the raw biostratigraphic data which was supplied by AGSO from their proprietary STRATDAT database.

The results of the sequence correlation were used throughout the study to date the tectonic evolution and basin-fill history.

3.3 High Resolution Chronostratigraphy

Only limited well control was available in the Roebuck Basin making it difficult to date the complete section accurately. Basin-fill determination was heavily dependent upon the interpretation of seismic data. This interpretation utilized the integrated sequence stratigraphic approach outlined above, combined with high resolution chronostratigraphic concepts.

Although the theory behind high resolution

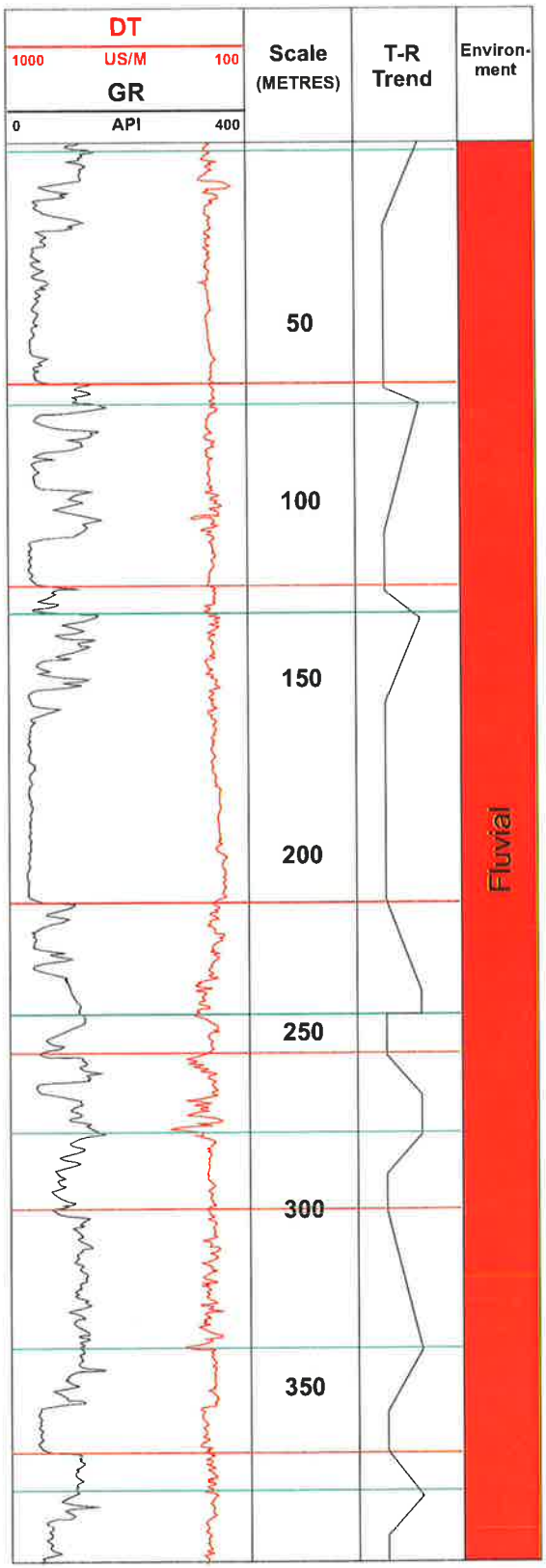

In fluvial sections, thin coal seams form just below the MFS during the transgressive system. These are identified on wireline log data by hot gamma spikes that correspond with slow sonic readings.

SB's are picked at the thickest amalgamation of channel sands between well development transgressive coal packages. The thickest sand body is formed when accommodation space is at a minimum. Meandering channels then snake across the alluvial plain incising and reworking previously deposited sand bodies into a thick fluvial sand sheet.

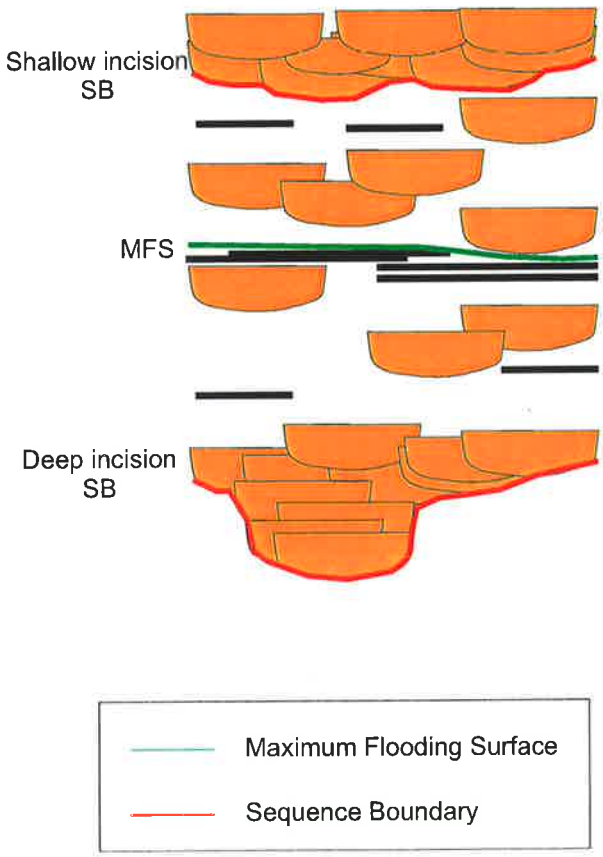

Figure 3.3 Major stratal surface pick methodology in non-marine section.

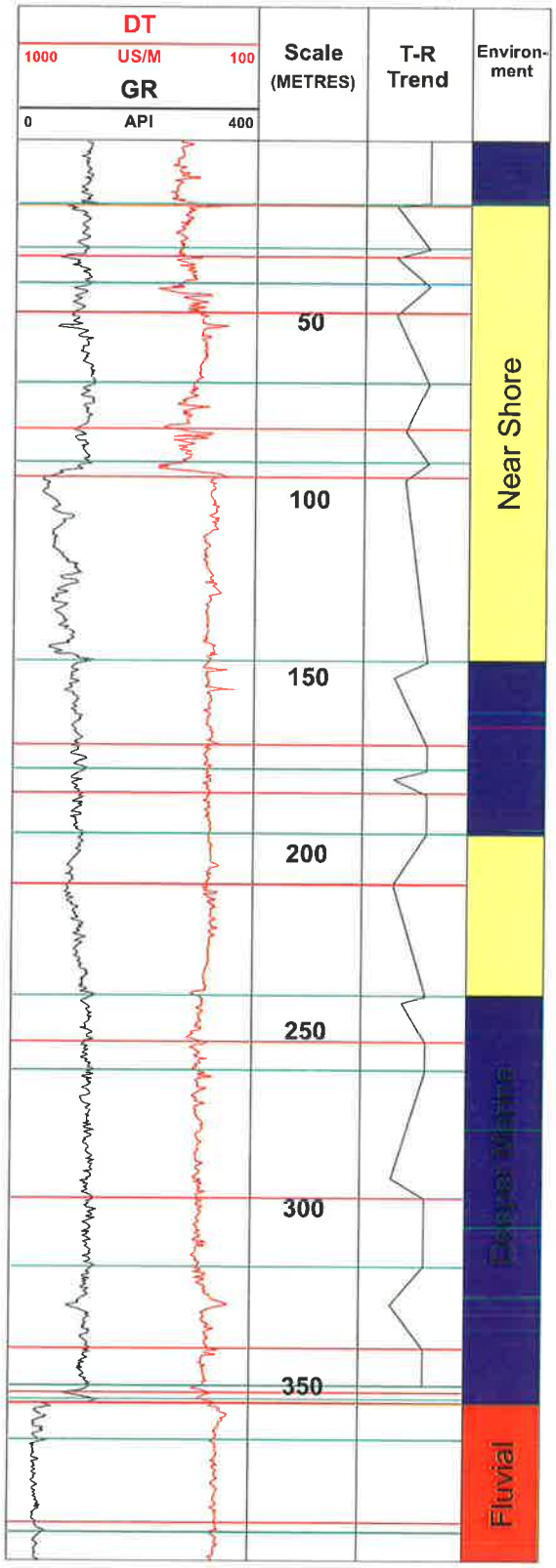

Deeper marine and nearshore systems have significantly different gamma trends. It is important to identify the palaeo-environment before interpreting the position

MFS's are picked as gamma peaks in near shore deposits. SB's are picked at the top of decreasing gamma trends. Decreasing gamma trends represent sand input during highstand times, were sufficient accommodation space exists on the shelf to preserve sediment. A highstand can be followed by a lowstand, producing a Type 1 SB, or a stillstand producing a Type 2 SB.

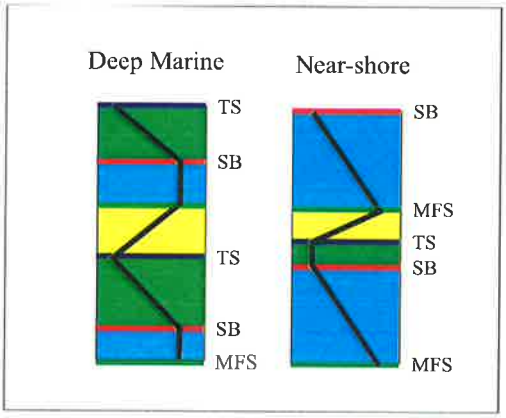

In deeper marine section MFS's are picked at the maximum gamma peak. Reasonable volumes of sand only reach the deeper part of the basin during lowstand. For this reason SB's are picked at the base of decreasing gamma trends and represent the correlative conformity.

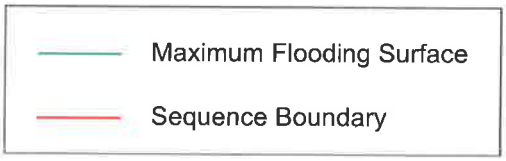

Figure 3.4 Major stratal surface pick methodology in nearshore to open marine section.

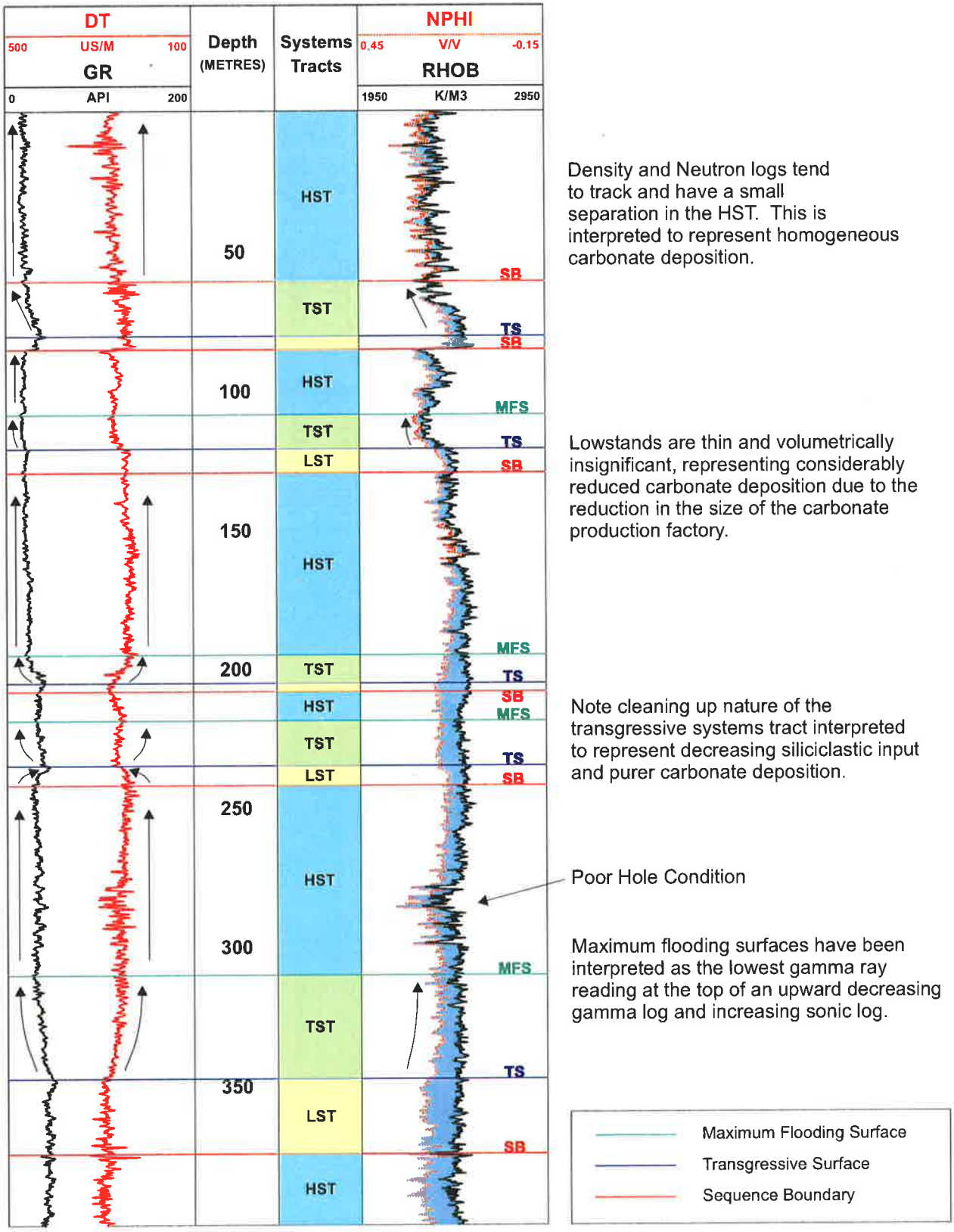

Figure 3.5 Major stratal surface pick methodology in carbonate dominated section.

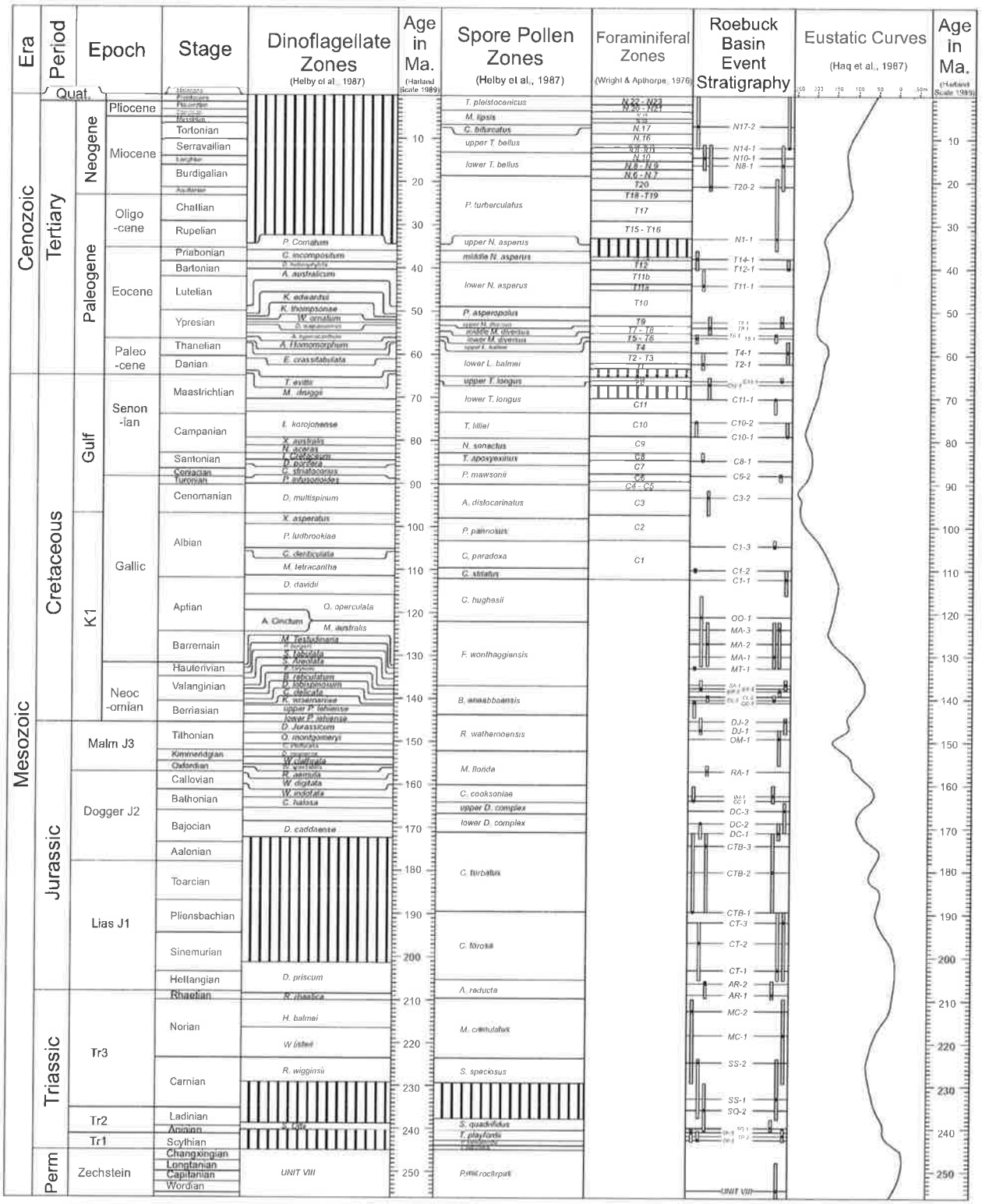

Figure 3.6 Stratigraphic event summary. Error bars show the most likely timing of each event (marked by the • marker) and also the possible position based on biostratigraphic constraints (marked by the bar).

chronostratigraphy is straightforward, the process has not commonly been used in geological studies to date as it is extremely time consuming. A rapid process for the chronostratigraphic breakdown of a group of 2D seismic sections and the construction of important geological products, such as coastal onlap curves and 3D Wheeler diagrams using this method is described in the following sections.

3.3.1 Chronostratigraphic Charts

Basic chronostratigraphic charts can be constructed from many types of data. However, they are most simply constructed from seismic data based on the assumption that primary seismic reflections follow time-significant chronostratigraphic correlation events such as bedding surfaces and unconformities, rather than time-transgressive lithostratigraphic units (Vail et al, 1977: Part 5). A seismic reflection thus approximates a time boundary (everything above the reflection is younger than everything below). Schultz (1982) proposed a hierarchical terminology for rock units bound by seismic-reflections or time planes. During this study the term "chronosome" (from Schultz, 1982) has been used to describe seismic-reflector bound packages at a variety of scales from parasequence to megasequence. This definition was useful during the chronostratigraphic mapping of the Roebuck Basin where the temporal duration of certain rock units was initially unknown.

Chronostratigraphic charts can be used to aid the understanding of the temporal and spatial distribution of each depositional system that makes up the basin-fill (Fig. 3.8) and identify areas of non-deposition due to erosion, bypass or condensation (distal proximity). Surfaces of non-deposition often prove to be excellent correlation markers both on seismic sections and in wells (Loutit, 1988), but have little thickness in the rock record. Their true significance can be better appreciated in the time dimension (Emery and Myers, 1996).

A thorough chronostratigraphic break-down of the basin was used to determine rates of sediment flux and tectonic subsidence. Plots of the proximal limit of topset deposition (coastal onlap) were used to estimate the frequency (but not the magnitude) of changes in relative sea-level. These variables provided useful information about the basin being studied and provided some of the essential input parameters used later in the forward sedimentary modelling of the basin.

3.3.2 Chronostratigraphic Reconstruction of the Roebuck Basin

Usually, one or two key seismic lines believed to be the most representative of the basin, are chosen to construct a chronostratigraphic chart. However, any one seismic line does not represent the complete stratigraphy of the basin. Emery and Myers (1996) describe the problem thus: *"there almost certainly will be depositional packages not represented on the chosen seismic line, as they were deposited out of plane of the section. The time of deposition of this package will be represented on the seismic section as a time of hiatus, condensation, bypass or erosion. A two-dimensional chronostratigraphic construction on a single line will not assign enough time to this hiatus, but will distribute the time through the deposition represented on the line".* It becomes obvious that, in order to accurately determine the location and duration of missing section in a basin, it is necessary to map the distribution of individual chronosomes through a 3D grid of lines. To do this by hand is an extremely complicated and time consuming exercise and almost impossible for large data sets without the aid of computer software.

3.3.3 The use of 3D-Chronostrat™ software in chronostratigraphic reconstruction

To produce a 3D chronostratigraphic framework for the Roebuck Basin a commercially available software suite (SRi's 3D-Chronostrat™, written by Ulf Nordlund) was used. This suite contains three Macintosh programs used to digitize (Digitize), sort (Chronostrat) and display (3D-Grid) chronosomes (demonstrated in Fig. 3.8). Griffiths

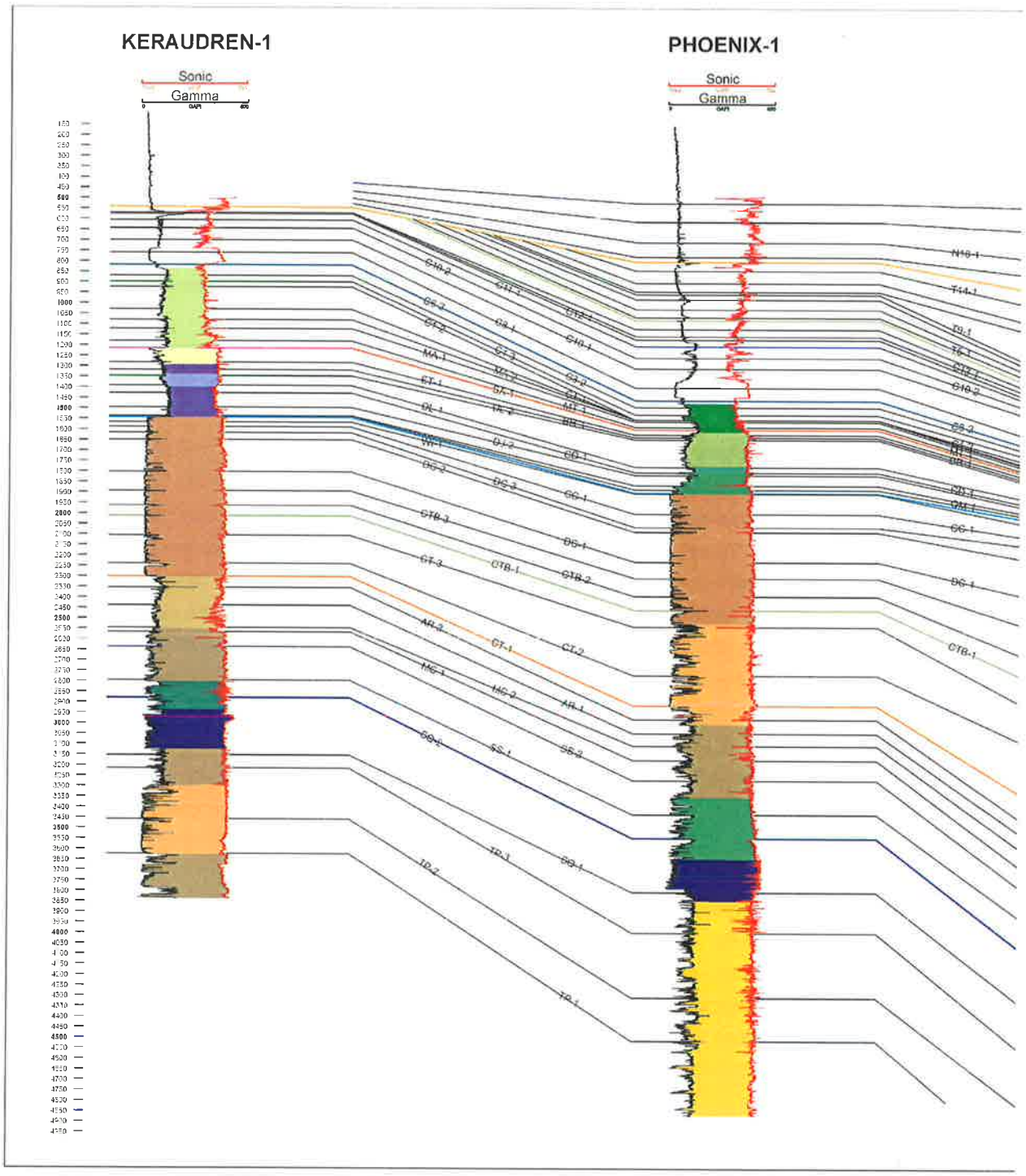

Figure 3.7 Wireline log correlation across the Bedout Sub-basin into the Beagle Sub-basin. Shading between logs represents the environmental interpretation based on Fig. 3.2. Con't over-page.

and Nordlund (1993), Nordlund and Griffiths (1993) and have described the use of this suite of software in relation to basin stratigraphy and Griffiths and Hadler-Jacobsen (1995) have described its role in forward sedimentary modelling.

3.3.3.1 Subdivision of the sediment fill using Digitize

The Digitize program enables rapid digitization of seismic horizons at an extremely high resolution (Fig. 3.8b). The program can handle up to 50 lines at a time with up to 15 lines being tied on screen at once.

A subset of data was selected from the Roebuck Basin from the overall seismic grid utilized for the structural and megasequence interpretation. Lines were selected using the following criteria; close proximity to the major depocentres, locality, quality and length. Thus, they represent the most

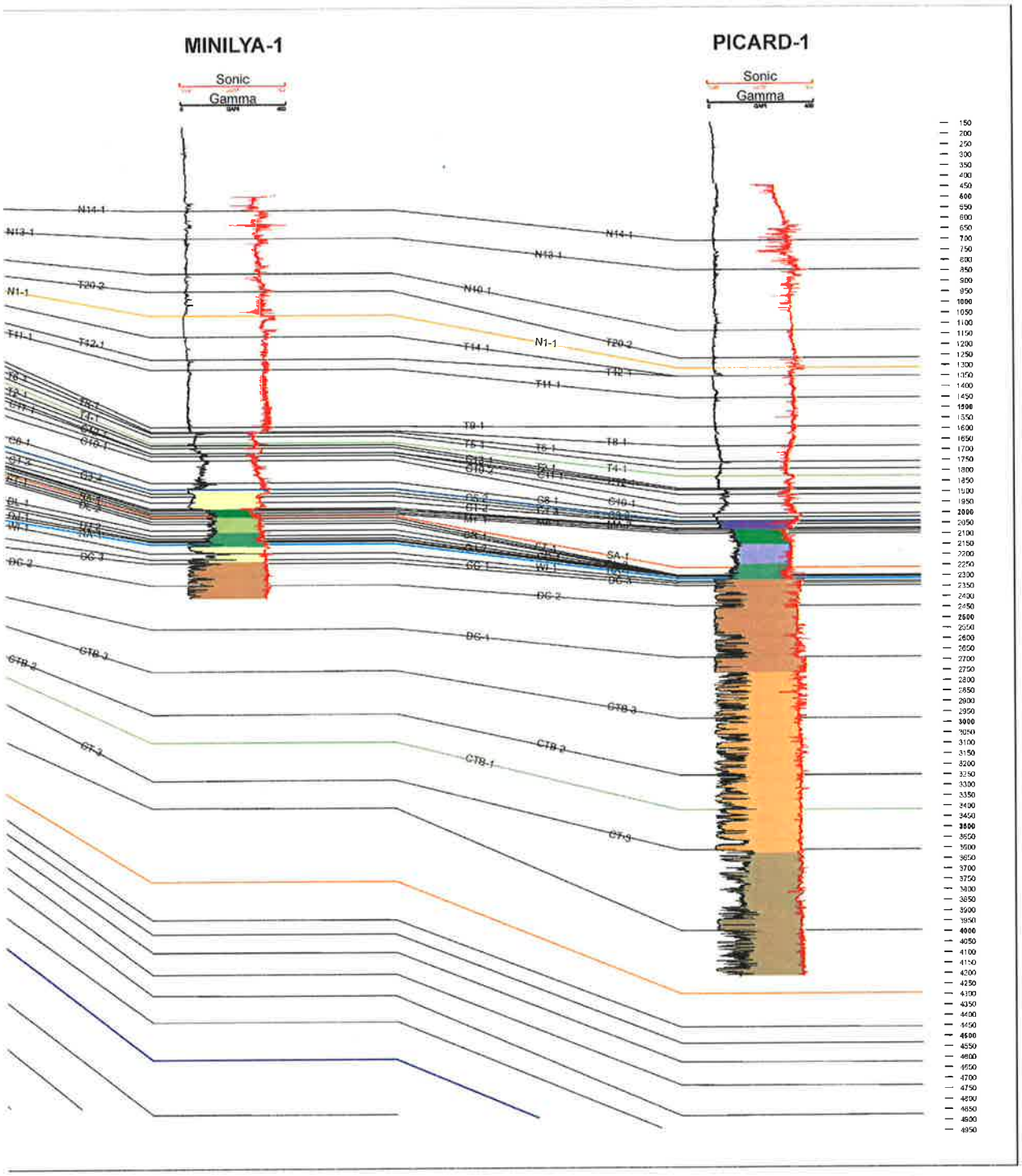

Figure 3.7 Con't.

complete record of chronosome distribution, both temporally and spatially, throughout the basin, with data of the highest quality and least number of ties.

Twelve of the fourteen AGSO, and three of the JNOC regional seismic lines, were chosen for chronostratigraphic mapping, making a subset of approximately 4500 km (Chapter 1 Fig. 1.3). The twelve AGSO lines, due to the regional nature of this survey, proved to be excellent candidates for the subset and where these types of regional surveys exist elsewhere around Australia, they will probably again make good candidates for chronostratigraphic work. The lines were downloaded from the regional database as raster images. The megasequence picks, synthetic seismic well ties and sequence stratigraphy picks were also included. Hence, the chronosome mapping was constrained by well information and structural mapping.

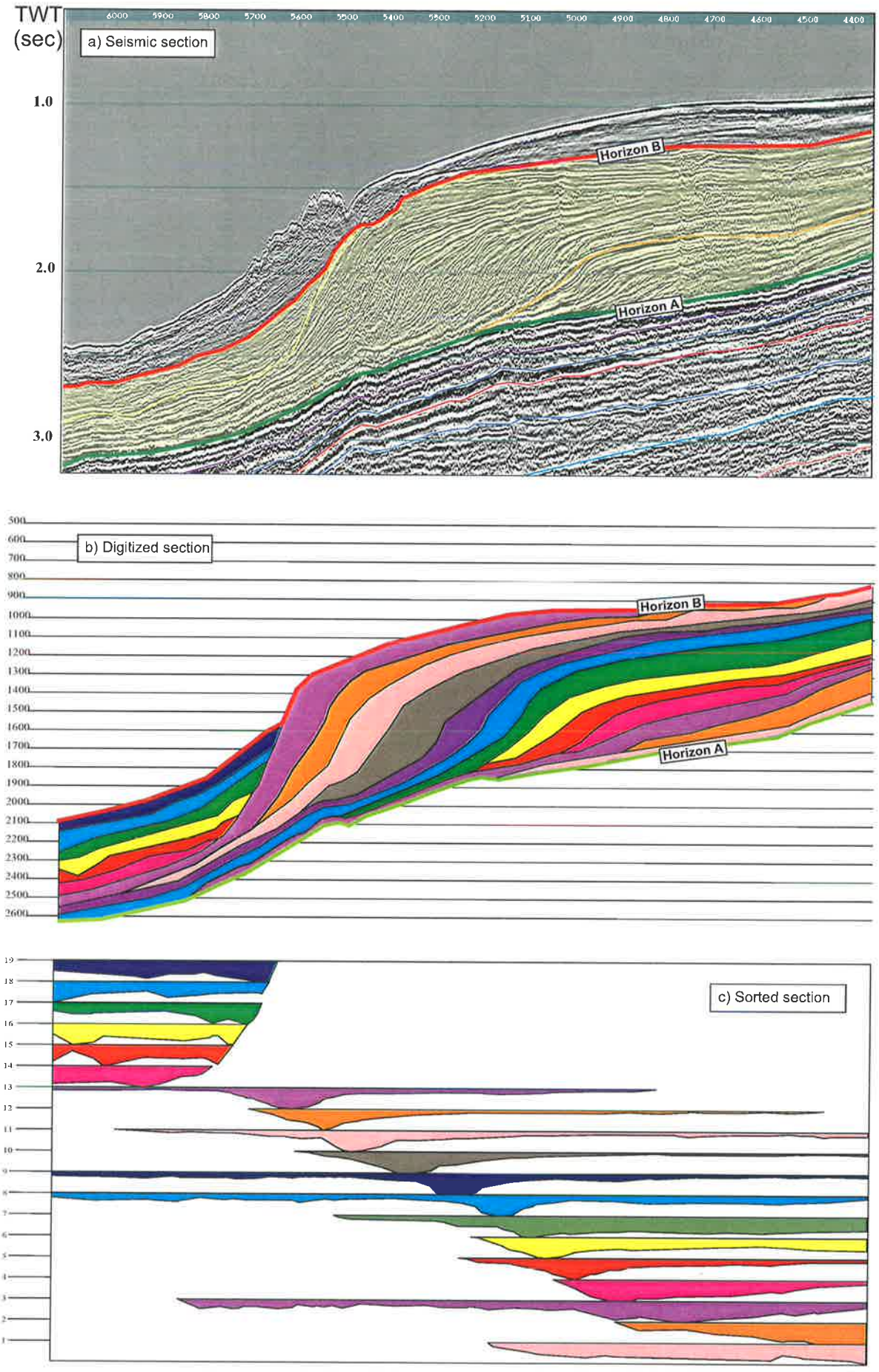

Figure 3.8 Construction of the chronostratigraphic framework. (a) Raw seismic (b) Digitized output from 3D-Chronostrat and (c) Sediment stacking order output from 3D-Grid.

Once the seismic line images were loaded into Digitize the seismic horizons were mapped. Two regionally extensive seismic events were required for the top and bottom bounding surfaces of the interpretation. Earlier on in the study a decision had been made to start the sequence stratigraphic interpretation at the Late Permian *Unit VIII* boundary, which is marked by a regional unconformity. This again seemed to be a suitable horizon for the base bounding surface due to high confidence in the seismic pick and its regional extent throughout the basin.

The choice of the top bounding pick was important as it would shape the nature, not only of the chronostratigraphic interpretation but also of the forward stratigraphic modelling. The top bounding pick had to include most of the section of interest from a petroleum perspective and encompass the areas of the basin that have yet to be explored. The obvious choice would be the seafloor, as this would include the complete section above *Unit VIII*. However, this would probably not have allowed sufficiently detailed work of high enough resolution in the time available. The late Cretaceous event *C6-2* was chosen, again, because of high confidence in the seismic pick and its wide regional extent.

One hundred and fifteen horizons were eventually used to divide the section into chronosomes. Initially, the megasequences were retraced using picks already made whilst interpreting the complete seismic database. The section was then subsequently divided up by mapping the most obvious seismic surfaces (surfaces of downlap, onlap, toplap and truncation (Mitchum et al., 1977 Part 6)) and then still further into smaller depositional sequences. The only constraint on the size of a chronosome that could be digitized was the resolution of the seismic data. Digitize was used to check for and flag mis-ties and ambiguous terminations. The identification of appropriate seismic surfaces and the nature of their termination constrains how the other computer programs in the suite will logically search and sort the data using basic laws of superposition.

3.3.3.2 Definition of the chronosome stacking order using Chronostrat

Once digitizing was completed the Chronostrat program was used to search for and sort horizon terminations on each 2D section, and determine the stratigraphic order of each horizon (Fig. 3.8c). The program then linked the tied horizons throughout the seismic grid to produce a chronostratigraphy in the form of a series of three-dimensional chronosomes of known stacking order.

3.3.3.3 Chronostratigraphic display using 3D-Grid

Once sorted, 3D-Grid was used to display single line chronostratigraphic summaries in 2D and the basin development in 3D. 3D-Grid was also used to output a wide variety of quantitative information concerning each 2D/3D chronosome in ASCII text file format which was imported into a standard spreadsheet. The information gained from 3D-Grid was used to provide many of the input parameters required for the forward stratigraphic modelling undertaken later.

3.3.4 Scaling the chronostratigraphy to absolute time

The chronostratigraphy that was constructed using the above methodology initially had a non-linear time scale where each chronosome had been plotted in relative stacking order in equal time increments. The chronostratigraphy was scaled to absolute time using well-ties to directly tie the time framework defined during sequence stratigraphic correlations undertaken earlier on in the study to each chronostratigraphic section. However, during the Triassic and Early Jurassic sedimentation was rapid and multiple chronosomes were deposited during single biostratigraphic/sequence stratigraphic intervals.

The simplest approach to dating these chronosomes would be to assign an equal time interval to each one by simply dividing the time between two well-defined time boundaries by the

number of chronosomes between those boundaries. Alternatively, a weighted method of time allocation could be used. Griffiths and Hadler-Jacobsen (1995) discuss the weighted method in some detail. They suggest that there is a relationship between the chronosome cross-sectional area to length ratio and its duration on a 2D seismic line. The concept they expressed is that clay-rich chronosomes are of large areal extent and are deposited over longer periods of time than sand-rich sediments. In other words "short fat chronosomes are sand-dominated and are deposited rapidly, whereas long thin chronosomes are clay dominated and are deposited slowly". The concept allows a prediction (in the absence of other data) regarding the age and grain-size content of a chronosome.

Griffiths and Hadler-Jacobsen (1995) suggest the following set of equations to scale the relative duration of each chronosome on a 2D seismic line to an absolute scale.

$$x_i = \left[\frac{(area)_i}{z_i / l_i}\right] \qquad (1)$$

$$\Delta t_i = x_i T \left[\sum_{j=1}^{n} x_j\right]^{-1} \qquad (2)$$

where x_i is the scaling ratio, $(area)_i$ is the cross-sectional area, z_i the maximum thickness, Δt_i is the duration, l_i is the length, of the i^{th} chronosome. T is the time duration of the complete 2D set of n chronosomes.

This equation assumes that there are no hiatuses in the section, something that Griffiths and Hadler-Jacobsen (1995) point out is incorrect. Applying the approach to a 3D data set yields:

$$x_i = \left[\frac{(volume)_i}{(area)_i}\right] \qquad (3)$$

where $(volume)_i$ and $(area)_i$ are the volume and area of the i^{th} chronosome in 3D, unlike equation (1) where measurements are from 2D sections.

Although there is still a possibility that sedimentary breaks will be missed in the 3D interpretation, with increased areal grid size there is less chance of this occurring. The underestimation of hiatus duration will be less using a 3D solution in equation (2) than a 2D solution.

For the Roebuck Basin 3D volumetric data were obtained directly from the 3D-Grid software package which was used to grid the upper and lower surface of each chronosome. A 60 by 60 grid was used to determine areas and volumes for the Roebuck Basin and these were utilized in equation (2) and (3).

The implications of using such a method should be considered carefully. This method could not be used *ad hoc* to a complete basin-fill with only a top and bottom time calibration as it would involve comparing chronosomes that have undergone different compaction histories - modifying the initial deposited volume to that preserved today. Such a method only works with chronosomes of approximately equal burial depths and reflecting similar compaction histories. Using the biostratigraphic and sequence stratigraphic framework the section was directly tied from wells at 32 surfaces. These act as control points thus breaking up the section into groups of chronosomes that have undergone similar compaction histories. In other words; equation (2) was not used once to date all the chronosomes but was used 31 times to data groups of chronosomes between calibration points based on biostratigraphy/sequence stratigraphy. During this study the largest number of untied chronosomes between calibration points was 6 which was hence the largest n value used in equation (2).

A second factor that must be considered is that, even using a large grid of data that covers the entire basin, not all chronosomes will be mapped in their entirety, resulting in an underestimate of total volume and area which may have an adverse effect on the ratio calculated in equation (3). Although this approach cannot be considered a perfect solution, the method described above is

considered a useful first approximation for dating the section in the absence of other geological data.

3.3.5 Chronostratigraphic Display

The scaled results of chronostratigraphic mapping were presented as a series of 2D line diagrams tied to a 3D grid to form a chronostratigraphic framework across the basin. An example of this 3D framework at the megasequence mapping level (9 chronosomes only) is shown in Figure 3.9. In total, 114 chronosomes were mapped across the basin. In 2D each line can be displayed in a more traditional manner as a series of stacked sediment packages in time. Chronosomes were displayed in time with a contemporaneous top and diachronous base, implying that each chronosome has only been partially deposited over certain areas of the basin. The program 3D-GRID actually displays relative thickness information of the chronosome along the line over the time interval represented by the thickest part of the package (i.e. relative thickness information is also being displayed on the time axis). This information is misleading when interpreted purely in a time framework and this functionality should probably be removed from the software.

Representative chronostratigraphic sections across the major depocentres, lines BMR120-01 (Fig. 3.10), BMR120-03 (Fig. 3.11), BMR120-07 (Fig. 3.12) and BMR120-11 (Fig. 3.13) are presented here. On each line, chronosomes have been picked to near seismic reflector resolution – resulting in similar TWT thickness for each chronosome. If the assumption is made that each chronosome represents a similar true thickness of sediment, then the chronostratigraphic chart can be used to infer additional information regarding the rate of sedimentation during time (i.e. low volume chronosomes are packages of sediment that have been deposited rapidly and chronosomes of large areal extent represent slow deposition). This concept has been more quantitative assessed in Section 3.4 and a detailed sediment supply budget calculated for the Roebuck Basin based on chronosome areas.

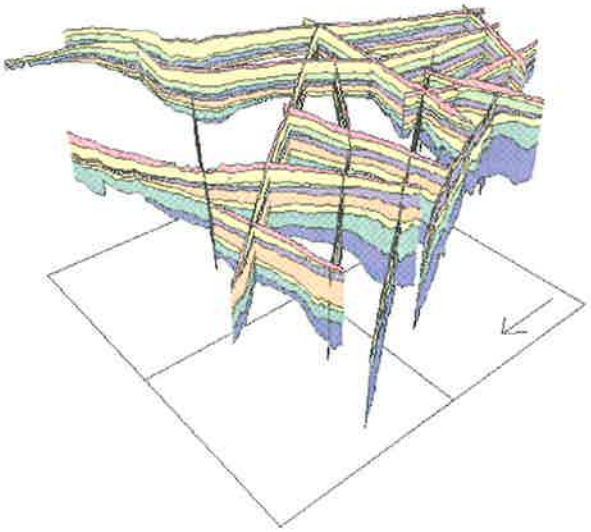

Figure 3.9 Fence diagram of megasequences viewed in 3D-Grid from the northwest (arrow represents N).

In addition to 2D chronostratigraphic sections each chronosome was gridded to produce a 3D surface and a 2D areal view (Figs. 3.14 and 3.15). Each 3D surface was compiled into a short animation so that the *in situ* (unbackstripped) depositional stacking pattern could be replayed in order, allowing a view of the depositional development of the basin.

3.4 Sediment Budget

Sediment supply is an important input parameter required for forward sedimentary modelling (Chapter 5). Modelling required a two end-member (sand and shale) library of sedimentation rates through time, expressed in the form of integrated thicknesses along a 2D line (the vertical by horizontal area of a 2D line filled per thousand years (km^2kyr^{-1})).

The shale and sand sediment budgets were calculated for the basin by decompacting on the assumption that the shape of a chronosome reflects its grain-size make-up and duration of deposition. More areally extensive chronosomes tend to be clay-dominated and more slowly deposited than sand-prone chronosomes (Griffiths and Hadler-Jacobsen, 1995). This assumption was used to predict the shale/sand ratio of each chronosome which was then decompacted using two algorithms, one for the shale fraction and one

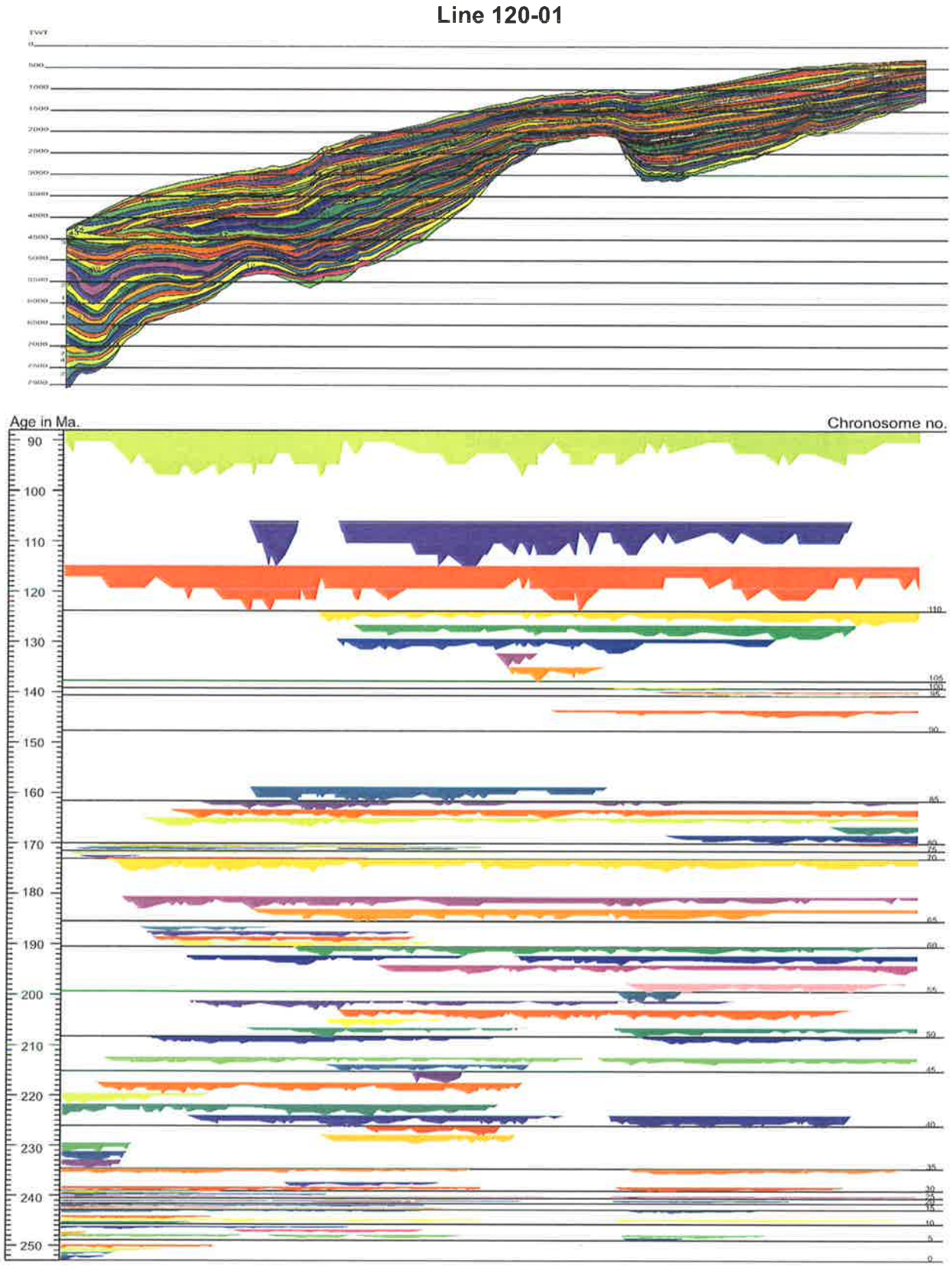

Figure 3.10 Chronostratigraphic display of line BMR120-01 across the Bedout Sub-basin, Bedout High and Rowley Sub-basin from Late Permian *Unit VIII* to Late Cretaceous *C6-2*.

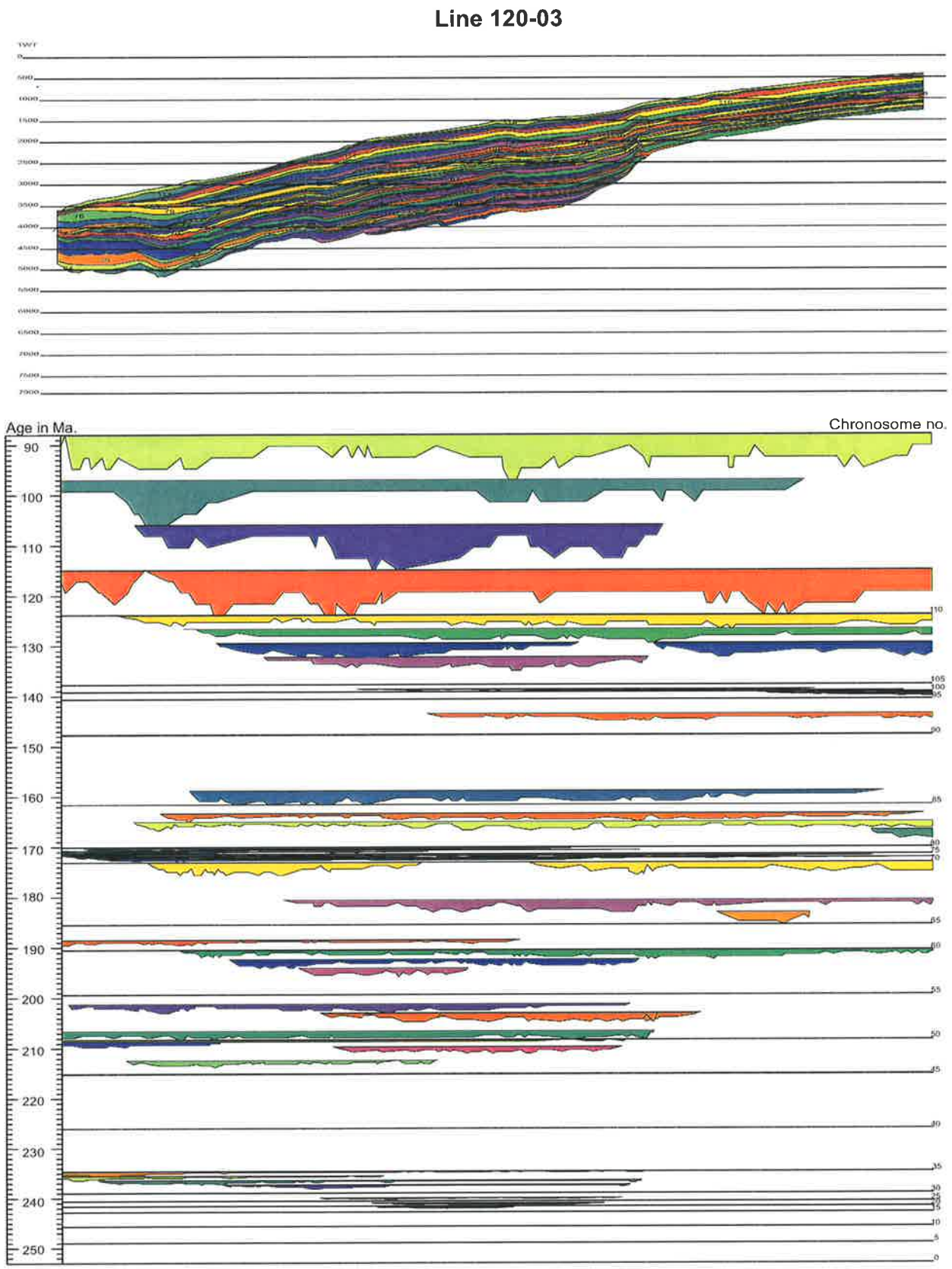

Figure 3.11 Chronostratigraphic display of line BMR120-03 from the Broome Platform across the Inner and Outer Rowley Sub-basin from Late Permian *Unit VIII* to Late Cretaceous *C6-2*.

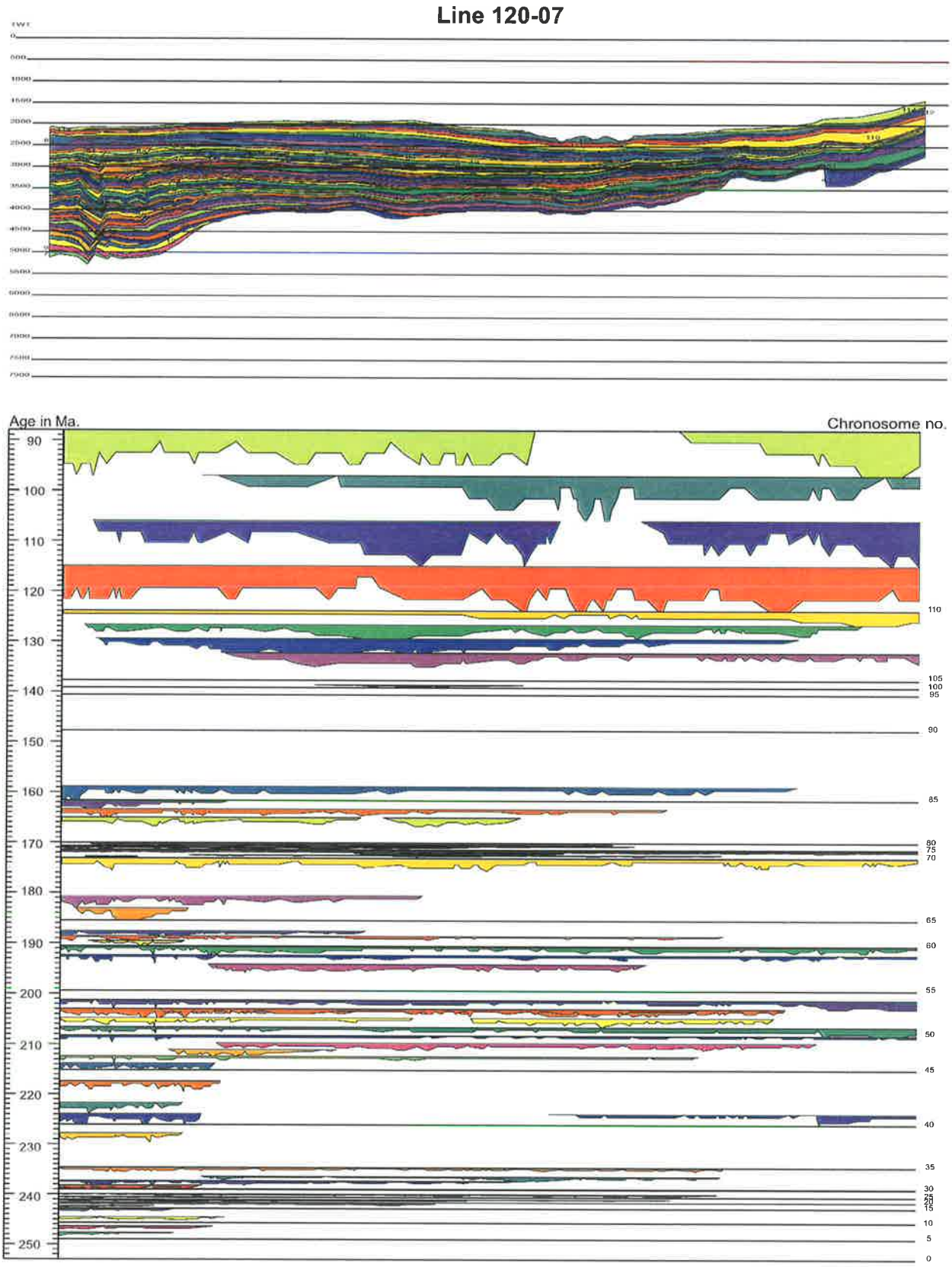

Figure 3.12 Chronostratigraphic display of line BMR120-07 in strike section across the Bedout and Inner Rowley Sub-basins from Late Permian *Unit VIII* to Late Cretaceous *C6-2*.

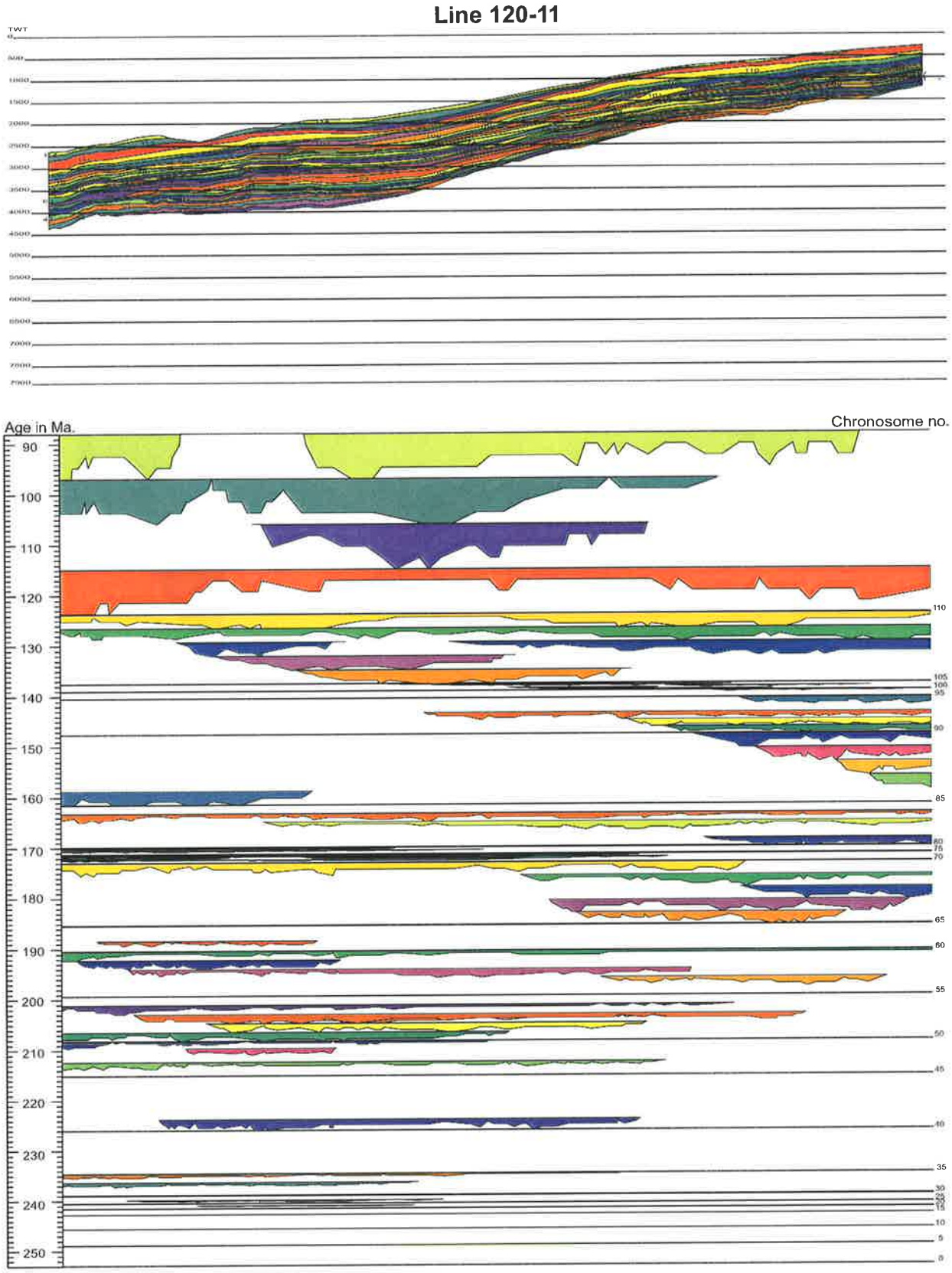

Figure 3.13 Chronostratigraphic display of line BMR120-11 across the Oobagooma and Rowley Sub-basins from Late Permian *Unit VIII* to Late Cretaceous *C6-2*.

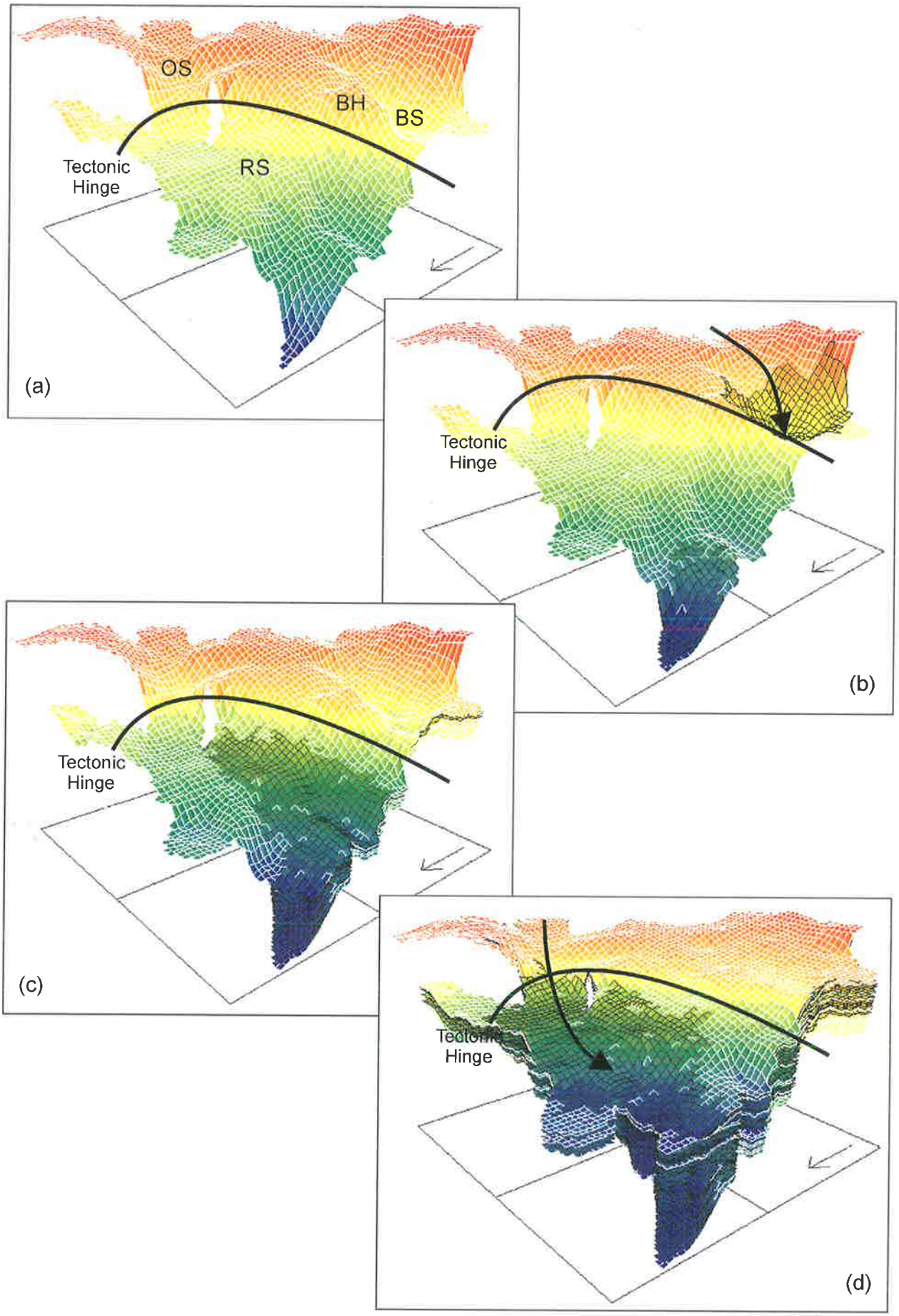

Figure 3.14 Chronostratigraphic surfaces displayed at (a) Late Permian (b) Early Triassic (c) Late Triassic and (d) Middle Jurassic. Depositional directions represented by arrows and major tectonic hinge also shown.

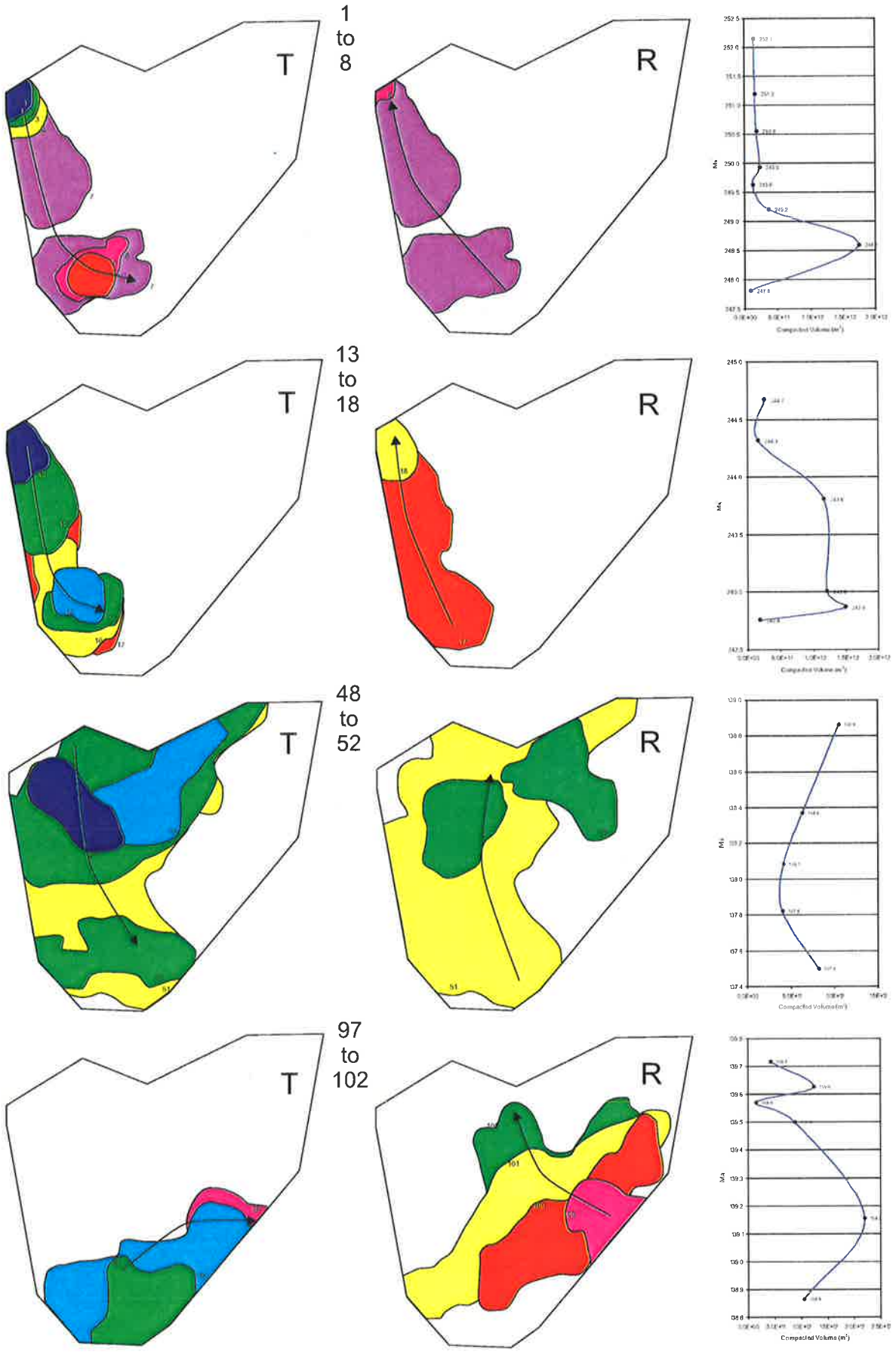

Figure 3.15 Areal distribution of selected representative chronosomes in T-R cycles. Chronosomes 1 to 8 and 13 to 18, deposited during the Early Triassic, demonstrate the restricted nature of deposition to the Bedout and Rowley Sub-basin during this time. Chronosomes 48 to 52 reflect more widespread deposition along the major Bedout and Oobagooma Sub-basin depositional axis during the Early Jurassic. Chronosomes 97 to 102 represent broad shelf-wide deposition associated with regional uplift during separation of India from Western Australia. Volume of preserved sediment for each chronosome is shown graphically on the right.

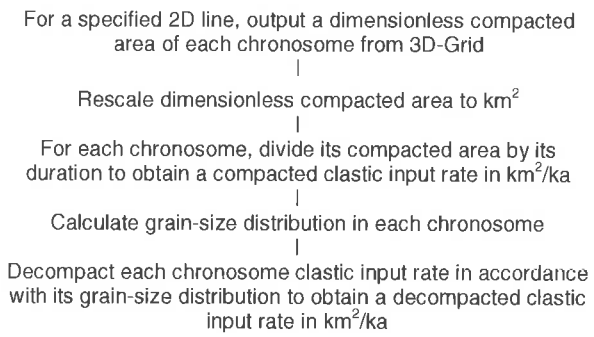

Fig 3.16 Determination of sediment input rate used for sedimentary modelling.

for the sand fraction, to obtain a decompacted area of sediment which was deposited during the duration of the chronosome. The method is shown in a flow diagram in Figure 3.16.

Firstly, the preserved compacted 2D area of each chronosome for the lines later selected for modelling were obtained directly from 3D-Grid in ASCII format. This output consisted of a chronosome area scaled by length in km in the horizontal plane by two-way-time (TWT) in milliseconds in the vertical plane. Within 3D-Grid a single user-specified depth conversion factor for TWT to metres may be entered to obtain a depth-converted chronosome area. This method has been used by (Griffiths and Hadler-Jacobsen, 1995) to rescale data sets but this approach is only valid for a data set distributed through a small depth range where the velocity profile remains fairly constant. This approach was not suitable for use during this modelling study where chronosome burial depths varied dramatically from 1 to 12 km and where individual chronosomes had large variations in burial depth over their areal extent, making a single velocity value unrealistic.

For the 2D section selected for forward modelling, chronosomes were rescaled to km^2 (cross-sectional area) by locating the chronosomes thickest TWT point on the 2D seismic line and calculating a TWT to thickness conversion ratio based on the interval velocity for that depth from the nearest stacking velocity panel on the seismic data. Long chronosomes were divided into sections, depth converted and summed to produce a total for the compacted area. Depth conversion at the thickest point of the chronosome ensured that the most volumetrically significant part of the cross-sectional area was depth converted with an appropriate value. Once compacted areas in km^2 were obtained for each chronosome, these were divided by chronosome duration to obtain the compacted sediment input rate in km^2kyr^{-1}.

The next step in obtaining a sediment input budget was to predict the sand:shale ratio of each chronosome. Using the assumption that the slowest sedimentation rate is clay dominated, Griffiths and Hadler-Jacobsen (1995) proposed the following equation for calculating the clay fraction of each chronosome;

$$\text{clay fraction } (F_{sh}) = \frac{\log(\text{clastic input rate}) - \log(\text{max. clastic input rate})}{\log(\text{min. clastic input rate}) - \log(\text{max. clastic input rate})} \quad (4)$$

where (clastic input rate) is the sedimentation rate for a given chronosome, (max. clastic input rate) is the highest sedimentation rate from the whole data set and (min. clastic input rate) is the lowest sediment input rate in the whole data set. It follows that;

$$\text{sand fraction } (F_{sd}) = 100 - \text{clay fraction \%} \quad (5)$$

Griffiths and Hadler-Jacobsen (1995) said, of equation (4), *"the basis for this equation is the assumption that there is a related, dependant gradual progression in both rate of deposition and grain-size. As grain-size increases so does the volumetric rate. A logarithmic relationship means that small additions of fine material have a disproportionately large negative effect on deposition rate"*. The validity of such a relationship in a two end-member system is incorrect as it assumes that two end-members of 100% sand and shale exist within the basin and that all chronosomes consist of a function of those members. However, the basic concept that size and thickness of a chronosome is directly related to duration rate is probably true. The equation

mathematically expresses the above statement and allows a first approximation of grain-size distribution which can be altered if lithological calibration from wells dramatically differ from simulations. It is possible that, through empirical testing in well-controlled data sets, such an expression could be improved and used in modelling where no well-control exists. However, the above expression was found to generate satisfactory results during Griffiths and Hadler-Jacobsen's (1995) study.

One problem does exist when using this relationship for grain-size prediction in the Roebuck Basin. In equation (4) compacted sedimentation rates were used to predict grain-size distribution in chronosomes. However, each chronosome has undergone a different burial history and hence a different degree of compaction. For example, using equation (4) a chronosome compacted to 1 km^2 at 1 km burial depth, if deposited in the same amount of time, will end up being assigned the same calculated sand:shale ratio as a chronosome compacted to 1 km^2 at 8 or 10 km burial depth, even though the deeper chronosome will have a higher sedimentation rate when decompacted.

In the case of Griffiths and Hadler-Jacobsen's (1995) work, most of their chronosomes were buried to a similar depth and can therefore be assumed to have undergone a similar burial history and, therefore, the application of equation (4) is reasonable. In the Roebuck Basin, chronosomes have undergone considerably different burial histories and it is necessary to take this into account. To overcome this problem in the Roebuck Basin, equation (4) was performed over three stratigraphic intervals - Unit VIII to CT-1, CT-1 to RA-1 and RA-1 to C6-2. These intervals were large enough to allow the definition of a good lithology distribution but allowed the comparison of similarly compacted chronosomes.

After calculation of the sand:shale ratio, decompaction of each chronosome was undertaken to obtain an uncompacted sediment input rate. The modelling software used in Chapter 5 uses two compaction algorithms, one for the sand fraction and one for the shale fraction to compact sediment. For sand, Sclater and Christie's (1980) algorithm, empirically derived from North Sea data, was used;

$$\ln\frac{\phi_0}{\phi_z} = \frac{z}{3.7} \qquad (6)$$

where z is the depth of burial in km, ϕ_0 is porosity at the seafloor and ϕ_z is the porosity at burial depth z. For shale, Baldwin and Butler's (1985) algorithm was used;

$$(1-\phi_z)^{6.35} = \frac{z}{6.02} \qquad (7)$$

where z is the depth of burial in km and ϕ_z is the porosity at burial depth z. Griffiths and Hadler-Jacobsen (1995) rearranged equations (6) and (7) to produce two decompaction algorithms, one for the shale content and one for the sand content in each chronosome. The sand content was decompacted using (modified form of equation (6));

$$Q_{sd} = \left[\frac{1-\left[\phi_0 \Big/ \exp(z/3.7)\right]}{1-\phi_0}\right] \times F_{sd} \times Q_{tc} \qquad (8)$$

where Q_{sd} is the decompacted sand input in km^2ka^{-1}, z is the midpoint depth of the thickest part of the chronosome, Q_{tc} is the total compacted sediment, F_{sd} the sand fraction of the total compacted sediment input and ϕ_0 the initial seafloor porosity of sand. The shale content was decompacted using (a modified form of equation (7));

$$Q_{sh} = \left[\frac{(z/6.02)^{1/6.35}}{1-\phi_0}\right] \times F_{sh} \times Q_{tc} \qquad (9)$$

where Q_{sh} is the decompacted shale input in km^2ka^{-1}, F_{sh} is the shale fraction of the total compacted sediment input in km^2ka^{-1} and ϕ_0 the

initial seafloor porosity of shale.

A value of 0.49 was used for ϕ_0 in equation (8) based on the work of Pryor (1973) a value of 0.75 was used in (9) based on the work of Baldwin and Butler (1985). The variable z was redefined as "*the midpoint depth of the thickest part of the chronosome*", rather than "*the depth to the midpoint of the chronosome*" as it was first defined in Griffiths and Hadler-Jacobsen (1995). As with the time to area conversion, this results in a more appropriate value for the decompaction of the bulk of the sediment that makes up the chronosome.

Depth conversion of each chronosome was semi-automated using a Fortran macro written by Mitchell (pers. com.) to depth convert TWT values using the Dix (1955) formula.

The sediment budgets calculated during this study were plotted against time and are shown in Figure 3.17. However, it is appreciated that the method used to derive them is an over-simplification of the sediment budget of the Roebuck Basin. In reality, the area of a preserved chronosome is the result of a number of processes, such as erosion and out-of-plane sedimentation.

In sedimentary modelling, if an open system where sediments may enter and leave is used, it is important to predict the amount of erosion products that have left the section in order to model the correct chronosome geometries. More sediment is required to construct a chronosome geometry than is preserved. One way that Griffiths and Hadler-Jacobsen (1995) suggested to predict eroded volumes was to compare observed chronosome geometry with a library of known geometries. A prediction can then be made as to the amount of missing section. Another possibility would be to compare the difference between the locally derived coastal onlap curve to other regionally derived onlap curves. Any short-fall in coastal encroachment between each curve may represent missing section and allow a semi-quantitative method of predicting the amount of truncation of the chronosome due to erosion.

Taking erosion products into account using the above methods does result in problems, as both methods increase the sediment input rate even though some volume of eroded sediment will be preserved in the section, usually in the form of lowstand products. These redeposited sediments will already be included in the sediment budget at a later time period. The problem is not so much one of predicting the total sediment volume but ensuring that sediment input timing is correct. In a small data set, identification and correlation of truncated chronosomes and their associated lowstand deposits may well resolve this problem and lead to the development of a more accurate sediment budget.

The Roebuck Basin is a rift basin, that represents only part of the sedimentary record that is preserved on the Australia continental margin. As no prediction of the sediment budget, subsidence history or original topography of the other rifted half of the basin could be made, it was necessary to close the system to preserve the sediment input during modelling undertaken later in Chapter 5. A "wall" was placed at the basinward end of each model to trap sediment in. This model is effectively a half-graben. In this case, no erosion products were lost from the system and extra sediment cannot be added to the system without increasing the overall volume of the final model, the size of which has been directly measured from the preserved section. As each line was regional in nature it was hoped that most of the autochthonous sediment was redeposited more distally "in-section" and little would have been lost from the basin. Evidence for such an assumption exists in the fact that on seismic data, sediment deposited after the CT-1 event tend to downlap out before reaching the present day margin.

3.5 Construction of coastal onlap and relative sea level curves

The coastal onlap curve represents the lateral movement through time of the proximal depositional edge of topset deposition (Emery and Myers, 1996). Coastal encroachment of coastal

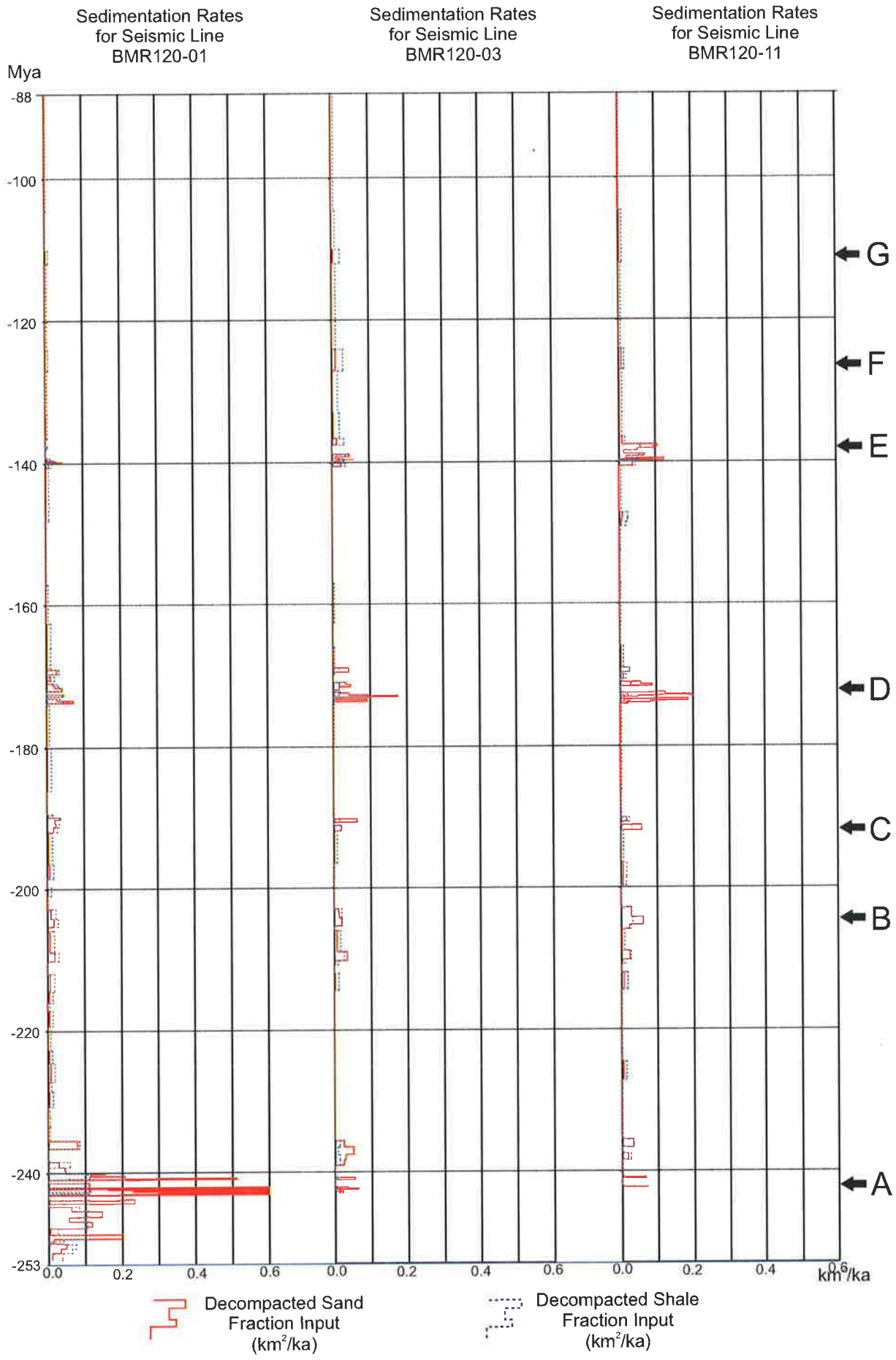

Figure 3.17 Sediment input rates for lines BMR120-01, BMR120-03 and BMR120-11. Major pulses of sedimentation were identified during tectonic episodes marked by A to G.

onlap is the result of a relative sea-level rise. Coastal toplap and a basinward shift in coastal onlap indicates a relative sea-level fall.

The chronostratigraphic chart provides the basis for the construction of a coastal onlap curve. The most landward point of each chronosome was simply plotted with time. As only the preserved coastal onlap can be plotted, encroachment of coastal onlap is inevitably always underestimated. Prolonged erosion will remove the upper portion of each chronosome resulting in a truncated landward termination. Coastal onlap that is preserved landward of the data set cannot be accurately recorded without extending seismic coverage. In addition to underestimation of coastal encroachment, the mis-identification of marine onlap deposition due to sedimentary by-pass can lead to an overestimate of the amount of regression occurring in the basin.

As with the construction of a chronostratigraphic chart there are several advantages of working with a 3D data set over 2D data. In 3D, an increased opportunity exists to record the maximum extent of coastal onlap and to identify periods of sediment by-pass. For the Roebuck Basin individual dip lines in each major depocentre and for the 3D data set were used so that a comparison of local versus regional conditions could be made.

Lines BMR120-01, 03 and 11 were each chosen as being the most representative dip lines for their respective sub-basins in the data set. Positional data in the form of X-Y coordinates for each chronosome were directly output for each 2D line from 3D-Grid and read in to a standard spreadsheet. The X-Y data were converted to a distance from the landward end of the line and re-scaled from 0 to 1 in accordance with the published onlap curves of Haq et al. (1987). In addition to the 2D lines, the 3D spatial outline of each chronosome was plotted out (Fig. 3.15). The most landward encroachment of each chronosome was then measured from a semi-circular reference line which has, from seismic interpretation, remained a fairly constant hinge-line since the late Permian *Unit VIII* event (Fig. 3.14). The resulting coastal onlap curves defined for each dip line and the whole 3D data set are shown in Figure 3.18. All curves were scaled to the Harland et al. (1992) time-scale.

Relative changes of sea-level can be determined from measurements of the vertical change in height of coastal onlap in marine sequences, deposited landward of the offlap break (Vail et al., 1977: Part 3). Relative sea-level changes result from the combination of fluctuations in eustatic sea-level change and total subsidence (tectonic and isostatic) (Fig. 3.19). The relative sea-level (Fig. 3.19) derived for a solitary one dimensional point in the basin relates to the subsidence curve at that unique location. The coastal onlap curve shown from the Roebuck Basin is, however, derived from a 3D data set and to a certain extent reflects overall eustatic and regional tectonics occurring in the basin. A comparison of the coastal onlap curve determined for the Roebuck Basin with that of the Haq et al. (1987) curves reveal several departures (Fig. 3.18). Although there is no *a prior* reason why the Haq et al (1987) eustatic curve should be expected to match the relative sea level curve derived for this basin, the comparison may be of interest. The departures are interpreted to result from regional tectonic events such as, regional uplift or rapid subsidence. However separating the local subsidence history from a true eustatic curve (assuming that the Haq curve is still subject to error) is still problematic.

Our ability to model the higher frequency small scale tectonic changes in subsidence is limited, especially those incorporating uplift where the amount of missing section is difficult to predict. However, the coastal onlap pattern does give a first approximation to the nature and extent of these events. To estimate the extent of the high-frequency tectonic fluctuations in the Roebuck Basin an attempt was made to scale the coastal onlap curve into a relative sea-level curve (measured relative to base level in similar fashion to the eustatic sea-level curve). This curve reflects both the eustatic and tectonic signal for the basin

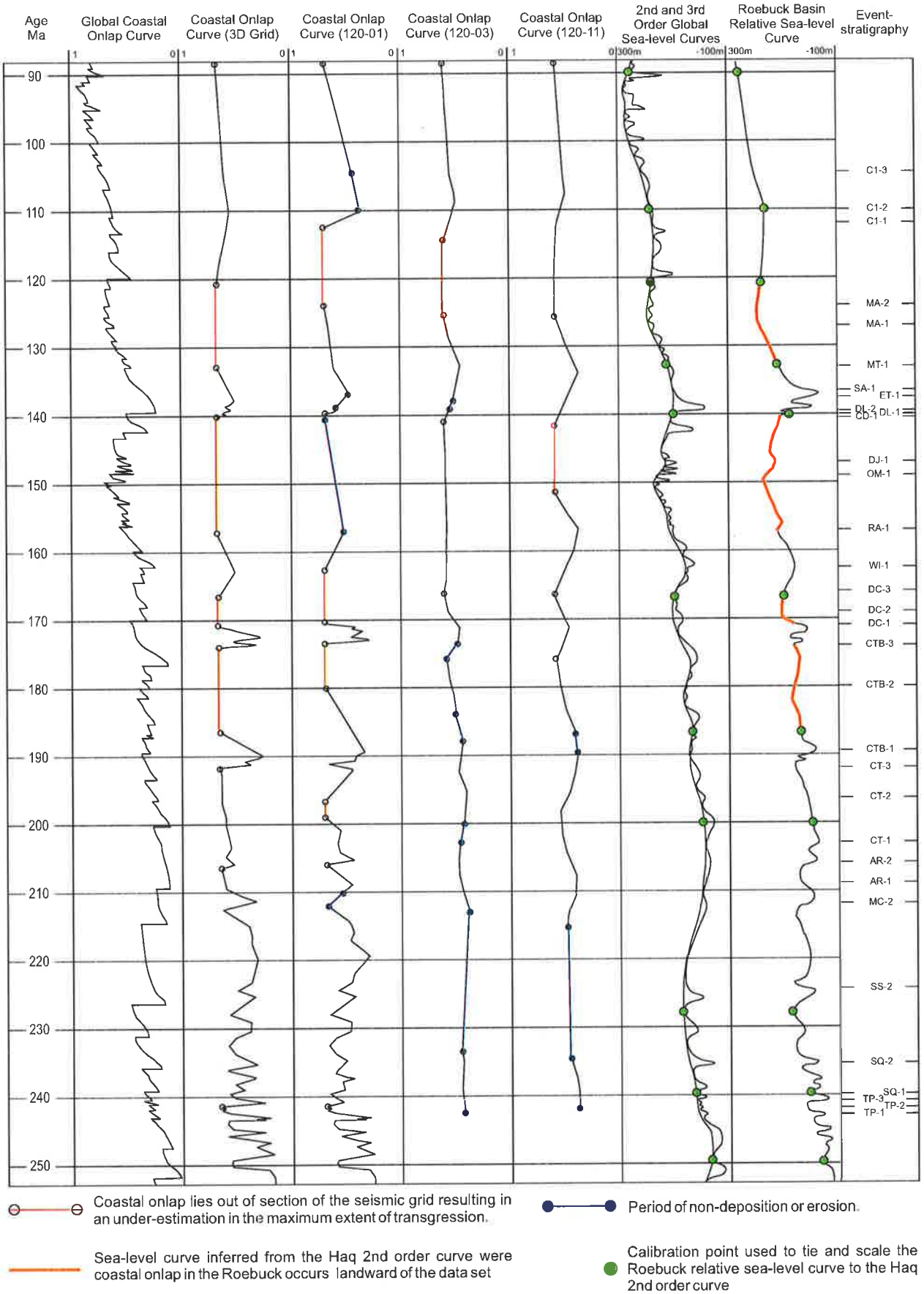

Figure 3.18 Coastal onlap curves for seismic lines BMR120-01, 03 and 11 and the 3D data set as a whole and the higher frequency 'relative sea-level' curve derived for the basin. The global Haq et al (1987) coastal onlap and eustatic sea-level curves are included for reference.

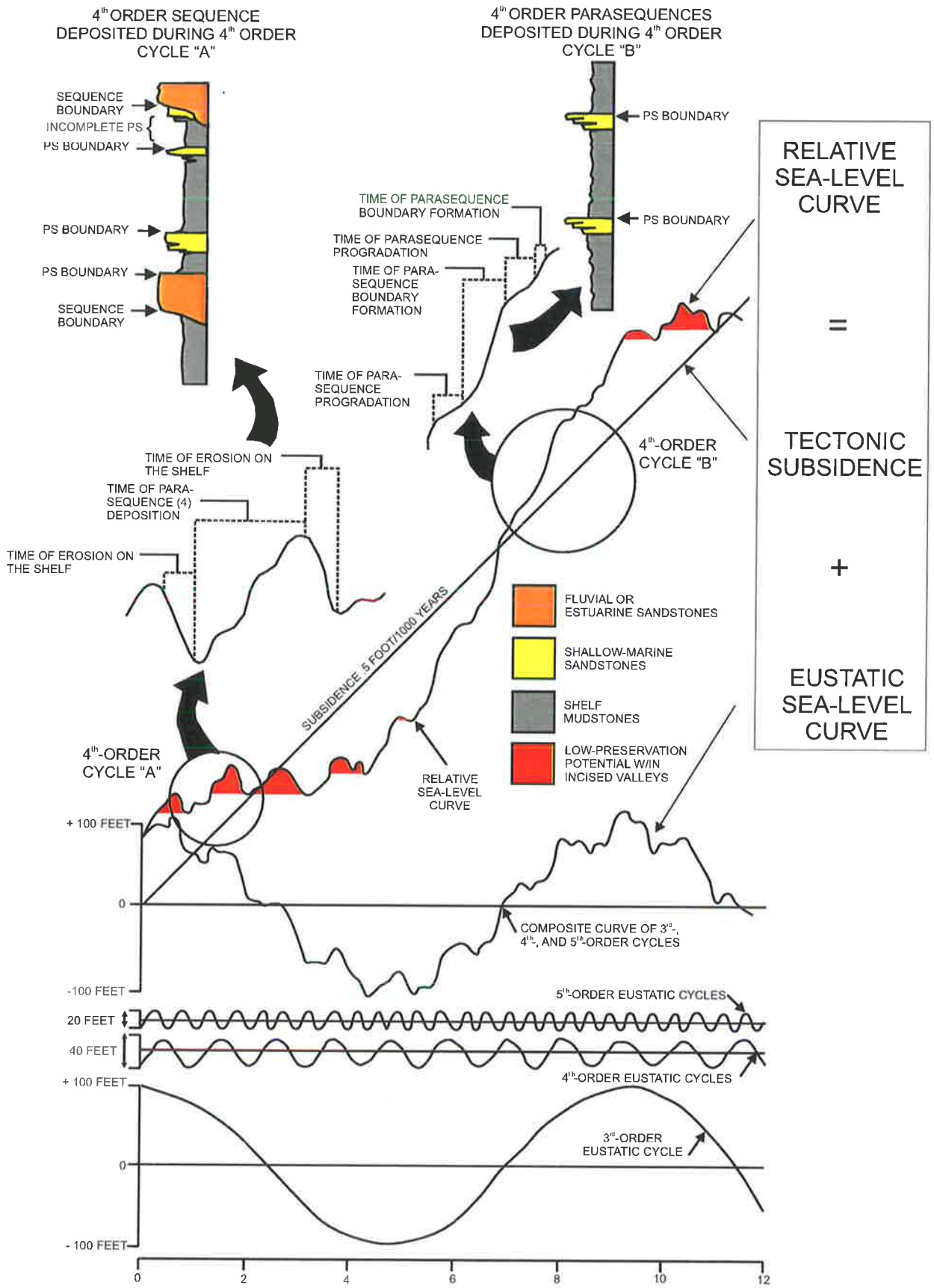

Figure 3.19 The definition of relative sea-level (from Van Wagoner et al. (1990)).

as a whole. To do this the combined onlap curve was rescaled relative to the Haq et al. (1987) 2nd order eustatic sea-level curve. On each curve points were tied in areas away from major departures between the two and then the onlap curve was rescaled using a linear function - relating relative change in coastal onlap to change in relative sea-level between each point. The results are shown in Figure 3.18. By pinning the coastal onlap curve to the global sea-level curve the effect of general basin subsidence is effectively removed and only eustatic and high frequency tectonic departures due to rapid subsidence or uplift were preserved. However, several major assumptions were made during the re-scaling operation:

- the basin is generally subsiding,
- each control point falls on part of the curve that is dominated by the eustatic signal,
- that the original scaling of the 2nd order global eustatic sea-level curve by Haq et al. (1987) (based on work by Pitmann (1978)) is accurate),
- between each control point the ratio of coastal onlap fluctuation to vertical relative sea-level fluctuation remains constant,
- that tectonic effects are of regional extent.

The validity of these assumptions in identifying and predicting the magnitude of high-frequency departures from any global sea-level curve are a controversial part of the methodology as the uncertainties in the processes are difficult to assess. For this reason the implications of using this derived sea-level curve are addressed in more detail in Section 4.4.4.

3.6 Chronostratigraphic Results

Chronostratigraphic mapping has provided information regarding sediment distribution, depositional style, sediment rates and regional sea-level fluctuations through time. These products were used in two ways; firstly, they were incorporated into an overall synthesis of the basin's development and basin-fill history detailed in Section 3.7, and secondly, they were used as input parameters for forward sedimentary modelling (Chapter 4). Here, the general results of chronostratigraphic mapping are presented.

Figure 3.20 shows an interpreted chronostratigraphic section (BMR120-01) across the Bedout Sub-basin, Bedout High and Rowley Sub-basin. On this line major periods of transgression, regression, non-deposition and erosion are highlighted. Distinct basin-fill styles can be interpreted that reflect changes in sedimentation rates and depositional processes. Five major depositional phases were identified in the basin during the Late Permian to Late Cretaceous interval. These depositional phases are interpreted to reflect changes in tectonic deformation of the basin and have been used to divide the sedimentary section into megasequences described in Section 3.7. The sediment distribution and style during each one of these depositional phases is presented here.

3.7 Tectonic Development and Basin-fill History

3.7.1 Megasequence Division

Regional structural and megasequence mapping undertaken during this study have shown that the area occupied by the Roebuck Basin developed as a result of a multiphase rift history under four main stress regimes:

- Stress I - NE-SW extension resulting in an intra-cratonic fracture sequence associated with the separation of the Chinese blocks from Gondwanaland during the Cambrian to Silurian. Three intra-cratonic fractures were developed; the Petrel, Canning and Southern Carnarvon Basins.
- Stress II - a transition phase from NE-SW to NNW-SSE extension associated with the separation of the China-Burma-Malaya-

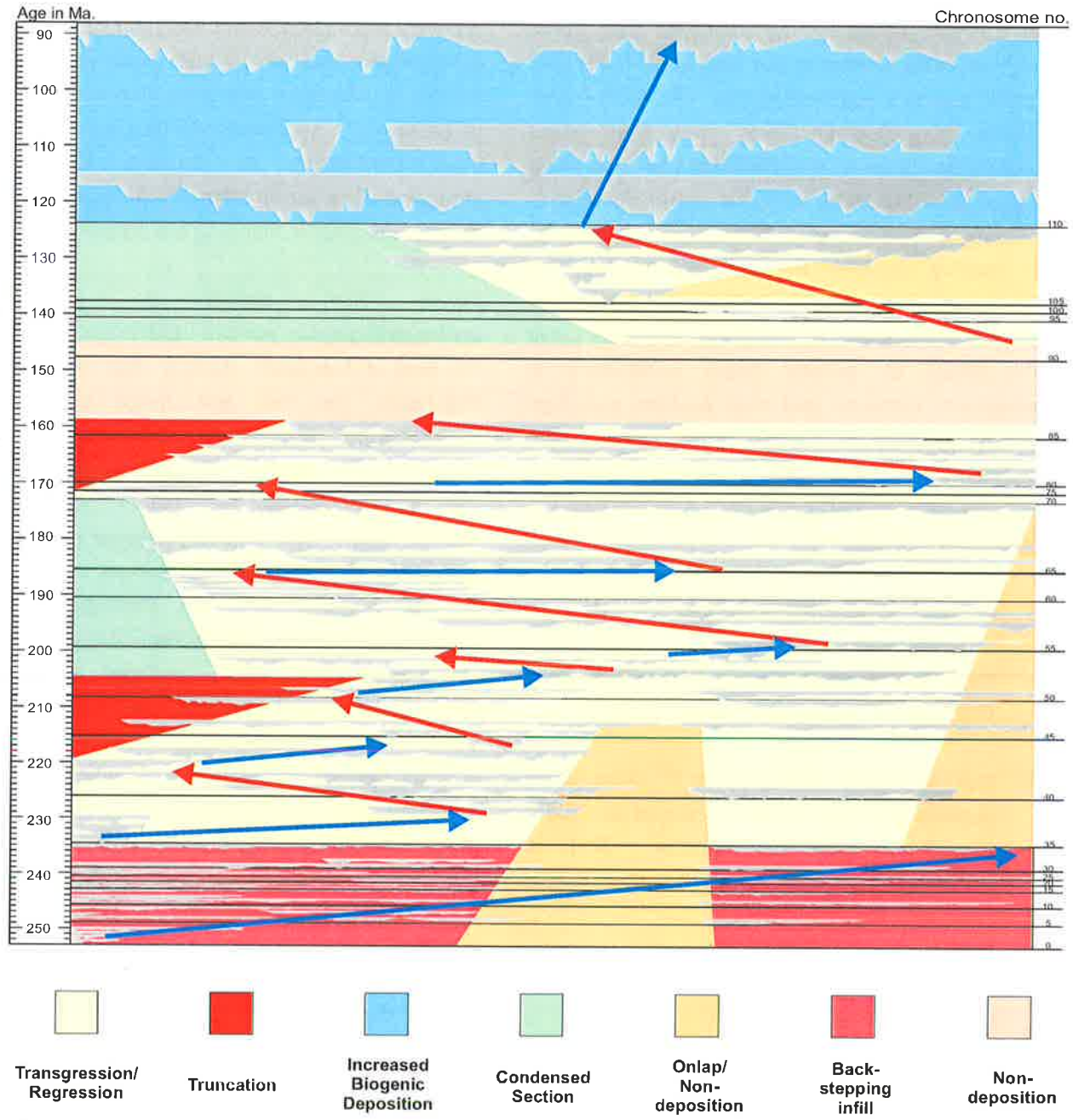

Figure 3.20 Interpreted chronostratigraphic summary of line BMR120-01 (showing gross trends).

Sumatra (SIBUMASU) blocks during the Late Carboniferous to Late Permian with development of both NW-SE and ENE-WSW oriented structures.

- Stress III - NNW-SSE post Late Permian extension during separation of 'Argoland' during the formation of the Westralian Superbasin sequence.

- Stress IV - NE-SW compression during collision with Asia during the Middle Miocene to Recent.

The area occupied by the Roebuck Basin can be considered as a series of stacked sedimentary basins consisting of the Canning Basin during the Ordovician to Late Carboniferous and the Roebuck Basin for the Permian to Recent.

During the four major stress regimes described above, eleven basin forming phases have been identified which have also been used to divide the basin-fill into megasequences:

1. Early Ordovician – *Base* (base Pz1 Extension Phase 1) – initiation of NE-SW intra-cratonic

extension. Triple junction development to the NNW of the Canning/Roebuck Basins and Chinese blocks separation from North West Shelf (NWS).

2. Late Devonian - *Dev* (base Pz2 Extension Phase 2) – a period of rejuvenated NE-SW extension during the Pillara, Van Emmerick and Red Bluffs Movements.

3. Late Carboniferous – *Stage 1* (base Pz3 Transition Phase 1) – transpression during the Meda Movement followed by a transition from NE-SW intra-cratonic extension to NW-SE extension during initiation of the Westralian Superbasin (Yeates et al., 1987) and the separation of the remaining China-Burma-Malaya-Sumatra (SIBUMASU) blocks from the North West Shelf.

4. Late Permian – *Unit VIII* (base Mz1 Sag Phase 1) – major uplift, erosion and faulting during the Bedout Movement (Forman and Wales, 1981). Deposition of volcanics and change in structural style from fault controlled subsidence to thermal subsidence.

5. Middle Triassic – above *SQ-2* (base Mz2 Extension Phase 3) – end of a major transgressive cycle resulting from rapid sag. Transpressional features seen in the Rowley, Bedout, and Oobagooma Sub-basins and the Fitzroy Trough as part of the Fitzroy Movement (Forman and Wales, 1981).

6. Early Jurassic – *CT-1* (base Mz3 Sag Phase 2) – a period of tectonics and erosion especially on the outer margin associated with rift shoulder development. Possibly related to the separation of an unknown sliver of continental block from the Rowley Sub-basin under NNW-SSE extension. End of the Fitzroy Movement of Forman and Wales (1981).

7. Early Jurassic – *RA-1* (base Mz 4 Sag Phase 3) – Argo Land plate separation NNW-SSE during extension. Rift shoulder development on outer margin. Initiation of sea-floor spreading in the Argo Abyssal Plain.

8. Early Cretaceous – *SA-1* (base Mz5 Sag Phase 4) – Australia-India plate separation during WNW-ESE extension. Initiation of sea-floor spreading in the Cuvier and Gasgoyne Abyssal Plains.

9. Middle Cretaceous – *C1-1* (base Mz6 Passive Margin Phase 1) – M0 spreading-ridge jump in the India Ocean and the Australia Southern Margin-Antarctica separation. NW-SE oblique-slip leading to inversion in the Oobagooma Sub-basin. Reduction in clastic sediment supply and passive margin development.

10. Base Tertiary – *C13-1* (base Cz1 Passive Margin Phase 2) – regional change in sedimentation style to predominantly carbonate deposition. Initiation of northward plate drift of Australia and a N-S compressional event.

11. Late Tertiary – *N14-1* (base Cz1 Passive Margin Phase 3) – Australia Northern Margin –Eurasia plate collision. NE-SW left-lateral oblique slip reactivation.

It is inherent from the above description that each basin phase is strongly related to the development of five break-up events that have affected the northwestern margin of Australia. Four rifts have been previously identified and well documented in the current literature, occurring in the Cambrian, Early to Late Permian, Middle Jurassic and Early Cretaceous. A possible fifth rift event which developed during the Early Jurassic has been identified during this study. This event has previously been considered to be the rift onset for the Middle Jurassic breakup episode.

Although the Palaeozoic evolution of the Roebuck Basin has been detailed as accurately as possible it should be emphasized that well constraint is poor. Observations are based heavily on seismic and the dating of events come from well-ties in the onshore area or the margins of the Fitzroy Trough/Oobagooma Sub-basin. The Mesozoic section is more accurately dated using chronostratigraphic techniques and well control.

3.7.1.1 Stress I - Palaeozoic NE-SW Extension

3.7.1.1.1 Extension Phase 1 – Early Ordovician to Late Devonian

Earliest structuring in the Canning Basin area occurred in the Early Ordovician in the Samphire Graben area during Samphire Marsh Movement (Kennard et al., 1994). The oldest rocks currently intersected in the Roebuck Basin are found below the Oobagooma Sub-basin in the Fitzroy Trough section and are Late Devonian in age. However, seismic and well correlations from onshore suggest that rocks as old as Ordovician may also be present at the base of this section. Seismic mapping suggests that sediments deposited throughout the Pz1 megasequence were mainly restricted to the south of the Oobagooma and Bedout Highs (the Willara Sub-basin, Samphire Graben and Fitzroy Trough) (Fig. A1.8 Appendix 1).

Examination of deep seismic data suggests that the Canning Basin succession developed as one of a series of intra-cratonic fractures resulting from brittle failure during upper-crustal thinning associated with the development of a series of triple junctions along the North West Shelf. These triple junctions, initiated in the Ediacaran (570 Ma) adjacent to the Bonaparte Basin and the Cambrian (505 Ma) adjacent to the Canning and Carnarvon Basins, eventually linked together to form the successful Cambrian rift of Chinese blocks from Australia and the development of the Palaeo-Tethys Sea (Veevers, 1988). The Bonaparte, Canning and Carnarvon Basins formed as a series of failed-rifts or 'aulacogens' adjacent to the successful rift margin.

Veevers (1988) suggested that the Chinese blocks rifted under a NW-SE extensional tectonic regime and the Bonaparte, Canning and Carnarvon Basins formed under dextral shear. More recently authors (O'Brien et al., 1993, AGSO, 1994, and Etheridge and O'Brien, 1994) have suggested a NE-SW extensional direction based on the development of predominantly extensional features of each intra-cratonic basin. Seismic evidence from the Roebuck Basin clearly suggests that extension occurred in a NE-SW orientation on NE and SW dipping normal fault systems, which resulted in the development of a deep narrow trough situated between the Leveque and Broome Platforms (Fig. A1.6 from 260 to 360 km Appendix 1).

Little is known about the nature of Palaeozoic sedimentation offshore, as few wells have penetrated the sequence. Most authors (Horstman & Purcell, 1988; Passmore, 1991; Lipski, 1993,1994; Colwell & Stagg, 1994) believe that the Palaeozoic sequence in the Roebuck basin is merely an extension of that seen in the onshore Canning Basin. A modified correlation of the onshore stratigraphy from Kennard et al. (1994) is shown in Fig. 3.21. Initial sedimentation is interpreted to have occurred directly on Precambrian crystalline basement originally associated with the Pilbara and Kimberley Cratons. Although basement has not been drilled in the Roebuck Basin, Leveque-1 on the adjacent Leveque Platform is interpreted to have bottomed in gabbroic basement. From well correlations early sedimentation is believed to consist of rift-related clastic deposits (*Nambeet Fm*) prior to the development of more widespread epeiric sea conditions that are known to have existed to the south. Carbonates similar to those found on the Broome Arch and northern Fitzroy Trough were probably deposited on the topographically higher offshore features, with clastic deposition occurring in the adjacent troughs (*Willara Fm and Nita Fm*). Organic rich shales (*Goldwyer Fm*) similar to those which sourced the Blina Field, were probably deposited in the Fitzroy Graben, but the likelihood of their presence in the Bedout Sub-basin to the west is unknown (Passmore, 1991).

Late Ordovician climatic conditions are interpreted to be arid as large volumes of evaporates were deposited in the current onshore area by Romine et al. (1994). Evidence from seismic suggests that salt deposition may extend into the offshore (salt-related detachment) (Fig. A1.10 Appendix 1).

Onshore Ordovician and Silurian sedimentation

was terminated by minor uplift and erosion in the earliest Devonian during a N-S compressional event known as the Prices Creek Movement (Kennard et al., 1994). In the offshore section this event has not been intersected and cannot be mapped with confidence on seismic.

Sedimentation recommenced in the Devonian with the deposition of marine clastics (*Tandalgoo Fm*) and carbonates (*Poulton Fm*). Contraction of the Devonian sea, caused by apparent uplift of the southern Canning Basin in the mid-Devonian, restricted deposition to the offshore Fitzroy Trough.

The oldest penetrations in the current offshore area occur on the Lennard Shelf at Perindi-1, Kambara-1 and Minjin-1, where all three wells penetrated reefal carbonate sequences of Late Devonian age (*Pillara Reef Complex*). Similar limestone reefs are expected on other flanking terraces of the Leveque Shelf, but it is unknown whether reefal build-ups were developed on graben edges to the west which were apparently emergent at this time.

Sedimentation resumed onshore during regional renewed NE-SW extension (Pillara Movement) followed by thermal sag up until the mid-Carboniferous (Kennard et al., 1994). Onshore thermal sag was interrupted by at least two further NE-SW extensional events, the Van Emmerick and Red Bluffs extensional movements (Kennard et al., 1994). In contrast to the onshore – the Latest Devonian Van Emmerick Movement led to uplift and erosion in the offshore section and the development of the deepest regionally correlatable event seen on seismic above basement. This event is interpreted to occur prior to the initiation of a second rejuvenated phase of extension in the offshore area.

3.7.1.1.2 Extension Phase 2 – Early to Middle Carboniferous.

Late Devonian extensional rejuvenation led to more widespread sedimentation over the whole Roebuck area sometime in the Early Carboniferous. Deposition became widespread, although localized depocentres were still active. An examination of the distal ends of lines BMR120-03 and 11 (Appendix 1 Figs. A1.3 and A1.8) show that mid-Carboniferous to Late Permian sediments (below *Unit VIII*) obtained considerable thicknesses basinward (up to 4 s TWT). However, on line BMR120-01 the section does not thicken considerably, suggesting that thickest sedimentation was still highly localized. The *Basement* and *Stage 1* TWT structure maps (Appendix 2 Figs. A2.1 and A2.2), show that these depocentres were restricted to the distal end of BMR120-03 and western end of BMR120-04 and BMR120-07 (Appendix 1 Figs. A1.3, A1.4 and A1.5).

The development of a basin low to the west during the Early Carboniferous is interpreted as a failed triple junction rift arm trending NNW-SSE. This failed rift arm has acted as a focus for crustal thinning and wrenching during the Late Carboniferous and subsequent rift events and has controlled the location of faulting and depositional axis during the Triassic and Jurassic.

Correlation from onshore well penetration suggests that nearshore Carboniferous sedimentation consists of shallow marine and lagoonal clastics (*Laurel and Anderson Fm*). The nature of sedimentation in the far offshore area is unknown, however, considerable thicknesses are interpreted to have been preserved. Large basin down-warps in the western Rowley Sub-basin may have offered restricted conditions for favourable source rock preservation.

Pz2 sedimentation was terminated at the end of Stress Regime I in the mid-Carboniferous during uplift and erosion associated with inversion on Devonian faults during the NE-SW oblique-slip Meda Transpressional Movement (Kennard et al., 1994). The event appears to be linked with the Alice Spring Orogeny in central Australia based on the timing of Shaw et al. (1992).

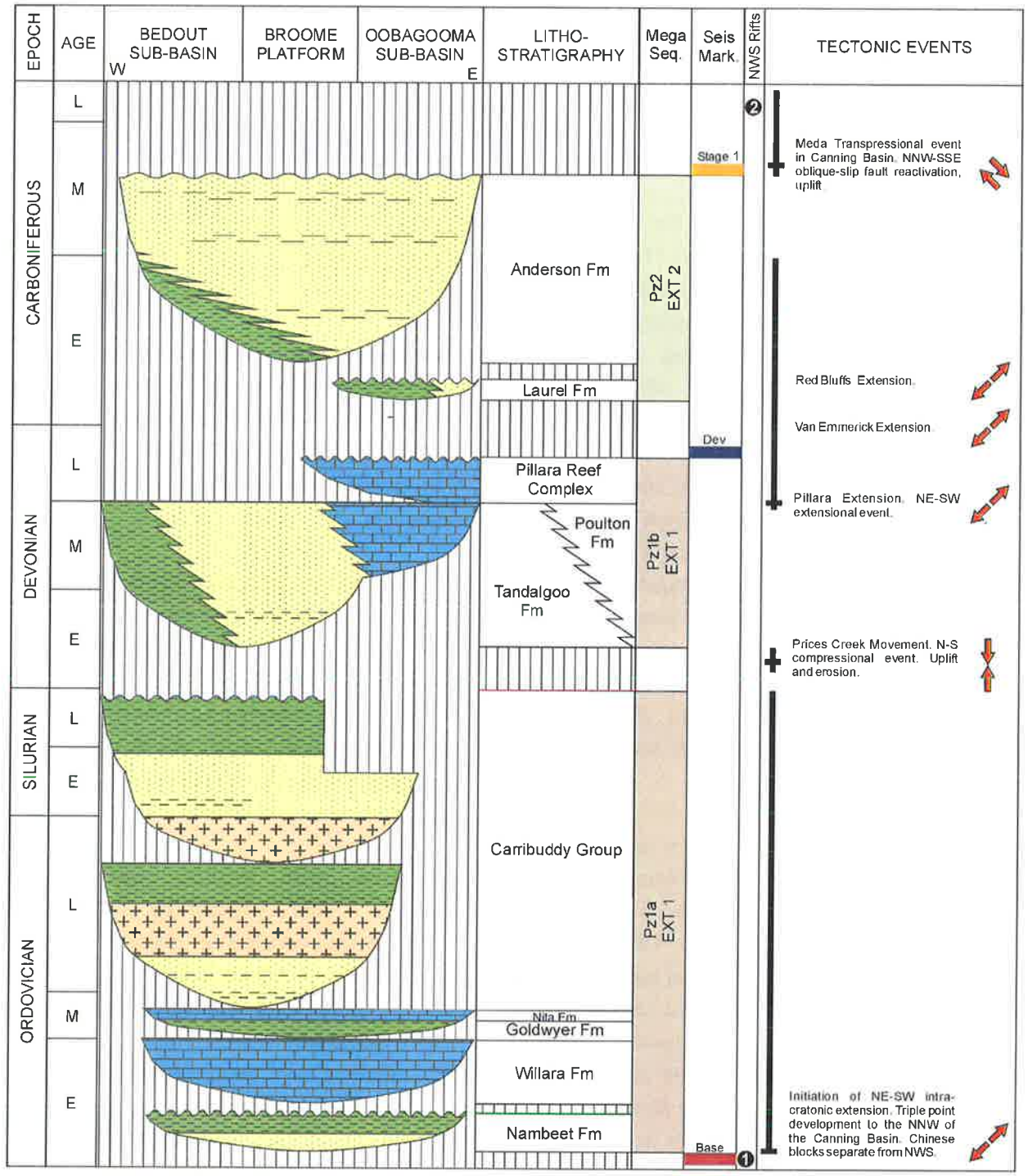

Figure 3.21 Chronostratigraphic summary of the Roebuck Basin. The Palaeozoic section is based on a E-W cross-section across the Oobagooma Sub-basin, Broome Platform and Bedout Sub-basin (modified from Kennard et al. 1994). The Mesozoic to Recent section is based on a N-S section across the Rowley Sub-basin, Bedout High and Bedout Sub-basin and was defined using chronostratigraphic mapping. Colour scheme for seismic markers and megasequences also used for regional cross-sections (Appendix 1).

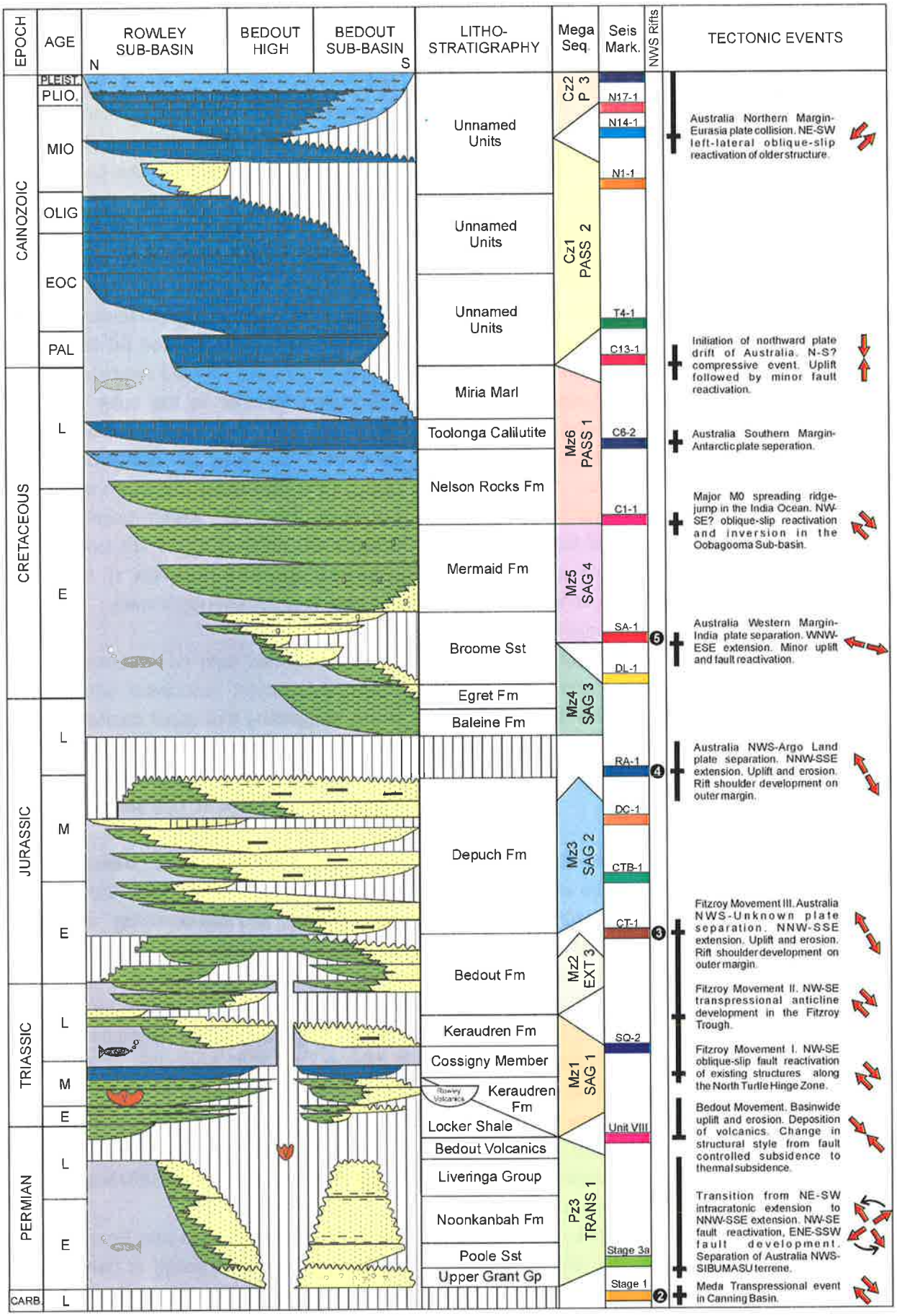

Figure 3.21 Con't.

3.7.1.2 Stress II - Transitional NE-SW to NNW-SSE Extension Phase

3.7.1.2.1 Transitional Phase 1 Latest Carboniferous to Late Permian

The onset of formation of the Westralian Superbasin defined the boundary between the NW orientated Palaeozoic intra-cratonic fracture elements of the Canning Basin and ENE orientated break-up elements of the Roebuck Basin. Although considered by Veevers (1988) to be Late Carboniferous, recent studies by AGSO (1994) suggest a Late Carboniferous to Early Permian time based on timing of regional unconformities across the shelf and the change in tectonic style seen by O'Brien et al. (1993) in the Bonaparte Basin. O'Brien et al., (1993) believe that the change in structural style from a NE-SW extensional direction to a NNW-SSE orientation occurred in the Late Carboniferous to Early Permian. Metcalfe (1988, 1993) considers that an Early Permian time is more appropriate based on the fact that palaeo-climatic, palyontological and palaeo-magnetic information found on remnant continental blocks of the SIMUBASU continental sliver are more closely related to Gondwanaland than the equatorial South China and Indo-China terrenes.

The base of the Westralian Superbasin is considered by other authors to be even later than initially suggested. Cockbain (1989), Hocking (1988), Hocking et al. (1994) and more recently Polomka and Lemon (1996) consider that the base of the Mesozoic succession is a more appropriate division. Polomka and Lemon (1996) suggest that during the Late Carboniferous to Triassic, the North West Shelf area developed from NE-SW intra-cratonic fracture to NNW-SSE orthogonal intra-cratonic downwarp with a distinct migration of structures from north to south in similar fashion to the development of the initial Cambrian rift development. The transition to downwarp first occurred in the Bonaparte area during the Late Carboniferous. However, further south in the northern Carnarvon Basin sag phase geometries only developed after a period of uplift, volcanism and faulting associated with the Bedout Movement in the Late Permian (Forman and Wales, 1981). The concept of a progressive rift history from north to south along the margin is important in explaining many of the transpressional wrench structures observed in the Fitzroy and Oobagooma Sub-basins and is discussed in Section 3.8.4.

In the Roebuck Basin significant NNW-SSE extension is interpreted to have commenced during the Late Carboniferous with the development of large isolated SE to ESE dipping normal faults which formed extensive asymmetric half-graben features in the outer Rowley Sub-basin up until the Late Permian. The best developed examples of half-graben formation occur in the NE Rowley Sub-basin where up to 12 km (5 s TWT) of syn-rift sediments thicken towards the north in a 120 km long half-graben (Fig. A1.3 and A1.8 Appendix 1). In contrast, to the west, less subsidence is seen.

On deep seismic data no evidence for a major crustal detachment associated with these faults exists, suggesting that upper crustal brittle failure occurred in response to lower crustal pure shear mechanisms, with the direction of extension occurring in a NNW-SSE orientation.

In addition to NNW-SSE extension, syn-rift sedimentation during the Late Carboniferous to Late Permian, was still occurring along the pre-existing intra-cratonic fractures of the onshore Canning Basin. Kennard et al. (1994) note that rapid NE-SW extension occurred in the onshore Fitzroy Trough at this time during the Point Moody Extension. NE-SW extension is interpreted to have occurred possibly up to the Late Permian on the bounding faults of the Oobagooma Sub-basin, before a period of major fault inversion during the Middle to Late Permian Bedout Movement.

The Late Carboniferous to Late Permian has been interpreted here as a period of transition from a regime of predominately NE-SW extension to predominantly NNW-SSE extension. The Late Permian Bedout Movement (Forman and Wales,

1981) (*Unit VIII*) is an important division in the Roebuck Basin between the Westralian Superbasin and underlying intra-cratonic fracture/transitional episodes. Not only is the style of structuring different below this horizon, it also marks the end of heavy igneous intrusion (Bedout-1, La Grange-1, Minjin-1, Pearl-1, Perindi-1 and Wamac-1). After volcanism and faulting associated with the Bedout Movement, wide spread transgression resulting from broad intra-cratonic downwarp occurred across the whole of the North West Shelf (Bradshaw et al., 1988). Although differential subsidence was still occurring in the majority of Palaeozoic depocentres of the Roebuck Basin, each became interconnected.

After the initiation of NNW-SSE extension at the end of the Late Carboniferous, sedimentation resumed in the Bedout Sub-basin with the deposition of Early Permian fluvio-glacial, fluvio-deltaic and marginal marine deposits consisting of interbedded sandstones conglomerates and shales (*Grant Group).* These basal units have been intersected in the nearby onshore wells Samphire Marsh-1, Chirup-1 and BMR 4A in the Samphire Graben and are interpreted to continue into the offshore area.

Following regional uplift in the late Early Permian marked by seismic event *Stage 3a*, interbedded sandstones, shales and minor coals, were deposited unconformably over the basal unit of Megasequence Pz3, in a fluvio-deltaic to marginal marine environment *(Poole Sst, Noonkanbah Fm and the Liveringa Group).* The top of the sequence is marked by the extrusion of mid-Late Permian volcanics at the Bedout High. These are the oldest rocks, so far, drilled in the Rowley and Bedout Sub-basins (Bedout-1 and Lagrange-1). Seismic interpretation suggests that sediments of Pz2 and Pz3 age were folded over the faulted core of the Bedout High and extensively eroded during the Late Permian Bedout Movement (Colwell & Stagg, 1994).

In total, five offshore wells; Lacepede-1, Pearl-1, Perindi-1, Minjin-1, and Kambara-1 have penetrated Permian sediments in the Oobagooma Sub-basin. At Lacepede-1A and Wamac-1, the intersected part of the sequence consists of interbedded sandstones, siltstones and claystones with some dolerite sills, minor coals and thin limestone beds. Lithologically, these sediments are significantly different to the present-day onshore part of the basin and are interpreted to reflect a marine depositional environment. High amplitude events of moderate continuity seen in the seismic data (Fig. 2.5 between 8 and 16 km at 1.6 s TWT) are interpreted as dykes or sills which have previously been identified and mapped on seismic in the area by Reeckmann and Meberson (1984).

3.7.1.3 Stress III - NNW-SSE extension

3.7.1.3.1 Thermal Sag Phase 1 – Late Permian to Late Triassic

Triassic development of the Roebuck Basin is dominated by the onset of a period of thermal sag and marine transgression that is characteristic of the whole of the North West Shelf. However, in the Roebuck Basin, only minor structuring was developed in the post-Permian to Recent section. This is unlike other basins on the North West Shelf which have developed large structural trends (the Rankin Platform) in response to Late Triassic and Middle Jurassic rifting (Stagg and Colwell, 1994).

Mesozoic sedimentation during major thermal sag/extension phases has been punctuated by a series of NW-SE transpressional events that have affected the margins of each sub-basin. One of these events was first recognized in the Fitzroy Trough by Forman and Wales (1981), who identified a series of *en echelon* style anticlinal features of Late Triassic age and, therefore, termed the event the Fitzroy Movement. The movement has traditionally been regarded as rift onset for breakup along the North West Shelf in the Callovian (Veevers, 1988), and has been identified in other basins (O'Brien et al,. 1993; Colwell and Stagg, 1994; Etheridge and O'Brien, 1994; Stagg and Colwell, 1994; Symonds et al., 1994). Although correlated across several basins,

the timing of the event is poorly constrained. In the Browse Basin, Symonds et al., (1994) identified movement in the Ladinian, in the Canning Basin the event is of Late Triassic age (Forman and Wales, 1981) and in the Roebuck Basin the event has been dated at Early Jurassic by Colwell and Stagg (1994).

During this study the Fitzroy Transpressional event has been sub-divided into three tectonic episodes occurring during the Middle Triassic (*SQ-1* 240 Ma), Late Triassic (*SS-2* 226 Ma) and Lower Jurassic (*CT-1* 203 Ma). Seismically, two of these events can be observed on the outer margin (Fig. 2.6 corresponding with the 240 Ma and the CT-1 events). On geohistories, the earlier two events are best observed in the Bedout Sub-basin on Figure 3.22 (c) and the youngest event can be seen on Figure 3.22 (b). These events cannot be observed in well data in the Rowley Sub-basin where no penetrations of Triassic sediments have yet been made or in the Oobagooma Sub-basin where a hiatus is developed at this time. The identification of the two oldest events are hindered on the Bedout High by numerous unconformities in the Early and Middle Triassic.

Of these movements Fitzroy Movement II and III represent major changes in depositional style in the basin and have been used to divide the Triassic and Early Jurassic into a predominantly sag controlled phase (Mz1 on Fig. 3.21), followed by an extension related phase (Mz2 on Fig. 3.21), again returning to sag in the Jurassic (Mz3 on Fig. 3.21).

Early Triassic sedimentation is dominated by transgression which is first observed on the outer-margin before migrating landward to onlap the flanks of the Bedout High and older Palaeozoic structures below the Bedout Sub-basin (Fig. 3.20 chronosomes 0 to 35). Dating of the base of the section is poorly constrained. The oldest well penetration of Triassic sediments consists of nearly a kilometre of dark shales in the *T. playfordii* biozone at Phoenix-1. Seismic mapping reveals that there is still some 500 ms of sediment between the base of the well and the Unit VIII seismic pick. These unsampled sediments were deposited over a period of about 10 Myr duration assuming that sedimentation commenced directly after volcanic emplacement used to date *Unit VIII* at the Bedout High and that dating of these volcanics is accurate. Maximum transgression is interpreted to occur towards the top of the *S. quadrifidus* biozone (below event *SQ-2*).

Initially, both accommodation space generation and sedimentation rates are interpreted to be rapid. Geohistory reconstructions of Phoenix-1 show that the basal 1800 m of sediment deposited at this well occurred in approximately 5 Myr (~360 $mMyr^{-1}$ of total subsidence (Fig. 3.22 (c)). From seismic mapping, 26 chronosomes were identified in the sequence dated 253 to 240 Ma (*Unit VIII* to *SQ-1*) and sediment rates were calculated to be three times greater than at any other time in the Mesozoic (Fig. 3.10 to 3.13 and Fig. 3.17 Pulse A).

Areally, early deposition was restricted to the western Rowley and Bedout Sub-basins and the sequence is observed to thin in an easterly direction and onlap Palaeozoic strata (Figs. A2.3 and A3.1 Appendices 2 and 3). Elongate chronosomes were initially developed due to topographic control of the subsiding margin (Fig. 3.15 (chronosomes 1 to 8 and 13 to 18)). Sediment stacking geometries were dominated by aggrading packages typical of 'steers-head' depositional infill. During the *T. playfordii* and earliest *S. quadrifidus* biozones four rapidly deposited sequences were identified in the area. According to Haq et al. (1987) global eustatic fluctuations were also of high frequency during this period (Fig. 3.18). These large lateral movements in coastal location are observed from chronostratigraphic mapping during this period, and are interpreted to result from eustatic fluctuations over a gentle depositional gradient where small vertical changes in sea-level resulted in large horizontal movements of the coastline. Sediments are interpreted to have kept pace with accommodation space generation, resulting in the development of a large coastal plain system in an overall transgressive environment.

The typical sediment volume for each chronosome during each T-R cycle is presented graphically in Figure 3.15. Preserved volumes were greatest during highstand when increased accommodation space was available for deposition, resulting in greater chronosome preservation in the study area.

Although the transgressive basal Triassic section has not been intersected, seismic facies for the basal section and the Early and Middle Triassic are similar, exhibiting higher continuity and frequency content, with less amplitude variability (Colwell & Stagg, 1994). Where this seismic facies has been drilled in the thicker parts of the basin (Phoenix-1), this sequence consists of over a kilometre of Triassic dark marine shales and siltstones (*Locker Shale*) and the basal Triassic is interpreted on its seismic character to be lithologically similar. Marine shales grade landward into Lower Triassic fluvial sands (Keraudren-1 in Fig. 3.7) and vertically into similar fluvial sands of Middle to Upper Triassic age (*Keraudren/Mungaroo Fm)*. From wire-line log character and palyontological environmental indictors these sediments are interpreted to have been deposited onto a coastal plain system in which Keraudren-1 intersected the fluvial non-marine section and Phoenix-1 the nearshore marine influence distal levee system. Strong marine influence is expected basinward. The Pilbara block is interpreted to have acted as the source for sediments which were shed on to the south western onshore Canning Basin and were transported across a prograding fluvial plain (Lipski, 1993).

Deposition was interrupted by Fitzroy Movement I during the Middle Triassic *S. quadrifidus* biozone (*SQ-1* 240 Ma). This event led to the formation of large transpressional wrench-related structures along North Turtle Hinge Zone (Fig. A1.4), faulted anticline highs on the outer margin (Fig. 2.6 horizon 240 Ma), a reduction in the rate of overall subsidence as seen at Phoenix-1 (~18 $mMyr^{-1}$) (Fig. 3.22 (c)) and reduction in sediment rate (Figure 3.17). The lateral nature of such structuring in response to this event is currently unknown due to poor seismic coverage, however, tectonic movement and inverted fault block development of a similar age has been identified by Symonds et al., (1994) along the outer margin of the Browse Basin. These inverted fault blocks in the Browse Basin contain the important Scott Reef and Brecknock gas/condensate reserves.

In addition to faulting, volcanism has also been interpreted on the outer margin (*Rowley Volcanics*) (Fig. A1.2 Appendix 1 between 120 and 160 km). These volcanics appear as a series of high angle bright chaotic reflectors typical of volcanic extrusives developed just above the termination of faulting. It is unknown whether these volcanics were sub-aerially or sub-aqueously deposited.

After structuring during Fitzroy Movement I, regional transgression peaked during the *S. quadrifidus* biozone resulting in the deposition of a carbonate member *(Cossigny Member)*. Regression commenced after the deposition of this carbonate member at around 234 Ma (*SQ-2*) forming a diachronous lithological boundary that youngs to the north, from older dark more marine influenced Lower Triassic shales to younger Middle to Upper Triassic fluvial sediments. Lipski (1993) interpreted this younging event as a northward retreat of the Early Triassic Tethyan Sea that allowed terrestrially sourced fluvial sediments to prograde from the south and southeast. However, seismic geometries do not support this interpretation and suggest instead that transition from marine transgression to regression occurred closer to the *SQ-2* event in the Middle Triassic (areal shape of transgression is indicated by Fig. A2.4 Appendix 2).

Globally, the Triassic is dominated by a major second order sea-level high at the top of the *S. specious* biozone (Haq et al. 1987), 7 Myr later than that observed in the Roebuck Basin. Sequence stratigraphic studies from the Northern Carnarvon Basin, based on more refined conodont biostratigraphy, date the onset of major regression in the very basal *S. specious* biozone (Gorter 1994 (dated 231 Ma on the absolute

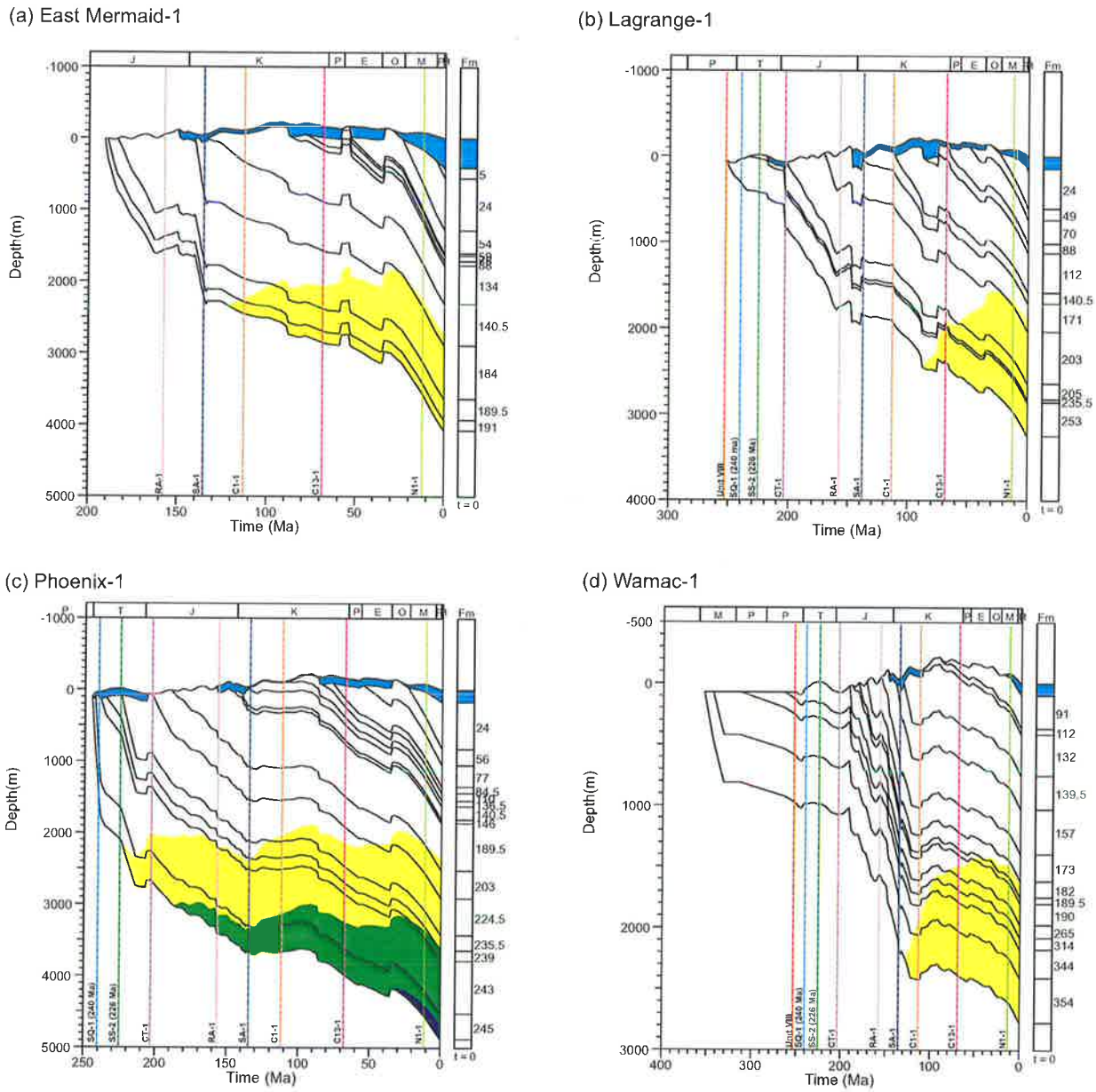

Figure 3.22 Total subsidence curves for key wells (generated from BasinMod™).

timescale of Nicoll and Foster (1994))). The exact timing of maximum transgression is interpreted to be effected by tectonic fluctuations associated with Fitzroy Movement I and II across the North West Shelf.

During the period between Fitzroy Movement I and II deposition rates and total subsidence slowed (~18 $mMyr^{-1}$) and are interpreted to represent the approach of thermal equilibrium in the crust (Fig. 3.17 and 3.22 (c)). 14 chronosomes were deposited in 14 Myr during the period from 240 to 226 Ma (*SQ-1* to *SS-2*) (Fig. 3.10). Although more widespread during maximum transgression, deposition once again became restricted to the western Rowley Sub-basin towards the end of the sequence.

Regressive Mz1 sediments consist of interbedded sandstones, siltstones, and claystones, with minor coals and limestones. Interbedding occurs more frequently at the base of the sequence representing meandering stream channels and overbank deposits (Lipski, 1993).

Renewed subsidence after structuring associated with Fitzroy Movement II at the SS-2 boundary has been taken here as the transition from thermal sag to renewed extension in the basin.

3.7.1.3.2 Extensional Phase 3 – Late Triassic to Early Jurassic

Fitzroy Movement II occurred in the Late Triassic close to the *S. speciosus* and *M crenulatus* biozone boundaries and is contemporaneous with major *en echelon* anticline development identified by Forman and Wales (1981) in the Fitzroy Trough. Offshore the event is not widely documented but appears to have led to uplift on the landward margin and marked the onset of increased rate of sedimentation and initiation of sea-level fall, resulting in a regional hiatus in the Oobagooma and eastern Rowley Sub-basin (Figs. 3.12 and 3.13 between 223 and 214 Ma). This sea-level fall can be observed in the coastal onlap curve and represents a major departure from the global response at this time (Fig. 3.18). Total subsidence in the Bedout Sub-basin and on the Bedout High also increased (~26 $mMyr^{-1}$) prior to uplift and erosion during Fitzroy Movement III (best seen in Fig. 3.22 (c), but also evident in Fig. 3.22 (b)).

The event marking Fitzroy Movement III has traditionally been associated with breakup onset along the North West Shelf. The event occurred during Early Jurassic at the base of the *C. torosa* biozone and marks the onset of a major progradational episode. The event is associated with major uplift across the basin, resulting in erosion on both the inner and outer flanks (sharp contact on wire-line logs and missing *A. reducta* and *M. crenulatus* biozones on the Bedout High (Figs. 2.1 and 3.7)). Structuring on the outer margin at this event appears on seismic to be similar in nature to a rift shoulder development; truncation below, downlap above (Fig. 2.6). Although the observed stratal geometries can be explained in several ways, sediments just below the CT-1 event may represent distal onlap onto a basinward high, thus appearing similar to truncation. However, both the distal onlap and truncation model requires the margin to be uplifted at this time, possibly due to increased heat flow during and flexural rebound after break-up. Truncation of the basinward end chronosomes 42 to 53 can be observed on the outer margin in response to uplift during the CT-1 event (Fig. 3.10 and 3.20).

It is speculatively suggested that this event actually marks a break-up episode previously un-interpreted on the North West Shelf. A small unidentified sliver may have separated from the Argo landmass adjacent to the Roebuck Basin at this time in a similar fashion to 'Argoland' 45 Ma later. The Rankin Platform in the Carnarvon basin may represent a remnant part of this rift system. The outer margin of the Roebuck Basin appears to have remained high as part of a rift-arch system during this time.

For these reasons the Mz2 megasequence has been interpreted as an extensional phase in the basin's development. Onset of deposition during this period marks the beginning of a transition in the overall style of sedimentation from an aggrading basin where sedimentation rates kept pace with increasing accommodation space during the Early Triassic, to one where generations of accommodation space out-paced sedimentation rates leading to prograding wedge type geometries which dominate the basin-fill style until the Late Cretaceous.

During the period prior to CT-1 uplift, between SS-2 and CT-1 (226 Ma to 203 Ma), 13 chronosomes (40 to 53) were deposited in the three major T-R cycles, each of approximately 6 Ma duration. Sedimentation at this time became widespread along the shelf, but deposition was predominantly restricted basinward of the well-developed tectonic hinge-line NW of the Bedout and Oobagooma Highs (Figs. 3.14 and A3.2 Appendix 3). Sediment preservation landward of this hinge-line was restricted to the depositional axis of the Bedout (Fig. 3.14b) and Oobagooma (Fig. 3.14d) Sub-basins during highstand conditions. Although sedimentation rates were low compared to the Early and Middle Triassic, a small sediment pulse was observed along the Oobagooma Sub-basin depositional axis during development of the CT-1 event, possibly representing rejuvenation of the Eastern sediment provenance at this time (Fig. 3.17 pulse B).

Late Triassic to Early Jurassic Mz2 sediments, where intersected in the Bedout Sub-basin, consist of an oxidized redbed succession of multi-coloured micaceous clay and siltstone with thin sandstone lenses. These are interpreted by Lipski (1993) to have been deposited in a low energy, oxidizing environment on a mature alluvial plain (*Bedout Fm*). The unit was 414 m thick in Phoenix-1. However, a lack of preserved palynomorphs precludes accurate internal dating. Sediments above are dated in the *C. torosa* biozone. This unit does not have a complete preserved equivalent in the Barrow and Dampier Sub-basins where this time interval is represented by a major angular unconformity. On seismic, the unit thins to the southeast and onlaps the Palaeozoic sequence at the basin margin. No wells have penetrated Triassic sediments in the Rowley Sub-basin, nevertheless, the presence of the upper portion of this redbed sequence in wells drilled on the Bedout High (low gamma logs below the CT-1 event in Figure 2.1) suggests that this unit extends into at least the southern part of the Rowley Sub-basin (Lipski, 1993, 1994). In the Oobagooma Sub-basin, the Triassic to earliest Jurassic is missing. Lower Jurassic sediments at Lacepede-1 and the Middle Jurassic at Wamac-1 immediately overlie the Late Permian unconformity. Marine regression during the Triassic confined deposition to the Bedout and Rowley Sub-basin and the area west of the Leveque shelf.

3.7.1.3.3 Sag Phase 2 – Middle Jurassic

The Middle Jurassic structural development occurred as a result of ' subsidence after Early Jurassic uplift and erosion during Fitzroy Movement III (chronosomes 54 to 86 (203 to 157 Ma)). Onset of renewed subsidence is evident from Figure 3.22 (b and c). Although the Mz 3 sequence was not penetrated in the Rowley Sub-basin and was absent in the Oobagooma Sub-basin, both East Mermaid-1 and Wamac-1 show subsiding profiles in the late Middle Jurassic (Figs. 3.22 (a) and (d)). Subsidence rates in the Rowley Sub-basin were higher during this period at a rate of 50 $mMyr^{-1}$, compared to 15-20 $mMyr^{-1}$ in the Bedout and Oobagooma Sub-basins.

During deposition of Mz3, a broad prograding wedge consisting of 4 distinct T-R cycles of 5, 12, 14 and 12 Myr were developed (Figs. 3.10, 3.11 and 3.20). Two sediment pulses were identified at around 190 Ma; at the *C. Torosa/C. turbatus* biozone boundary when five chronosomes (60 to 65) were deposited in 3 Ma, and at 172 Ma at the *C. turbatus/D. complex* biozone boundary when 20 chronosomes (70 to 80) were also deposited in 3 Ma (Fig. 3.17 Pulse C and D). These rapid increases in sediment rate correspond with major regressions in the basin (Fig. 3.18), and were interpreted to represent tectonic uplift and rejuvenation of the sediment province associated with events CTB-1 and DC-1 respectively. The occurrence of major biozone boundaries at these major deposition/environmental breaks on the North West Shelf is probably not coincidental but are related to stress-inducing environmental changes experienced by floral/faunal assemblages at this time.

Wire-line log interpretation reveals that the *CTB-1* event coincides closely with a sedimentological change from a braided to a more channel dominated fluvial system. Examination of the isopachs at this time (Figs. A3.3, A3.4 and A3.5 Appendix 3) show that, although major deposition was more widespread, the NW corner of the data area remained a focus for active extension and underwent increased subsidence during formation of a failed rift arm to the major NE oriented rift axis (Thouin Graben). Syn-depositional rifting is evident on the isopachs up until the RA-1 event (Fig. A3.5 Appendix 3). Major localised subsidence during deposition of the CTB-1 to DC-1 isopach has resulted in a 'bulls-eye' on Figure A3.4 (Appendix 3).

In the Bedout Sub-basin, Lower to Middle Jurassic sediments, deposited during sag, consist of a regional blanket of sandstones, interbedded with claystones, siltstones and coals (*Depuch/Legrendre Fm*) that are up to 0.7 s TWT (~1.3 km) thick and represent fluvio-deltaic

sedimentation with occasional marine influences.

In the Rowley Sub-basin a thick Jurassic section (1.3 s TWT, ~2.5 km) developed in the central part of the basin. This section thins towards the west as a result of downlap before being truncated at the margin due to thermal uplift prior to final break-up in the Callovian. The sequence is relatively unstructured.

In the Oobagooma Sub-basin, a broad sag blanket was developed that onlaps the basement of the Leveque Platform in the NE (Colwell & Stagg, 1994). The sequence is thickest along the main axis of the Oobagooma Sub-basin and exhibits only minor fault reactivation. The succession consists of interbedded fluvio-deltaic sandstones, siltstones, shale and coal.

Although most fill consists of fluvial section, nine stratigraphic sequences were identified that could be correlated across the basin during this time interval. Although predominantly in a global rising stage eustatic phase (Haq et al. 1987), little marine influenced section has currently been intersected in wells, and it appears that the Bedout Sub-basin at least has been dominated by sediment supply during this time. The interaction between accommodation space and sediment supply is better balanced in the Rowley Sub-basin and marine incursion is interpreted to be more significant.

During the equivalent time interval in the Barrow and Dampier Sub-basins, rapid subsidence resulted in the deposition of *Lower and Middle Dingo Claystones,* important source rocks on the North West Shelf. Corresponding marine depocentres did not form in the Bedout Sub-basin.

At the time of Callovian breakup (separation of Argoland), the Roebuck Basin's margin underwent a second prominent phase of uplift and erosion with strong truncation of chronosomes 81 to 86 during rift shoulder development (Fig. 3.20 and 2.6). The event can be observed on all total subsidence histories where a hiatus can be seen at this time (Fig. 3.22)

All truly extension style structuring was restricted to the outer margin where failure occurred on a series of massive down-to-the-north normal faults. Deformation occurs over a narrow zone of approximately 10 to 15 km at the apex of the rift system (near the northern end of Fig. A1.2 Appendix 1). The zone widens with distance from the apex to approximately 50 km at the northern end of Figure A1.3 (Appendix 1). Elsewhere, only minor fault reactivation can be observed, except along the Thouin Graben in the NW corner of the study area where rapid sag took place (Fig. A3.5 Appendix 3).

Dredging of the margin has encountered widespread volcanics along both the Roebuck and Browse Basin margins (Ramsey and Exon, 1994) at the time of breakup. Oceanic crust was emplaced adjacent to the present day margin and is imaged well on deep seismic data. The lack of evidence for upper crustal extension suggests that rifting followed by breakup is the result of deep crustal/upper mantle thinning followed, ultimately, by high angle failure of the rigid crust and oceanic crustal emplacement.

3.7.1.3.4 Thermal Sag Phase 3 – Late Jurassic to Early Cretaceous

Late Jurassic break-up marks the end of active rifting along the margins directly adjacent to the Roebuck Basin. The Late Jurassic to Recent development of the basin is best described in terms of a 1st order eustatic continental encroachment cycle (associated with the breakup of a super-continent and controlled by changes in the ocean basin volume related to plate tectonic cycles (Pitman, 1978)). Eustatic continental encroachment was punctuated by tectonic events associated with rifting in adjacent basins rather than along the margin of the Roebuck Basin itself.

Deposition recommenced after final break-up along the margin of the basin. The base of the post break-up sequence is marked by a well-developed regional unconformity associated with outer margin uplift (Fig. 2.6 RA-1 event). During the Oxfordian, the vertical stress regime changed

from a phase of flexure to a phase of slow thermal relaxation and gentle sag resulting in initiation of transgression. The nature of transition from rebound to subsidence is slightly different in each sub-basin (Fig. 3.22). A relatively short period of uplift/non-deposition was identified in wells in the Bedout and Oobagooma Sub-basins (Fig 3.22(c) and (d)), whereas a longer period of uplift and non-deposition was observed on the Bedout High and in the Rowley Sub-basin (Figs. 3.22 (a) and (b)). Timing of subsidence onset between each sub-basin is interpreted to be controlled by relative proximity to the rift axis. East Mermaid-1 in the Rowley Sub-basin was closer to the rift axis and is interpreted to have undergone increased uplift and having been starved of sediment for a longer period. When subsidence returned to this location it was more rapid (~140 $mMyr^{-1}$) than at other well locations (average of approximately ~15 $mMyr^{-1}$ (Fig. 3.22(a)), probably as a result of rapid cooling of thinner crust at this location and the greater potential energy available for subsidence due to increased vertical uplift at this point.

The oldest preserved sediment sampled above the unconformity to date is *R. aemula* in age and occurs near the Leveque Shelf (Lynher-1). Along the margins of the Beagle and Bedout Sub-basins and in the Rowley Sub-basin *W. spectabilis* has been sampled (Jarman-1). Sediments below the unconformity are *W. digitata* in age suggesting a *R. aemula* age for rift onset. However, the exact nature and timing of events during this period are not best predicted in the Roebuck Basin. This is due to sedimentation supply being restricted at this time, resulting in a depositional time break that probably consisted of a degree of erosion followed by condensed section during rapid transgression. Further offshore, initial oceanic crust emplacement is interpreted to have occurred during the last episode of major rifting adjacent to the Roebuck Basin and has been dated at 155.3 +/- 3.4 Ma (Ludden, 1992). This date corresponds closely to an *R. aemula* break-up time (157 Ma). Oceanic crust is overlain by thin distal Tithonian turbidites (Gradstein, 1992).

Faulting associated with the Callovian break-up in the Roebuck Basin was mild and little topography has been generated at the break-up unconformity. In contrast, break-up structuring in the Northern Carnarvon Basin was strong and gave rise to the development of two obliquely intersecting fault-sets trending northeast-southwest and north-south which resulted in horst and graben development in the Beagle and Dampier Sub-basins.

In the Roebuck Basin, initial sedimentation was interpreted to occur in a broad rift-rim basin sag during rapid transgression after break-up due to rapid rates of subsidence combined with low rates of sediment supply (Fig 3.17). Sediments of the transgressive cycle are only poorly developed and the *W. spectabilis* to *E. torynum* sequence is only thinly developed in the Roebuck Basin and is often below seismic resolution. Where preserved, this sequence consists of transgressive marine, commonly glauconitic sandstone (*Egret Formation)* (Lipski, 1993; Colwell & Stagg, 1994). From log data this unit is interpreted to back-step and grade into predominantly shalely marine section until a maximum flood in the Tithonian (*D. jurassicum*) (seen at Phoenix-1 between the RA-1 and DJ-2 event). The onshore time equivalent consists of a fine grained marine siltstone (*Jarlemai Siltstone*). Maximum flood in the Roebuck Basin coincides with a global 2nd order flood and development of a worldwide anoxic event globally associated with the formation of high potential source rocks. The development of this global anoxic event combined with development of restricted Late Jurassic depocentres in the Northern Carnarvon Basin resulted in ideal conditions for source rock development in that area (the important *Upper Dingo Claystone* source rock). Unfortunately, gentle structuring in the Roebuck Basin was not conducive for equivalent development in this area.

Seismically resolvable sedimentation recommenced initially as delta development along the depositional axis of the Oobagooma Sub-basin (Fig. 3.13 chronosomes 86 on). In the Bedout and Rowley Sub-basin after deposition of the transgressive and condensed section, return of major sediment was marked by increased

sedimentation rates between 141 to 138 Ma (chronosomes 95 to 105) (Figs. 3.10 and 3.13 and Fig. 3.17 Pulse E). This was due to rejuvenation of the sediment provenance in response to increased regional uplift associated with the onset of separation of India from Australia.

The first major influx of lowstand sand occurred in the Valanginian *D. lobispinosum* biozone which marks the beginning of a series of 3rd order fluctuations during tectonically enhanced 2nd order sea-level fall (*Broome Sandstone*). From seismic, the Broome Sandstone is interpreted to have formed during forced regression, resulting in shingled geometries and progradation to the north (major basinward fluctuations can be observed on the coastal onlap curves at this time (Fig. 3.18)). The best-developed sands occur in the inboard areas and to the northeast (Wamac-1, Lacepede-1 (Fig. 2.3) and during *S. areolata* deposition, at Keraudren-1). The unit thins and shales out to the north and west where only distal shaley equivalents exist. The isopach of the RA-1 to SA-1 unit clearly shows a transition from syn-rift controlled deposition to delta-fan controlled deposition with point sources from the Fitzroy Trough and the Broome Platform. Sediment supply into the Bedout Sub-basin appears to decrease at this time (Fig. A3.6 Appendix 3).

Although in a more proximal location than either Minilya-1 or Phoenix-1, the section intersected at Keraudren-1 consists of deepwater distal facies. Keraudren-1 is interpreted to be predominantly condensed until deposition during the *E. Torynum-S. areolata* biozones as a result of major sediment switching to the Oobagooma Sub-basin at this time. The depositional axis through the Bedout Sub-basin appears to come from the east and pass to the south of Keraudren-1 prior to *S. areolata* time (Fig. A3.6 Appendix 3).

During *D. lobospinum* deposition at Minilya-1, Keraudren-1 and Phoenix-1, time-equivalents consist of marine fine-grained sediments that, from log motifs, appear to have been reworked into a gentle fine-coarse-fine cycle. Palaeo-environmental indicators suggest that these deposits were formed in marine to deep-marine environments, indicating that deeper-water geostrophic flow was possibly active on the North West Shelf as early as the Lower Valanginian (Fig. 3.7 represented by a thick package at approximately 1600 m in Phoenix-1). Unfortunately, these packages proved difficult to map and their overall depositional shape was difficult to determine.

Contourite or geostrophic flow deposits have been identified in the Northern Carnarvon Basin where they have been attributed to increased ocean circulation patterns after separation of India and Australia (Romine et al., 1997). Change in shape of chronosomes during later outbuilding may represent an increase in the effect of lateral oriented depositional processes such as long shore drift and mark the onset of more open marine conditions (Fig 3.15 chronosomes 97 to 102). More open marine conditions may have developed earlier in the Roebuck Basin, where transition from rift to drift occurred earlier along the outer margin and effects of the India plate separation were more subdued in this area, when compared to other North West Shelf basins.

Later, outbuilding occurred across the basin in a broad, laterally extensive shelf-wide delta front, with highest sedimentation rates occurring in the Oobagooma Sub-basin (Fig. 3.15 chronosomes 97 to 102 and Fig. 3.17). The distribution of high quality Cretaceous sands is interpreted to be partially controlled by a northeast flowing long-shore drift process. Progradation in the Oobagooma Sub-basin occurs to the NNE towards the Browse Basin. At the top of the sand unit a thinly developed blocky sand package was deposited during the final stages of a tectonically enhanced relative sea-level fall of *S. areolata* age at the SA-1 boundary. This package is interpreted to mark the break-up unconformity formed during the separation of India from Australia.

The TWT structure map of SA-1 is presented in Figure A2.9 (Appendix 2). Sediments below SA-1 form a wedge geometry, the downlap edge of which can be seen on the TWT structure map.

Isopach analysis confirms that the Oobagooma Sub-basin was the focus for delta development and deposition during this period of the Lower Cretaceous (Fig. A3.7 Appendix 3).

3.7.1.3.5 Sag Phase 4 – Early Cretaceous to Middle Cretaceous

The separation of India from Australia marked the final break-up along the North West Shelf and led to the development of the 'Cuvier-Gascoyne' abyssal plain. Colwell and Stagg (1994) describe the 'Cuvier-Gascoyne breakup' unconformity as either absent or not recognized over much of the basin. However, uplift associated with break-up, resulted in unconformity development during the Valanginian *S. areolata* biozone and gave way to a very slow period of subsidence in the Rowley and Bedout Sub-basin (~5 $mMyr^{-1}$). Subsidence remained higher (20 $mMyr^{-1}$) in the Oobagooma Sub-basin as a result of isostatic loading due to lowstand wedge/sediment controlled regression (Fig. 2.3), and further proximity from the tectonic disturbance to the west.

Although subsidence was relatively weak over the Rowley and Bedout Sub-basins, increasing accommodation space was developed due to a rising eustatic sea-level associated with this first order coastal encroachment cycle. From chronostratigraphic mapping a change in depositional style can be observed from shorter, rapidly deposited packages to more areally extensive ones (Figs 3.10 to 3.14 at chronosome 105). This possibly reflects increasing wave effect in the basin. On logs, transgression is best observed at Keraudren-1 and Bedout-1, where a transition from progradational to transgressive/aggradational geometries can be observed over the SA-1 boundary (Fig. 2.1 and 3.7).

Although predominantly transgressive, the 1st order flood is punctuated by a series of minor T-R cycles which are predominately below seismic resolution but can be observed on logs. The most pronounced fall can be observed in the Oobagooma Sub-basin during the *M. australis* biozone (between 127 and 123 Ma (events MA-2 and MA-3)) (Fig. 2.3 tie approximately two thirds of the way up between SA-1 and C1-1 and the sediment pulse F on line BMR120-03 and BMR120-11 on Fig 3.17). However, over most of the basin these sea-level falls were weak, forming type 2 sequence boundaries only. Coarse grain sediment input has been observed in the Northern Carnarvon Basin by Romine et al. (1997) who attribute this event to the M5 ridge jump in the Indian Ocean. Important reservoir facies have been deposited in both the Dampier Sub-basin (Wandoo-1) and Browse Basin (Asterias-1) at this time.

Elsewhere on the North West Shelf the *M. australis/A. cinctum* second order sea-level high resulted in a TOC peak in sediments (Loutit et al. (1997). This was not observed in the Roebuck Basin suggesting that more open-marine conditions were prevalent in this area or that organic rich sediments have not yet been sampled in well programs.

Deposition of coarse grained sediment became increasingly restricted to lowstand/stillstand wedges of interbedded glauconitic sandstone in the shelfal areas of the Oobagooma and Bedout Sub-basins that were deposited in an overall transgressive marine to marginal marine unit consisting of claystone *(Mermaid Fm)* (Lipski, 1994; Horstman & Purcell, 1988). Other sediments deposited during this sequence consist predominantly of aggrading marine silts and shales that thin basinward.

Although still undergoing, an overall transgression phase, sea level fall in the Late Aptian resulted in the development of a major regional unconformity in the Roebuck and Northern Carnarvon Basins.

3.7.1.3.6 Passive Margin Development Phase 1 – Middle Cretaceous to Late Cretaceous

The boundary between passive margin and thermal sag phase has been placed arbitrarily at a period of tectonism which is easily correlatable across the whole of the North West Shelf.

The unconformity is associated with plate clearance of India beyond the Exmouth Plateau (Veevers, 1984). Romine et al. (1997) also identify this event as a major sequence boundary, again associated with the M0 plate ridge jump in the Indian Ocean (their date ~113 Ma). The TWT structure map of this event is shown in Figure A2.10 (Appendix 2). Sediment below the event extends further basinward than the SA-1 event, but is truncated landward due to sea-level fall associated with the regressive phase of the first order eustatic cycle.

In the Oobagooma Sub-basin, plate clearance in the Indian Ocean resulted in oblique-slip reactivation and inversion on most of the N-S orientated early Palaeozoic faults, producing a good seismic marker (C1-1). Subsidence rates also slowed dramatically in the sub-basin (Fig. 3.22(d)). In the Rowley and Bedout Sub-basins the resulting unconformity from this event is easily identifiable on wire-line logs and biostratigraphic correlation, however, its character on seismic is very weak. After inversion the Roebuck Basin became part of a broader shelf system incorporating all of the major depocentres of the North West Shelf. Change in depositional unit morphology from a lobate, to elongate, wave reworked longshore drift controlled morphology, can be observed on the isopach map of the unit (Fig. A3.8 Appendix 3).

The basinward shift in deposition due to sea-level fall was quite long lived, spanning approximately 17 Ma (Fig. 3.18 between 127 Ma and 110 Ma). Deposition at this time was dominated by lowstand coarser grained material reworked from the more proximal part of the basin. Increased sediment rates were observed across the area (pulse G in Fig. 3.17). A good example of heavily reworked sediment containing both Jurassic and Lower Cretaceous palynomorphs, deposited during the C1-1, C1-2 and C1-3 events, is observed at Minilya-1 (Fig. 3.7), but can also be seen at Phoenix-1 (Fig. 2.2). Elsewhere in the basin, aggrading marine claystones and minor carbonates were deposited during return to transgressional conditions *(Nelson's Rocks Fm)*.

Gentle subsidence was punctuated by a regionally correlatable erosive event (C6-2) dated at 88 Ma (Fig. A2.11). This event corresponds to break-up on the Southern Margin between Australia and Antarctica and change in spreading rates between Australia and India. The nature of erosion appears from palaeontological indicators to be submarine in nature, possibly as a result of sediment starvation during increased geostrophic circulation. Romine and Durrant (1996) also observed enhanced sub-marine erosion in the Northern Carnarvon Basin which they attribute to increased ocean circulation patterns associated with increasing separation of India from Australia at this time. Submarine canyon development is also evident on seismic data at the northern end of the Oobagooma Sub-basin, suggesting that high-density currents were entering the basin at this time (Fig. 2.9). Upwelling associated with increased ocean circulation, combined with a reduction of terrigenious input into the Roebuck Basin area during extended highstand conditions, has resulted in increased biogenic content of Late Aptian to Santonian sediments. A total organic content high is observed at Pheonix-1 during the *D. multispinum* sea-level high.

According to the Haq et al. (1987) sea-level curve, highest global sea-levels were attained in the Turonian. In the Roebuck Basin the greatest level of transgression and 1st order maximum flood occurs immediately above the regional C6-2 seismic marker at the top of the C6 biozone during the Coniacian. The event marks the transition from middle neritic claystones and marls, to bathyal marls, shale and calcilutites. In starved areas of the basin a carbonate hard ground has been developed as a highly condensed section spanning 10 to 15 Myr. The calicilutite has been termed the Toolonga Calcilutite but its initiation of deposition occurred some 4 Myr earlier in the Roebuck Basin than its named formation equivalent in the Carnarvon Basin. Developed directly above this unit, a bright package with a strong downlap surface can be seen on seismic. A good example of hard-ground followed by down-lap is seen in Figure 2.2. On wire-line logs the Turonian flood is marked by a cleaning up cycle

with the development of purer carbonates as water deepened. The base of the carbonate forms a strong sonic break from fast to slow. The fraction of carbonate within the section diminishes with the influx of highstand shales and is marked by the development of a down-lap surface. This surface marks a very important transition from overall transgressive to regressive basin fill.

Peak marine transgression resulted in landward migration of the major depositional axis and this resulted in the deposition of thin but areally large chronosome packages dominated by fine grained pelagic and distal sediments in the offshore area. As the section became more condensed the biogenic carbonate content of each chronosome increased. The final three chronosomes (111 to 114) were deposited over a period of 25 Myr and the lithological makeup of the last chronosome consists predominantly of calcilutites. Due to the condensed nature of sediments at this time the coastal onlap curve derived during this time is very coarse (Fig. 3.18). After the Late Cretaceous 1st order MFS long-term eustatic sea-level fall was initiated, and increased sediment-flux resulted in reduction in carbonate content of sediments during the C8 biozone.

3.7.1.3.7 Passive Margin Development 2 – Late Cretaceous to Late Tertiary

Later passive margin development was punctuated by several regionally correlatable tectonic events. The first readily identifiable unconformity developed during the basal Tertiary C13 biozone and produced an important seismic marker (C13-1). The C13-1 event appears related to major global second order sea-level fall, possibly associated with the onset of collision of India with Asia and the onset and migration of Australia in a northward direction. A second seismic marker, the T4-1 event was developed during the Paleocene and appears related to a major second order sea-level fall on the Haq et al. (1987) chart. Both events show strong truncation below (Fig. 2.1 and 2.2). However, no sand was recorded in any of the wells at these time intervals and sediments consist of deep water marine mudstones, marls and carbonates. Increase in carbonate deposition probably reflects change to a more favourable climate for carbonate deposition during the northward migration into low latitudes.

Final separation of Antarctica from Tasmania during the Oligocene enabled the development of the Circum-Antarctic Current which resulted in the thermal isolation of Antarctica. Development of thick continental ice-sheets resulted in rapid global sea-level fall and development of the N1-1 sequence boundary. In the Roebuck Basin the event marks an increase of sand into the basin and truncates older Early Tertiary stratigraphy (Fig 2.1).

Post Oligocene deposition is dominated by the development of a massive steep-fronted prograding carbonate foreset wedge system which extends across the inner Rowley Sub-basin. The wedge is clearly visible on seismic and on isopachs (Figs. A1.2 at 220 km and A1.3 at 180 km, 1.5 s TWT (Appendix 1) and Fig. A3.12 (Appendix 3)). Deposition of the wedge has resulted in increased isostatic loading of the shelf resulting in increased subsidence rates (Fig 3.22 (a to d)). Where intersected, wedge sediments consist of shelf to lagoonal calcarenites and dolomites.

3.7.1.4 Stress IV - NE-SW compression

3.7.1.4.1 Passive Margin Development 3 – Late Tertiary to Recent

After a long northward migration, the Australia plate finally collided with Eurasia during the Late Miocene (N17-2). The collision resulted in transpressional inversion of older NNW-SSE trending Palaeozoic faults in the north eastern Oobagooma Sub-basin and Browse Basin, and lead to transtensional wrenching along the footwalls of NE-SW orientated Palaeozoic half-grabens in the Rowley Sub-basin. Late Miocene increased tectonic subsidence is also evident (Fig. 3.22 (a-d)). The development of such features can be clearly seen on seismic data (Fig. A1.3 at 250

km Appendix 1). East Mermaid-1 was drilled on such a feature.

Although only a limited number of inversion features have been identified, when compared with a simple Harding stress diagram they suggests that collision occurred under a NE-SW left lateral stress regime. Major inversion features appear to be focused around the edges of older rigid blocks (the Leveque Platform) and along older Palaeozoic structures. Compressional stresses appear to have been focused along the outer half of the basin during collision.

3.8 Discussion

3.8.1 Comparison of the Roebuck Basin Chronostratigraphy with previous studies

Several studies using sequence stratigraphic and chronostratigraphic approaches have been conducted on the North West Shelf. A non-exhaustive list of the more significant works in terms of approach and findings includes; Kirk (1985), Erskine and Vail (1987), Hocking (1992), Wulff (1992), Arditto (1993), AGSO (1994), Barber (1994), Exon and von Rad (1994), Ross and Vail (1994), Gorter (1994), Labutis (1994), Jablonski (1997), Loutit et al. (1997), Romine et al. (1997) and Blevin et al. (1998).

Most of these studies are basin and interval specific, however, a few are more regional, including the work of; Labutis (1994) who incorporated data from the Northern Carnarvon Basin and Timor Sea areas to build a sequence stratigraphic framework for the Triassic to Cretaceous section of the North West Shelf, Blevin et al. (1998) who defined the sequence stratigraphy for the complete basin-fill of the Browse Basin, and Romine et al. (1997) who described the sequence breakdown of the Cretaceous and Tertiary of the Northern Carnarvon Basin. The latter two studies have presented accurate datings of the major bounding surfaces which provide a means of comparing them with this study's findings. Comparison of previous studies in neighbouring basins with results from the Roebuck Basin is not simple, as structural and sediment processes combine to produce subtle variances in the timing of boundary development. Parkinson and Summerhayes (1985) describe a possibility where, during a sea-level fall, three adjacent basins with subtle differences in their subsidence rates develop unconformities at differing times. In their discussion, the basin undergoing slow subsidence developed a sequence boundary earliest and the basin with the most rapid subsidence did not develop a sequence boundary at all. The sea-level fall in this example did not occur synchronously across these basins. Miall (1992) has argued that the interaction of sediment supply, subsidence and eustasy, can be large enough to make dating of a large majority of the Haq et al. (1987) 3rd order eustatic curve impossible.

In addition to issues of synchronicity, Loutit et al. (1997) point out that for the Early Cretaceous of the North West Shelf, age determination of sequences is difficult due to the scarcity of age-diagnostic bio-stratigraphic markers. This statement is true for much of the North West Shelf biostratigraphic zonation scheme of Helby et al. (1987). To highlight this issue Loutit et al. (1997) plotted error bars on their stratigraphic breakdown for the Early Cretaceous of the Northern Carnarvon Basin to demonstrate the range of possible overlap in sequence boundary dating.

With the above statement in mind, a direct comparison of the dating of major seismic surfaces identified during this study, with those of Romine et al. (1997) for the Cretaceous to Recent of the Northern Carnarvon Basin and Blevin et al (1998) for the Jurassic and older section of the of the Browse Basin, has been made (Fig. 3.23).

Within the Browse Basin the Late Permian (*Unit VIII*) event was identified and dated at approximately the same time as in the Roebuck Basin. An equivalent to the SQ-2 event was also identified but not mapped during the Blevin et al. (1998) study. A distinct event was identified in wells in the Roebuck Basin (*SS-2*) for the *Trmid* event of Blevin et al. (1998). This event was not

mapable on seismic in the Roebuck Basin but has been observed in the Canning Basin where it was termed the Fitzroy Movement, during which transpressional anticline features, uplift and erosion developed in the Fitzroy Trough (Forman and Wales, 1981). Three seismic events were identified and mapped in the Jurassic section of the Browse Basin and timing of the basal and top event correspond to the *CT-1* and *RA-1* events in the Roebuck Basin. Timing of the middle *Jearly* and CTB-1 event is different and highlights the problem of coarse biostratigraphy in the Middle Jurassic. Both events are interpreted in this study to probably represent a period of rift onset and are interpreted to be the same event. In the Browse Basin the *Jearly* event falls within the *C. turbatus* biozone with sediments below and above containing diagnostic assemblages. In the Roebuck Basin this event was also found to fall at the base of the zone but was usually constrained by the *C. torosa* directly below. Unfortunately, the *C. turbatus* biozone spans 17.5 Myr and the potential error in placing the event (shown by the error bar) shows that discrepancies in dating between the two studies could easily be accommodated.

3.8.2 Interaction of sediment supply, coastal onlap and preserved geometries

From an examination of the sediment budget calculated for each line (Fig. 3.17), it is clear that the majority of preserved sediments were deposited during five main sediment pulses with relatively limited background sedimentation between. In addition, each pulse of sedimentation is associated with rapid basinward migration of coastal onlap. Two processes could produce similar sediment geometries to those observed, regression may have resulted from increased sediment supply with little or no corresponding tectonic subsidence so that top-lap was developed and interpreted as coastal onlap, or relative base-level fall/regional uplift occurred resulting in true basinward migration of coastal onlap. Comparison with the global onlap curve shows that these events do not have a global signature.

During this study these events have been interpreted to represent regional episodes of tectonic uplift, which have resulted in rejuvenation of the sediment source province and a basinward shift in coastal onlap. Observations that support this interpretation include, unconformities in wells, truncation on seismic, termination of faulting at these events and major facies changes over these events. However, none of these relate uniquely to an uplift signature – a eustatic fall or combination would also produce these signatures.

Although sedimentation is greatest along the Bedout Sub-basin depositional axis, the Oobagooma Sub-basin depocentre axis became increasingly important for sediment supply during the Cretaceous (Fig. 3.17). The reason for this is unknown, however the importance of this sediment input in relation to good reservoir development in the basinward section of the NE Rowley and SW Browse Basins may be significant from a hydrocarbon prospectivity perspective.

3.8.3 Comparison of coastal onlap and eustatic curves

The onlap patterns that were derived in the Roebuck Basin were compared with the global curve of Haq et al. (1987) (Fig. 3.18). The coastal onlap curve derived for line BMR120-01 and for the 3D data set as a whole has a higher frequency than that of the other two lines. This is a reflection of the fact that BMR120-01 consists of a more complete data set than BMR120-03 or BMR120-11, so more data points were available to construct a curve. In addition, the frequency component of the Early and Middle Triassic section of BMR120-01 and 3D data set is higher than that of the Jurassic and Cretaceous section, again reflecting the number of chronosomes and hence temporal resolution used to define each section.

Ignoring high resolution fluctuations, the general "second order" trends of coastal onlap of each line and the 3D set are similar. When compared with the global curve, similar overall trends were observed. However, frequency differences and

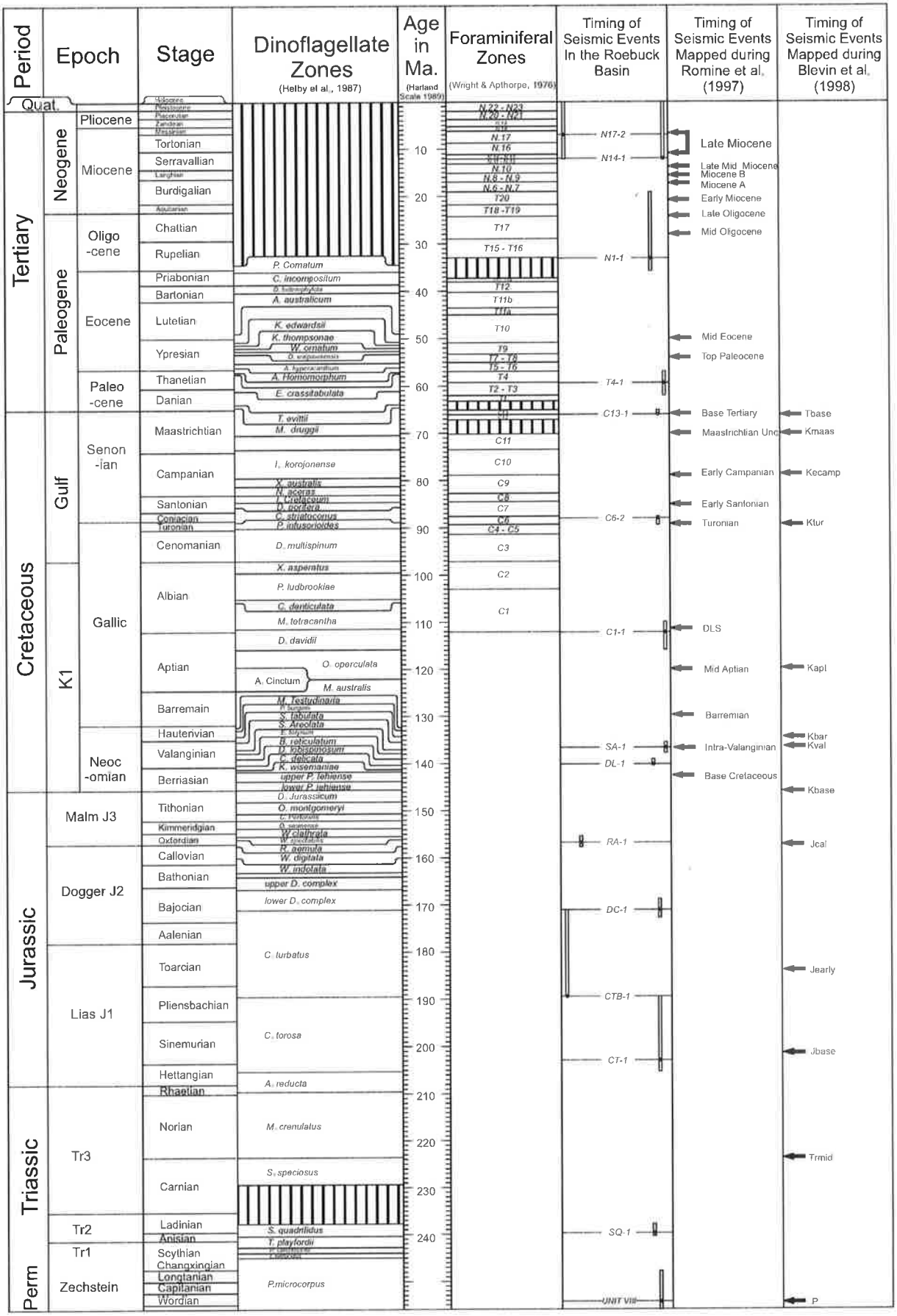

Figure 3.23 Comparison of the dates of major seismic horizons identified during this study with two recent sequence stratigraphic projects. All events are included from Romine et al. (1997). No accurate biostratigraphic data was presented for events younger that Tbase in Blevin et al. (1998).

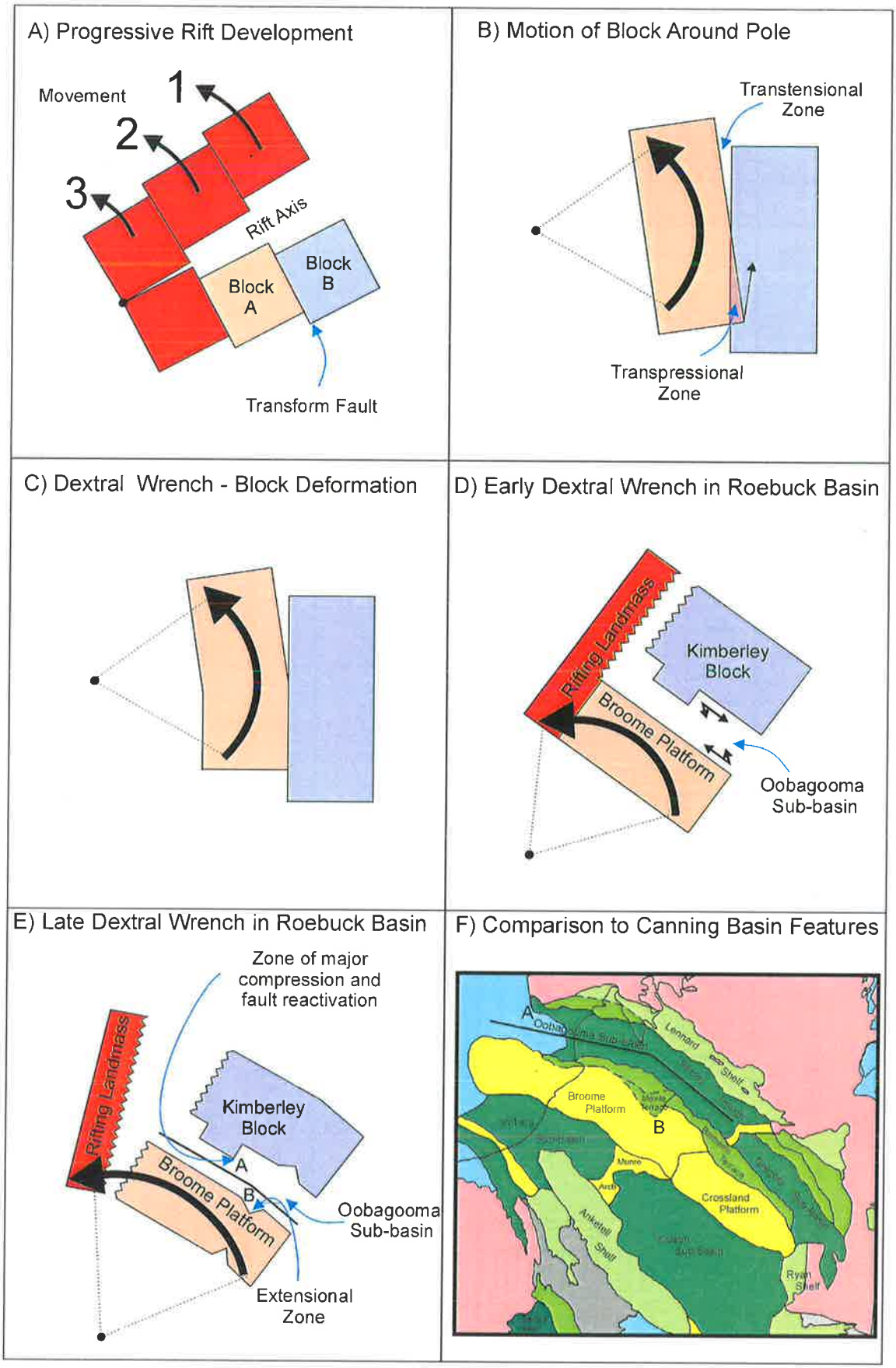

Figure 3.24 Model for progressive rift development along the North West Shelf. (a) Progressive rifting along the shelf showing three distinct movements. (b) Individual block movements showing zones of transpression and transtension. (c) Potential block deformation due to dextral rotation. (d) Effect of early wrenching in the Roebuck Basin. (e) Effect of late wrenching in the Roebuck Basin. (f) The present day structural framework (from Hocking et al.1994) of the onshore Canning Basin.

departures between each curve can be observed. Onlap curves defined for the Roebuck Basin appear to represent a mixture of third order fluctuations on a predominantly second order onlap trend. Departures between the curves are of third order duration and correspond to the tectonically developed sequence boundaries related to rifting that is interpreted to have occurred in the basin. Most noticeable departures occur between 226 to 213, 207 to 203, 192 to 187 and 174 to 171 Ma which correspond to the SS-2, CT-1, CTB-1 and DC-1 boundaries (Fig. 3.18).

Rescaling and smoothing of the coastal onlap curve to form a high frequency relative sea-level curve resulted in a very similar trending curve when compared to the Haq et al. (1987) second order eustatic sea-level curve. The low frequency 'Haq' curve can therefore be considered as representative of onlap patterns developed on the North West Shelf of Australia.

3.8.4 Progressive rift model for the North West Shelf

A comparison of the dating of rift development along the North West Shelf suggests that rifting was initiated in the NE and slowly spread to the SW as progressive blocks separated from Australia. The first magnetic ocean lineaments are dated M26 in the Argo Abyssal Plain, M10 in the Cuvier and Gascoyne Abyssal Plains and M7 in the Perth Abyssal Plain. Oceanic crust to the NE of the Roebuck Basin has been subducted into the Java Trench. The development of older rift sequences also appears to be progressive from NE to SW based on the dating of intra-cratonic rifting in the Bonaparte (Ediacaran), Canning (Cambrian), and Southern Carnarvon (Silurian) Basins.

Figure 3.24 shows a potential theoretical model for progressive rift development around a pole or hinge point, for the North West Shelf, that helps explain the formation of transpressional features during rift development. The model predicts that as rifting progresses from NE to SE transtensional/transpressional stresses will be developed due to differential rotational movement between adjacent blocks. Zones of extensional necking and distortion associated with irregular block shape will also be developed. This model could be developed further using sand/clay-box modelling techniques.

CHAPTER 4

SEDIMENTARY MODELLING

"Now would I give a thousand furlongs of
sea for an acre of barren ground – long heath,
brown furze, anything. The wills above be done,
but I would rather fain die a dry death"

The Tempest
Shakespeare (1611)

4.1 Introduction

Forward modelling is a powerful tool, which if implemented appropriately, is capable of predicting facies distribution away from well control. Not only can modelling be used in a predictive role, but also as an interactive interpretation tool, able to test geological hypotheses for their sedimentological feasibility. In the petroleum industry, forward modelling can be used to identify and test new plays ahead of drilling and can therefore reduce costs.

Due to the current data availability in the Roebuck Basin the area is ideal for sedimentary modelling. Only limited well control, restricted to the inboard margin, exists and only limited regional seismic data has been acquired over the area. Very little is therefore known about the stratigraphy of the outer margin, and thus forward sedimentary modelling can be used directly as a tool for palaeogeographic and lithology prediction as well as hypothesis testing. Such predictions were used to directly develop hydrocarbon exploration play concepts and play element distribution and fairway maps in the area.

Although obviously useful, sedimentary modelling is not a panacea for the undrilled basin. Models are only as good as the input parameters and the algorithms used to drive them. If the results obtained are not reflected in the rock record, it is usually a reflection of the input parameters driving the model.

4.2 Choice of model

The deposition and accumulation of sediments and strata are controlled by a complex set of variables, many of which are not fully understood (Bezdek et al., 1990). Most models are simplifications of the sedimentation process and model only the critical variables required to emulate stratal geometries observed in nature. There are two major types of model available:

- Empirical models based on simple rules of geometry that govern sediment stacking patterns determined by user-defined conditions of sediment supply, sea-level and subsidence, such as SEDPAK (Bezdek et al., 1990).

- Process driven models that go someway to actually model the physical processes of sediment-water fluid dynamics, such as SEDSIM.

Generally, process driven models tend to be highly CPU intensive and usually require greater iteration to make them stable and produce meaningful results. In addition to the method of simulation, both 2D and 3D modelling can be conducted. 2D modelling has limitations when compared to 3D modelling including;

- limited spatial distribution of the simulation,

- requirement to identify a line of section along

true sedimentary dip rather that modelling in 3D the depositional direction,

- only limited control of out-of-plane erosion and sedimentation.

However, advantages of 2D modelling include;

- easily examinable results which can be readily compared with real data, such as seismic data,
- not as CPU intensive,
- input parameters are quicker to obtain and require less information so that input files are easier to set-up.

In general, 3D modelling, due to CPU constraints and the availability of data, is more appropriate where reasonable seismic coverage is available, and the area and time interval of interest is limited. 2D modelling is highly flexible and can be used at a variety of different scales. However, it is more appropriate than 3D when only regional seismic lines are available, the area is large and the time interval of interest is of a long duration. As computers become more powerful 3D models will be increasingly used for regional work.

In consideration of the above comments 2D modelling was deemed more appropriate in the Roebuck Basin. Sedpak modelling software was chosen due to its ready availability at the NCPGG in 1996.

4.3 The Sedpak Modelling Package

Sedpak v4.0 is a 2D stratigraphic basin-fill modelling package written in C for Unix workstations. It is produced under the supervision of Prof. Chris Kendall by the staff and students of the University of South Carolina, USA (Strobel et al., 1989). Sedpak is a geometric model based on empirical principles. It is designed to model and reconstruct clastic and carbonate sediment geometries which are produced as a response to changing rates of tectonic movement, eustasy and sedimentation (Bezdek et al., 1990). Sedpak does not actually emulate the physical processes involved in deposition; transport and erosion. Instead, it tries to simulate them using simple heuristics such as *"if sediment is transported into a cell and the existing slope of the floor of a cell is below a certain critical value, then sediment is deposited - otherwise it is transported to the next cell"* (Griffiths and Hadler-Jacobsen, 1995). Such simple heuristics probably express our current knowledge of long-term depositional processes.

The use of Sedpak has been described by several authors, including Kendall et al. (1986,1991), Strobel et al. (1989) and Griffiths and Hadler-Jacobsen (1995). Griffiths and Hadler-Jacobsen (1995) produced a benchmark paper outlining the use of 3D-Chronostrat™ software as a means of input parameter definition for forward sedimentary modelling and Sedpak in particular. Griffiths and Hadler-Jacobsen's (1995) paper is acknowledged as the framework for the sedimentary modelling undertaken during this study.

4.3.1 How Sedpak Works and the Sedpak sediment budget

A sedimentary basin-fill model, in its most basic form, simply fills available accommodation space through time. Accommodation is defined as the volume that exists between a sedimentary base-level, usually sea-level in a marine environment or the fluvial equilibrium profile in the fluvial environment, and a lower sedimentary marker, often basement, if considering a complete basin (Posamentier and Vail, 1988).

This concept was developed by Jervey (1988) who summarized the major components contributing to changes in accommodation space thus;

$$\Delta\text{accommodation} = \Delta\text{eustasy} + \Delta\text{subsidence} + \Delta\text{compaction} \quad (1)$$

If sediment is introduced into the system and accumulates at a rate that exceeds accommodation space addition, then

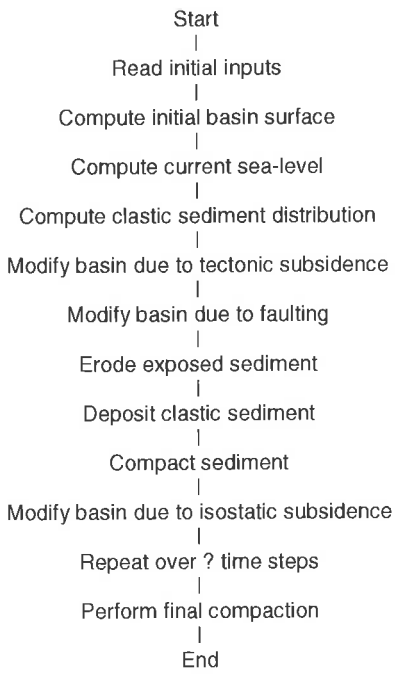

Figure 4.1 Flow diagram of steps in a typical Sedpak simulation (from Strobel et al (1989)).

accommodation space is filled and the basin water depth (remaining accommodation that can be filled) is reduced (Jervey, 1988). Jervey (1988) defined the change in water-depth as a function of eustasy, subsidence, compaction and sediment accumulation:

$$\Delta\text{water depth} = \Delta\text{eustasy} + \Delta\text{subsidence} + \Delta\text{compaction} + \Delta\text{sediment accumulation} \quad (2)$$

The above term represents the basic equation that defines the boundary conditions of a volume that can be filled during forward sedimentary modelling.

Sedpak constructs an empirical model of stratal geometries by simply infilling a 2D basin with a combination of clastic and carbonate sediment (Bezdek et al., 1990). Values are entered for initial basin configuration and as a function of time via a graphical user interface (Bezdek et al., 1990). During this study the following parameters (discussed in more detail in the following section) were defined and modified to examine their effects on over-all stratal architecture; initial topography, clastic sediment supply, tectonic subsidence and eustatic sea-level. Geometries of clastic fill were modelled through time in response to depositional processes previously described. Sediment geometries are plotted and viewed immediately so that parameters can be changed interactively and the program re-run until the resultant geometries are satisfactory (Bezdek et al., 1990).

A discussion of the nature of the input parameters required by Sedpak goes some way towards explaining how the model works. A more detailed description can be found in Strobel et al. (1990) and in the Sedpak Manual (Bezdek et al., 1990). The overall steps involved in the model are as shown in a flow diagram modified from Strobel et al. (1989) (Fig. 4.1).

Sedpak models the input and distribution of sediment across a number of columns over a number of time steps. The number of time steps and columns in the model is user-definable depending on the required resolution of the model. Sediment is distributed between each column, and each column is then treated as a separate 1D model for the purposes of compaction and isostatic loading.

Sediment is input into the model at each time step in the form of a right-angle triangle (Fig. 4.2). The base of the triangle represents a penetration length into the basin (Section 4.5.4). The penetration length is grain-size dependent and variable through time. The triangle of sediment is first distributed over the columns covered by the sediment penetration length. Sediment is allowed to accumulate on a column up until a user-defined depositional angle between neighbouring cells is reached (Section 4.5.5). Once the depositional angle has been reached for a particular cell, extra sediment bypasses that cell until it reaches one where the depositional angle has not been exceeded. Erosion of a column occurs when a user-defined alluvial or submarine angle of repose between two columns is exceeded.

After each sediment distribution step, each column of sediment is then compacted and isostatic subsidence calculated. Combined with tectonic subsidence and sea-level variations,

sediment is distributed throughout the model.

4.4 Sedpak input parameters

All sedimentary modelling packages require quantitative sedimentary input parameters. In the Roebuck Basin, where very little work has previously been conducted, it has taken most of this study to provide the parameters necessary to undertake the modelling. However, the information gathered greatly increased the understanding of the basin. In a sentence, good basin analysis provides the foundation for good modelling.

To run SEDPAK successfully, appropriate lines for modelling must be selected. Then accurate sediment budgets, subsidence histories and sea-level curves must be defined for the duration of each simulation. The derivation of these components for the Roebuck Basin are discussed here.

4.4.1 Line selection

After slope analysis of the chronosome output of 3D-Grid, two major and one minor sediment input points were identified for the Roebuck Basin (Fig. 4.3). Lines BMR120-01, 03 and 11 were chosen as being representative seismic dip sections from these sediment input points across the Bedout and Rowley, the Rowley and the Oobagooma Sub-basins respectively. From isopach analysis, sedimentation in the Bedout has been shown to be more oblique to BMR120-01 during the Early Cretaceous (Fig. A3.6 Appendix 3). This should be considered when analysing the simulations at the Cretaceous level.

4.4.2 Sediment Supply

Sediment supply was derived by decompacting chronosome volumes obtained from 3D-Chronostrat. The methodology and results of this

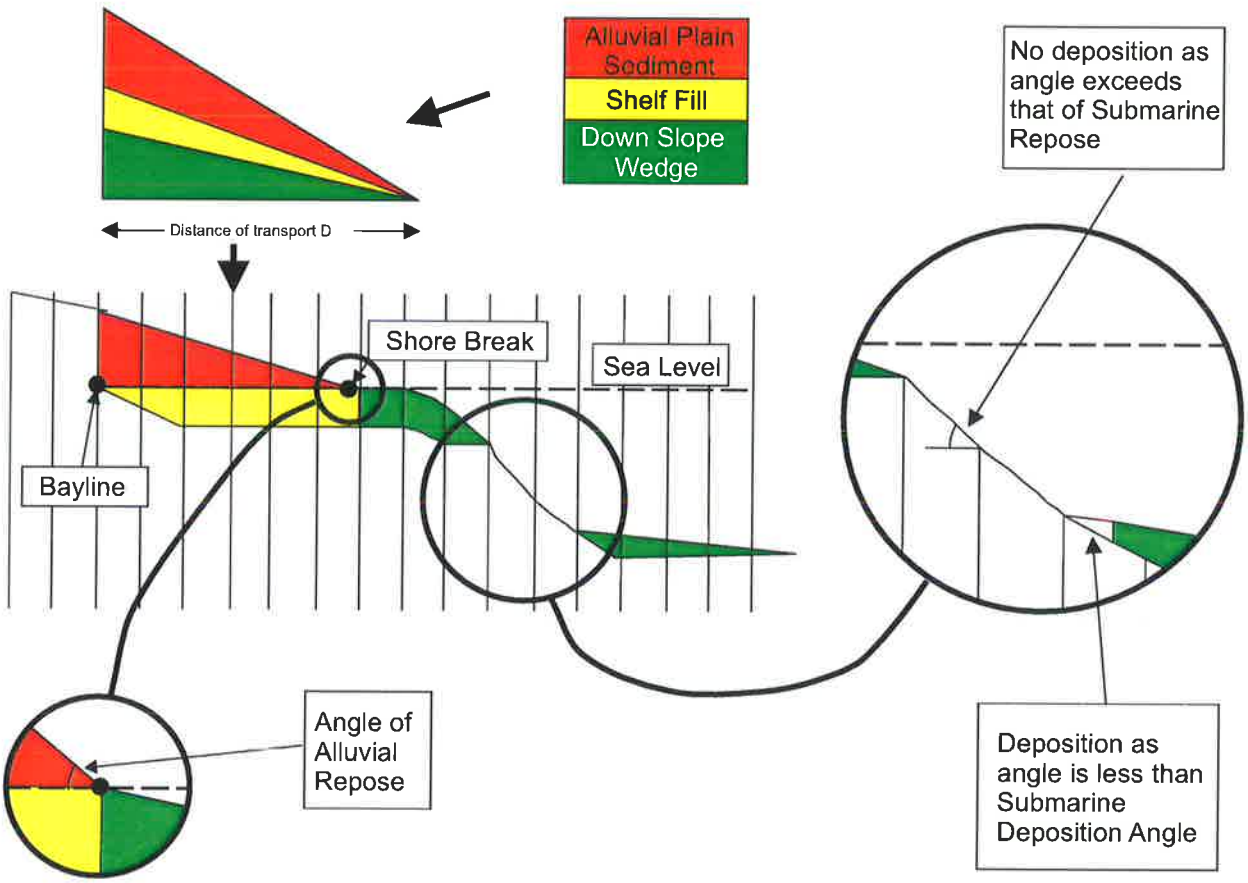

Figure 4.2 Sedpak model for sediment input, deposition, transport and erosion (from Bezdek et al. (1990)).

process have previously been described in Section 3.4 and are displayed graphically in Figure 3.17.

4.4.3 Subsidence History

Subsidence in a basin results from three main components; tectonic subsidence, isostatic loading and compaction of underlying sediment. Sedpak models local Airy-type isostatic response and sediment compaction using the standard empirically derived equation, but models tectonic subsidence explicitly using a number of user-defined curves of subsidence rate at specified points along the length of the model. Sedpak performs a straight line interpolation between each point to construct a 2D tectonic subsidence history for the basin. It was necessary to define this series of tectonic subsidence curves for each line.

Derivation of tectonic subsidence can be performed using a method termed "geohistory analysis" (Van Hinte, 1978). A geohistory is a 1D analysis of the subsidence and sediment accumulation in a specific part of the basin. To perform geohistory analysis, three values for each sedimentary unit are required; decompaction, palaeobathymetry and eustatic sea-level (Allen and Allen, 1990). At a well, palaeobathymetry information and sediment type is available, however, in an undrilled basin these parameters must be predicted.

Geohistory analysis was conducted for all wells in the basin using BasinMod™ software. Lithology information was obtained from composite well logs. Palaeobathymetry information was predicted using palaeontological indicators, wire-line log interpretation and seismic interpretation of palaeo-water depths, such as, topset systems, shelf-breaks, bottomset systems and clinoform heights. Eustatic sea-level corrections were made using the Haq et al., (1988) second order sea-level curve. Results for some key wells are shown in Figure 3.22.

The above technique was then used to predict

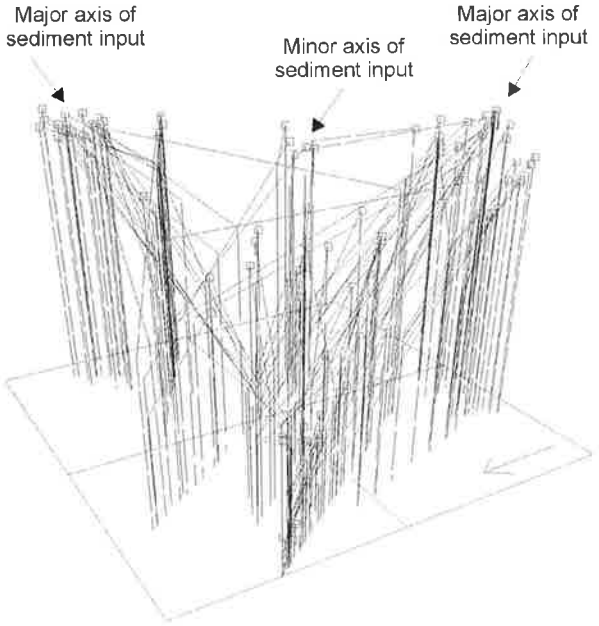

Figure 4.3 Major sediment input axis identified using highest and lowest points on each chronosome (viewed from the NW (arrow points to N)).

subsidence along each line. Subsidence curves were generated for each model by backstripping a simple burial-depth versus time plot curve. Burial depths were calculated at 30 stations (1D pseudo wells) along each line using seismic average velocities extracted from stacking velocities using the Dix formula (Dix, 1955). When compared with Bedout-1, East Mermaid-1 and Wamac-1 the depth conversions of each horizon were within ± 5% of their check-shot corrected values at each well location and often as close as ± 1%. As a first approximation lithologies at each station were derived from the chronosome lithological composition predicted in Section 3.4. If dramatic differences between modelled lithologies and well intersections occurred then the process of predicting subsidence could be recalculated.

After removing basinward tilting from the section, some estimation of palaeobathymetry could be made from chronosome geometry. Flat geometries landward of clinoforms were interpreted as representing some degree of topset geometry and were interpreted as being deposited at, or near, sea-level. Geometries basinward of clinoforms were interpreted to represent bottomsets deposited in deeper water. A simplified model of palaeobathymetry was constructed at each station. Water depth was assumed to be 0 m

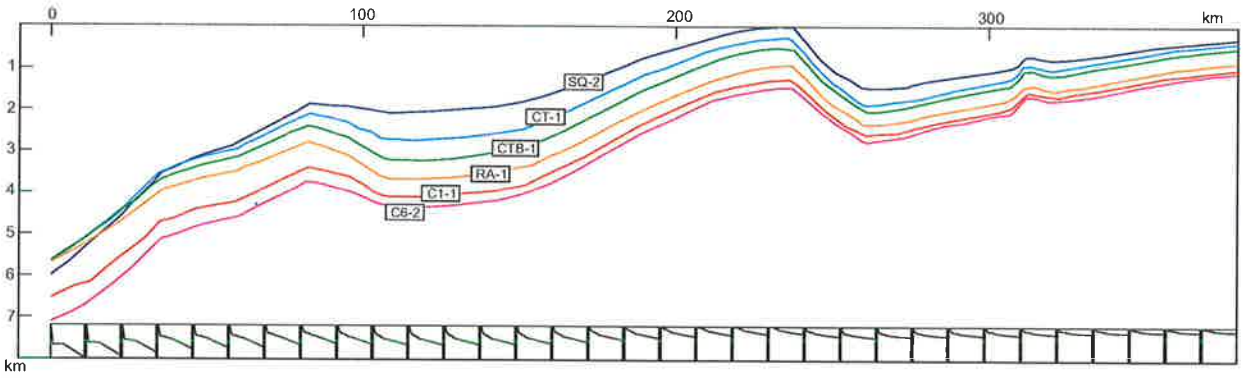

Figure 4.4 2D tectonic subsidence along line BMR120-01 (1D models used to generated the 2D model are shown along the bottom of the section).

(e.g. shallow) in the topset system and 200 m (e.g. deep) in the bottomset system. A more refined approach would have been to measure the clinoform heights from topset to bottomset to find depth to the bottomset and then increase water depth basinward in relation to a slope angle.

Eustatic sea-level fluctuation and missing section were not accounted for, but hiatus duration at major boundaries was directly measured from the Wheeler diagram of each line.

With this information in hand each model was backstripped using BasinMod™, and their tectonic subsidence histories resolved. The final results for line BMR120-01 are shown in Figure 4.4.

4.4.4 Sea-level

In Chapter 3 the construction of the relative sea-level curve for the Roebuck Basin was discussed. This, along with six other curves, were used to drive sea-level during modelling (Fig. 4.5). The Haq et al., (1987) curves were rescaled in time to match the Harland et al. (1992) time scale used for this study and run in the model as a direct comparison to the Roebuck relative sea-level curve. A filtered version of the Roebuck sea-level curve was also used. This curve was smoothed with a hi-cut filter designed from a Fast-Fourier Transform (FFT) of the Roebuck Basin relative sea-level curve. The FFT (Fig. 4.6) reveals that the highest frequency of any reasonable amplitude (30 m at 0.25 Hz dropping to 15 m at 0.30 Hz) was 4 Myr in duration. A hi-cut filter was designed to remove all frequencies above this.

In addition to the above curves, two sine-waves were also used as sea-level curves. It has been shown that, cyclothem sedimentation of the order of 20 kyr can been simulated by using a perfectly sinusoidal sea-level curve superimposed on a constant tectonic subsidence (Turcotte and Willeman, 1983). Mitchum and Van Wagoner (1991) suggest that the eustatic sea-level response is the result of a number of the superimposed cycles of different periodicity. However, the validity of the use of eustatic sea-level fluctuations in the generation of sequences of onlap and offlap has been questioned. Two other mechanisms have been described which could result in the second and third order onlap and offlap changes in the stratigraphy of a basin. These are; flexural response at the rift-drift transition of continental breakup (Watts et al., 1982; Watts, 1982) and plate boundary reorganizations due to in-plane stress (Bally, 1982).

The transition from local weak Airy-type isostatic response to a flexural type response has been modelled by Watts et al., (1982). They found that an onlap-offlap-onlap pattern of sedimentation occurred during the rift-drift cycle in continental breakup. Sediments initially onlap basement until the transition from Airy isostasy to flexural subsidence. Here, lateral heat flow due to secondary convection causes thermal-uplift on the coastal plain, which terminates onlap. Approximately 16 Myr after rifting, flexural subsidence begins to outstrip thermal uplift and sediments again begin to onlap the basin flanks. Other mechanisms for vertical plate movements

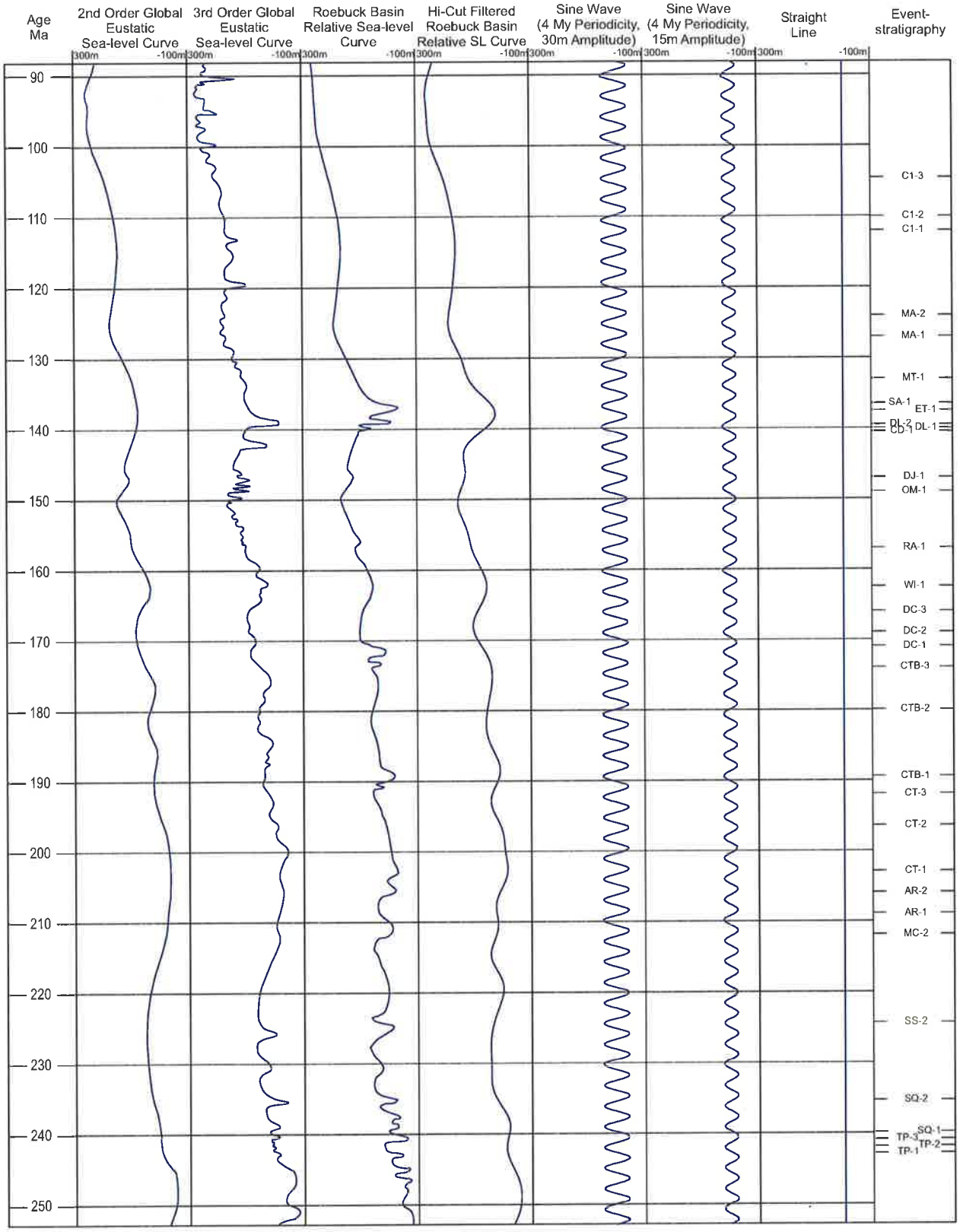

Figure 4.5 Sea-level curves used during modelling (global curves from Haq et al. (1987)).

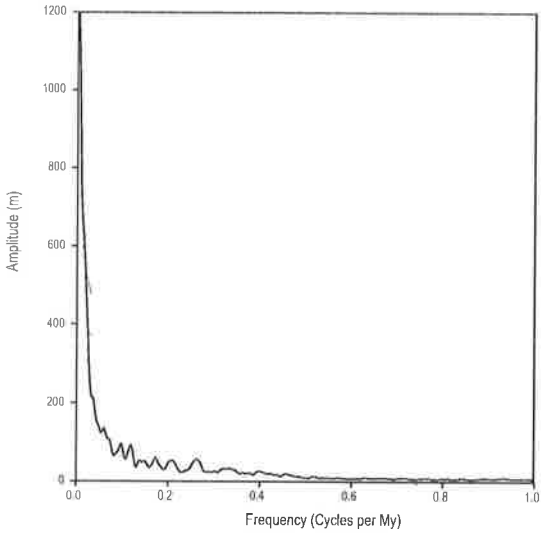

Figure 4.6 Frequency-amplitude analysis of the Roebuck Basin 'relative sea-level curve' using Fourier analysis. Sea-level fluctuations exceeding 25 m occur up to 0.25 cycles per Myr (every 4 Myr).

are described by Cloetingh et al. (1985), Karner (1986) and Kooi and Cloetingh (1992).

The two sine curves were used to test the possibility of a sinusoidal component to the relative sea-level changes, the driving mechanism, being either a periodical rigid flexure of the plate or a eustatic signal. The sine curves were also designed from the FFT. As mentioned above, the highest order sea-level fluctuation of significant amplitude was found to be of 4 Myr duration and to have an amplitude of 30 m. A sine curve of this, and of 15 m amplitude, were run as models.

To test if the section could be reasonably simulated with subsidence and sediment input alone, a model was run with no sea-level curve (the straight line in Figure 4.5).

4.5 Model setup

Final model parameters, such as, model duration, sediment penetration length and initial topography, were derived by performing several iterations and matching the results to seismic geometries and well lithologies to find stable simulations. The Sedpak modules used for all simulations are shown in Table 4.1. Twelve models were selected as the 'best' solutions (shown in Table 4.2), and represent simulations along the three depositional lines, using differing sea-level curves. Each line required slightly different modelling parameters to obtain similar characteristics to well and seismic data. Key parameters used for the "best" model for each line are shown in Table 4.3 and discussed in more detail here.

4.5.1 Model Dimensions and Duration

The length of each model was taken directly from the seismic line, with an extra 10 km added to the basinward end to "construct" a retaining wall. The retaining wall closes the system and prevents sediment loss from the distal end of the section. Vertical height does not affect the modelling process but is set at a value such that all the sections can be displayed at the end of the simulation.

The duration of each model was taken from the age of first sedimentation on each line, determined from the 3D chronostratigraphy (253 to 248 Ma) to 88 Ma (the *C6-2* event).

4.5.2 Temporal and Spatial Resolution

Ideally, a resolution should be chosen that avoids aliasing effects. To do this it is necessary to select a temporal and spatial resolution at half of the smallest chronosome in terms of length and duration. However, there has to be a compromise between computation time and resolution.

The smallest chronosomes in terms of both length (11.167 km) and duration (55 kyr) were located on line BMR120-01. To prevent aliasing in the length domain, a sample length of 5.584 km would be necessary, which would require 68 columns. Each line was divided into 2 km wide columns, 200 across BMR120-01, 160 across BMR120-03 and 130 across BMR120-11, which easily captures the required resolution to prevent aliasing. This column width is smaller than required but improves the spatial resolution.

To avoid aliasing in the time domain a sample interval of approximately 27.5 kyr was required.

Module	*Clastic source direction*	*Carbonate deposition switch*	*Sediment compaction switch*	*Deposition switch*	*Hardground switch*	*Lagoonal switch*	*Subsidence switch*	*Wave damping switch*	*Sediment winnowing switch*	*Airy isostasy switch*
Status	Right-side	Off	On	On	Off	Off	On	Off	Off	On

Table 4.1 Sedpak modules and parameters used for all simulations undertaken during study.

Seismic Line	*Roebuck Basin SLC*	*Haq 2nd order SLC*	*Haq 3rd order SLC*	*Sine curve with 30m amplitude*	*Sine curve with 15m amplitude*	*No SLC*
BMR120-01	✓	✓	✓	✓	✓	✓
BMR120-03	✓	✓	✓	-	-	-
BMR120-11	✓	✓	✓	-	-	-

Table 4.2 Final simulations conducted using Sedpak to investigate the effect of differing rates and amplitudes of sea-level fluctuation on sediment distribution.

Simulation line	*Start time (M.a.)*	*Finish time (M.a.)*	*Basin length (km)*	*No. of timesteps*	*No. of columns*	*Sand penetration length*	*Shale penetration length*	*Alluvial angle of repose*	*Submarine angle of repose*	*Shallow deposition angle*	*Deep deposition angle*
120-01	253.0	88.0	400	1650	200	20	300	0.01	24.0	1.2	0.55
120-03	242.8	88.0	316	1548	160	20	150	0.01	24.0	1.0	0.40
120-11	242.2	88.0	260	1542	130	20	150	0.01	24.0	1.1	0.50

Con't	*Transition depth from shallow to deep (m)*	*Last stage of burial (M.y.)*	*Shale density (g/cm^3)*	*Sand density (g/cm^3)*	*Mantle density (g/cm^3)*	*Sea-level offset (m)*	*Erosion enhance-ment*	*Temp. increment (^oC)*	*Arrhenius activation energy (cal/mol)*	*Frequency Factor*	*Thermal gradient ($^oC/100m$)*
120-01	500	50	2.65	2.70	6.0	0	0.5	25	50000	$3.155x10^{27}$	2.55
120-03	200	50	2.65	2.70	6.0	0	0.6	25	50000	$3.155x10^{27}$	2.40
120-11	400	50	2.65	2.70	6.0	0	0.5	25	50000	$3.155x10^{27}$	2.55

Table 4.3 Parameters used in Sedpak for each line simulation.

Over the duration of the models (from 253 Ma to 88 Ma) this would require 6000 time steps to adequately resolve the shortest duration chronosome. Unfortunately, a model with this number of time steps would not run on the computer platform available for this modelling exercise (a Silicon Graphics Indigo 2 with 256 Mb of RAM) as Sedpak array usage would exceed available memory at this resolution. If a model of this magnitude could have been run on this platform its estimated completion time would be in the order of 48 hours.

A time step value of 100 kyr (1650 time-steps in BMR120-01) was chosen for each model. At this resolution aliasing of 16 % of the chronosomes is expected. The average runtime of a model was approximately 12 hours.

The use of an equal time-step approach will cause unnecessary resolution over large durations of the simulation and inadequate resolution over others. Griffiths and Hadler-Jacobsen (1995) suggest as an improvement of Sedpak, that using a variable resolution, with higher resolution when required, as determined by chronosome statistics, would offer a more ideal solution. This approach is often used in reservoir simulation modelling packages.

4.5.3 Initial Basin Floor Topography

With little or no palaeobathymetry data the design of an initial basin floor topography for each line was not easy and required an iterative process. Knowledge of age, geometry and location of sediment and the initial tectonic history along each line was used to predict where and when first accommodation space occurred. Interpretation of 3D chronostratigraphic sediment distributions and an examination of 2D seismic lines suggest that a well-developed hinge line existed, which confined much of the early sedimentation to the outer part of each sub-basin. This tectonic hinge was built into each line's initial basin configuration (Fig. 4.7).

For BMR120-01 a slope of 0.38° to the outer margin was constructed. This slope made

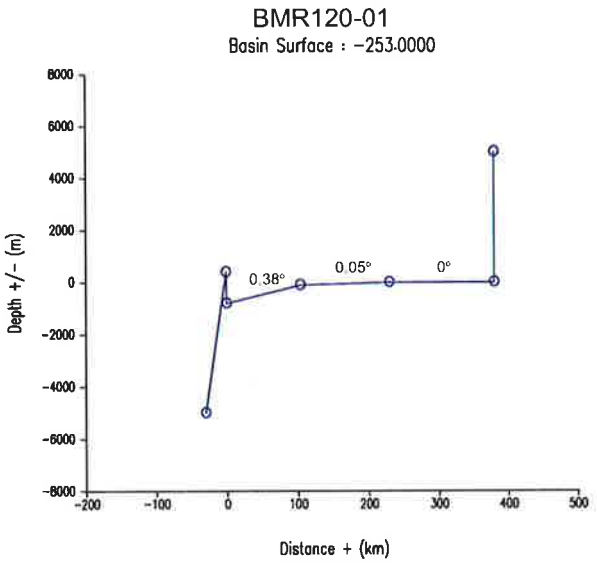

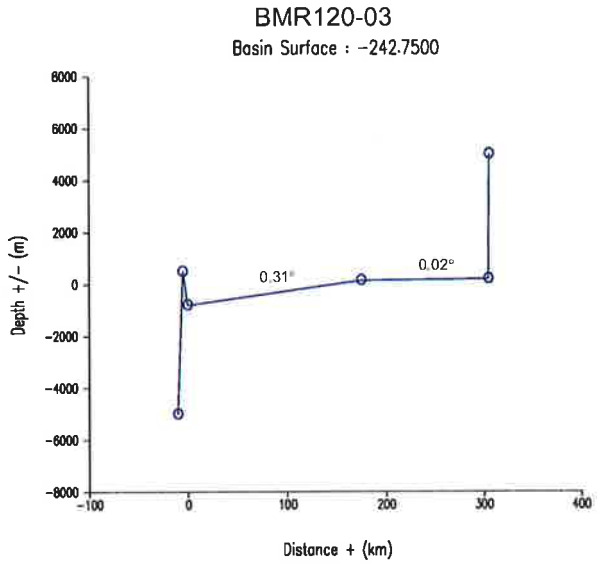

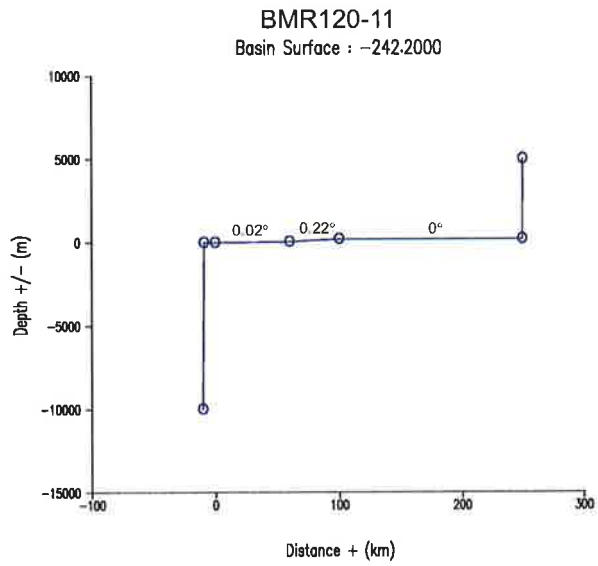

Figure 4.7 Initial basin topographies (basin surfaces ages given in negative Ma).

sedimentation unstable, forcing it out to the distal margin during the initial part of the simulation where sediment is first recorded in chronostratigraphic reconstructions. Landward of the hinge a very gentle to flat dip was designed to mimic a fluvially dominated coastal plain. With an appropriate alluvial angle of repose (discussed later) this ramp and flat configuration also allowed sediment by-pass during the initial stages of the model. The initial topography of BMR120-03 and BMR120-11 have a similar design to that of BMR120-01 (Fig. 4.7).

4.5.4 Sediment Penetration Lengths

Fine grained sediment travels further in a basin than coarser material. This is due to the different initial transport and sorting processes that occur in sediments of different grain size. Sand travels as bedload and clay as suspended load. Sedpak has no explicit method of modelling sediment transport due to suspension. Instead, Sedpak employs user-defined sediment penetration lengths for clay and sand, to determine how far sediment, of each particular grain-size, is likely to travel into the basin during its initial deposition. Sedpak, thus implicitly distinguishes between suspension and bedload transport. After initial deposition, sediment is then redistributed using the slope criteria as described earlier (Section 4.3.1). Penetration lengths represent the base length of each sediment input triangle (Fig. 4.2) and for this study were 150-200 km for clay and 20 km for sand.

4.5.5 Depositional Slopes

As initially described in Section 4.3, Sedpak uses a series of user-defined depositional angles and angles of repose. These angles are critical in controlling the deposition and redistribution of sediment through the basin. They are lithologically and temporally independent and are fixed throughout the duration of the model, even though we know that sediments of different grain-size have differing angles of repose. Five key angles are considered by Sedpak;

- shallow and deep deposition angles control the amount of initial build-up of sediment with a transition from shallow to deep that is user-defined,

- alluvial, shallow submarine and deep submarine angles of repose that control the redistribution of sediment after deposition, again at different user-defined depth levels.

These angles have a dramatic impact on the final preserved geometries in the section. The angles used during this study (shown in Table 4.3) were iteratively fine tuned but were first chosen to represent typical values recorded for present-day depositional lobes (Galloway, pers. com. and course notes (1994)). Two of the angles, the alluvial angle of repose and the deep submarine angle, have lower and higher values respectively, than those expected in the depositional environment.

It was found that a high alluvial angle of repose "captured" most of the sediment on the coastal plain and starved the basin of sediment. The alluvial angle had to be lowered to allow enough sediment to by-pass into the basin to obtain realistic geometries. This has probably led to an underestimate of the amount of fluvial section and an over-estimate of the amount of coastal section preserved in BMR120-03 and BMR120-11.

In an attempt to model sediment unloading along the margin during the time of final rift, the retaining wall was removed at 157 Ma (RA-1) on lines BMR120-01 and BMR120-03 and sediments allowed to redistribute. The margin has an extremely high slope angle of 20°, measured directly from seismic section, which was represented by the deep marine angle of repose. This angle is unrealistic for unconsolidated sediments and so the transition from shallow to deep angle of repose was set at a large depth on each line so as not to affect redistribution of recently deposited sediments. Overall, similar results were obtained in the bulk of the section using runs with the higher figure, compared to

runs with a more realistic figure. When rifted, using a lower deep marine angle of repose, erosion occurred considerably more landward into the shelf than observed from seismic, effectively redistributing up to half of the Rowley Sub-basin sediments off the line.

4.5.6 Thermal Modelling

In addition to sedimentological modelling, Sedpak has a 2D thermal modelling module able to produce TTI (time-temperature index) plots and simple single value Arrhenius activation energy kinetic plots of thermal maturity. For calibration of Sedpak thermal modelling, simple BasinMod™ models were also constructed for selected wells in the basin (see Section 5.4).

4.5.7 Other parameters

Sedpak has the ability to further enhance sediment distribution through the basin with a number of wave parameter modules. The most important of these to clastic deposition is the sediment winnowing module. Although we can make some prediction as to the palaeo-fetch and strength of waves from palaeo-plate, climate and latitude reconstructions, they were often the most difficult to quantitatively describe during the past. For this reason, most extra modules were turned off during simulations (Table 4.2). One implication of such an act is that fine and coarse sediments are probably slightly more sorted than represented in the results of this study.

4.6 Modelling Results

4.6.1 Modelling iterations

Few iterations of each model were required to stabilize each simulation. None of the parameters defined during chronostratigraphic mapping required modification – suggesting that the sea-level curve, sediment budget and subsidence history derived for the basin are good approximations and are useful in delineating the basin development and fill-history. Certain parameters did require modification – the initial basin surfaces, the depositional angles and mantle density. Initial basin surface was defined iteratively to allow sedimentation to develop in the correct position based on chronostratigraphic mapping as no other data was available to constrain these initial surfaces.

Depositional angles were constrained using modern analogues but still require minor modification to obtain the most representative results. Mantle density also initially proved problematic. Using a realistic figure (3.2 gcm^{-3}) led to rapid subsidence in the basin. To overcome this, mantle density was treated as a 'rigidity function' rather than a realistic parameter. After several iterations a value of 6 gcm^{-3} was found to yield the most realistic results.

During assessment of driving parameters of formation and sediment-fill for the basin these parameters were kept constant so a comparison of like with like could be made.

4.6.2 Well and section comparisons to simulation results

As an assessment of the validity of each simulation, comparisons were made with well-data and seismic sections. Figure 4.8 shows the comparison at megasequence level between the overall geometries obtained during modelling with the Roebuck Basin derived sea-level curve (part (a) of each line section in Fig. 4.8) versus the actual depth converted section (part (b) of each section in Fig. 4.8). It is important to note that the depth converted sections represent the present day geometries which have been loaded with a significantly thick carbonate wedge, whereas, the simulations represent geometries at 88 Ma. The loading effects of the wedge (the top of which is marked by the red horizon in Fig. 4.8), must be taken into account when considering isostatic loading of the basement and compaction of the sediment fill.

After initial examination obvious discrepancies between the finer scale geometries between the sections and simulations can be observed.

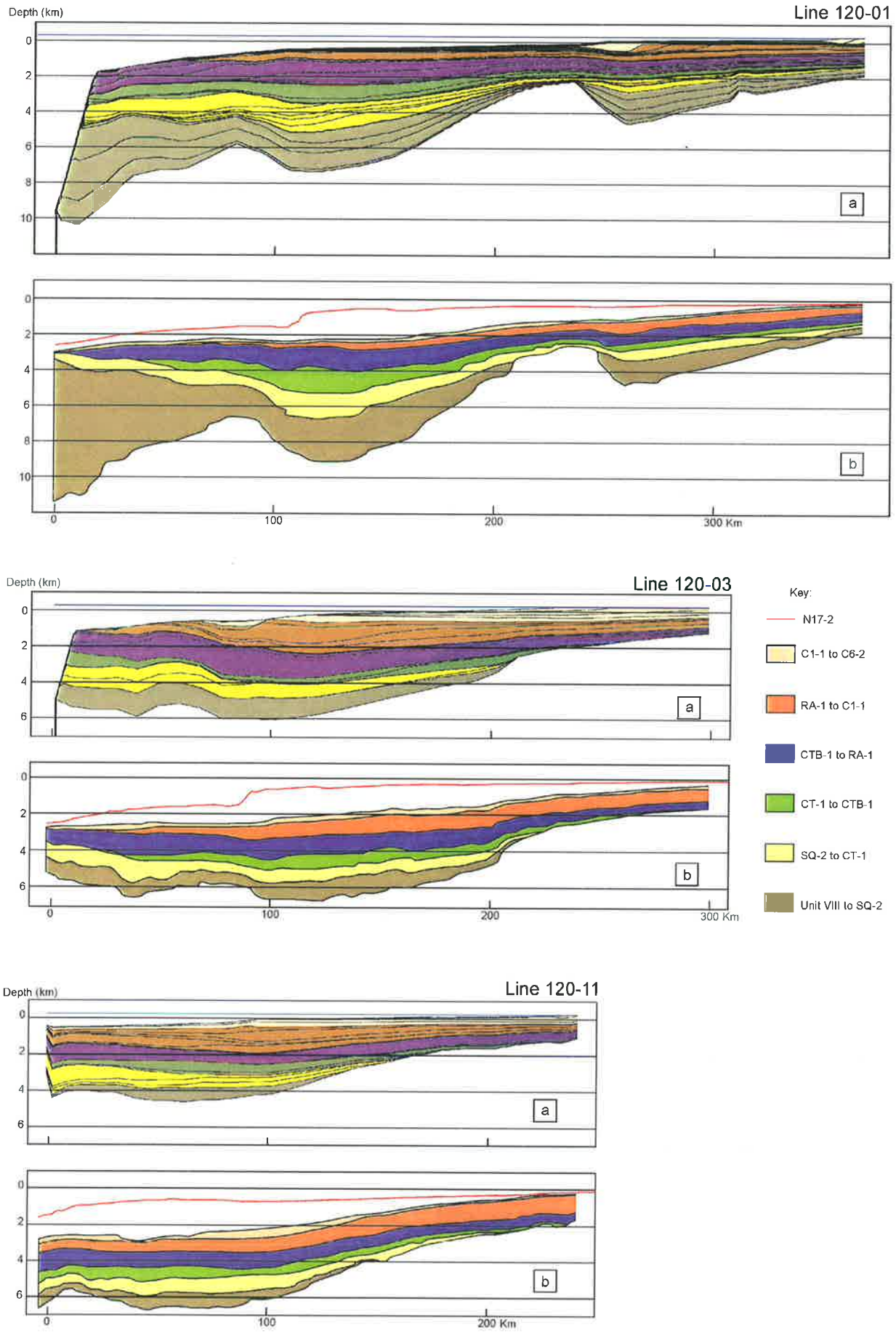

Figure 4.8 A comparison of final megasequence geometries generated from Sedpak using the Roebuck Basin relative sea-level curve with depth converted seismic - (a) simulation finishing at 88 Ma (b) present day geometry from depth converted seismic.

However, it is clear to see that the overall geometries and volumes of each have been matched. One conclusion that can be drawn from this observation is that, on a basin-wide scale, the sediment budget that has been predicted for the basin is of the correct order of magnitude.

One discrepancy that stands out in the model is that sediments deposited from *CT-1* to *CTB-1* tend to have been deposited basinward of where they should be. All evidence from this study suggests that the shelf margin during this time consisted of an uplifted rift shoulder which would have acted to restrict sediment movement to the north. Figure 4.4 shows that most differential subsidence occurs prior to the SQ-2 event with over 5.5 km of subsidence occurring on the outer margin. After the SQ-2 event subsidence is relatively even across the whole of the basin. During definition of tectonic subsidence the amount of uplift on the outer margin was difficult to predict. With further experimentation with the subsidence curves at this time, an accurate prediction of the amount of uplift required to retain sediments in a landward position could be made.

Confident that the overall sediment volumes had been accurately simulated, the validity of the internal geometries of each sequence were further assessed by comparison with well data (Fig. 4.9). Gamma wire-line log data and environmental interpretation of each control well, represented by column (a) in Figure 4.9, was plotted against four simulations using different sea-level curves; (b) the Roebuck Basin relative sea-level curve, (c) the Haq second order sea-level curve, (d) the 15 m amplitude sine curve and (e) the 30 m amplitude sine curve.

Simulations using the Roebuck Basin and Haq second order curves emulated most major environmental facies and lithology changes satisfactorily (usually within one facies belt). However, one discrepancy between modelled and actual section occurs above the *CTB-1* event where a major marine incursion has been modelled but is not present in the actual section. This transgression is of very short duration and 20 km landward of the well the sediment thickness of this event is almost negligible. Internal sediment geometries are not as well matched using the Sine curves.

4.6.3 Display

Figures 4.10, 4.11 and 4.12 represent final simulations generated for each line using the Roebuck Basin relative sea-level curve over the duration 253 to 88 Ma. Three versions of each simulation have been presented representing environmental facies distribution, lithofacies distribution and thermal maturity. Time markers at the *SQ-2* event (-235), the *CT-1* event (-203), the *CTB-1* event (-189.5), the *RA-1* event (-157) and the *C1-1* event (-112) were used to allow easy identification of the age of each section. Black dots on the environmental facies distribution sections represent the shoreline position through time. The overall geometries and facies distribution of each line have adequately matched those observed in the wells and on seismic. The simulations can therefore be used as a reasonable visualization tool for the distribution of sediment fill throughout time. Figure 4.13 shows results for line BMR120-01 using six different sea-level curves.

4.6.4 Basin-fill assessment

Early and Middle Triassic (pre –235 marker) sedimentation on each line is similar, with facies distributions being strongly controlled by sediment rates. Facies consists of predominantly fluvial and shore-faces sediments which, at their base, are interbedded with more marine sediments. This distribution of facies and sediment geometries reflect the rapid increase in sediment rates from the Early to Middle Triassic with sediments strongly onlapping the older basin-fill.

At approximately 240 Ma there is a distinct transition in sediment style from one of aggrading and onlapping, to one of prograding as sediment supply and thermal sag slowed. The distribution of each prograding delta system throughout the Jurassic and Early Cretaceous has also been

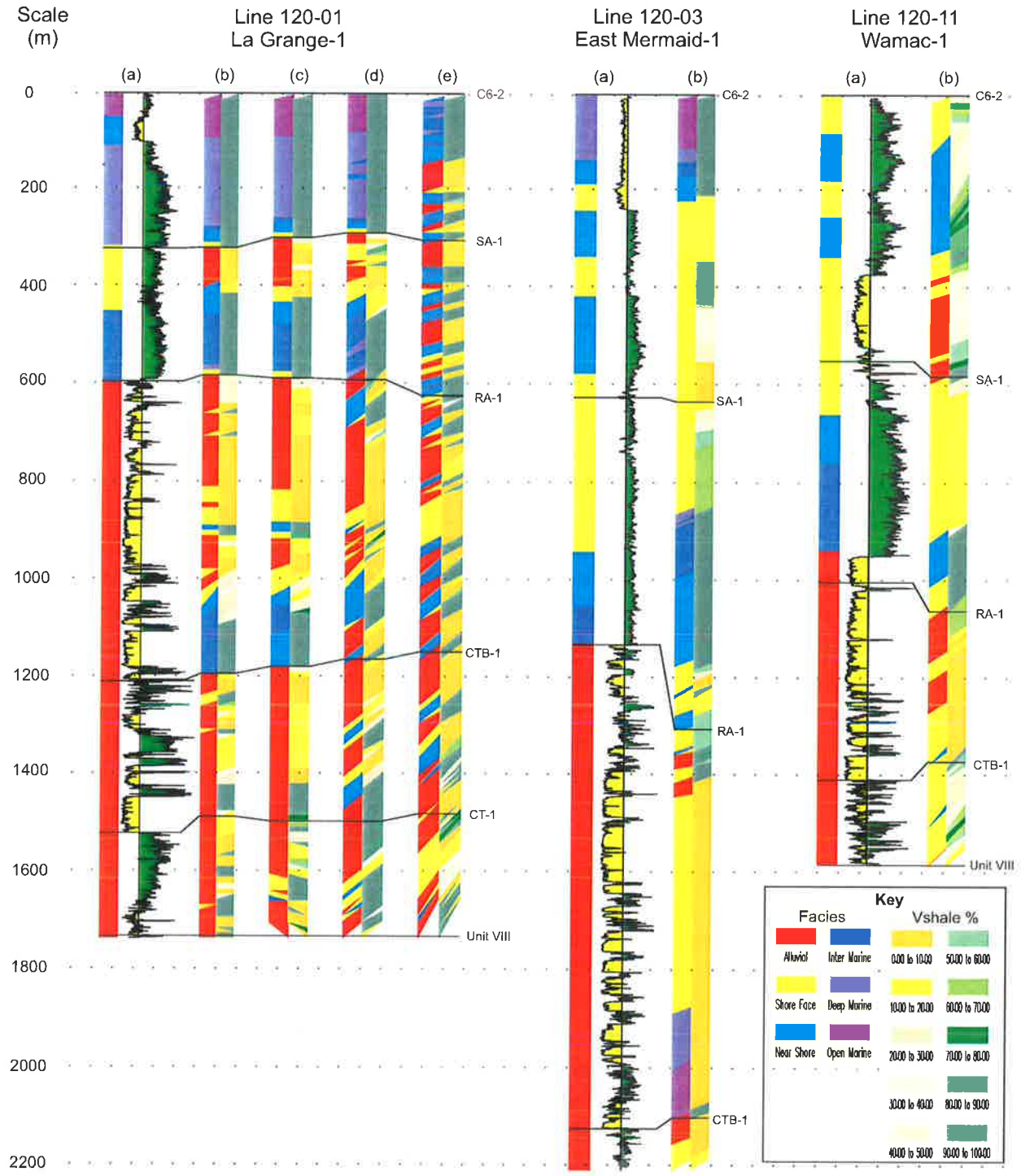

Figure 4.9 Comparison of well data with simulations using different sea-level curves – (a) interpreted well data and gamma log (b) Roebuck Basin relative sea-level curve (c) Haq 2nd order eustatic curve (d) 15 m amplitude sine curve (e) 30 m amplitude sine curve.

clearly visualized. Major lithological and environmental changes occur in the untested Rowley Sub-basin. In the tested Bedout Sub-basin a homogeneous fluvial to nearshore fill has been modelled which reflects findings in wells. Early drilling results in this homogeneous modelled fill were not encouraging to early exploration. These observations are very important in the assessment of the petroleum potential of the basin and are discussed further in Chapter 5

4.6.5 Palaeogeographies

Palaeogeographies were calibrated using well data, Sedpak simulations, TWT structure and isopach maps and chronosome maps to obtain basin depositional trends. Timeslices at every 10 Ma were generated and facies boundaries used to

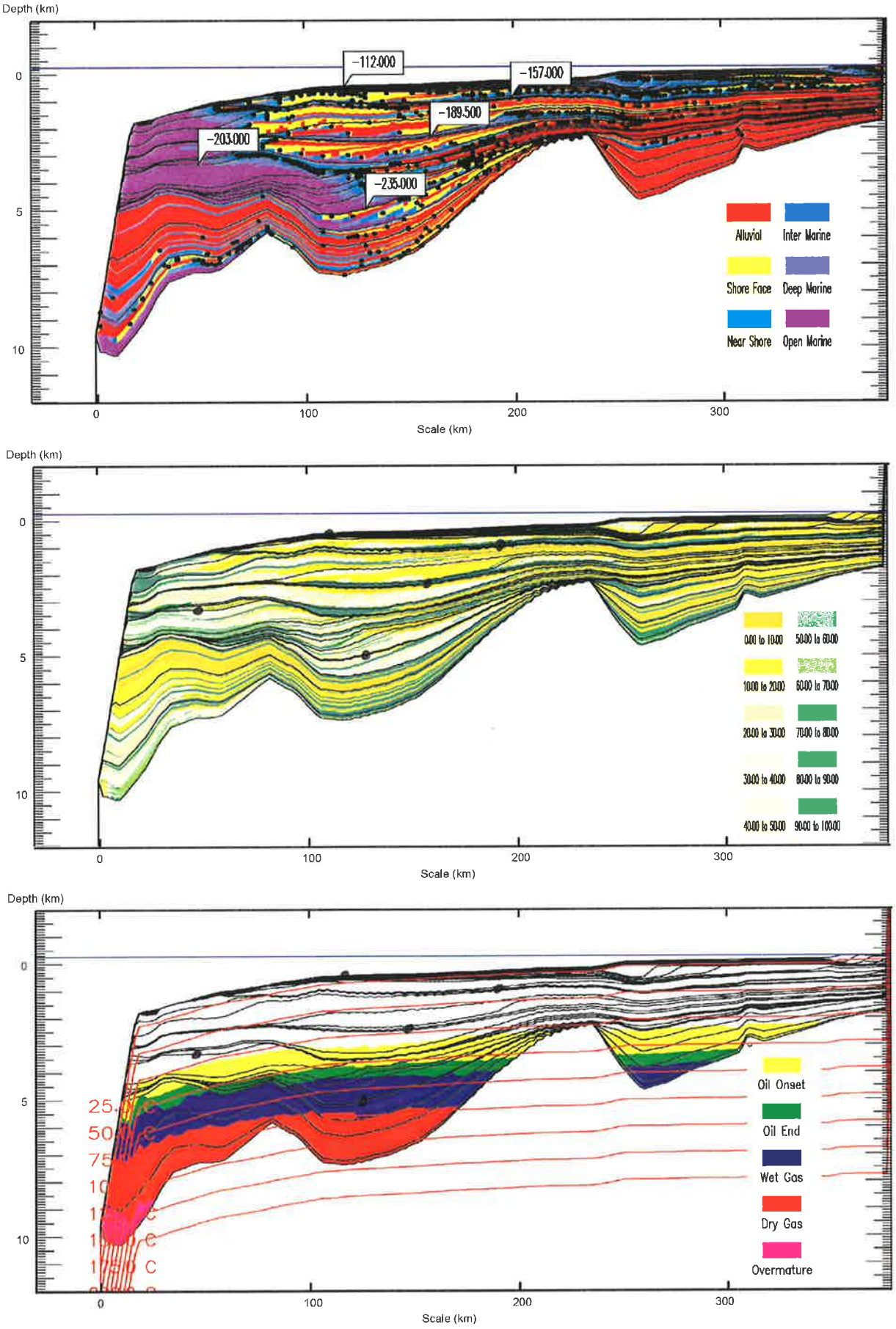

Figure 4.10 Sedpak simulations of line BMR120-01 from 253 to 88 Ma using the Roebuck Basin relative sea-level curve - (top) environmental facies distribution (middle) lithofacies distribution showing % of shale (bottom) thermal maturity.

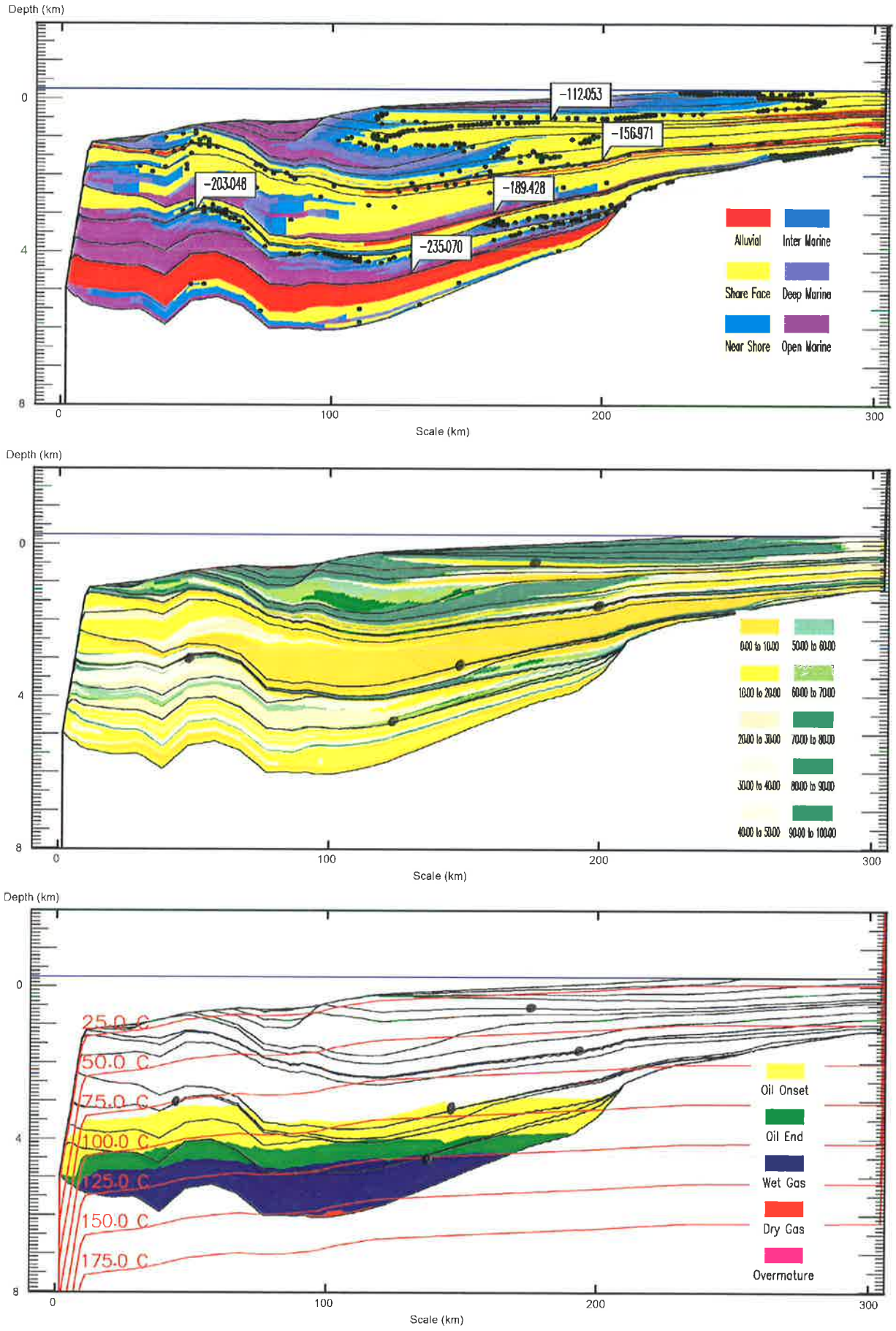

Figure 4.11 Sedpak simulations of line BMR120-03 from 253 to 88 Ma using the Roebuck Basin relative sea-level curve - (top) environmental facies distribution (middle) lithofacies distribution showing % of shale (bottom) thermal maturity.

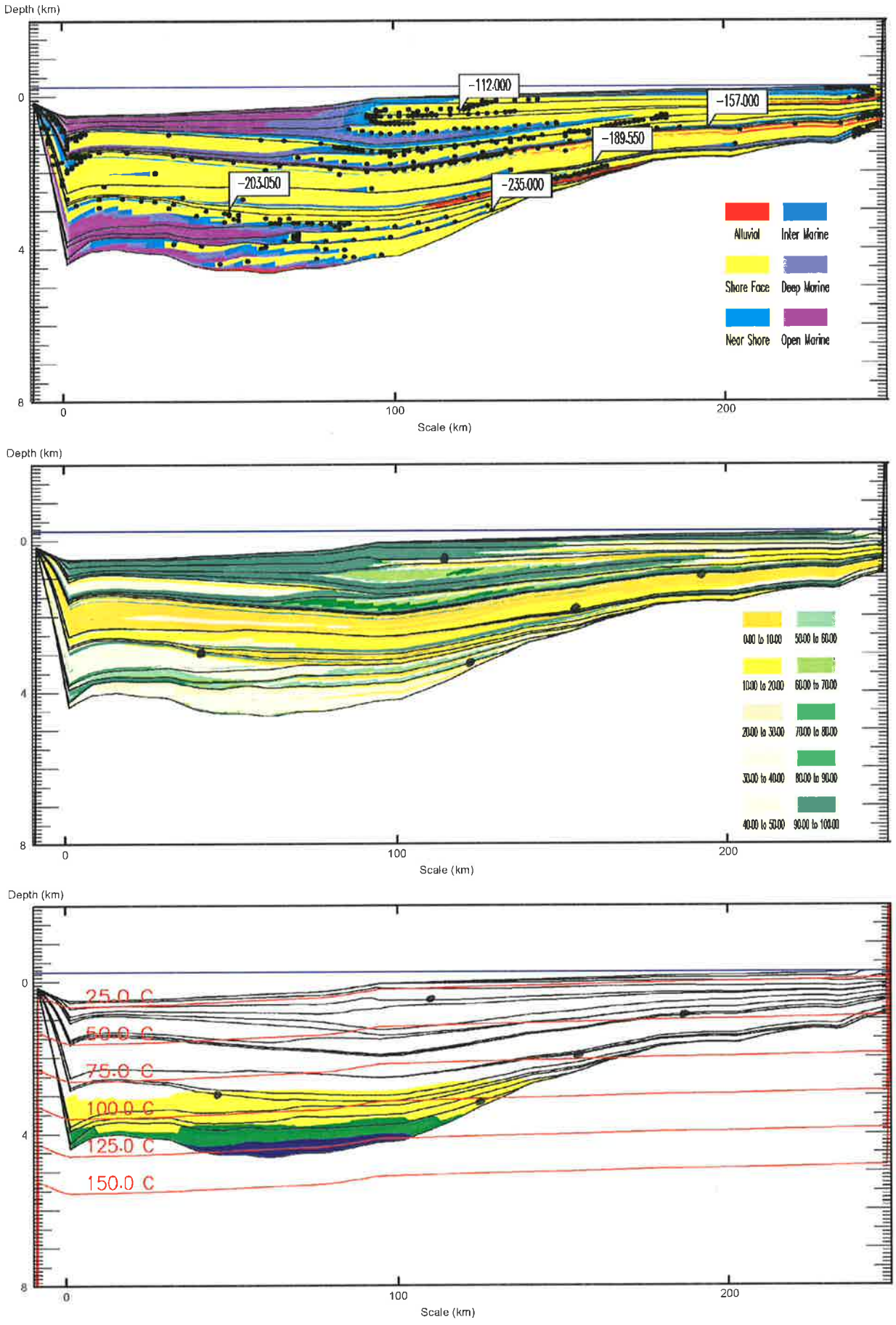

Figure 4.12 Sedpak simulations of line BMR120-11 from 253 to 88 Ma using the Roebuck Basin relative sea-level curve - (top) environmental facies distribution (middle) lithofacies distribution showing % of shale (bottom) thermal maturity.

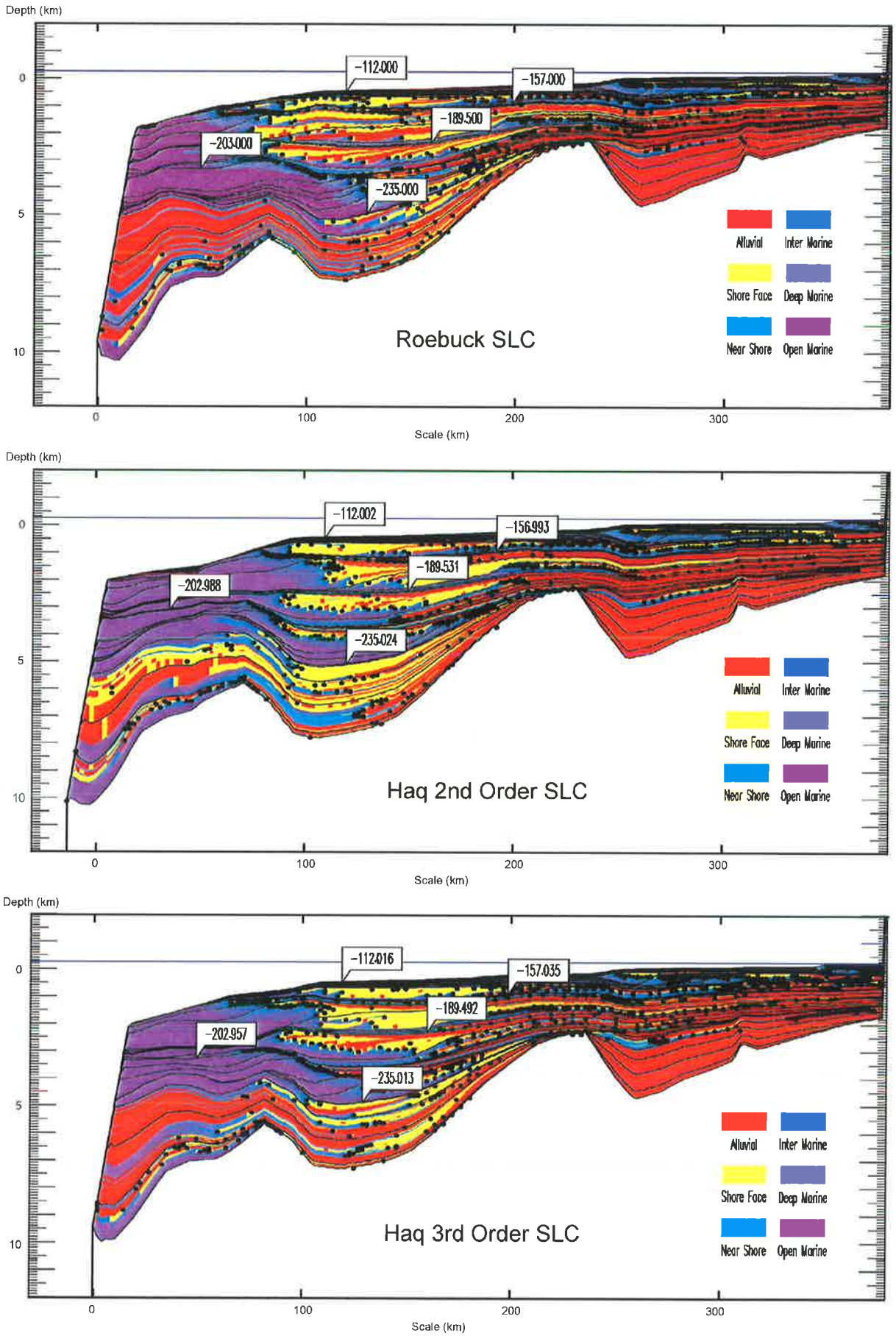

Figure 4.13 Sedpak environmental facies simulations of line BMR120-01 using different sea-level curves – (top) Roebuck Basin relative sea-level curve (middle) Haq 2nd order sea-level curve (bottom) Haq 3rd order sea-level curve.

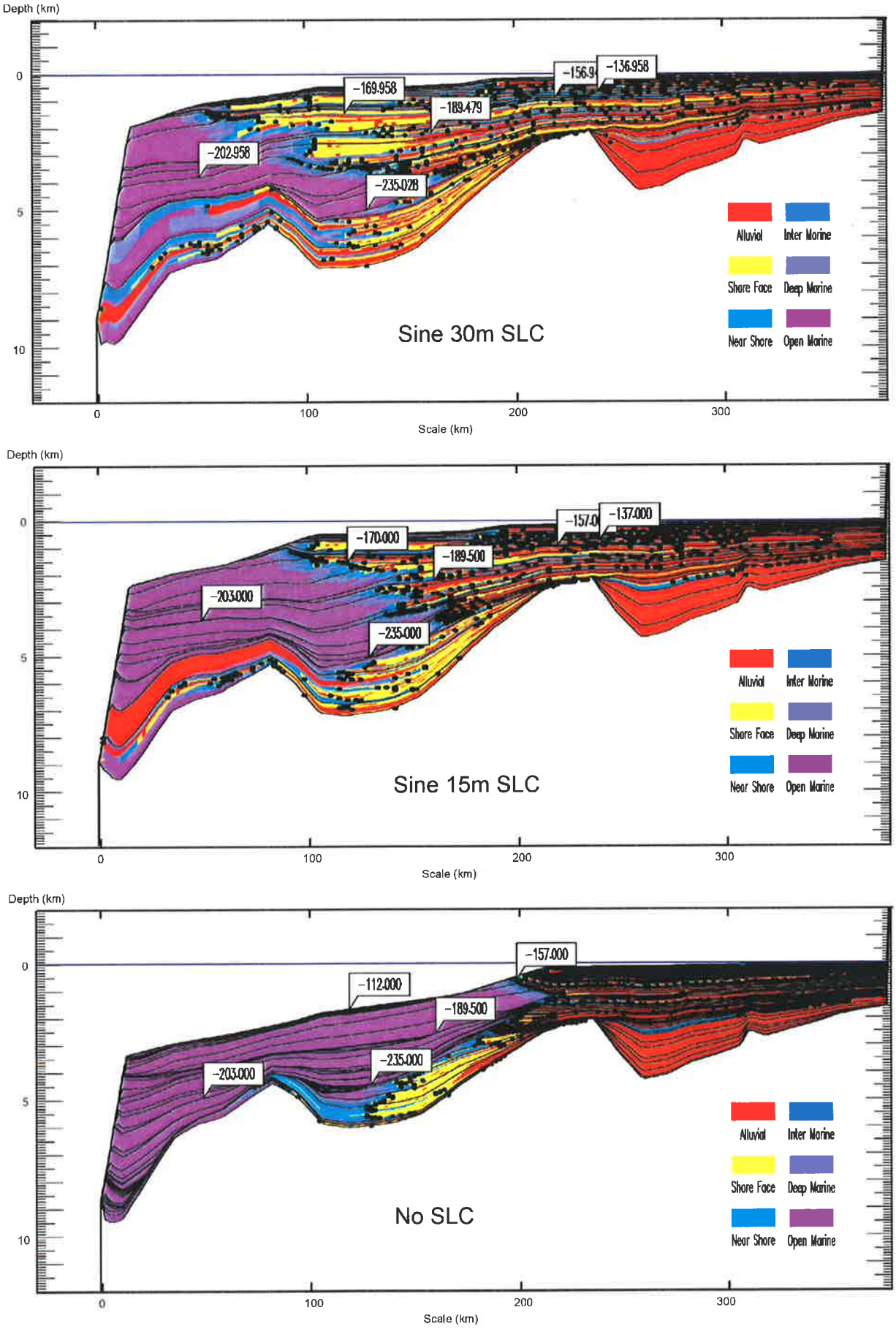

Figure 4.13 Con't – (top) 30 m amplitude sine curve (middle) 15 m amplitude sine curve (bottom) no sea-level curve.

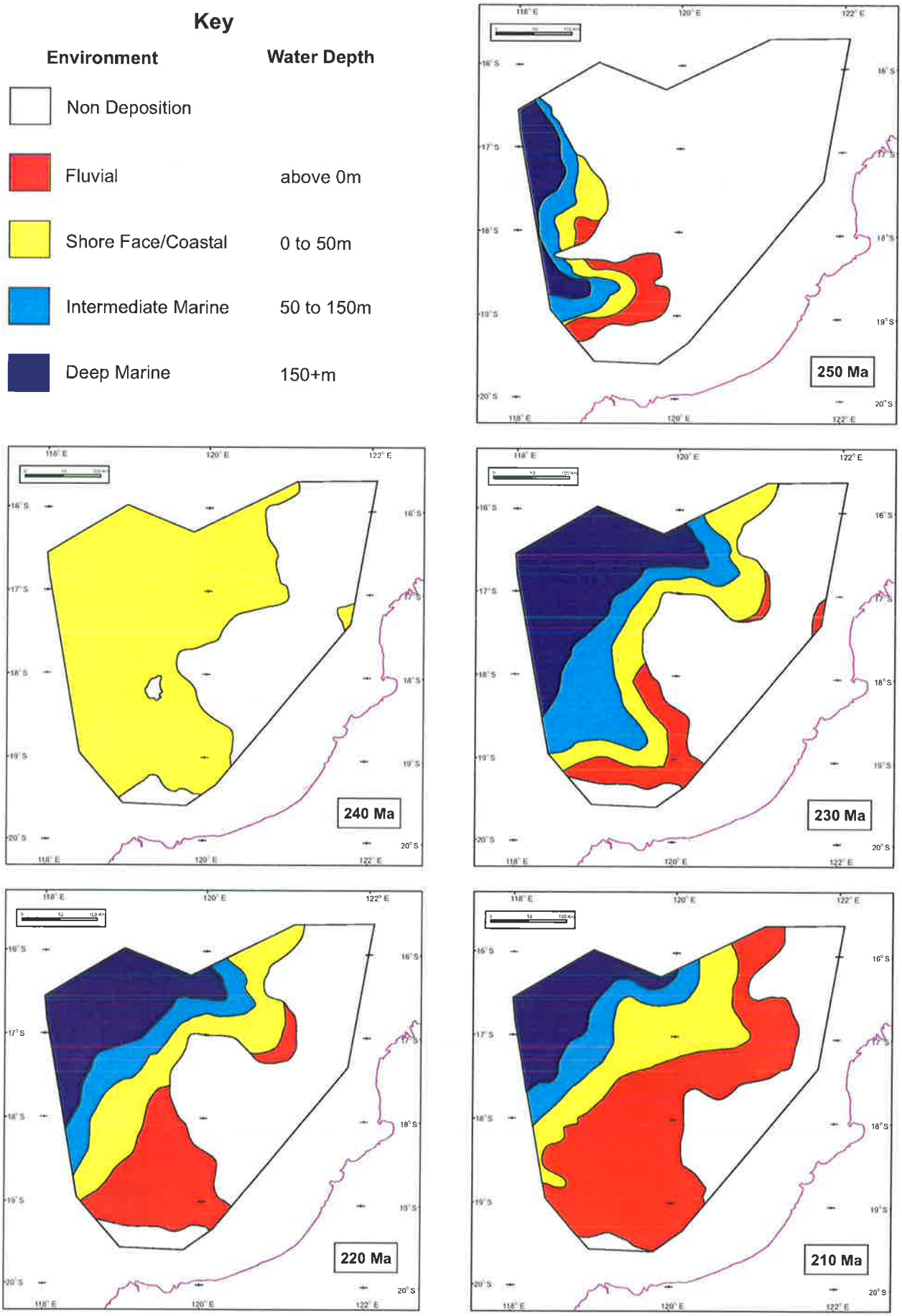

Figure 4.14 Palaeogeographic interpretations through the Mesozoic at 10 Myr time-slices.

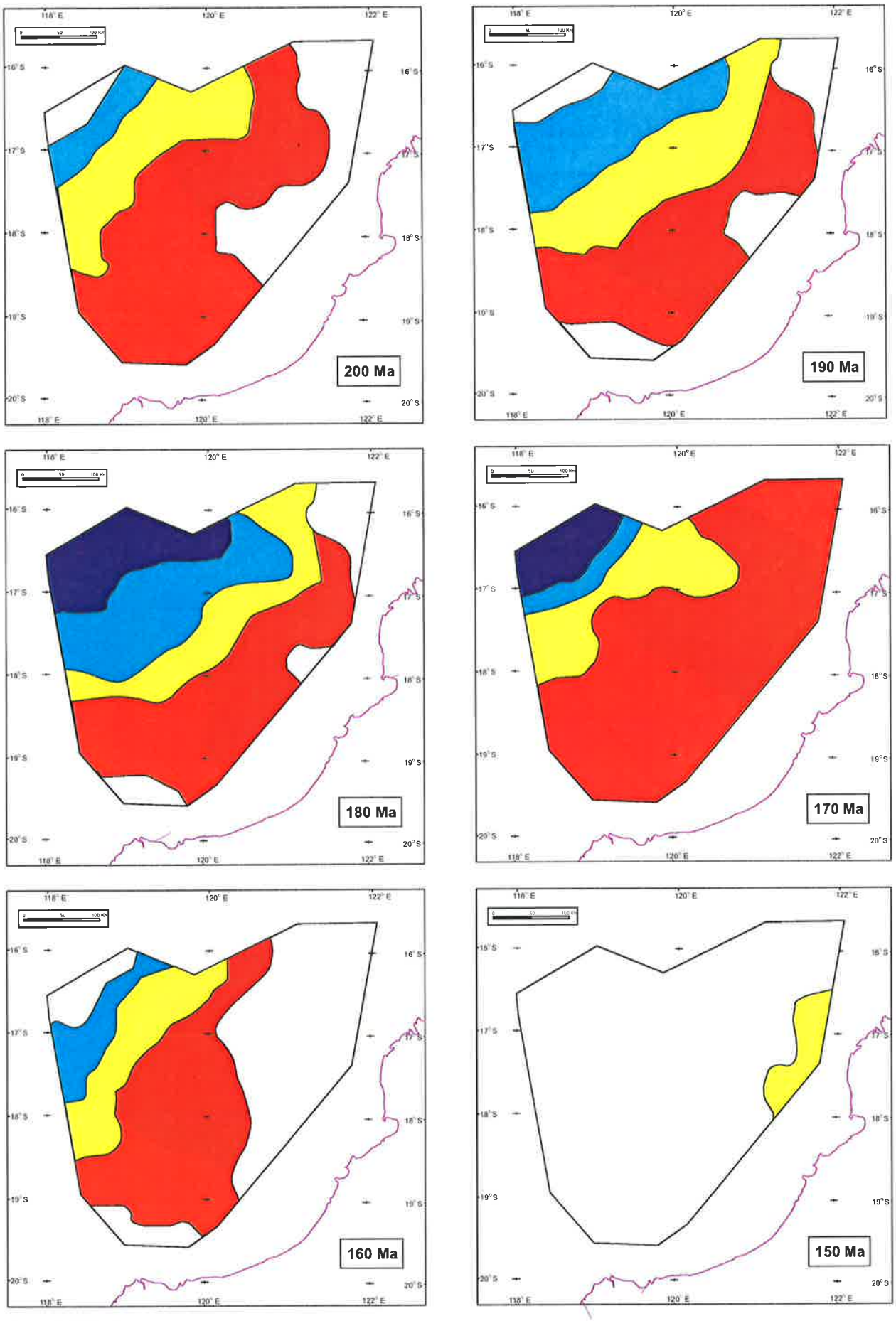

Figure 4.14 Con't.

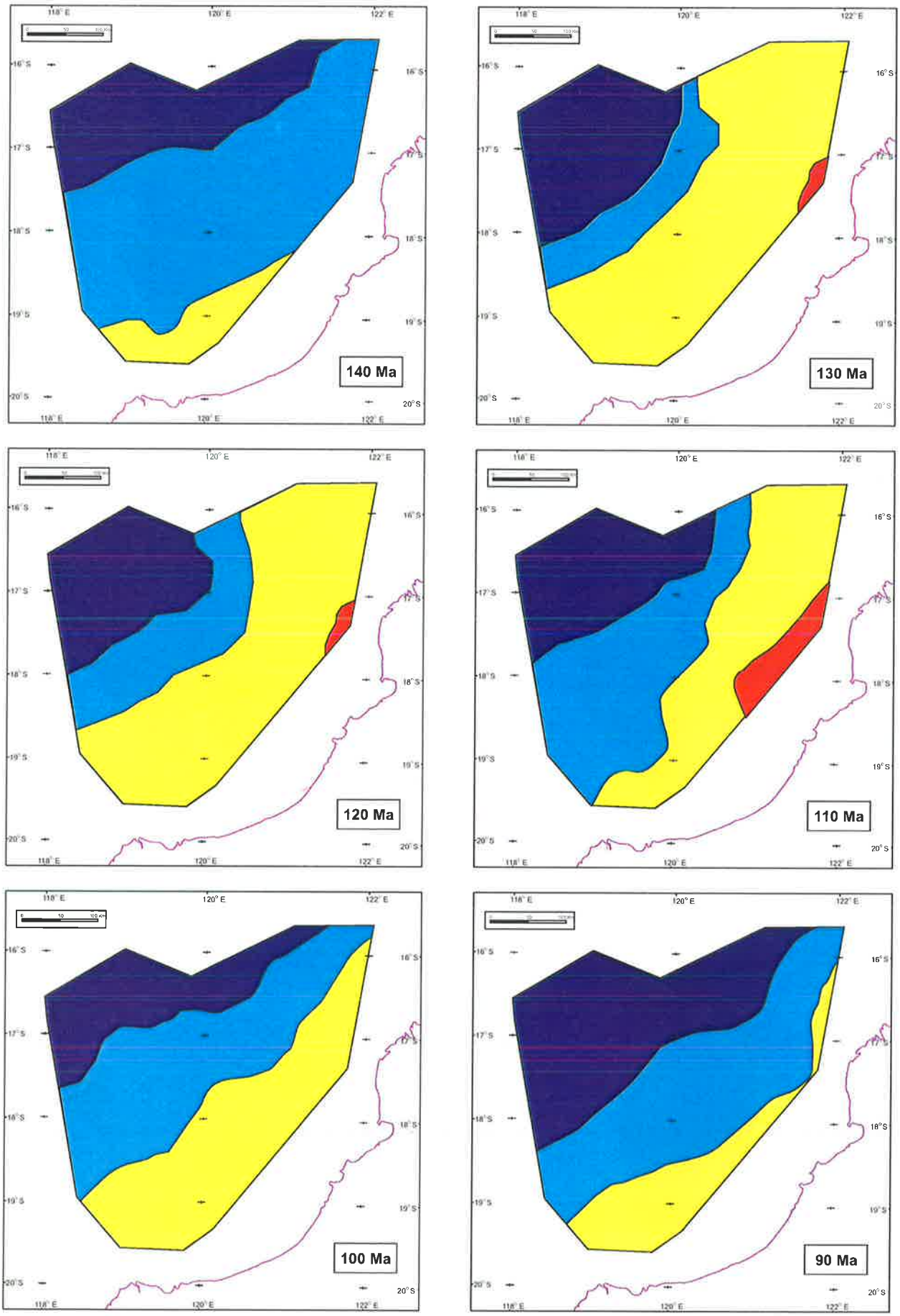

Figure 4.14 Con't

delineate environment of deposition (Fig. 4.14). Palaeogeographies were used in the assessment of the basin's petroleum potential and are also addressed in Chapter 5.

4.7 Discussion

4.7.1 Controls on sediment fill in the Roebuck Basin

To assess major controlling parameters on the sediment-fill in the basin a number of different sea-level curves were used during simulations (Fig 4.13). Simulations produced using the Roebuck Basin sea-level curves, the Haq second order eustatic sea-level curve and Haq third order eustatic sea-level curves produce similar overall geometries and internal characters which matched well with observed geometries in wells and seismic data. All offered reasonable and possible solutions. Simulation with 30 m amplitude sine curve also produce representative overall geometries However, the internal character was not as consistent with well-data (Fig. 4.9). Seismic geometries were not matched using the 15 m amplitude sine curve or with tectonic subsidence alone (no sea-level curve).

These simulations can be used to examine the interaction of sediment supply with fluctuation in eustatic sea-level. Of interest were the simulations of 30 m and 15 m amplitude sine curves and subsidence only. Simulation with the 30 m amplitude curve matched gross observed seismic geometries reasonably well, whereas subsidence only, gave unrealistic results. It is clear that, to emulate observed geometries, some form of base-level modulation is required. The amplitude of modulation of base-level appears important within Sedpak, however, it is difficult to assess the geological significance of this.

Observations during this study suggest that relative sea-level is an important factor controlling sediment by-pass into the basin. If there is no modulation, sediments tend to stack-up on the shelf. With a large enough base-level fall sediments by-pass the shelf, and are deposited in the basin. The Roebuck Basin, Haq second order and Haq second order sea-level curve, although similar in nature, are of differing frequencies and amplitudes but produce similar results when used during simulations. The Haq third order simulation is significant in the fact that it contains a much higher frequency than that of the other two curves but still replicates similar geometries. At a large scale (10-100's km) it appears that sediment supply rate is more important than sea-level curve frequency and magnitude, provided that base-level is fluctuated beyond a critical threshold. On a smaller scale (1-10's km) however, the internal distribution of each depositional unit appears strongly controlled by frequency and magnitude of the sea-level curve.

Accurately derived sea-level curves from onlap patterns in the basin can be used to model basin-fill satisfactorily. Results from this study suggest that the curves derived by Haq et al. (1987) are reasonable approximations of the high-frequency basin-level modulations that have occurred in the Roebuck Basin and could potentially be used as a first approximation to simulate basin-fill at other locations globally. However, the definition of an accurate sediment budget through time is also critical in basin modelling.

CHAPTER 5

PETROLEUM POTENTIAL

"Eye of newt and toe of frog,
Wool of bat and tongue of dog,
Adder's fork and blindworm's sting,
Lizard's leg and howlet's wing,
For a charm of pow'rful trouble,
Like a hell-broth boil and bubble."

"Double, double, toil and trouble;
Fire burn and caldron bubble."

Conjuring of the first apparition from ***Macbeth***
Shakespeare (1605)

5.1 Introduction

Commercial production has been established onshore in the northern Canning Basin from Devonian carbonates, and from Permian and Carboniferous sandstones. Although these objectives have been targeted in the near onshore they are probably buried too deeply to be prospective further seaward and Mesozoic plays are interpreted to be of more importance in the offshore area. However, due to the lack of wells in the Roebuck Basin an assessment of hydrocarbon prospectivity is very speculative.

Drilling efforts to date highlight the fact that lack of source rock, seal potential and timing of maturation, are the major factors contributing to the low petroleum potential and failure to find commercial hydrocarbons in the Roebuck Basin (Table 5.1). The identification of high quality source rock, and understanding of its context within the petroleum system are essential in assessing the petroleum potential of the basin. In other North West Shelf basins, and elsewhere in the world, Upper Jurassic and Lower Cretaceous claystone source rocks are commonly present. In the Roebuck Basin structural deformation at this time was mild and did not lead to the development of the restricted depocentres required for good source rock development and preservation.

During this study an attempt was made to assess the development and distribution of potential sources and seals in the basin and to discuss the petroleum potential in terms of petroleum systems. Only the potential of the Mesozoic fill has been assessed in detail here as few penetrations of the Palaeozoic exist offshore. The method used here was to review existing play concepts based on well information and then characterise further play concepts using the improved structural, stratigraphic and modelled information derived during this study.

5.2 Traditional Petroleum Play Elements

5.2.1 Reservoirs

Petroleum play elements identified during this study are summarized in Figure 5.1. Seven reservoir units have been identified, ranging in age from Early Triassic to Tertiary. Passmore (1991) also identified Early Permian clastics as forming both reservoir and seal in several of the onshore fields. Where intersected in the offshore Fitzroy graben, these early Permian sandstones have good porosity (Passmore, 1991). However, quality is unknown over most of the Bedout Sub-basin due to a lack of well data, and reservoir potential is probably limited due to deeper burial.

Primary objectives within the basin consist of the

Well	Spud data/ operator	Water depth (m)	T.D. depth and age.	Objectives	Hydrocarbons	Structure validity	Remarks
Bedout-1	1971 Bocal	153	3073 L. Permian	Late Triassic sands in anticlinal dome with 4 way dip closure	None	Subtle	Volcanics intersected at base. Proven good quality reservoir, but poor main seal (sandy).
East mermaid-1	1973 Shell	420	4068 E. Jurassic	Upper and Middle Jurassic sands within an anticlinal feature	Gas show in Jurassic	Minor closure	Mature source rocks around T.D., but structure is young (Miocene to Recent).
Keraudren-1	1973 Hematite	95	3844 M. Triassic	Middle Triassic and Jurassic sands in north tilting fault block	Minor gas shows	No	Triassic fault breaching at lower targets, no closure at Jurassic level.
Lacepede-1	1970 Bocal	63	2477 L. Carb.	Dip closed hanging wall anticline	None	Yes	Structuring is young (Miocene to Recent). Charge-timing problem.
Lagrange-1	1982 BP	147	3252 L. Permian	Late Triassic sands in anticlinal dome with 4 way dip closure	Minor gas shows	Yes	Volcanics not breached.
Lynher-1	1971 Bocal	58	2725 ?L. Permian	Jurassic sands within a hanging wall anticline	None	Missed crest	Structuring is young (Miocene to Recent). Crest of structure tested negatively by Trochus-1.
Minilya-1	1974 Bocal	146	2400 Jurassic	Fault bounded anticline	Minor gas shows	No	Unknown source potential.
Minjin-1	1984 Esso	21	1850 Devonian	Permo/Carb sst in a closed domal structure associated with intrusives	None	Yes	Lack of mature adjacent source rocks. Secondary objective also tight (Devonian carbonates).
Nebo-1	1993 Kufpec	171	3132 M. Jurassic	Middle Jurassic sands in faulted anticlinal structure.	Oil 1840 BOPD 42^0 API	Yes	Primary bjective was 136m low to prognosis. Oil encountered in thin sands in secondary objective.
Pearl-1	1983 Home	18	2203 E. Carb.	Permo/Carboniferous sands within an old faulted Palaeozoic anticline	None	Subtle	Porosity was low in the Carboniferous but fair in the Permian.
Perindi-1	1983 Esso	23	1867 Devonian	Permo/Carb sands in domal crest associated with igneous intrusion	Oil shows in Permo/Carb.	Fault breach	Early Permian intrusion locally matured Palaeozoic sources, otherwise immature.
Phoenix-1	1980 BP	139	4850 Triassic	Mid-Late Triassic sst in fault bounded anticlinal structure	Oil/gas shows in Triassic	Yes	Well was suspended without testing after significant gas shows below 4133m. Poor reservoir.
Phoenix-2	1982 BP	140	4967 Triassic	Middle Triassic sst in fault bounded anticlinal structure	Minor gas shows	Yes	Poor reservoir characteristics (tight). No Late Jurassic seal in Phoenix area.
Wamac-1	1973 Amax	77	2754 E. Carb.	Devonian carbonates in partly fault controlled feature on basement high	None	Subtle	Carbonates not reached, tight Palaeozoic section instead.

Table 5.1 Well objectives and failure analysis. Several valid structures have been tested. Failure is attributed to lack of source/seals and timing of migration.

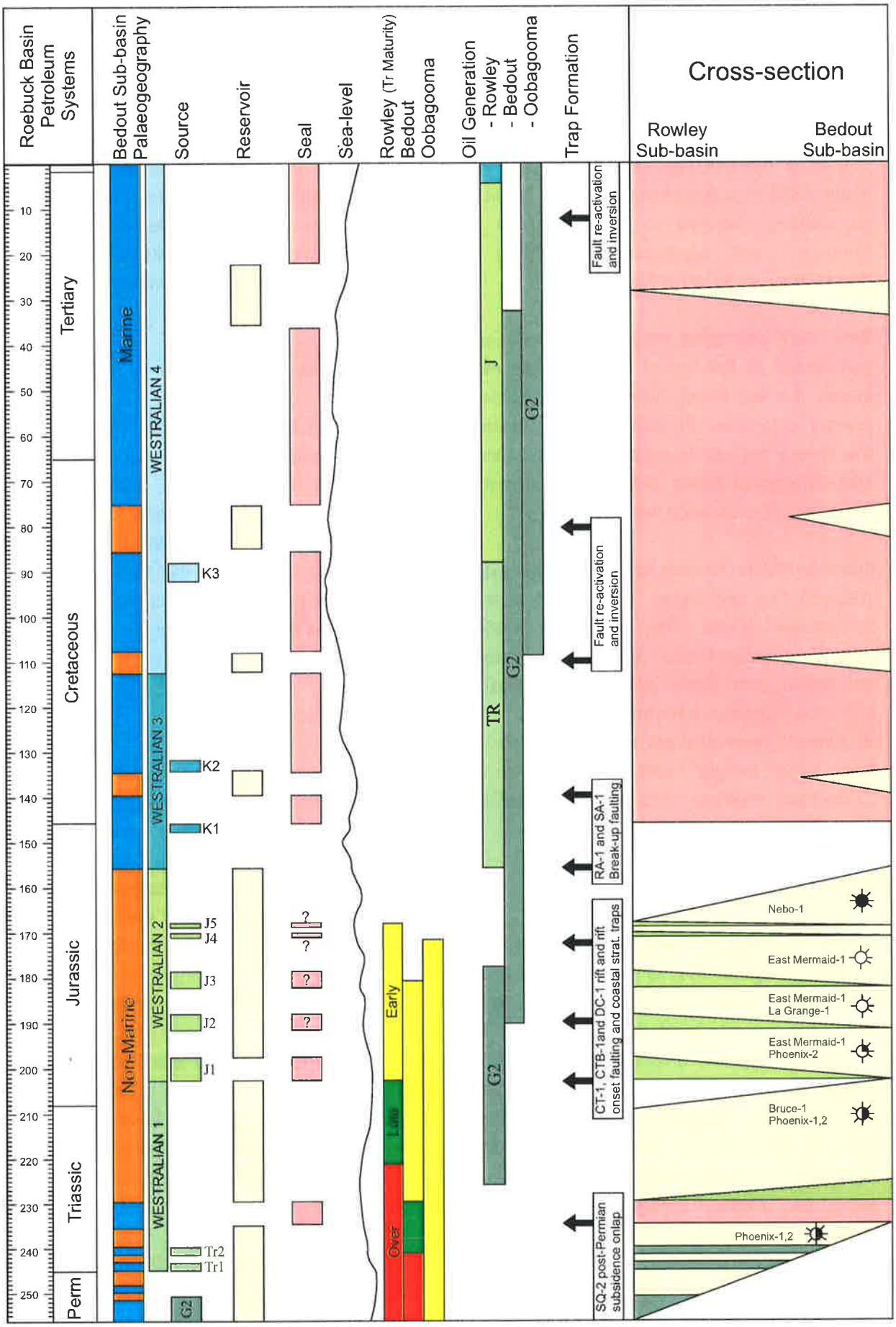

Figure 5.1 Petroleum systems summary diagram.

Middle to Upper Triassic fluvial sandstones *(Lower and Upper Keraudren Formation)* where encouraging hydrocarbon shows have been intersected in both Phoenix wells from this stratigraphic interval. In Phoenix-1, an interpreted 110 m of net gas pay occurred in tight sands below 4322 m at the base of the unit. Higher up, oil staining occurred in side-wall core from Phoenix-1 and significant gas shows and fluorescence occurred in Phoenix-2.

Secondary objectives may include interbedded sandstones at the top of Early Triassic marine shales *(Locker Shale)*, which lie just below the primary objectives. Phoenix-1 and 2 penetrated this interval but both found poor porosity, although intra-formational sands did have significant gas shows and fluorescence within closure.

Lower to Middle Jurassic fluvio-deltaic sandstones *(Depuch Fm)* and Upper Jurassic transgressive sandstones *(Erget Fm),* represent shallower secondary objectives. However, structuring associated with these reservoirs is mild and migration pathways from mature Triassic sources to Jurassic reservoirs are probably limited away from basin margin faults. Migration to Early Cretaceous reservoir units is also limited away from basin margins.

5.2.2 Seals

Several possible seals were developed at various stages throughout the sequence. A thick Early Cretaceous marine claystone forms a regional seal over the whole of the North West Shelf *(Mermaid Formation)*. It acts as a seal over Middle to Late Jurassic sandstones in the western part of the basin but is expected to become increasingly sandy to the east as it grades into a sandstone *(Broome Sandstone)*. Within the Middle Jurassic sandstone *(Depuch Formation)* thin claystone interbeds may form intra-formational seals.

The thick Late Triassic to Earliest Jurassic red-bed claystone *(Bedout Formation)* is expected to form a regional seal over Late Triassic sandstones. It was 437m thick in Phoenix-2, 313m thick in Phoenix-1 and 188m thick in Bedout-1 and can be traced on seismic eastward, where it onlaps Permian Strata at the basin margin.

A Middle Triassic regional limestone marker *(Cossigny Member)* which grades into a claystone with calcilutite lenses near the basin margins, acts as an intra-formational seal between Middle Triassic sandstones. Intra-formational shales were also found to act as individual seals for gas-bearing sands in Phoenix-1.

5.2.3 Source

As highlighted in the introduction, failure of all thirteen wells is surprising, and may suggest that the basin is deficient in source rock. Major sourcing Upper Jurassic shales found in the post-rift sequence of the North West Shelf are either thin or not present in the Roebuck Sub-basin, which has a sandstone sequence instead. Source rock issues are discussed in the latter part of this chapter.

5.2.4 Traps

Structural movement associated with rifting has resulted in trap formation throughout the Mesozoic to Recent section (Fig. 5.1). Stratigraphic pinch-out traps are formed against the flanks of the Bedout High and basin margins. Reactivation during the Miocene collision event has also led to the development of trapping configurations.

5.3 Source Rock Characterization

During this study, source rocks were identified and their distribution predicted using a number of techniques, some of which have been described in previous chapters, including; sequence stratigraphic correlation, seismic mapping, forward sedimentary modelling and geochemical analysis. Unfortunately, only a very limited geochemical data set is currently available from the Roebuck Basin, as few wells have been drilled in the area (Table 5.2).

Current open-file geochemical studies have been

Well	*TOC*	*Rock-Eval*	*GC-MS*	*Visual Kerogen*	*Tmax*	*SCI*	*Ro*	*No. BHT meas.*	*PST*	*PHF*	*PGG*
Bedout-1	✓	✓	✓	✓	✓	✓	✓	3	19.0	36.5	27
E. Mermaid-1	✓	✓		✓	✓	✓	✓	3	14.0	31.2	23.5
Keraudren-1	✓	✓		✓	✓	✓	✓	3	21.0	37.5	26.0
Lagrange-1	✓	✓	✓	✓			✓	3	17.0	36.0	26.0
Lynher-1	✓	✓		✓	✓	✓	✓	2	23.0	49.0	37.0
Minilya-1	✓	✓	✓	✓			✓	1	19.0	45.0	35.0
Phoenix-1	✓	✓	✓	✓		✓	✓	4	19.0	37.5	25.5
Picard-1	✓	✓		✓			✓	0	19.0	42.0	27.0
Wamac-1	✓	✓	✓	✓		✓	✓	3	22.0	38.0	27.5

TOC=Total Organic Carbon GC-MS=Gas Chromotography-Mass Spectrometry SCI=Spore Colouration Index Ro=Vitrinite Reflectance PST=Present Surface Temp.

PHF=Present Heat Flow PGG=Present Geothermal Gradient

Table 5.2 Gehemical data available for thermal maturity and hydrocarbon potential analysis.

conducted by Robertson Research (1979, 1986) and by the Japan National Oil Corporation (JNOC) (1987, 1989). JNOC's (1987, 1989) evaluations were undertaken by Robertson Research using over 500 samples from nine wells and include; total organic carbon content (TOC), Rock-Eval pyrolysis, pyrolysis-gas chromatography (PYGC), gas chromatography-mass spectrometry (GCMS), visual kerogen analysis, and vitrinite reflectance (Ro) (Table 5.2). These studies were used to identify all zones of potential organic rich rocks of Triassic, Jurassic and Cretaceous age. An estimate of the interval thickness of each organic rich zone was made using gamma, resistivity and sonic wire-line log signatures. Summaries of typical well results from the Bedout Sub-basin, Bedout High and Oobagooma Sub-basin are presented in Tables 5.3, 5.4, and 5.5.

Once each well had been analyzed, a correlation of each interval was attempted between wells using the high resolution stratigraphic breakdown described in Chapter 3. The timing of each interval was plotted on a chart and correlated with Haq et al. (1987) second order eustatic sea-level curve (Fig. 5.2). A good correlation was obtained between periods of highstand and known global anoxic events and the timing of development of organic rich facies in the Roebuck Basin.

In addition to wire-line correlations, the high resolution chronostratigraphic seismic correlations and forward sedimentary modelling techniques were also used to visualise where and how source rocks may develop.

Using the above methods, ten source rock intervals were identified that could be correlated over considerable distances and offer basin-wide source potential (Triassic and Jurassic intervals throughout the basin) or identified upside potential (Cretaceous intervals in Phoenix-1) (Table 5.6). These source rocks have been correlated to the Triassic to Recent Westralian petroleum super-system first identified and described by Bradshaw et al (1994). A summary of the details of the timing of deposition and maturity of these petroleum systems are shown in the petroleum systems event summary (Fig. 5.1).

5.4 Thermal Maturity

Basin thermal maturity was assessed using simple 1D thermal models at each well location produced by BasinMod™, which were used to calibrate less constrained 2D models produced using Sedpak. The geochemical and thermal maturity data available for each modelled well is given in Table 5.2.

Geohistories for each well were produced using the method described by van Hinte (1978). Surface temperatures for thermal modelling were assumed to be 25 °C throughout the duration of each model. However the sediment/water interface temperature was calculated based on water depth using the following formula; 25 °C at the surface, 25 °C minus 4 °C100m^{-1} for first 200 m, then minus 2 °C100m^{-1} for any depth below 200 m. Palaeo-water depths were predicted using biostratigraphic and wire-line log indicators (Section 3 Fig. 3.2). Each model was referenced to present day sea-level and absolute fluctuations in sea-level were removed using the Haq et al. (1987) second order eustatic sea-level curve. Present day bottom hole temperatures (BHT) were obtained from relevant well completion reports and bottom hole temperatures were corrected using the method of Andrews-Speed et al. (1984). Lithologies, and thermal maturity data, were also obtained from well completion reports.

Initially, simple thermal models were calculated using a constant heat flow based on the current values calculated from present BHT data (Fig. 5.3(a)). Present day heat flows are mainly low ranging from 31 to 38 mWm^{-2} with only Lyher-1 and Minilya-1 having significantly higher values at 45 and 49 mWm^{-2} respectively. The present day heat flow calculated for the wells suggest that the area has a low to normal heat flow consistent with its current stable tectonic condition.

Initial modelling, holding present heat flow constant through time, showed that calculated maturities are commonly greater than measured

Well: PHOENIX-1

Depth	*Age*	*Lithology*	*Net thickness of source and average TOC (%)*	*Maturity VR(% Ro)*	*Oil Generation Capacity MBBLS/km²*	*Oil Currently Generated MBBLS/km²*	*Keragen Composition*	*Comments*
1490-1510m	Late Cretaceous (C3)	Dark grey mudstones	10m (2.05%)	Immature (0.40)			40% Inert. 50% Vit. 10% Waxy	
		Grey green mudstones	10m (9.84%)		3.7	-	35% Inert. 15% Vit. 25% Algal 25% Waxy	Developed above the C1-3 event.
2034-2085m	Middle Jurassic (C. cooksoniae)	Grey mudstones	11m (3.91%)	Immature (0.43)	4.9	-	38% Inert. 19% Vit. 22% Algal 21% Waxy	Developed above the DC-2 event.
2454-2460m	Lower Jurassic (C. turbatus-C. torosa)	Dark grey mudstones	6m (6.90%)	Early Mature (0.50)	1.0	-	48% Inert. 29% Vit. 12% Algal 11% Waxy	Developed above the CT-3 event.
2522-2586m	Lower Jurassic (C. torosa)	Organic rich dark-grey mudstones	30m (4.67%)	Early Mature (0.42)	2.5	-	51% Inert. 28% Vit. 7% Algal 14% Waxy	Developed above CT-1 event.
3920-4240m	Middle Triassic (T. playfordii)	Dark-grey mudstones	95m (4.07%)	Middle Mature (0.80)	16	8.6	35% Inert. 27% Vit. 14% Algal 24% Waxy	Developed above the TP-1 and TP-2 events.

Table 5.3 Potential source intervals identified in Phoenix-1 in the Bedout Sub-basin (modified from JNOC 1989).

Well: BEDOUT-1

Depth	*Age*	*Lithology*	*Net thickness of source and average TOC (%)*	*Maturity VR(% Ro)*	*Oil Generation Capacity MBBLS/km²*	*Oil Currently Generated MBBLS/km²*	*Keragen Composition*	*Comments*
2159-2195m	Middle Jurassic (D. complex)	Black coals and grey black very mudstones (interbedded in sandstones)	4m (24.68%)	Early Mature (0.53)	1.2	0.5	48% Inert. 40% Vit. 4% Algal 8% Waxy	Developed above DC-1 event.
2262-2280m	Middle Jurassic (C. turbatus)	Dark grey mudstones with black coals (interbedded in sandstones)	3.4m 23.59%	Early Mature (0.54)	1.5	0.7	40% Inert. 35% Vit. 10% Algal 5% Waxy	Developed above CTB-3 event.
2304-2332m	Lower Jurassic (C.turbatus)	Dark grey mudstones with black coals (interbedded in sandstones)	4m 25.15%	Early Mature (0.54)	1.7	0.7	40% Inert. 40% Vit. 5% Algal 10% Waxy	Developed above CTB-2 event.
2417-2527m	Lower Jurassic (C. turbatus-C. torosa)	Dark grey mudstones (interbedded in sandstones)	20m 21.21%	Early Mature (0.57)	9.9	6.2	44% Inert. 38% Vit. 7% Algal 11% Waxy	Developed above CTB-1 event.
2563-2566m	Lower Jurassic (C. torosa)	Dark grey mudstones (interbedded in sandstones)	3.4m 9.58%	Early Mature (0.60)	2.0	1.2	15% Inert. 35% Vit. 20% Algal 20% Waxy	Developed above CT-2 event.

Table 5.4 Potential source intervals identified in Bedout-1 on the Bedout High (modified from JNOC 1987).

Well: WAMAC-1

Depth	*Age*	*Lithology*	*Net thickness of source and average TOC (%)*	*Maturity VR(% Ro)*	*Oil Generation Capacity MBBLS/km²*	*Oil Currently Generated MBBLS/km²*	*Keragen Composition*	*Comments*
1620-1740m	Middle Jurassic (C. turbatus)	Black coals and grey black very organic rich mudstones (interbedded in sandstones)	8m (32.55%)	Immature to Early Mature (0.50)	4.7	0.5	50% Inert. 25% Vit. 10% Algal 15% Waxy	Developed above CTB-1 event.
1876-1940m	Lower Jurassic (C. torosa)	Dark grey organic rich mudstones (interbedded in sandstones)	30m 8.65%	Early Mature (0.55)	5.4	2.0	40% Inert. 35% Vit. 10% Algal 15% Waxy	Developed above the CT-3 event.

Table 5.5 Potential source intervals identified in Wamac-1 in the Oobagooma Sub-basin (modified from JNOC 1989).

Source Unit	*Average TOC%*	*Typical N/G Thickness*	*Algal Content %*	*Oil Generative Potential MMBBL/km²*
K3	9.8	10	25	1.0
K2	2.1	22	15	2.0
K1	3.5	9	10	2.1
J5	3.9	11	22	4.9
J4	24.7	4	10	1.2
J3	23.6	4	5	1.5
J2	7.2	20	7	9.9
J1	4.7	30	7	2.5
Tr2	4.0	50	7	8.4
Tr1	4.1	45	14	9.2

Table 5.6 Potential source rock characteristics (modifed from JNOC 1987, 1989).

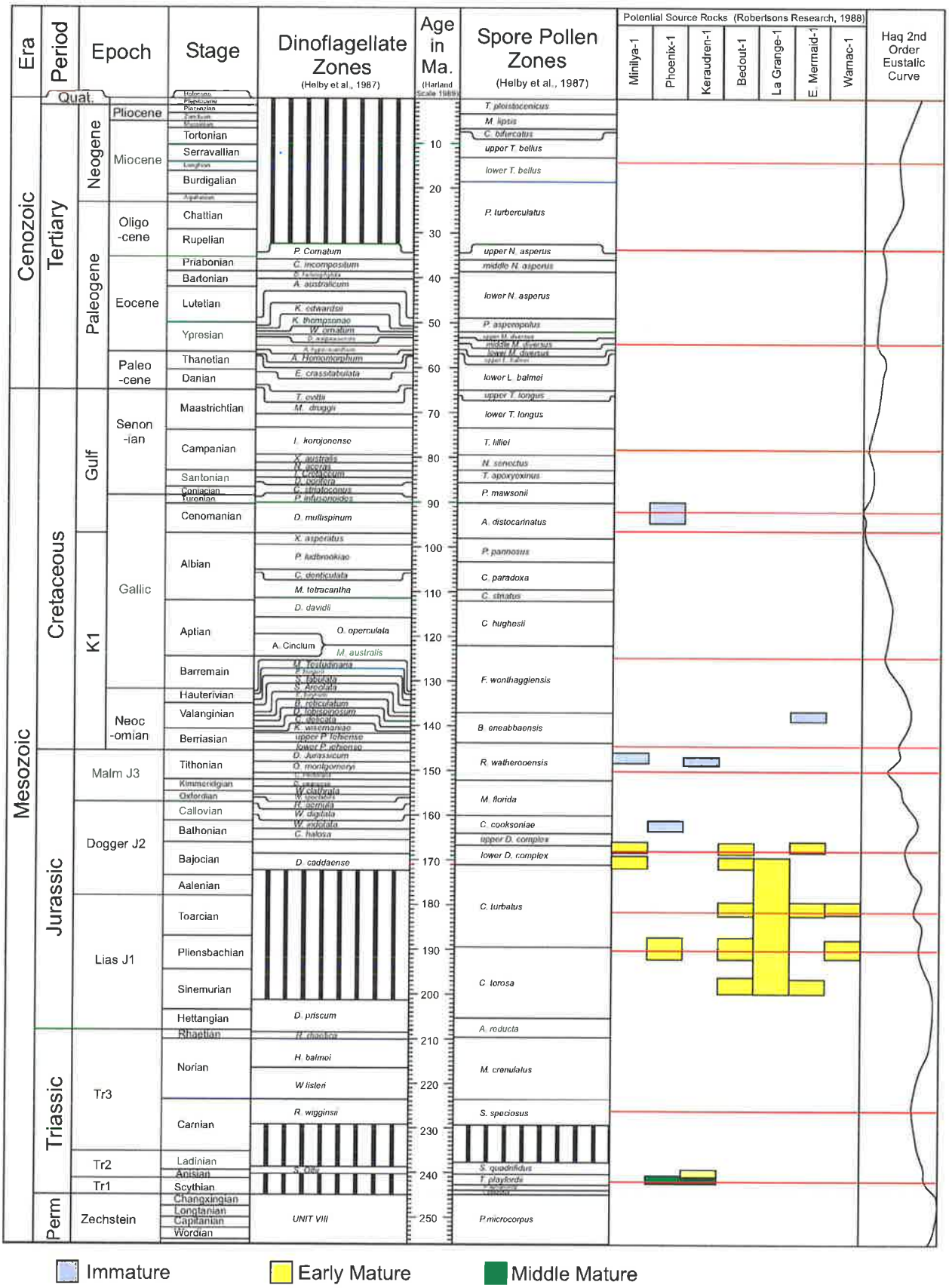

Figure 5.2 Zones of potential source rock identified in each well based on high resolution log and seismic correlations and geochemical studies commissioned by JNOC (1987, 1988). Identified zones correlate well with global sea-level highs.

values (see Table 5.7, Fig. 5.4 and 5.5(a)). A reasonable correlation was observed between low measured maturity and marine influence in depositional environment. Anomalously low measured vitrinite is a common phenomenon on the North West Shelf in marine sequences (Wilkins et al. 1992). Assuming a similar condition in the Roebuck Basin then most of the wells from the Roebuck Basin have maturity/depth relationships consistent with being at maximum temperatures now.

Three wells were identified that have measured maturity values greater than calculated; Lagrange-1, Bedout-1 and Wamac-1. Wamac-1 has a high maturity value in the Palaeozoic section whereas Lagrange-1 and Bedout-1 have high values in Triassic to Early Jurassic section. In the case of Wamac-1, dolerite intrusions are probably related to the high measured maturity (Fig. 5.4(c)).

For Bedout-1 and Lagrange-1 higher palaeo-heat flow was used to try to model the high maturity values. Using the rifting heat flow option in BasinMod™, models were generated with rifting between 250 and 240 Ma, however, these did not generate calculated values close to the measured data (Fig. 5.3(b) and Fig. 5.5(b)). For Lagrange-1 a model using high palaeo-heat flow and erosion was generated which gave a reasonable fit to the data (Fig. 5.3(c) and Fig. 5.5(c)). Approximately 4000 m of sedimentation and erosion at around 200 Ma would be required to model the vitrinite reflectance profile observed in the well. No evidence exists to suggest that such a model is a realistic geological representation, but it does show the thermal properties required to obtain a match. To accurately model the vitrinite reflection profile, the basal unit (253 Ma) requires heating by approximately 40 °C above its present temperature at sometime before 150 Ma, suggesting that the Bedout High area had high heat flow associated with it sometime before the Middle Jurassic.

In addition to 1D models generated using BasinMod™ 2D models were also produced using Sedpak (Fig. 5.6 and Figs. 4.10, 4.11 and 4.12). Details of the generation of these models is given in Section 5.6. Care must be taken when interpreting these 2D models as they are poorly constrained and reflect maturity profiles at the end of each simulation (88 Ma). However, each 2D profile was calibrated by direct comparison with well-data. For example, a comparison of the maturity of Fig. 5.6 (time C6-2) at location 220 km (the location of Lagrange-1), with maturity during the early Late Cretaceous in Fig 5.5(a) reveals that, in both models, the basal unit is about to reach early maturity. Using a similar approach with Fig. 4.11 at 180 km (the location of East Mermaid-1) and Fig. 5.4(a), it can be shown that 2D modelling has slightly underestimated predicted maturity (sediments deposited at 189 Ma are just entering the early mature window in the 2D model, whereas sediments deposited at 184 Ma are reaching early maturity in the 1D model). A similar slight underestimate was obtained between Fig. 4.12 at 215 km and Fig. 5.4(c).

Devonian and Ordovician rocks have not been sampled and maturity of the section is unknown. However, generated hydrocarbons are likely to have already migrated into Palaeozoic traps. On the Broome arch, onshore Ordovician source rocks have reached maturity prior to Devonian sedimentation (Passmore, 1991). Based on modelling in Wamac-1 (Fig. 5.4(c)) Carboniferous source rocks are presently within the oil window in much of the offshore Fitzroy graben.

Using results from 2D modelling, the thermal maturity profile of the basin through time can easily be visualized (Fig. 5.6). In the Bedout and Rowley Sub-basins, early to middle Triassic source rocks are presently within the oil window (Fig. 5.4(b)), unlike the Rankin Trend where maturity modelling has shown it is over-mature (peaked prior to Tithonian) (Brikke 1982). Large portions of the western Rowley Sub-basin have potentially been generating liquid hydrocarbons from the Middle Triassic and a mixture of liquid and dry hydrocarbons from the Early Jurassic on. Maturity in the eastern Rowley Sub-basin (Figs. 4.11 and 4.12) is lower than the deeper buried

Bedout-1			*E. Mermaid-1*			*Keraudren-1*			*La Grange-1*		
Strat Int	Dep Env	Fit	Strat Int	Dep Env	Fit	Strat Int	Dep Env	Fit	Strat Int	Dep Env	Fit
145-0	M	VR≤C	160-0	M	VR<C	157-0	M	VR<C	171-0	M	VR=C
206-145	NM	VR≤C	190-160	NM	VR≤C	203-157	NM	VR=C	253-171	NM	VR>C
253-243	M	VR>C				235-203	M	VR<C			
						245-235	NM	VR<C			
Maturity Timing		For Unit 253			For Unit 191			For Unit 245			For Unit 253
a) Early		>120Ma			>120Ma			>200Ma			>80Ma
b) Middle								>90Ma			
c) Late											

Lynher-1			*Minilya-1*			*Phoenix-1*			*Wamac-1*		
Strat Int	Dep Env	Fit	Strat Int	Dep Int	Fit	Strat Int	Dep Env	Fit	Strat Int	Dep Env	Fit
214-0	M	VR<C	170-0	M	VR<C	160-0	M	VR<C	91-0	M	
						220-160	NM	VR≤C	157-91	M	VR<C
						245-220	M	VR<C	265-157	NM	VR≤C
									NM	NM	VR≤C
Maturity Timing		For Unit 214			For Unit 170			For Unit 240			For Unit 264
a) Early		>120Ma			>30Ma			>230Ma			>110Ma
b) Middle		>60Ma						>190Ma			
c) Late								>30Ma			

Key

Stratigraphic Interval	Units=Ma	
Depositional Environment	M=Marine	NM=Non-Marine
Fit	VR=Measured Vitrinite Reflectance	C=Calculated VR

Table 5.7 Results of thermal modelling for six wells in the Roebuck Basin.

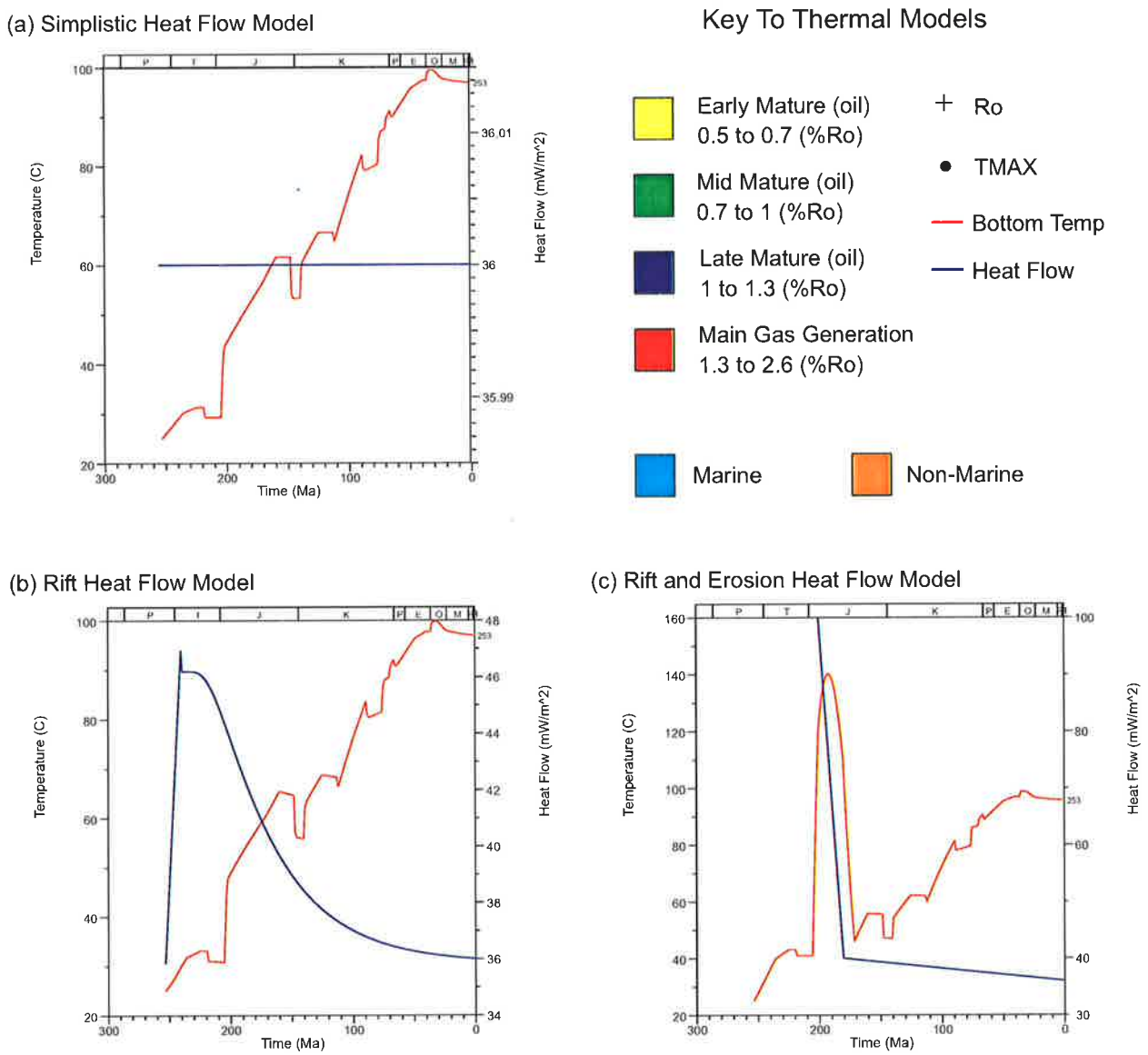

Figure 5.3 Heat-flow models and key to thermal models: (a) Simple heat-flow rate used for all thermal models (b) Rift heat-flow rate used to model increased maturity at Lagrange-1 (c) Rift and erosion heat rate used to model increased thermal maturity at Lagrange-1.

western Rowley Sub-basin. Less gas flushing of potential accumulations would be expected in this area. The Triassic is likely to be over-mature in the deeper water areas (Fig 5.6). Early to Middle Jurassic source rocks appear to have just entered the mature zone in the eastern and central Rowley Sub-basin (Fig. 5.6). In deep water areas Late Triassic, Lower Jurassic and possibly middle to Late Jurassic source rocks may be presently generating hydrocarbons.

Maturity implications for each identified source interval is discussed in more detail in Section 5.5.1.

5.5 Discussion

5.5.1 Petroleum Systems

5.5.1.1 Pre-Westralian Petroleum Systems

Although not addressed in detail in this study, work in the onshore Canning Basin by Kennard et al. (1994) has identified several viable petroleum systems in Permian and pre-Permian sediments, which include the Larapintine 2, 3 and 4 and Gondwanan 1 and 2 supersequences. Seismic interpretation suggests that these petroleum systems extend into the offshore area along the older Palaeozoic trends that underlie the Bedout

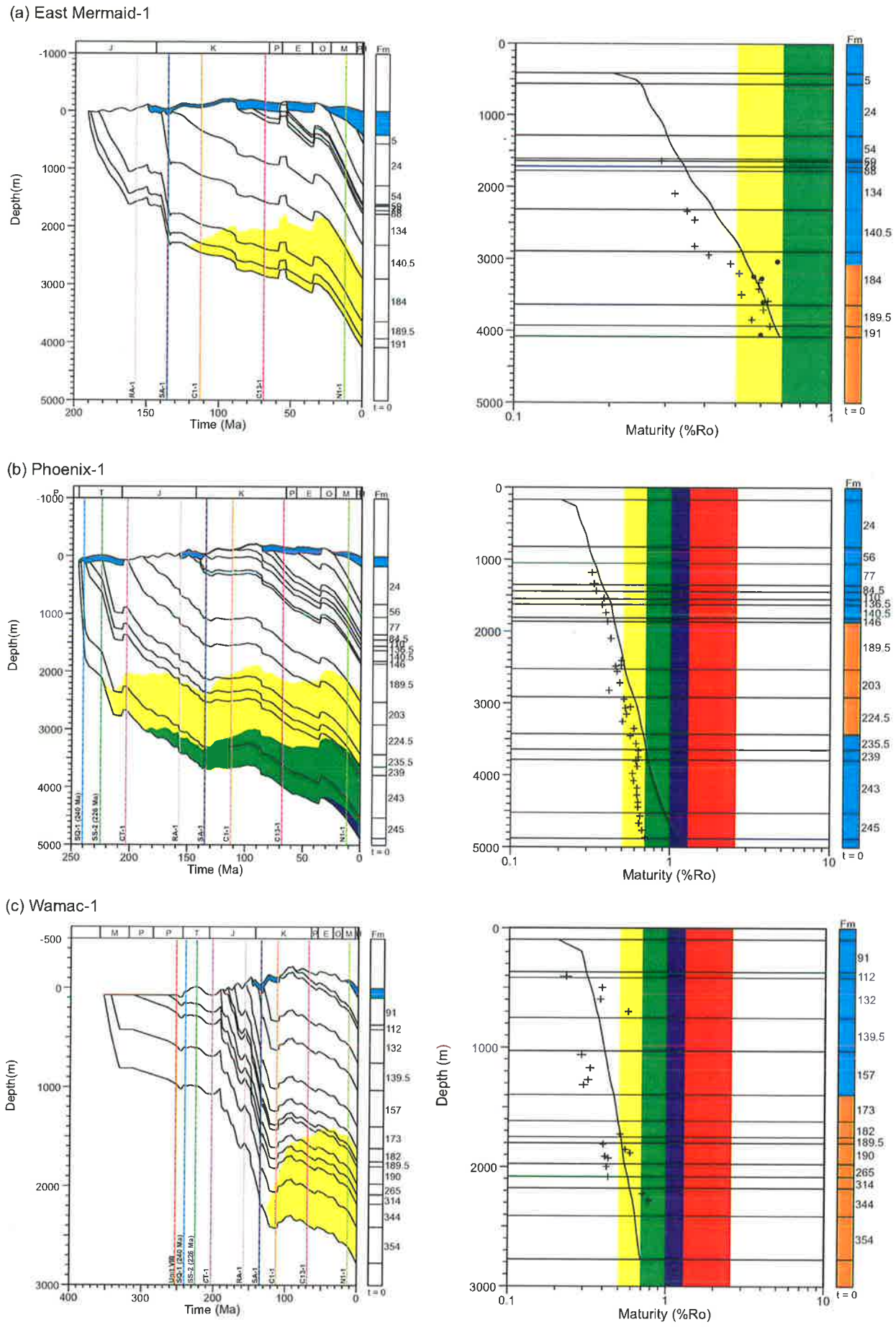

Figure 5.4 Simple 1D thermal models from across the basin: (a) East Mermaid-1 from the Rowley Sub-basin (b) Phoenix-1 from the Bedout Sub-basin (c) Wamac-1 from the Oobagooma Sub-basin.

(a) Lagrange-1 Simplistic Model

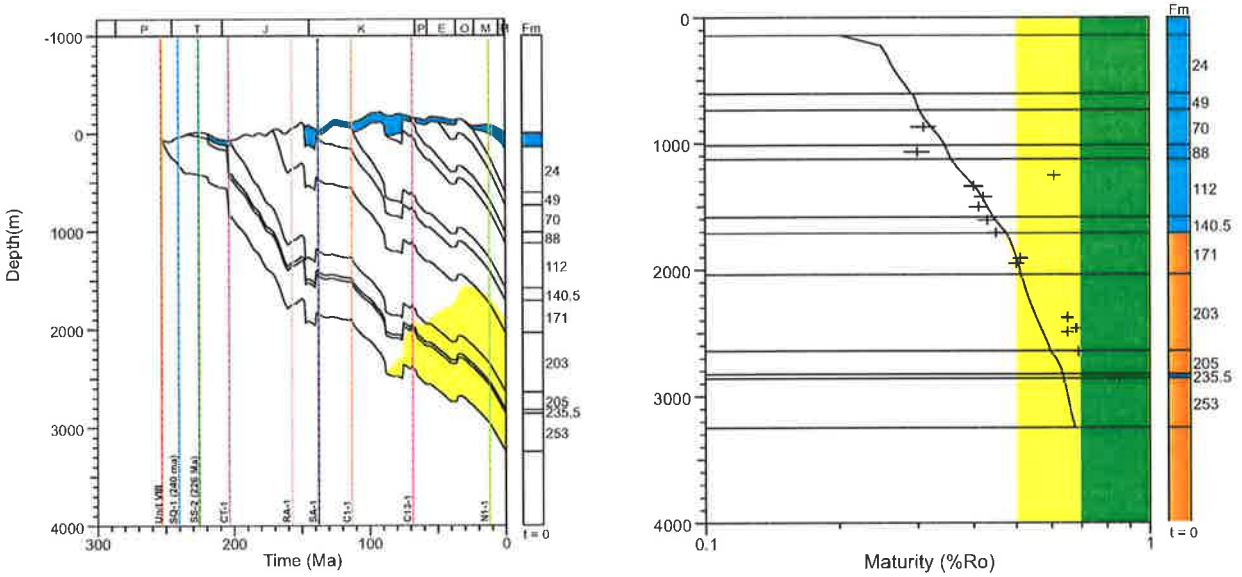

(b) Lagrange-1 with Rift Heat Flow

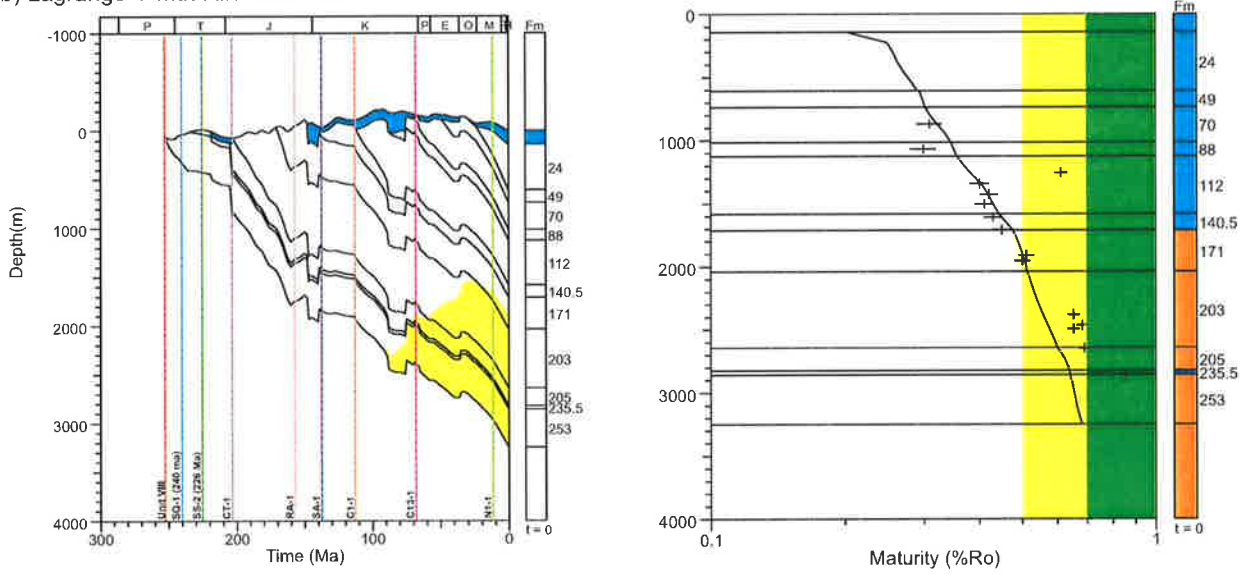

(c) Lagrange-1 with Rift Heat Flow and Erosion

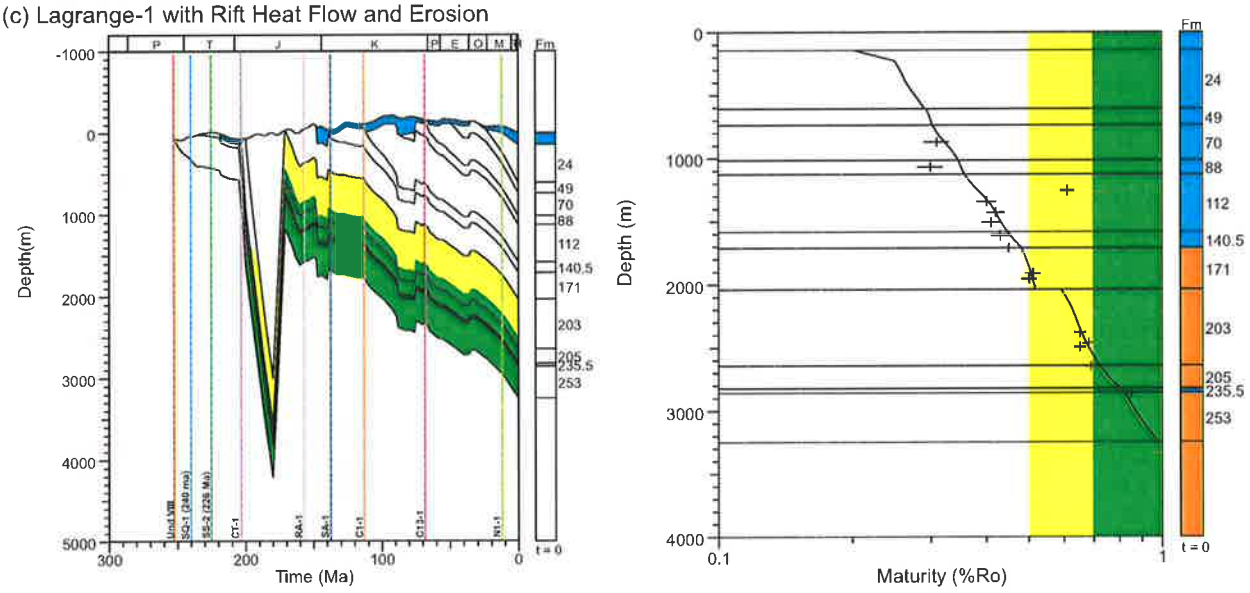

Figure 5.5 More advanced 1D thermal models for Lagrange-1: (a) Simple heat-flow model (b) Rift heat-flow model (c) Rift heat-flow and 4000 m burial and erosion prior to the Callovian.

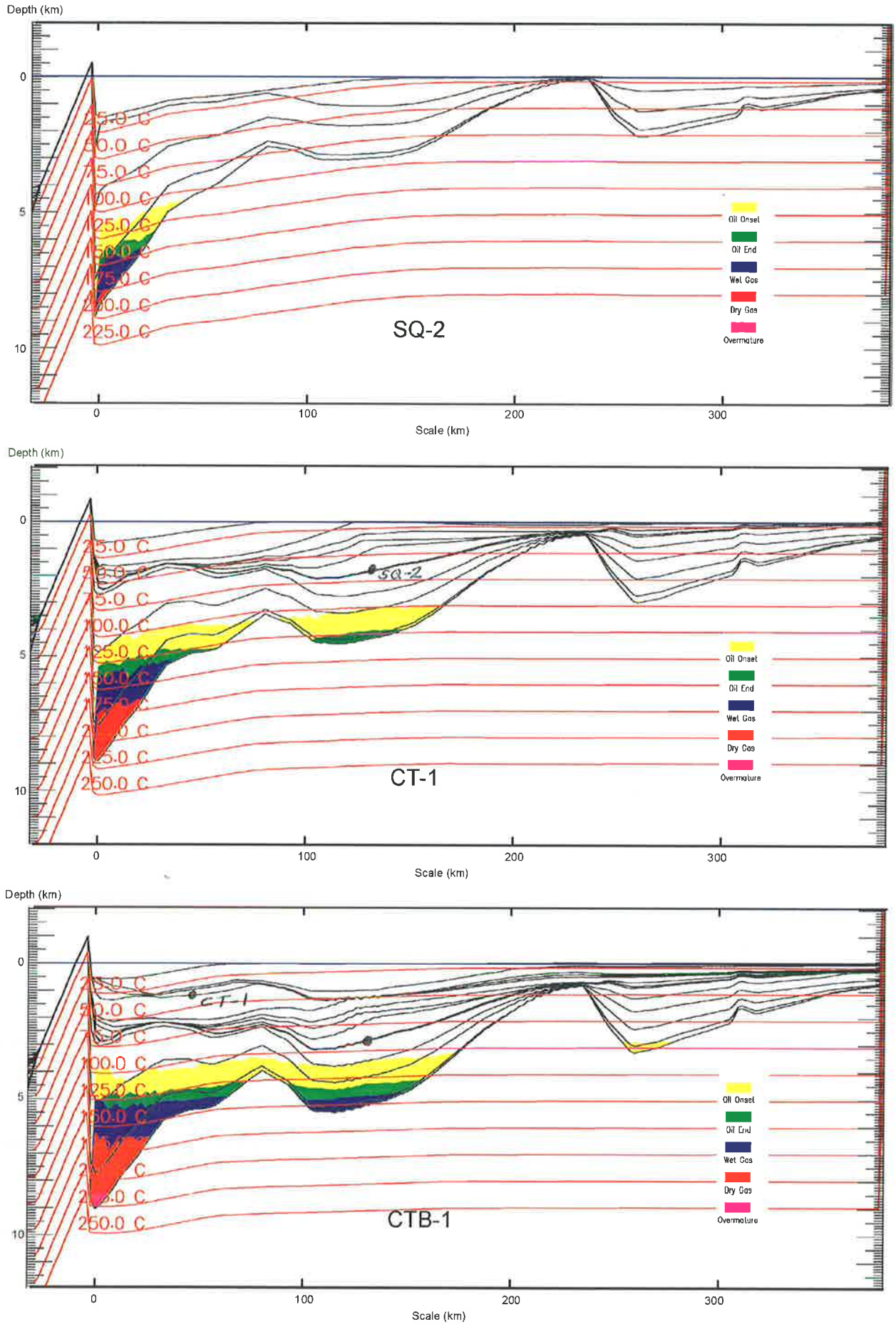

Figure 5.6 Sedpak maturity simulations of line BMR120-01 through time – (top) at *SQ-2* (middle) at *CT-1* (bottom) at *CTB-1*.

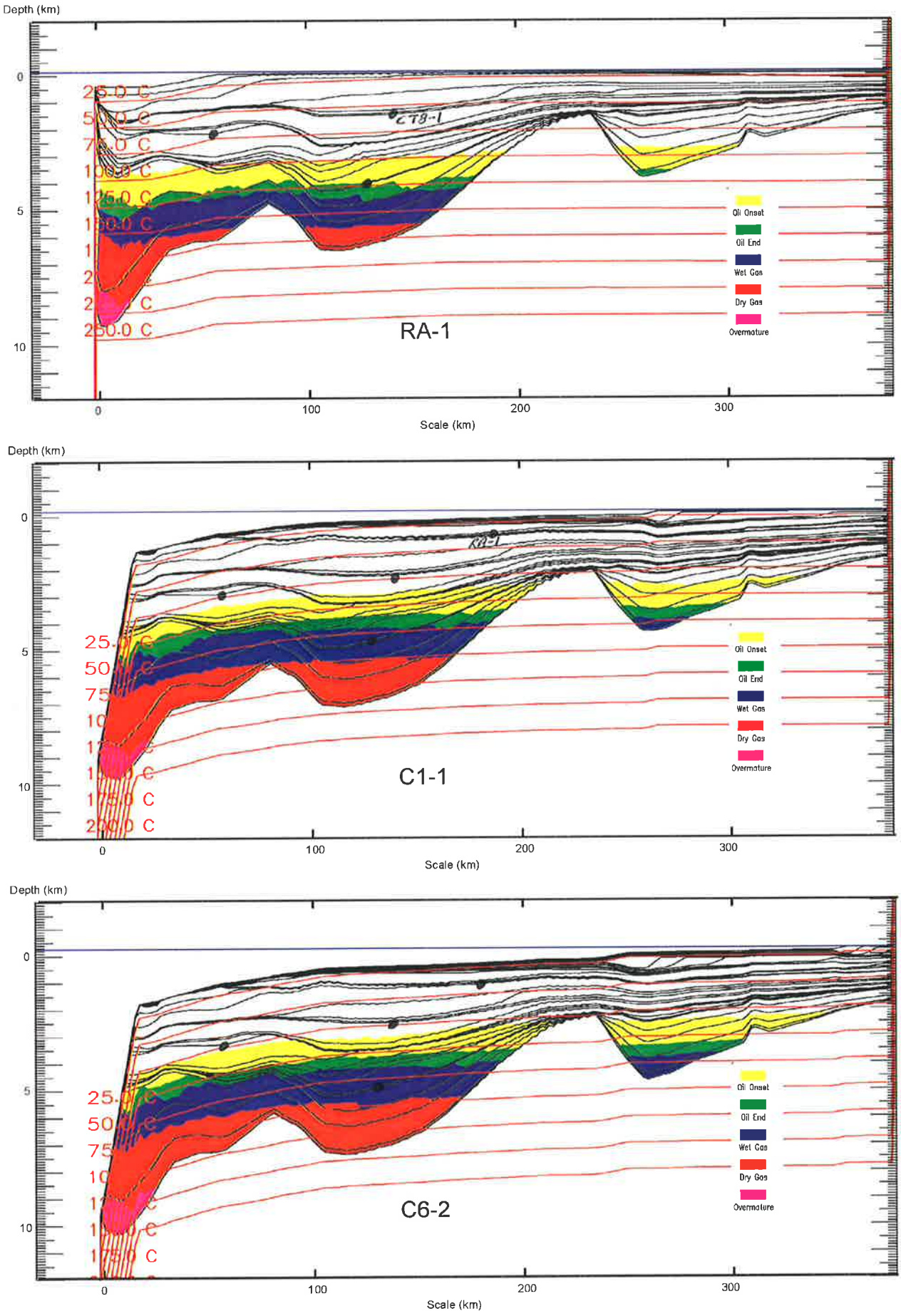

Figure 5.6 Cont. – (top) at *RA-1* (middle) at *C1-1* (bottom) at *C6-2*.

and Oobagooma Sub-basins. However, wells drilled to date in the Bedout and Oobagooma Sub Basins have not penetrated these petroleum systems. Provided they have been preserved, and where migration pathways exist, these source rocks may be a significant hydrocarbon source for the present shallower offshore Paleozoic and Mesozoic traps.

5.5.1.2 Westralian Petroleum Systems

The ten identified source rock intervals in the Roebuck Basin can be sub-divided into four groups of units depending on their tectono-depositional setting. Tr1 and Tr2 were deposited during rapid thermal sag, J1 to J5 were deposited during gentle thermal sag and infill, K1 and K2 were deposited during rift and post-rift sedimentation, and K3 was deposited during passive margin conditions. These four groups are believed to have a wide geographic distribution along the North West Shelf as similar sub-divisions have been identified by McConachie et al. (1996) in the Petrel Sub-basin. The four groups have been termed the Westralian 1, 2, 3, and 4 petroleum super-systems. This differs slightly from the original Westralian petroleum system classification of Bradshaw et al (1994) who grouped the Lower Triassic in the Gondwanan petroleum system. In the Roebuck Basin Lower Triassic sedimentation appears related to early thermal sag during Westralian break-up.

5.5.1.2.1 Westralian 1 (Units Tr1 and 2)

Westralian 1 sediments consist of Lower Triassic marine shales and deltaic sands (Locker Shale equivalents and Lower Keraudren Formation) first deposited during a phase of rapid thermal sag shortly after a period of uplift and erosion that is associated with the Bedout Movement (Forman and Wales, 1981). During this time, sedimentation rates kept pace with subsidence leading to the development of a typical McKenzie-type 'steer's head' sedimentary stacking geometry.

The oldest section of the Westralian 1 unit has been penetrated in Phoenix-1 and 2, and Keraudren-1. JNOC (1987) identified a zone in Phoenix-1 from 3,900 to 4,280 m with high TOC values of up to 6% (12 samples greater than 3%). This interval was interpreted to consist of type I and II kerogen based on Van Krevelen plots, however visual analysis revealed only gas prone inertinite and vitrinite. Pyrolysis-gas chromatography (PYGC) confirm the land-derived waxy content of the source interval with peaks greater than C20 dominant. There may be several reasons for the discrepancy between Van Krevelen plots and visual studies, including bias due to hand picking of samples richer in oil-prone algal material for bulk Rock-Eval analysis. In addition, Triassic samples are middle mature for oil generation (Figs. 5.4(a) and (b)) so some of the oil prone kerogen will already have been converted to hydrocarbons leaving behind inertinite as the dominant kerogen type in the bulk of samples selected for visual analysis. However, the input of land-derived material is believed to be high in Western Australian marine source facies (Scott, 1994). The presence of large amounts of terrestrially derived inertinite during Rock-Eval has been cited as the cause of under-estimation of the HI of source rocks, as inertinite does not contribute to the S2 fraction but does contribute to the TOC value (Scott, 1992; Horstman, 1994). For this reason many of the source rocks previously evaluated as gas prone in the Roebuck Basin may have more liquid potential than first estimated. Many liquid hydrocarbons of the North Rankin, Goodwyn, Angel and Eaglehawk fields show biomarker affinities to a Lower Triassic source (Brikke, 1982) and Triassic biomarkers were also noted in the Saladin field, suggesting a possible contribution from Triassic source rocks (Tait et al., 1989).

Large amounts of land-derived material in Westralian source rocks imply that fresh-water run-off was high (Scott, 1998). Both thermocline and halocline development would be expected in a restricted basin with positive fresh-water balance, leading to anoxic conditions and the deposition of black laminated shales. Although core data are limited, shale successions contain a variety of grey colours rather than black,

suggesting that anaerobic conditions prevailed (Scott, 1998). Terrestrial material is probably preferentially preserved compared to marine algal material under anaerobic conditions (Scott, 1998). Algal material was probably only preserved basin-wide during regional anoxic events.

Two potential anoxic intervals, units Tr1 and Tr2, which contained a higher algal composition, were identified in the Triassic section (Table 5.6). The basal unit Tr1 is richer in oil prone algal material than the upper unit. Similar observations have been made in the Perth Basin by Thomas (1984) suggesting that this phenomenon may be regional. The algal content of many Triassic samples in Keraudren 1 exceed 40 %.

Maturity of both the Tr1 and Tr2 units varies across the basin. Vitrinite reflectance data (excluding single measurement data points) from JNOC (1987) are plotted on Figure 5.4 and 5.5. Although vitrinite data suggest that the Westralian 1 super-sequence is early mature at this location, thermal modelling results using present thermal conditions suggest that it is middle mature for oil generation. The difference in modelled versus measured vitrinite reflectance is likely to be the result of vitrinite suppression which has been observed elsewhere on the North West Shelf (Wilkins et al, 1992; Kaiko and Tingate, 1996). There is a general correlation between marine sequences and increased suppression in the Roebuck wells examined so far. Further thermal maturity data (e.g. FAMM, VRF and apatite fission track) would be useful for future, more detailed, thermal modelling.

Assuming that the calculated vitrinite maturity trend is correct, the basal unit is still relatively immature considering burial in excess of 5,000 m. Modelling with a constant thermal gradient (2.5 to 3.0 °C100 m-1) based on current thermal conditions suggests that the Westralian 1 super-sequence source rocks entered the oil window in the Early Jurassic. Maturities would increase and the timing of generation would occur earlier where burial depth is greater, and towards the main rift axis where heat flows were elevated in the past. For example, East Mermaid-1 located in the inner Rowley Sub-basin did not penetrate the Westralian 1 super-sequence unit but shows higher levels of maturity at time-equivalent units than Phoenix-1 due to deeper burial (Fig. 5.4a).

The spatial distribution of the Westralian 1 super-system can be mapped seismically by the onlap/unconformity surface of the top Triassic (CT-1) event (Fig. A2.5 Appendix 2). Marine sediments of latest Permian and earliest Triassic age, such as the Chirup and Blina Shales, have been intersected in Chirup-1 and Wallal-4,4a located on the coastline, landward of this onlap surface. These sediments are interpreted to represent the remnants of a well-developed marine incursion that occurred during the Early Triassic but were subsequently exposed during the Middle Triassic Fitzroy Movement I.

Organic preservation during the Early Triassic is believed to have occurred during basal marine transgression over irregular topography formed during Late Permian rifting (Scott, 1998). These small basins had restricted circulation and helped promote localized anoxic conditions. Isolated depocentres also formed during tectonic movement associated with the Fitzroy Movement I along the northern margin of the basin and along the western margins of the Bedout and Rowley Sub-basins (Appendix 1 Fig. A1.5). More widespread anoxic conditions were restricted to periods of higher productivity or increased fresh water run-off. High sedimentation rates during this period resulted in rapid burial of organic material below the sediment-water interface, further aiding organic preservation. The dilution in concentration of organic material during rapid sedimentation does not appear to have been detrimental to source rock development during this period. As sediment infilled each depocentre and the transgression progressed, more open marine conditions prevailed, accounting for the upward decrease in source quality (Scott, 1998).

Only limited analysis of the hydrocarbon accumulations that occur in the Roebuck Basin has been conducted. Accumulations that are

associated with the Westralian 1 super-system include discoveries at Phoenix-1 and 2. Both wells encountered gas and oil in Middle and Upper Triassic sandstones, possibly sourced from the Lower Triassic. However, deeper Palaeozoic or down-dip Jurassic source rocks cannot be discounted as the generative source for these accumulations.

In the western half of the basin Tertiary faulting creates potential migration pathways to younger reservoir units. Faulting is more limited in the central and eastern parts of the basin and migration pathways to younger reservoirs may be limited. In these areas sources may form self-sourcing reservoir systems similar to those described by Scott (1998). Onlap plays of Triassic age have previously been identified in the Bedout Sub-basin (Lipski, 1994), and offer attractive hydrocarbon targets. Similar style onlap plays have been identified around the Bedout High and in the Rowley and Oobagooma Sub-basins throughout the Lower and Middle Triassic section (Appendix 2 Fig. A2.4).

5.5.1.2.2 Westralian 2 (Units J1 to J5)

Units J1 to J5 were deposited under fluvio-deltaic conditions during declining thermal sag. Sediments consist of braided and stacked channel sands interbedded with transgressive shales, lagoonal coal beds and sapropels, overbank deposits and deltaic facies. TOC values for shales generally average between 1 and 5% but in intervals rich in coals and sapropel zones exceed 20%. Rock-Eval analysis of algal rich intervals, especially the J2, J4 and J5 sequences, appear to have exceptional oil generation potential (S2 values of 10 to 20 mg/g and HI values of 250 to 400) and appear similar in nature to the 'Type B' Jurassic facies identified by Scott on the North West Shelf (1998). Unfortunately, these facies are only thinly developed and Scott (1998) has highlighted the fact that these facies can vary locally from oil prone to gas prone between wells only 20 km apart. Units J1 and J3 have large TOC values but are dominated by gas prone coaly material.

Only the more proximal sediments of these sequences have been intersected in the Phoenix wells and potential upside exists in the Rowley Sub-basin where more distal shales may be expected.

Units J1 to J5 were deposited during a series of well-developed prograding wedges that can be observed on seismic data and mapped on chronostratigraphic cross-sections. The chronostratigraphic section at the top of Figure 3.10 shows the development of a strong downlap surface and basinward shift in sediment depocentre between sediment packages 55 and 80 at the western end of the line from 200 to 170 Ma (also see Fig. 2.6). Episodes of progradation appear to be triggered by major tectonic readjustments of the shelf — an observation similar to that of Jablonski (1997). During the Jurassic each tectonic event is associated with a landward shift in coastal onlap followed by the development of a pronounced downlap surface. During the development of these downlap surfaces sedimentation rates, which have been calculated from preserved sediment volumes on the chronostratigraphic sections, are seen to increase.

Development or preservation of source rock material in the Roebuck Basin has been strongly influenced by these tectonic processes. Source rock development is associated with the deposition of sapropelic and coal-rich material in lacustrine lakes and restricted embayments that developed during the formation of irregular topography during periods of rifting and subsequent rapid transgression. Additional organic preservation is also likely to have occurred in the pro-delta setting during later delta outbuilding caused by increased sediment rates. Increased sedimentation rates are believed to have resulted from rejuvenation of the sediment province during tectonic activity.

Sedimentary modelling has been used to simulate the depositional processes that occurred during deposition of the Mesozoic section in the Roebuck Basin (Fig. 4.10, 4.11 and 4.12). As shown in the

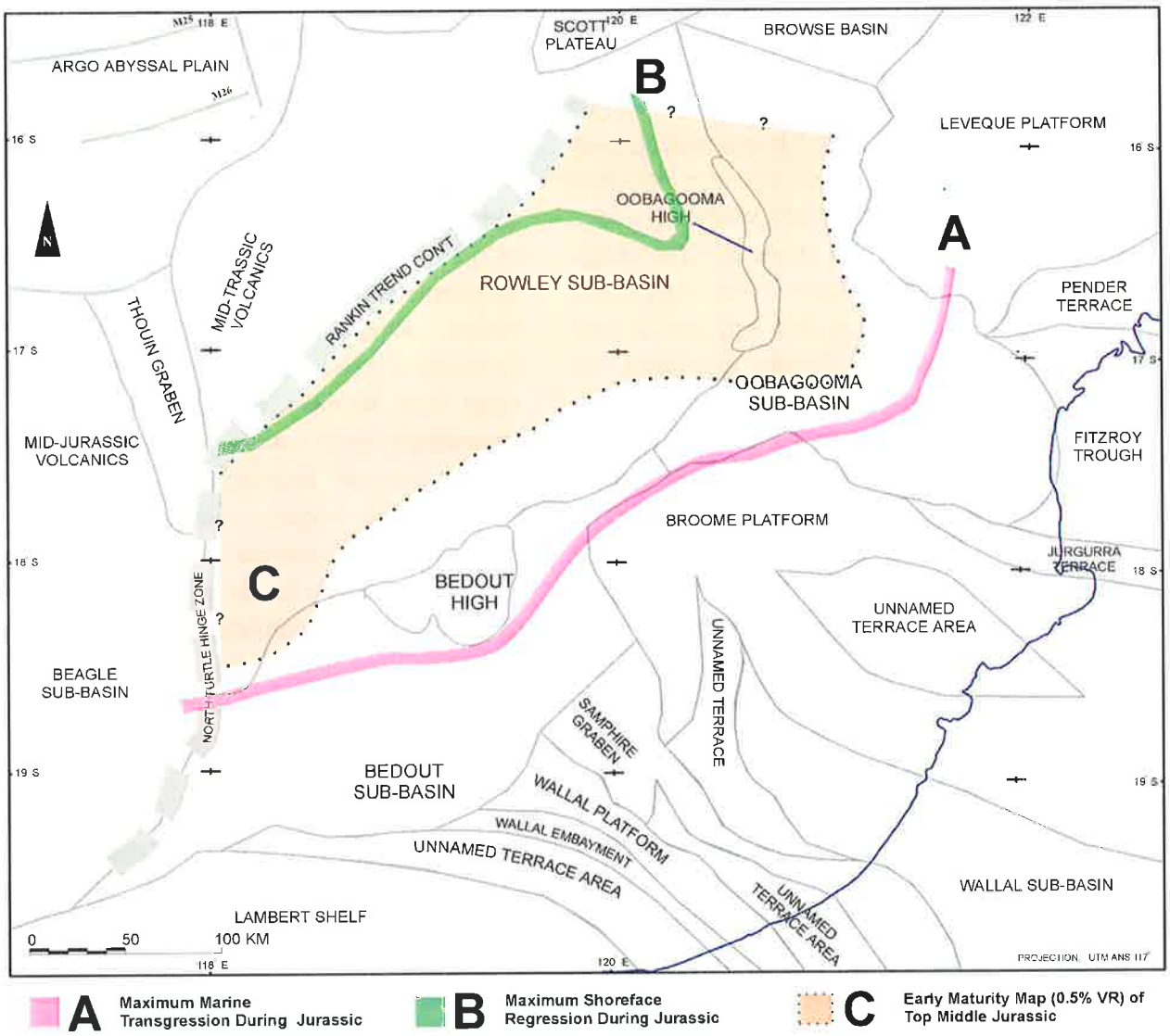

Figure 5.7 Jurassic play fairways map showing the potential distribution of interbedded source and reservoir/seal pairs. Estimated area of early mature Middle Jurassic is shown by shading.

above figures, J1 to J5 were deposited between time markers –203 Ma and –157 Ma. During this time interaction of sea level, tectonics and sedimentation, resulted in a series of transgressive–regressive cycles across the basin. Although this model offers only a coarse temporal representation, four marine incursions, each of which are followed by the development of a progradational wedge, are clearly identifiable. Modelling also suggests that the thickest delta front development occurred in the inner Rowley Sub-basin to the north-west of the Bedout High, that is between 80 km and 150 km on the model section (Fig. 4.10) and between 160 km and 240 km on seismic line BMR120-01 (Appendix 1 Fig. A1.2). Focused delta development in this area is most probably related to Jurassic depositional isostatic loading, preferentially occurring in the region as a result of differential compaction around the Bedout High. This region offers many attractive stratigraphic exploration targets such as isolated channel systems, coastal sand deposits and barrier-bar systems. These reservoir-trap systems are potentially sourced/sealed by high-quality source rich, pro-delta, shale systems. Although detailed seismic facies analysis was not conducted during this study, a quick-look examination of seismic line BMR120-01 does reveal higher amplitude, mounded and channeled features in this interval (Appendix 1 Fig. A1.2 between 220 and 240 km, 3 to 3.7 s TWT).

The 2-D maturity profile reveals that at 90 Ma the base of the Jurassic was currently in the early

maturity oil generation window (Fig. 4.10) in the western part of the Rowley Sub-basin. Sedimentation rates slowed down after the Turonian, and consequently thermal maturity over the majority of the basin would not have increased until development of the thick carbonate wedge during the Oligocene and Miocene. This wedge can be clearly seen on seismic line BMR120-03 (Appendix 1 Fig. A1.3 at 180 km) and is best developed in the inner Rowley Sub-basin. An isochron map of the Base Oligocene to Middle Miocene section (Appendix 3 Fig. A3.12) shows the spatial distribution of this wedge. Sediments underlying this wedge will have been subject to increased temperatures since the onset of its development at the base of the Oligocene. Increased source rock maturities are to be expected below it, which would push the Tr1 and Tr2 units into the dry gas window, thus presenting a possibility of gas flushing for prospects within this area. The Jurassic and the lowest Cretaceous section are predicted to lie within the oil window. Towards the basin margins maturity diminishes due to thinner overburden, although, conversely, towards the rift margin the thermal gradient will be greatly increased due to crustal extension and thinning. The Jurassic play-fair resulting from juxtaposition of all major play elements is shown in Figure 5.7.

No hydrocarbon accumulations have been discovered in the Roebuck Basin which have been attributed to a Jurassic source. However, oil staining has been observed in the Jurassic section in some wells (see Fig. 5.1).

5.5.1.2.3 Westralian 3 and 4 (Units K1 to K3)

Within the Roebuck Basin Cretaceous sediments were preserved under similar tectonic conditions to Jurassic sediments. During both periods, sediments prograded into gently sagging, post-rift basins, without major faulting. However, by Cretaceous times, as Argoland and India drifted away from Australia, conditions were becoming increasingly open marine. Total organic carbon values average approximately 2 to 4% and kerogen type became increasingly gas-prone. Although large volumes of source rock were deposited, maturity for oil generation only occurs below the Tertiary carbonate wedge (Appendix 3 Fig. A3.12). Potential for oil generation from Cretaceous source rocks is difficult to predict but is believed to be small compared to that from the Jurassic and Triassic.

Cretaceous to Recent reservoir distribution was increasingly restricted to the basin margin areas due to increased water depth. Significant sand development only occurred during increased uplift associated with the separation of India and Australia in the Valanginian. Sedimentary modelling suggests that delta building was focused along the inner axis of the Rowley Sub-basin at this time. Unfortunately, no hydrocarbon accumulations have been found in the Cretaceous to Recent section in the Roebuck Basin.

CHAPTER 6

CONCLUSIONS

"So flashed and fell and brand Excalibur:
But ere he dipt the surface, rose an arm
Clothed in white samite, mystic, wonderful,
And caught him by the hilt, and brandished him
Three times, and drew him under in the mere.
And lightly went the other to the King."

"Then spoke King Arthur, drawing thicker breath:
'Now see I by thine eyes that this is done.
Speak out: what is it thou hast heard, or seen?' "

Morte D'Arthur
Alfred, Lord Tennyson

6.1 Background

The Roebuck Basin is one of four major sedimentary basins that makeup Australia's North West Shelf. Although the basin is situated in the middle of Australia's rich hydrocarbon province, only sub-economic gas discoveries have been made to date leading to a down-grading of the basin's prospectivity, so that over the past few decades, only brief syntheses of regional data have been conducted within the basin. During this study the key aim was to provide a structural and stratigraphic framework for the evolution of the basin based on sequence stratigraphic concepts. This framework was then used as the basis for understanding and ultimately predicting the timing, distribution and nature of petroleum systems in the basin.

The major findings of this study are summarised here under the general headings; tectonic framework, chronostratigraphic sub-division, basin development, stratigraphic simulations and petroleum potential.

6.2 Tectonic framework

The major results of regional mapping are shown in Figure 2.11. Regional mapping has enabled accurate delineation of the structural features in the Roebuck Basin which were only crudely defined using older vintage seismic data. Using deep seismic data, new features have also been identified. Of note is the Oobagooma High, a newly identified Palaeozoic structure that separates the Oobagooma Sub-basin from the Rowley Sub-basin at the Palaeozoic level. Structural discontinuity can be observed in sediments stretching from the Oobagooma High across the front of the Broome Platform to the Bedout High feature. Both the Oobagooma and Bedout Highs are interpreted to have formed due to compressional forces over a major crustal detachment possibly related to an accommodation zone formed during earlier NE extension (the North West Shelf Megashear of AGSO (1994)).

In general, structuring is complex along the margins of the basin and changes from asymmetrical half-graben extension onshore to symmetrical graben extension in the near offshore to thin-skinned detachment in the outer offshore area. Style of extension appears to be controlled by the location of the more rigid elements of the basin, with normal faults developing near the stable bounding Kimberley Craton and Leveque Platform to the NE and the Broome Platform to the SW. These structural provinces were used to divide the Oobagooma Sub-basin at the Palaeozoic level into three compartments separated by hardlinked transfer zones. Each compartment is interpreted to control the

distribution of petroleum play elements during the Palaeozoic. Greatest potential is interpreted to occur along the NE margin of the onshore compartment which is believed to have been restricted at this time resulting in better development of source rock.

6.3 Chronostratigraphic sub-division

In addition to regional mapping, more detailed interpretation was conducted in conjunction with sequence stratigraphic analysis of available well data. This proved problematic in the upper part of the section which is carbonate-dominated. For carbonate-rich sediments wire-line methods have not been well documented. In addition, the mid Cretaceous to Recent section of the Roebuck Basin has traditionally been over-looked during biostratigraphic sampling due to its perceived lack of hydrocarbon potential, making prediction of the timing of events even more problematic. To resolve this, a new method of log interpretation was utilised for the upper part of the section based on the following observations (see Fig. 3.5). During carbonate production lowstand systems tracts are characterized by an increase in gamma and irregular sonic readings associated with increased clastic input and reduction in area available for carbonate production. During transgression the gamma log cleans up due to predominantly carbonate deposition as siliciclastic deposition is relocated in a landward direction and an increased proportion of the shelfal area becomes flooded and available for carbonate production. The maximum flooding surface is represented at the lowest gamma reading at the top of the distinctive cleaning up transgressive package. The subsequent highstand systems tract shows constant gamma and sonic values up until the following sequence boundary where fine grained siliciclastic input causes a sharp increase in gamma and sonic.

Sixty-four boundaries were identified that could be partially correlated throughout the basin and used to date the section. Using this chronostratigraphy, the major events in the basin were dated and used to divide the basin-fill. Results of this sub-division are shown in Figure 3.21.

6.4 Basin development

Structurally, the Roebuck Basin is interpreted to have developed as a result of a multiphase rift history under four main stress regimes: NE-SW extension resulting in an intra-cratonic fracture sequence associated with the separation of the Chinese blocks from Gondwanaland during the Cambrian to Silurian; a transitional phase from NE-SW to NNW-SSE extension associated with the separation of the China-Burma-Malaya-Sumatra (SIBUMASU) blocks during the Late Carboniferous to Late Permian with development of both NW-SE and ENE-WSW structures; a NNE-SSW post Late Permian extensional phase resulting in formation of the Westralian Superbasin sequence (separation of Argoland and India); and a NE-SW compression phase during collision with Asia during the Middle Miocene to Recent. Each extensional basin phase is strongly related to the development of five break-up events that have effected the northwestern margin of Australia. Four break-up events have been previously identified and well documented in the current literature, occurring in the Cambrian (Chinese), Early to Late Permian (SIBUMASU), Middle Jurassic (Argoland) and Early Cretaceous (India). A possible fifth break-up event which developed during the Early Jurassic has been identified during this study which has previously been identified in the past as rift onset for the Middle Jurassic breakup episode.

During the four major stress regimes described above, eleven basin forming phases were identified which have also been used to divide the basin-fill into megasequences related to the development of the five break-up events described above. These events are summarized in Figure 3.21.

Structuring, initiated during the Ordovician, occurred on a series of NW oriented normal faults that formed along the margins of the Oobagooma Sub-basin and the Willara Sub-basin and Samphire Graben. These features developed

under the same stress regime, NE-SW intra-cratonic extension, as the onshore Canning Basin during brittle failure due to upper-crustal thinning.

Transition from NE-SW to NNW-SSE extension during the Late Carboniferous to Early Permian, is marked by the development of gentle thermal sag due to lower crustal thinning and limited upper crustal brittle deformation. Periodic extension in both a NNW-SSE and NE-SW orientation appears to have occurred during this time.

By the Late Permian structuring associated with NE oriented intra-cratonic extension ceased along the Bedout and Oobagooma Sub-basins. Fault inversion resulting from periodic tectonism became prominent along the eastern margin of the Oobagooma Sub-basin at the edge of the Leveque Platform. Renewed NNW extension in the Triassic and Jurassic led to the development of two major structural provinces; 'book-shelf' faulting on a major detachment system to the west and relatively gentle structuring to the east, however, faulting is not interpreted to have contributed significantly to upper crustal extension due to its sub-vertical nature.

Large scale differences in structuring between the Roebuck Basin (subtle) and its adjacent basins (pronounced) suggest that either the crustal composition or stress regime was different in this area. In contrast to the other basins, the Roebuck Basin has undergone NE extension prior to NNW extension which may have altered the crustal composition. Annealling of the upper crust by period heating and cooling during early rifting may strengthen it (strain hardening in Kusznir and Park (1987)).

Triassic thermal sag and marine transgression was punctuated by a series of NW-SE transpressional events that occurred along the margins of each sub-basin, known as the Fitzroy Movement. During this study the Fitzroy Movement has been sub-divided into three tectonic episodes occurring during the Middle Triassic (*SQ-1* 240 Ma), Late Triassic (*SS-2* 226 Ma) and Lower Jurassic (*CT-1* 203 Ma). Of these events Fitzroy Movement III has traditionally been associated with breakup onset along the North West Shelf. The event marks the onset of a major progradational episode and is associated with major uplift across the basin. The outer margin appears on seismic to be a rift shoulder and it is speculatively suggested that this event marks a break-up event previously unrecognised on the North West Shelf. A theoretical model for progressive rift development around a pole or hinge point, that helps explain the formation of transpressional features during rifting, has been developed for the North West Shelf. The model demonstrates that as rifting progresses from NE to SE transtensional/transpressional stresses will be developed due to differential rotational movement between adjacent blocks (Fig. 2.23).

The Middle Jurassic structural development is marked by thermal subsidence after Early Jurassic uplift and erosion associated with Fitzroy Movement III. At the time of Callovian breakup the Roebuck Basin margin underwent a second prominent phase of uplift and erosion with strong truncation of the outer margin during rift shoulder development. Final breakup resulted in the development of massive down-to-the-northwest faulting with the failed rift arm to this rift system running from the north towards the Lambert Shelf. During NNW extension, basin forming processes are interpreted to have involved lower crustal/upper mantle thinning through pure shear processes. A 'flexural-cantilever' model has been proposed for the formation of the basin (Fig. 2.17).

Callovian break-up marked the end of active rifting along the margin directly adjacent to the Roebuck Basin. Late Jurassic to Recent development of the basin can be described in terms of a 1st order eustatic continental encroachment cycle, which is punctuated by tectonic events associated with rifting in adjacent basins rather than along the margin of the Roebuck Basin itself. The oldest preserved sediment sampled above the unconformity to date is *R. aemula* in age, although major thicknesses of sediment were not developed until rejuvenation of the sediment province in response to increased regional uplift

associated with the onset of separation of India from Australia. Palaeo-environmental indicators suggest that offshore deposits have been reworked in marine to deep-marine environments indicating that deeper-water geostrophic flow currents were possibly active on the North West Shelf as early as the Lower Valanginian.

The boundary between thermal sag and passive margin phase has been placed at an unconformity resulting from sea-level fall, and is associated with plate clearance of India beyond the Exmouth Plateau which is associated with the M0 plate ridge jump in the India Ocean. Unconformities were also developed on the North West Shelf during break-up on the Southern Margin between Australia and Antarctica and change in spreading rates between Australia and India.

The greatest level of transgression and 1st order maximum flood occurs immediately above the regional C6-2 seismic marker. Later passive margin development was punctuated by several regionally correlatable tectonic events associated with the onset of collision of India with Asia and the onset and migration of Australia in a northward direction.

Final separation of Antarctica from Tasmania during the Oligocene enabled the development of the Circum-Antarctic Current which resulted in the thermal isolation of Antarctica and rapid global sea-level fall. Post Oligocene deposition is dominated by the development of a massive steep fronted prograding carbonate foreset wedge system which extends across the inner Rowley Sub-basin. After northward migration, the Australia plate collided with Eurasia during the Late Miocene (N17-2) resulting in sinistral wrenching.

Due to limited availability of data, dating of events has been extremely difficult in the Roebuck Basin. A direct comparison of the dating of major seismic surfaces identified during this study was made with those of Romine et al. (1997) for the Cretaceous to Recent of the Northern Carnarvon Basin and Blevin et al (1998) for the Jurassic and older section of the Browse Basin. All studies identify similar surfaces but with slightly different timing. This is interpreted to be a result of slight diachronous formation of sequence boundaries in response to different sediment budgets and tectonic regimes in each basin.

6.5 Stratigraphic Simulation

Forward sedimentary modelling using SEDPAK was employed directly as a tool for palaeogeographic and lithology prediction as well as hypothesis testing. Such predictions were used to directly develop hydrocarbon exploration play concepts and play element distribution and fairway maps in the area.

Comparison of modelling results with well and seismic data suggests that overall geometries and facies distributions along each line had adequately matched using the available input parameters. The simulations can therefore be used as a reasonable visualization tool for the distribution of sediment fill throughout time and the sea-level curve, sediment budget and subsidence history derived for the basin are reasonable approximations and are useful in delineating the basin development and fill-history.

Six sea-level curves were used to derive sea-level during modelling; the Roebuck Basin derived curve and its hi-cut frequency filtered equivalent, the Haq 2nd and 3rd order sea-level curves, two sine curves with an amplitude of 30 m and 15 m and a frequency of 4 Ma. To test if the section could be reasonably simulated with subsidence and sediment input alone, a model was run with no sea-level curve. Simulations using the Roebuck Basin sea-level curves, the Haq second order eustatic sea-level curve and Haq third order eustatic sea-level curves, produce similar overall geometries and internal characters which matched well with observed geometries in wells and seismic data. All offered reasonable and possible solutions. Simulation with a 30 m amplitude sine curve also produced representative overall geometries, however, the internal character was not as consistent with well-data. Seismic

geometries were not matched using the 15 m amplitude sine curve or with tectonic subsidence alone (no sea-level curve).

Simulations using the Roebuck Basin, Haq second order and Haq third order sea-level curve, although of differing frequencies and amplitudes, produced similar results. It appears that sediment supply rate is more important than higher order sea-level curve frequency and magnitude, provided that base-level is fluctuated beyond a critical threshold. On a smaller scale the internal distribution of each depositional unit appears strongly controlled by frequency and magnitude of the sea-level curve.

Results from this study suggest that the curves derived by Haq et al. (1987) are reasonable approximations of the high-frequency relative sea-level oscillations that have occurred in the Roebuck Basin and could potentially be used as a first approximation to simulate basin-fill at other locations globally. However, comparison of the global onlap curve with the locally derived Roebuck Basin curve, highlight departures between the two. During this study these departures have been interpreted to represent regional episodes of tectonic uplift, rejuvenation of the sediment source province and basinward shifts in coastal onlap that have occurred in the Roebuck Basin.

6.6 Petroleum Potential

Major petroleum play elements in the Roebuck Basin are summarized in Figure 5.1. Failure to find commercial hydrocarbons in the basin is attributed to lack of source rock, seal potential and timing of maturation. During this study, source rocks were identified and their distribution predicted using a number of techniques, including; sequence stratigraphic correlation, seismic mapping, forward sedimentary modelling and geochemical analysis. Using the above methods, ten source rock intervals were identified. These source rocks have been correlated to the Triassic to Recent Westralian petroleum super-system first defined by Bradshaw et al (1994).

The ten identified source rock intervals in the Roebuck Basin can be sub-divided into four groups of units depending on their tectono-depositional setting. Tr1 and Tr2 were deposited during rapid thermal sag, J1 to J5 were deposited during gentle thermal sag and infill, K1 and K2 were deposited during rift and post-rift sedimentation, and K3 was deposited during passive margin conditions.

Westralian 1 sediments consist of Lower Triassic marine shales and deltaic sands (Locker Shale equivalents and Lower Keraudren Formation). Although source potential of the Triassic is predominately gas prone, units Tr1 and Tr2 contain a higher algal composition.

Organic preservation during the Early Triassic is believed to have occurred during basal marine transgression over irregular topography formed during Late Permian rifting (Scott, 1998). In the Roebuck Basin, isolated depocentres also formed during tectonic movement associated with the Fitzroy Movement I along the northern margin of the basin and along the western margins of the Bedout and Rowley Sub-basins.

Units J1 to J5 were deposited under fluvio-deltaic and consist of braided and stacked channel sands interbedded with transgressive shales, lagoonal coal beds and sapropels, overbank deposits and deltaic facies. TOC values for shales generally average between 1 and 5% but in intervals rich in coals and sapropel zones exceed 20%. Rock-Eval analysis of algal rich intervals, especially the J2, J4 and J5 sequences, appear to have exceptional oil generation potential.

Units J1 to J5 were deposited during a series of well-developed prograding wedges that can be observed on seismic data and mapped on chronostratigraphic cross-sections. Episodes of progradation appear to be triggered by major tectonic readjustments of the shelf. Source rock development is associated with the deposition of sapropelic and coal-rich material in lacustrine lakes and restricted embayments that developed during the formation of irregular topography during

periods of rifting and subsequent rapid transgression.

Sedimentary modelling of the Jurassic has been used to simulate the basin fill. Four marine incursions, each of which are followed by the development of a progradational wedge, are clearly identifiable. Thickest delta front development occurred in the inner Rowley Sub-basin to the north-west of the Bedout High and may offer many attractive stratigraphic exploration targets such as isolated channel systems, coastal sand deposits and barrier-bar systems. These reservoir-trap systems are potentially sourced/sealed by high-quality source rich, pro-delta, shale systems.

During maturity analysis vitrinite data suggests a thermal maturity lower than modelled maturities using present thermal conditions. The difference in modelled versus measured vitrinite reflectance is likely to be the result of vitrinite suppression which has been observed elsewhere on the North West Shelf. There is a general correlation between marine sequences and increased suppression in the Roebuck wells examined so far.

Development of the thick carbonate wedge during the Oligocene and Miocene has increased maturities in this location pushing the Tr1 and Tr2 units into the dry gas window thus presenting a possibility of gas flushing for prospects within this area. The Jurassic and the lowest Cretaceous section are predicted to lie within the oil window.

During the Cretaceous large volumes of potential source rock were deposited, but maturity for oil generation is only marginal below the thickest section of the Tertiary carbonate wedge. The significance of oil generation from Cretaceous source rocks is difficult to predict but is believed to be small compared to that from the Jurassic and Triassic.

CHAPTER 7

RECOMMENDATIONS

"Explain it as you like.
I offered you, if you remember,
a choice of explanations,
before I began the story.
I have not yet found the
explanation that can satisfy me."

In the Dark
E. Nesbit

Recommendations at the conclusion of this study can been divided into two: those concerned with improving understanding of the Roebuck Basin and those concerned with enhancing scientific methodology. Recommendations that fall into the former category are listed firsts:

- During this study direct predictions have been made regarding the sediment distribution within the basin. The first approach in confirming these results would be to undertake high resolution seismo-stratigraphic/facies interpretations of key seismic lines. This will fast-track exploration acreage and test the depositional models presented here. Although sequence mapping was undertaken during this study, the process was not exhaustively pursued and would benefit from further work.

- Recent petroleum exploration activity associated with the re-gazettal of the Roebuck Basin, has led to the reprocessing and acquisition of a considerable amount of seismic data, especially over the largely unexplored outer margin of the basin. This data could be vital in determining the break-up history of the Roebuck Basin and North West Shelf, which from this study appears more complicated than previously thought. In particular more seismic over the margin will help clarify the nature of the Fitzroy Movement III event which appears similar in nature to a break-up event.

- Well data re-sampling could be used to better constrain timing, geochemical and sedimentary properties in the basin. Unfortunately, beneficial results maybe limited during such an approach, as most wells are now over 15 years old and the material available is limited to side-wall cores and ditch cuttings. Extensive sampling should be undertaken during any renewed drilling campaign in the area to address these issues.

In addition to enhancing our understanding of the Roebuck Basin some recommendations for future development of predictive stratigraphic analysis and a suggestion for potential data sets that could be used are presented here. During this study a great effort was made to break-down the sedimentary sequence and some interesting and innovative methods were used to do this. Results from this approach have helped defined the chronostratigraphy, sediment budget and sediment distribution in the Roebuck Basin. However, due to its regional nature, poor quality and limited well control the data set was far from suitable for defining some of the key relationships that could help refine the understanding of our key depositional models.

One of the more challenging tasks undertaken during this study was the prediction of sediment rates and lithological content of chronosomes

through time. Although reasonably well confined at the resolution of this study, the limited data set used here made it difficult to test the assumptions used. Of note are the use of chronosome areal distribution to predict grain-size distribution or depositional duration. To really understand this relationship further work using 3D seismic data tied to high resolution biostratigraphic studies in areas with good well control are essential. Accurate plots of chronosome size, duration and grain-size distribution could then be examined and analysed rigorously. One potential data set for the North West Shelf of Australia could be the Cornea 3D survey acquired by Shell in 1997. Ten wells all with high-resolution biostratigraphic breakdowns have been drilled in this area providing ample well control. Such a data set analysis using the same basic techniques utilised during this study could help aid our understanding of several sedimentary depositional processes.

REFERENCES

AGSO NORTH WEST SHELF STUDY GROUP, 1994—Deep reflections on the North West Shelf: changing perceptions of basin formation. In: Purcell, P.G. and R.R. (eds), The sedimentary basins of Western Australia. Proceedings of the West Australian Basins Symposium, Petroleum Exploration Society of Australia, 14-17 August, Perth, 63-76.

ALLEN, P.A. AND ALLEN, J.R., 1990—Basin analysis: principles & applications. Blackwell Scientific Publications, p451.

ANDREWS-SPEED, C.P., OXBURGH, E.R. AND COOPER, B.A., 1984—Temperatures and depth-dependent heat flow in western North Sea. Bull. Am. Assoc. petrol. Geol., 68, 1764-1781.

ARDITTO, P. A., 1993—Depositional sequence model for the post-Barrow Group Neocomian succession, Barrow and Exmouth sub-basins, Western Australia, APEA Journal, 33(1), 151-60.

BALDWIN, B. AND BUTLER, C.O., 1985—Compaction Curves. Am.Assoc. Pet. Geol., Bull., 69: 622-626.

BALLY, A.W., 1982—Musings over sedimentary basin evolution. Phil. Trans. R. Soc. London, A305, 325-338.

BARBER, P., 1994—Sequence stratigraphy and petroleum potential of Upper Jurassic-Lower Cretaceous depositional systems in the Dampier Sub-basin, North West Shelf, Australia. In: Purcell, P.G. AND R.R. (eds), The sedimentary basins of Western Australia, Proceedings, PESA Symposium, Perth, 525-42.

BEZDEK, J.C., BIZWAS, G., CANNON, R.L. AND KENDALL, C.G.St. C., 1990—Expert Explorer. SEDPAK Manual. May 1990.

BLEVIN, J.E., STEPHENSON, A.E., AND WEST, B.G., 1994—Mesozoic Structural Development of the Beagle Sub-basin – Implications for the Petroleum Potential of the Northern Carnarvon Basin. In: Purcell, P.G., R.R. (eds), The sedimentary basins of Western Australia. Proceedings of the West Australian Basins Symposium, Petroleum Exploration Society of Australia, Perth, 14-17 August, Perth, 479-496.

BLEVIN, J.E., BOREHAM, C.J., SUMMONS, R.E., STRUCKMEYER, H.I.M. AND LOUTIT, T.S., 1998—An effective Lower Cretaceous petroleum system on the North West Shelf: Evidence from Browse Basin. In: Purcell, P.G. AND R.R. (eds), The sedimentary basins of Western Australia 2. Proceedings of PESA Symposium, Perth, 397-419.

BP, 1982—Well completion report for Lagrange-1, unpublished.

BRADSHAW, M., 1993—Australian Petroleum

Systems. Petroleum Exploration Society of Australia Journal, 21, 43-53.

BRADSHAW, M.T., BRADSHAW.J., MURRAY, A.P., NEEDHAM, D.J., SPENCER, L., SUMMONS, R.E., WILMOT, J. AND WINN, S. 1994—Petroleum systems in west Australian basins. In: Purcell, P.G., and R.R. (eds), The sedimentary basins of Western Australia. Proceedings of the West Australian Basins Symposium, Petroleum Exploration Society of Australia, Perth, 14-17 August, Perth, 63-76.

BRADSHAW, M.T., YEATES, A.N., BEYNON, R.M., BRAKEL, A.T., LANGFORD, R.P., TOTTERDELL, J.M. AND YEUNG, M., 1998—Palaeogeographic evolution of the North West Shelf region. In: Purcell, P.G. and R.R. (eds), The North West Shelf, Australia, Proceedings of PESA Symposium, Perth, 1998, 29-54.

BRIKKE, I., 1982—Geochemical Interpretation of Some Oils and Condensates from the Dampier Sub-basin of Western Australia, APEA Journal, 22, 1.

BROWN, S.A., BOSERIO, I.M., JACKSON, K.S. AND SPENCE, K.W.,1984—The geological evolution of the Canning Basin, implications for petroleum exploration. In: Purcell, P.G. (ed), The Canning Basin, W.A. Published by the Geological Society of Australia and by Petroleum Exploration Society of Australia, 85-96.

BURKE, K.., AND DEWEY, J.F., 1973—Plume-generated triple junctions: key indicators in applying plate tectonics to old rocks. Journal of Geology. 81, 406-433.

CALVERT, S.E., AND PEDERSEN, T.F., 1990—Anoxia vs. productivity: what controls the formation of organic-carbon-rich sediments and sedimentary rocks? The American Association of Petroleum Geologists Bulletin. V 74, No 4, 454-466.

CHALLINOR, A., 1970—The Geology of the Offshore Canning Basin, Western Australia: APEA Journal, 10(2), 78-90.

CHRISTIE-BLICK, N. AND BIDDLE, K.T., 1985—Deformation and basin formation along strike-slip faults. In: Christie-Blick, N. and Biddle, K.T., (Ed.) Strike-slip deformation, basin formation, and sedimentation. Spec. Publ. Soc. Econ. Paleont. Mineral., 37, 1-34.

CLOETINGH, S., McQUEEN, H. AND LAMBECK, K., 1985—On a tectonic mechanism for regional sea level variations. Earth Planet. Sci. Letters, 75, 157-166.

COCKBAIN, A.E., 1989—The North West Shelf. The APEA Journal, 29(1), 529-45.

COLWELL, J.B. AND STAGG, H.M.J., 1994—Structure of the offshore Canning Basin: first impressions from a new regional deep, seismic data set. In: Purcell, P.G., R.R. (eds), The sedimentary basins of Western Australia. Proceedings of the West Australian Basins Symposium, Petroleum Exploration Society of Australia, Perth, 14-17 August, Perth, 757-68.

DIX, C.H., 1955—Seismic velocities from surface measurements. Geophysics, 20, 68-86.

DRUMMOND, B.J., ETHERIDGE, M.A., DAVIES, P.J., & MIDDLETON, M.F., 1988—Half-graben model for the structural evolution of the Fitzroy Trough, Canning Basin, and implications for resource exploration. The APEA Journal, 28(1), 76-86.

DRUMMOND, B.J., SEXTON, M.J., BARTON, T.J., & SHAW, R.D., 1991—The nature of faulting along the margins of the Fitzroy Trough, and implications for the tectonic development of the trough. Exploration Geophysics, 22, 111-116.

ELLIOT, R.M.L., 1990—Browse Basin. In Geology and mineral resources of Western Australia. Western Australia Geological Survey Memoir, 3, 535-47.

EMBRY, A.F., 1995—Sequence boundaries and

sequence hierarchies: problems and proposals. In: Steel, R.J., Felt, V.L., Johannessen, E.P. and Mathieu, C., (eds), Sequence stratigraphy on the Northwest European margin. Proceedings, Norwegian Petroleum Society Conference, 1-3 February, Stavenger, Norway 1-11.e

EMERY AND MYERS 1996—Sequence stratigraphy. Blackwell science, p297.

ERSKINE, R.D., AND VAIL, P.R., 1987—Seismic stratigraphy of the Exmouth Plateau. In: Bally, A.W., (ed), Atlas of seismic stratigraphy, American Association of Petroleum Geology, Studies in Geology, 2, Tulsa. OK. 163-173.

ETHERIDGE, M.A., AND O'BRIEN, G.W, 1994—Structural and tectonic evolution of the Western Australian margin basin system. Petroleum Exploration Society of Australia Journal 22, 45-63.

EXON, N.F. AND VON RAD, U., 1994—The Mesozoic and Cainozoic sequences of the Northwest Australian margin, as revealed by ODP core drilling and related studies. In: Purcell, P.G., R.R. (eds), The sedimentary basins of Western Australia. Proceedings of the West Australian Basins Symposium, Petroleum Exploration Society of Australia, Perth, 14-17 August, Perth, 181-99.

FORMAN, D.J. AND WALES, D.W., 1981—Geological evolution of the Canning Basin, Western Australia. Australia, Bureau of Mineral Resources, Geology and Geophysics Bulletin 210, 91p.

GALLOWAY, W.E., 1989—Genetic stratigraphic sequences in basin analysis: architecture and genesis of flooding surface bounded depositional units. Am.Assoc. Petrol. Geol. Bull., 73, 125-142.

GIBBS, A.D., 1984—Structural evolution of extensional basin margins. Journal of the Geological Society of London, 141, 609-20.

GORTER, J.D., 1994—Triassic Sequence Stratigraphy of the Carnarvon Basin, Western Australia. In: Purcell, P.G., R.R. (eds), The sedimentary basins of Western Australia. Proceedings of the West Australian Basins Symposium, Petroleum Exploration Society of Australia, Perth, 14-17 August, Perth, 397-413.

GORTER, J.D., 1996—Speculation on the origin of the Bedout High – A large, circular structure of pre Mesozoic age in the offshore Canning Basin, Western Australia. PESA News, October/November, 32-33.

GRADSTEIN, F.M., 1992—Legs 122 and 123, Northwestern Australian margin – A stratigraphic and palaeogeographic summary. In: Gradstein, F.M., and Ludden, J.N., et al (eds), Proceedings of the Ocean Drilling Program, Scientific Results, Vol. 123.

GRIFFITHS, C.M., AND HADLER-JACOBSON, F., 1995—Practical dynamic modelling of clastic basin fill. In: Steel, R.J., et al (eds), Sequence Stratigraphy on the Northwest European Margin. NPF Special Publication 5, pp. 31-49.

GRIFFITHS, C.M. AND NORDLUND, U., 1993—Chronosomes and quantitative stratigraphy. Goeinformatices, 4: 327-336.

HAQ, B.U., HARDENBOL, J. AND VAIL, P.R., 1987—Chronology of fluctuating sea levels since the Triassic, Science, v.235, 1156-1167.

HAQ, B.U., HARDENBOL, J. AND VAIL, P.R., 1988—Mesozoic and Cenozoic chronostratigraphy and cycles of sea-level change, In: Wilgus, C.K., et al (eds), Sea-level change: an integrated approach, Society of Economic Paleontologists and Mineralogists Special Publication, 42, 71-108.

HARDING, T.P. AND LOWELL, J.D., 1979—Structural styles, their plate tectonic habitats and hydrocarbon traps in petroleum provinces. Bull. Am. Assoc. Petrol. Geol., 63, 1016-1058.

HARLAND, W.B., ARMSTRONG, R.L., COX, A.V., CRAIG, L.E., SMITH, A.G. AND SMITH, D.G.,

1992—A Geological Time Scale, Cambridge University Press.

HELBY, R., MORGAN, M., AND PARTRIDGE, A.D., 1987—A Palynological zonation of the Australian Mesozoic. In: Jell, P.A. (ed), Studies in Australian Mesozoic Palynology: AAP Memoir 4, 1-94.

HOCKING, R.M., 1988—Regional geology of the northern Carnarvon Basin. In: Purcell, P.G., and R.R., (eds), The North West Shelf, Australia. Proceedings of the Petroleum Exploration Society of Australia Symposium, Perth, 97-114.

HOCKING, R.M., MORY, A.J. AND WILLIAMS, I.R., 1994— An atlas of Neoproterozoic and Phanerozoic basins of Western Australia. In: Purcell, P.G., and R.R. (eds), The sedimentary basins of Western Australia. Proceedings of the West Australian Basins Symposium, Petroleum Exploration Society of Australia, Perth, 14-17 August, Perth,21-43.

HOCKING, R.M., 1992—Jurassic deposition in the southern and central North West Shelf. Geological Survey of WA, 1992, 7.

HORSTMAN, E. L., 1994—The effect of inertinite on kerogen appraisal by programmed pyrolysis, North West Shelf, Australia. APEA Journal, 34 (1), 297-306.

HORSTMAN, E.L. AND PURCELL, P.G. & R.R., 1998—The offshore Canning Basin – a review. In: Purcell, P.G. AND R.R., (eds), The North West Shelf, Australia, Proceedings of Petroleum Exploration Society Australia Symposium, Perth, 1988, 253-257.

HUBBARD, R. J., PAPE, J. AND ROBERTS, D. G., 1985—Depositional sequence mapping as a technique to establish tectonic and stratigraphic framework and evaluate hydrocarbon potential on a pasiive continental margin. In: Berg, O. R. and Woolverton, D. (ed.)—Seismic stratigraphy II: an intergrated approach. Am. Assoc. petrol. Geol. Mem. 39, 79-91.

HUBBARD, R. J., 1988—Age and significance of sequence boundaries on Jurassic and Early Cretaceous rifted continental margins. Bull. Am. Assoc. petrol. Geol., 72, 49-72.

HULL, J.N.F., SMITH, S.A., AND YOUNG, H.C., 1998—Sequence stratigraphic interpretation of carbonate wireline log motifs: an example from the North West shelf of Australia. APPEA Journal, 188-198.

JABLONSKI, D., 1997—Recent advances in the sequence stratigraphy of the Triassic to Lower Cretaceous succession in the northern Carnarvon Basin, Australia. Australian Petroleum Production and Exploration Association Journal, 37(1), 429-54.

JERVEY, M.T., 1988—Quantitative geological modelling of siliclastic rock sequences and their seismic expressions, In Wilgus, C.K., et al (eds), Sea level changes: an integrated approach, Society of Economic Paleontologists and Mineralogists Special Publication, 42, 47-69.

JNOC, 1987—A petroleum analysis of six wells from the offshore canning basin. 35pp.

JNOC, 1988—Geological and geophysical study of the offshore Canning Basin in the Northwest Shelf of Australia. Japan National Oil Corporation Report (unpublished).

JNOC, 1989—Geochemistry of 3 wells, Pearl-1, Perindi-1, Kambara-1, Offshore Canning Basin, North West Shelf of Australia. 39pp.

KAIKO, A.R., AND TINGATE, P.R., 1996—Suppressed vitrinite reflectance and its effect on thermal history modelling in the Barrow and Dampier Sub-basins. Australian Petroleum Production and Exploration Association Journal, 36(1), 428-44.

KARNER, G.D., 1986—Effects of lithospheric in-plane stress on sedimentary basin stratigraphy. Tectonics, 5, 573-588.

KENDALL, C.G.St.C., LERCHE, I. AND NAKAYAMA, k., 1986—Simulation of continental margin sedimentation. Am. Assoc. Pet. Geol., Bull., 70: 606.

KENDALL, C.G.St.C., MOORE, P., STROBEL, J., CANNON, R., PERLMUTTER, M., BEZDEK,J. AND BISWAS, G., 1991—Simulation of the sedimentary fill of basins, In: Franseen, E.K., Watney, W.L., Kendall, C.G.St.C., and Ross, W.C., (eds), Sedimentary Modeling: Computer Simulations and Methods for Improved Parameter Definition. Kansas Geological Survey Publication, Lawrence, Kans., pp. 9-32.

KENNARD, J.M., JACKSON, M.J., ROMINE, K.K., SHAW, R.D. AND SOUTHGATE, P.N., 1994—Depositional sequences and associated petroleum systems of the Canning Basin, WA. In: Purcell, P.G., and R.R. (eds), The sedimentary basins of Western Australia. Proceedings of the West Australian Basins Symposium, Petroleum Exploration Society of Australia, Perth, 14-17 August, Perth, 657-676.

KIRK, R.B., 1985—A seismic stratigraphic case history in the eastern Barrow Sub-basin, North West Shelf, Australia. In: Berg, O.R., and Woolverton, D.G., (eds), Seismic stratigraphic 11 – an integrated approach to hydrocarbon exploration, American Association of Petroleum Geologists Memoir 39, 183-207.

KOOI, H., AND CLOETINGH, S., 1992—Lithospheric necking and regional isostasy at extensional basins 2. Stress-induced vertical motions and relative sea level changes. Journal of Geophysical Research, Vol. 97, 573-91.

KOPSEN, E. AND MCGANN, G., 1985—A Review of the Hydrocarbon Habitat of the Eastern and Central Barrow-Dampier Sub-basin, Western Australia, APEA Journal, 25, 1, 154-1

KUSZNIR, N.J., AND PARK, R.G., 1987—The extensional strength of the continental lithosphere: its dependence on geothermal gradient, and crustal composition and thickness. In: Coward, J.F., Dewey, J.F., and Hancock, P.L. (eds), Continental Extensional Tectonics, Spec. Publ. Geol. Soc. London, 28, 35-52.

KUSZNIR, N.J., MARSDEN, G. AND EGAN, S., 1991—Forward and reverse modelling of rift basin formation. In: Lambiase, J.J., (ed) Hydrocarbon Habitat in Rift Basins. Special Publication of the GSL, 80, 33-56.

LABUTIS, V.R., 1994—Sequence stratigraphy and the North West Shelf of Australia. In Purcell, P.G. AND R.R. (eds), The sedimentary basins of Western Australia, Proceedings, PESA Symposium, Perth, 159-80.

LIPSKI, P., & BEATTIE, B., 1992—A Triassic play in the eastern Bedout Sub-basin. Oil & Gas Australia, July, 1992, 24-26.

LIPSKI, P., 1993—Tectonic setting, stratigraphy and hydrocarbon potential of the Bedout Sub-Basin, North West Shelf. Australian Petroleum Exploration Association Journal, 33 (1), 138-50.

LIPSKI, P., 1994—Structural framework and depositional history of the Bedout and Rowley Sub-basins. In: Purcell, P.G., and R.R. (eds), The sedimentary basins of Western Australia. Proceedings of the West Australian Basins Symposium, Petroleum Exploration Society of Australia, Perth, 14-17 August, Perth, 769-77.

LISTER, G.S., ETHERIDGE, M.A., AND SYMONDS, P.A., 1986—Application of the detachment fault model to the formation of passive continental margins. Geology 14, 246-50.

LOUTIT, T.S., HARDENBOL, J., VAIL, P.R., BAUM, G.R. 1988—Condensed sections: the key to age determination and correlation of continental margin sequences. In: Wilgus, C.K., Hastings, B.S.,Kendall, C.G.St.C., Posamentier, H.W., Ross, C.A. and Van Wagoner, J.C. (eds), 1998—Sea-level Changes: An Integrated Approach. Special Publication, Society of Economic Paleontologists and Mineralogists, Tulsa, 42, 407 pp.

LOUTIT, T.S., ROMINE, K.K. AND FOSTER, C.B., 1997—Sequence biostratigraphy, petroleum exploration and *A. cinctum*. APPEA Journal, 272-284.

LUDDEN, J.N., 1992—Radiometric age determinations for basement from Sites 765 and 766, Argo Abyssal Plain and northwestern Australian margin. In: Gradstein, F.M., Ludden, J.N., et al., 1990. Proceedings of Ocean Drilling Program, Scientific Results, 123. ODP, College Station, Texas, 557-559.

MAGOON, L.B. AND DOW, W.G., 1991—The petroleum system, from source to trap. AAPG 1991 annual convention abstracts, AAPG Bulletin 75(3), p.627.

MCCONACHIE, B.A., BRADSHAW, M.T. AND BRADSHAW, J., 1996—Petroleum systems of the Petrel Sub-basin , an integrated approach to basin analysis and identification of hydrocarbon exploration opportunities. Australian Petroleum Production and Exploration Association Journal 36(1), 248-268.

McKENZIE, D.P., 1978—Some remarks on the development of sedimentary basins. Earth and Planetary Science Letters, 40, 25-32.

METCALFE, I., 1988—Origin and assembly of Southeast Asian continental terranes. In: Audley, C.M.G., and Hallam, A. (eds), Gondwana and Tethys. Geological Society of London Special Publication 37, 101-18. 1988.

METCALFE, I., 1993—Southeast Asian terranes, Gondwanaland origins and evolution. In: FINDLAY, R. H., Unrug, R., Banks, M.R. and Veevers, J.J. (eds), Assembly, evolution and dispersal, proceedings of the Gondwana eight symposium. International Gondwana Symposium 8, 181-200.

MIALL, A.D., 1986—Eustatic sea level changes interpreted from seismic stratigraphy: a critique of the methodology with particular reference to the North Sea Jurassic record, AAPG Bulletin, v. 70, 131-137.

MIALL, A.D., 1992—Alluvial deposits. In: Facies Models – Response to sea level change. Walker, R.G. and James, N.P., (eds), Geological Association of Canada, Waterloo, Ontario, pp. 119-142.

MILLER, L.R., 1997—Sedimentary architecture of rift-related depositional systems in the Dampier Province, North West Shelf, Australia. University of Adelaide PhD thesis, unpublished.

MITCHUM, R.M. Jr, VAIL, P.E. AND THOMPSON, S. III 1977—The depositional sequence as a basic unit for stratigraphic analysis. In: Payton, C.E., (ed), Seismic Stratigraphy – Applications to Hydrocarbon Exploration, Am. Assoc. petrol. Geol. Mem. 26, 53-62.

MITCHUM, R.M., 1977—Seismic stratigraphy and global changes of sea level, Part 1: Glossary of terms used in seismic stratigraphy, In: Payton, C.E., (ed) Seismic stratigraphy-applications to hydro-carbon exploration, AAPG Memoir 26, 205-212.

MITCHUM, R.M.Jr. AND VAN WAGONER, J.C., 1991—High frequency sequences and their stacking patterns: sequence stratigraphic evidence of high frequency eustatic cycles. Sediment. Geol., 70, 135-144.

NICOLL, R.S. AND FOSTER, C.B., 1994—Late Triassic conodont and palynomorph biostratigraphy and conodont thermal maturation, North West Shelf, Australia. AGSO Journal of Australian Geology and Geophysics, Special Issue, 15(1), 101-118.

NORDLUND, U. AND GRIFFITHS, C.M., (1993a)—An example of the practical use of chronosomes in quantitative stratigraphy. Geoinformatics, 4: 3.

NORDLUND, U. AND GRIFFITHS, C.M., (1993b)—Automatic construction of two- and three-dimensional chronostratigraphic sections

from digitized seismic data. Comput. Goesci., 19: 1185-1205.

O'BRIEN, G.W., ETHERIDGE, M.A., WILLCOX, J.B., MORSE, M., SYMONDS, P., NORMAN, C. AND NEEDHAM, D.J., 1993—The structural architecture of the Timor Sea, north-western Australia: implications for basin development and hydrocarbon exploration. Australian Petroleum Exploration Association Journal 33(1) 258-78.

O'BRIEN, G., HIGGINS, R., SYMONDS, P., QUAIFE, P., COLWELL, J., AND BEVIN, J., 1996—Basement control on the development of extensional systems in Australia's Timor Sea: An example of hybrid hard linked/soft linked faulting? APEA Journal, 36 (1), 161-201.

OSBORNE, D,G., 1994—Nebo oil discovery, Beagle Sub-basin. In: Purcell, P.G. AND R.R. (eds), The Sedimentary Basins of Western Australia, Proceedings PESA Symposium, Perth, 653-57.

PARKINSON, N. AND SUMMERHAYES, C. 1985—Synchronous global sequence boundaries. Bull. Am. Assoc. petrol. Geol. 69, 685-687.

PASSMORE, V.L., 1991—Promising hydrocarbon potential seen in Canning Basin off Australia. Oil & Gas Journal, August 26, 1991, 65-70.

PITMANN, W.C., 1978—Relationship between eustacy and stratigraphic sequences of passive margins. Bull. Geol. Soc. Am. 89, 1389-1403.

POLOMKA, S.M. AND LEMON, N.M. 1996—Tectono-stratigraphic evolution of the Barrow Sub-basin, North West Shelf: A discussion on nomenclature revision. PESA Journal 24, 105-15.

POSAMENTIER, H.W. AND VAIL, P.R. 1988—Eustatic controls on clastic deposition, II, sequence and systems tract models. In: Wilgus, C.K., et al (eds), Sea Level Changes: An Integrated Approach, Spec. Publ. Soc. Econ. Paleont. Mineral. 42, 125-154.

POSAMENTIER, H.W., ALLEN, G.P., AND JAMES, D.P., 1992—High-Resolution Sequence Stratigraphy – The East Coulee Delta. Journal of Sedimentary Petrology.

PRYOR, W.A., 1973—Permeability-porosity patterns and variations in some Holocene sand bodies. Bull. Am. Assoc. petrol. Geol., 57, 162-189.

RAMSEY, D.C. AND EXON, N.F., 1994—Structure and tectonic history of the northern Exmouth Plateau and the Rowley Terrace, northwest Australia. AGSO Journal of Australian Geology & Geophysics, Special Issue, 15(1), 55-70.

REECHMANN, S.A. AND MEBERSON, A.J., 1984—Igneous intrusions in the north-west Canning Basin and their impact on oil exploration. In: Purcell, P.G.(eds), The Canning Basin, WA. Proceedings, GSA/PESA Symposium, Perth, 389-400.

REIJMER, J.J, TEN KATE, W.G.H.Z., SPRENGER, A. AND SCHLAGER, W., 1991—Calciturbidite composition related to the exposure and flooding of a carbonate platform (Triassic, Eastern Alps). Sedimentology, 38, 1049-1074.

ROBERTSON RESEARCH INTERNATIONAL 1979—A petroleum geochemical study of the Australian North West Shelf, P1-87, unpublished.

ROBERTSON RESEARCH INTERNATIONAL 1986—A petroleum geochemical study of the North West Shelf, Australia, Phase II, unpublished.

ROMINE, K.K, SOUTHGATE, P.N., JACKSON, M.J., KENNARD, J.M., 1994—The Ordovician to Silurian phase of the Canning Basin, WA: structure and sequence evolution. In: Purcell, P.G. AND R.R. (eds), The Sedimentary Basins of Western Australia, Proceedings PESA Symposium, Perth, 459-75.

ROMINE, K.K. AND DURRANT, J.M., 1996—

Carnarvon Cretaceous-Tertiary Tie Report, AGSO Record 1996/36, confidential report, unpublished.

ROMINE, K.K., DURRANT, J.M., CATHRO, D.L. AND BERNARDEL, G., 1997—Petroleum play element prediction for the Cretaceous-Tertiary Basin phase, Northern Carnarvon Basin. APPEA Journal, 315-339.

ROSS, M.I. AND VAIL, P.R., 1994—Sequence stratigraphy of the lower Neocomian Barrow Delta, Exmouth Plateau, Northwestern Australia. In: Purcell, P.G. AND R.R. (eds), The sedimentary basin of Western Australia, Proceedings, PESA Symposium, Perth, 435-48.

SCHULTZ, E.H., 1982—The Chronosome and Supersome: terms proposed for low-rank chronostratigraphic units. Can. Pet. Geol., Bull., 30: 29-33.

SCLATER, J.G., AND CHRISTIES, P.A.F., 1980—Continental stretching: an explanation of the post Mid-Cretaceous subsidence of the central North Sea basin. J. geophys. Res., 85, 3711-3739.

SCOTT, J., 1992—Accurate recognition of source rock character in the Jurassic of the North West Shelf, Western Australia. APEA Journal, 32 (1), 289-99.

SCOTT, J., 1994—Source rocks of Western Australian basins. In: Purcell, P.G. and R.R. (eds), The sedimentary basins of Western Australia. Proceedings of PESA Symposium, Perth, 315-31.

SCOTT, J., 1998—Continuous oil pools and self-sourcing reservoirs: International examples and Australian possibilities. In: Purcell, P.G., and R.R. (eds), The sedimentary basins of Western Australia 2. Proceedings of PESA Symposium, Perth, 155-68.

SENGOR, A.M.C., 1987, Tectonics of the Tethysides: orogenic collage development in a collisional setting. Annual Reviews of Earth & Planetary Science, 15, 213-44.

SHAW, R.D., ZEITLER, P.K., McDOUGALL, I. AND TINGATE, P.R., 1992—The Paleozoic history of an unusual intracratonic thrust belt in central Australia based on ^{40}Ar- ^{39}Ar, K-Ar and fission track dating. Journal of Geological Society, London, 149, 937-954.

SMITH, S.A., HULL, J.N., AND YOUNG, H.C., 1997—A sequence stratigraphic wall chart of the North West Shelf. APEA Journal., 37(1): 825.

STAGG, H.M.J., 1993—Tectonic elements of the North West Shelf, Australia. Scale 1:2500000. Australian Geological Survey Organisation, Canberra.

STAGG, H.M.J. AND COLWELL, J.B., 1994—The structural foundations of the Northern Carnarvon Basin. In: Purcell, P.G., and R.R. (eds), The sedimentary basins of Western Australia. Proceedings of the West Australian Basins Symposium, Petroleum Exploration Society of Australia, Perth, 14-17 August, Perth, 349-64.

STROBEL, J., CANNON, R., KENDALL, C.G.St.C., BISWAS, G. AND BEZDEK, J., 1989—Interactive (SEDPAK) simulation of clastic and carbonate sediments in shelf to basin settings. Comput. Geosci., 15: 1279-1290.

STROBEL, J., SOEWITO, F., KENDALL, C.G.St.C., BISWAS, G., BEZDEK, J., AND CANNON, R., 1990—Interactive simulation (SEDPAK) of clastic and carbonate sedimentation in shelf to basin settings. In: Cross, T.A., (eds), Quantitative Dynamic Stratigraphy. Prentice-Hall, Englewood Cliffs, N.J., pp. 433-444.

STRUCKMEYER, H.I.M., BLEVIN, J.E., SAYERS, J., TOTTERDELL, J.M., BAXTER, K. AND CATHRO, D.L., 1998—Structural evolution of the Browse Basin, North West Shelf: new concepts from deep-seismic data. In: Purcell, P.G. and R.R. (eds), The Sedimentary Basins of Western Australia. Proceedings of Petroleum Exploration Society of Australia Symposium, Perth, WA, 1998, 345-67.

SUMMONS, R.E., BRADSHAW, M., CROWLEY, J., EDWARDS, D.S., GEORGE, S.C., AND ZUMBERGE, J.E. 1998—Vagrant Oils: Geochemical signposts to unrecognized petroleum systems. In: Purcell, P.G., and R.R. (eds), The sedimentary basins of Western Australia 2. Proceedings of PESA Symposium, Perth, 155-68.

SYMONDS, P.A., COLLINS, C.D.N. AND BRADSHAW, J., 1994—Deep structure of the Browse Basin: implications for basin development and petroleum exploration. In: Purcell, P.G., and R.R. (eds), The sedimentary basins of Western Australia. Proceedings of the West Australian Basins Symposium, Petroleum Exploration Society of Australia, Perth, 14-17 August, Perth, 315-31.

TAIT, A.M., BARTLETT, R.M., SAYERS, M.J., McLERIE, M.K. AND McKAY, D.M., 1989—The Saladin Oil Field, APEA Journal, 29, 1, 212-219.

THOMAS, B.M., 1984—Hydrocarbons, source rocks and maturity trends in the Northern Perth Basin, Australia. In: Demaison, G. and Murris, R.J., (eds), Petroleum geochemistry and basin evaluation. American Association of Petroleum Geologists Memoir 35, 391-403.

TURCOTTE, D.L. AND WILLEMAN, R.J. 1983—Synthetic cyclic stratigraphy. Earth and Planetary Science Letters. 63 no. 1, 89-96.

VAIL, P.R., MITCHUM, R.M. Jr., TODD, R.G., WIDMIER, J.M., THOMPSON, S., SANGREE, J.B., BUBB, J.N. AND HATLEID, W.G. 1977—Seismic stratigraphy and global changes in sea level. In: Payton, C.E. (eds), Seismic Stratigraphy – Applications to Hydrocarbon Exploration, Memoir of the American Association of Petroleum Geologists, Tulsa, 26, 49-62.

Van HINTE, J.E., 1978—Geohistory analysis-application of micropalaeontology in exploration geology. Bull. Am. Assoc. petrol. Geol., 62, 201-222.

VAN WAGONER, J.C., POSAMENTIER, H.W., MITCHUM, R.M., VAIL, P.R., SARG, J.F., LOUTIT, T.S. AND HANDENBOL, J., 1990—An overview of the fundamentals of sequence stratigraphy and key definitions. In: Sea Level Changes: an Integrated Approach, Spec. Publ. Soc. Econ. Paleont. Mineral., 42, 39-45.

VEEVERS, J.J., (eds), 1984—Phanerozoic earth history of Australia, Oxford University Press, Oxford, 418.

VEEVERS, J.J., 1988—Morphotectonics of Australia's Northwestern Margin - A Review. In: The North West Shelf, Australia, Petroleum Exploration Society of Australia, Perth, 10-12 August, Perth, 19-27.

VON RAD, U., AND EXON, N.F., 1983—Mesozoic-Cenozoic sedimentary and volcanic evolution of the starved passive margin off northwest Australia. American Association of Petroleum Geologists Memoir, 34, 253-281.

WATTS, A.B., KARNER, G.D. AND STECKLER, M.S., 1982—Lithospheric flexure and the evolution of sedimentary basins, Phil. Trans. R. Soc. London, A305, 249-281.

WATTS, A.B., 1982—Tectonic subsidence, flexure and global changes in sea level. Nature, 297, 469-474.

WERNICKE, B., 1985—Uniform-sense normal simple shear of the continental lithosphere. Can. J. Earth. Sci. 22 108-125.

WERNICKE, B. AND BURCHFIEL, B.C., 1982—Modes of extensional tectonics. J. Struct. Geol., 4, 105-115.

WILGUS, C.K., HASTINGS, B.S.,KENDALL, C.G.St.C., POSAMENTIER, H.W., ROSS, C.A. AND VAN WAGONER, J.C. (eds), 1998—Sea-level Changes: An Integrated Approach. Special Publication, Society of Economic Paleontologists and Mineralogists, Tulsa, 42, 407 pp.

WILKINS, R.W.T., WILMSHURST, J.R., HLADKY, G., ELLACOTT, N.J., AND BUCKINGHAM, C.P., 1992—The suppression of vitrinite reflectance in some North West Shelf wells: Barrow-1, Jupiter-1, and Flamingo-1. Australian Petroleum and Exploration Association Journal, 32(1), 300-12.

WULFF, A.C., 1992—Depositional history and facies analysis of the upper Jurassic sediments in the eastern Barrow Sub-basin. APEA Journal, 32 (1), 104-22.

YEATES, A.N., BRADSHAW, M.T., DICKINS, J.M., BRAKEL, A.T., EXON, N.F., LANGFORD, R.P., MULHOLLAND, S.M., TOTTERDELL, J.M., & YEUNG, M., 1987—The Westralian Superbasin: an Australian link with Tethys. International Symposium on Shallow Tethys, 2, A.A. Balkema, Rotterdam, 199-213.

APPENDIX 1

Regional Cross-sections

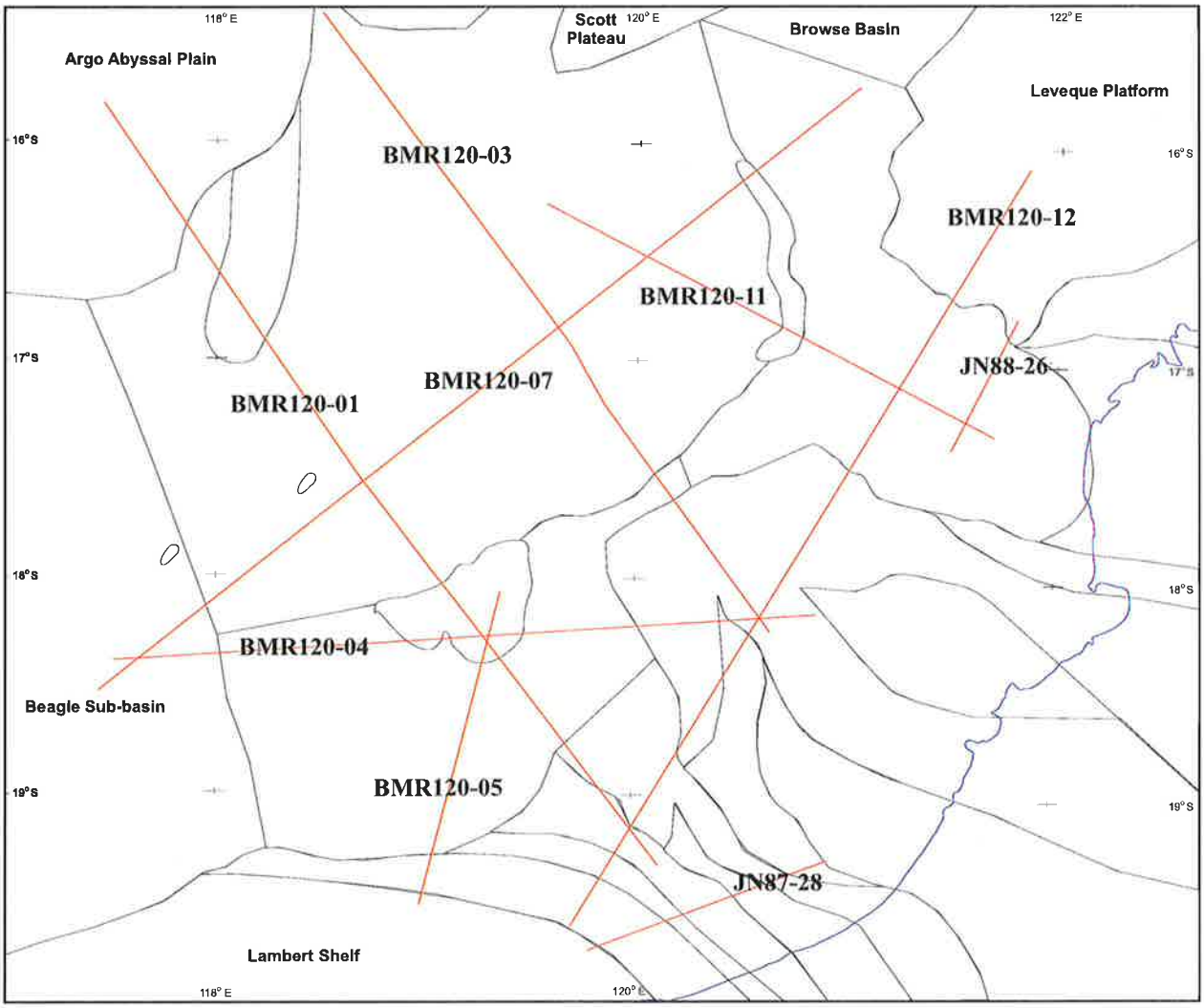

Figure A1.1 Location of regional cross-sections in relation to major structural elements in the basin.

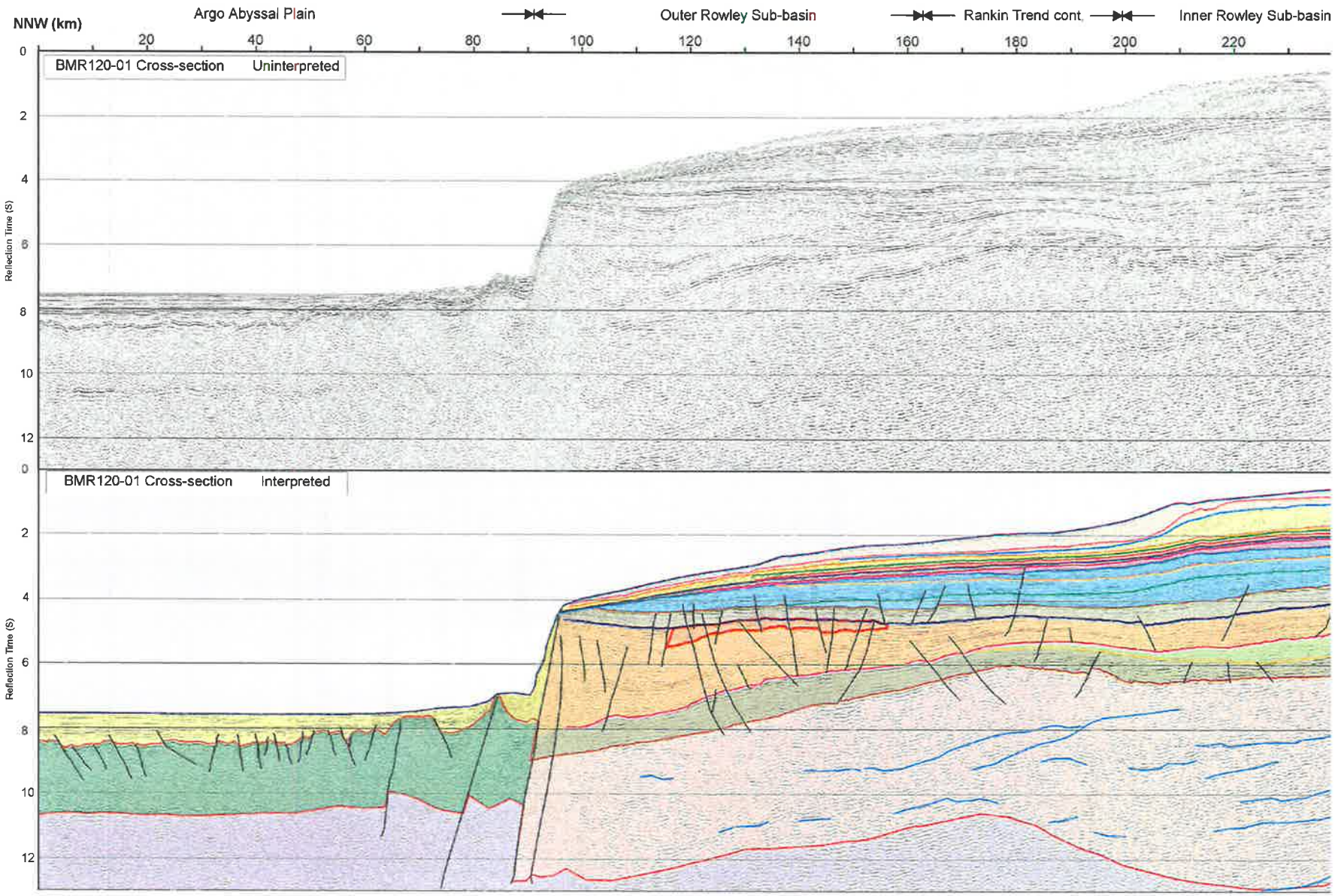

Figure A1.2 Interpreted and uninterpreted regional cross-section (seismic line BMR120-01). Continued over page.

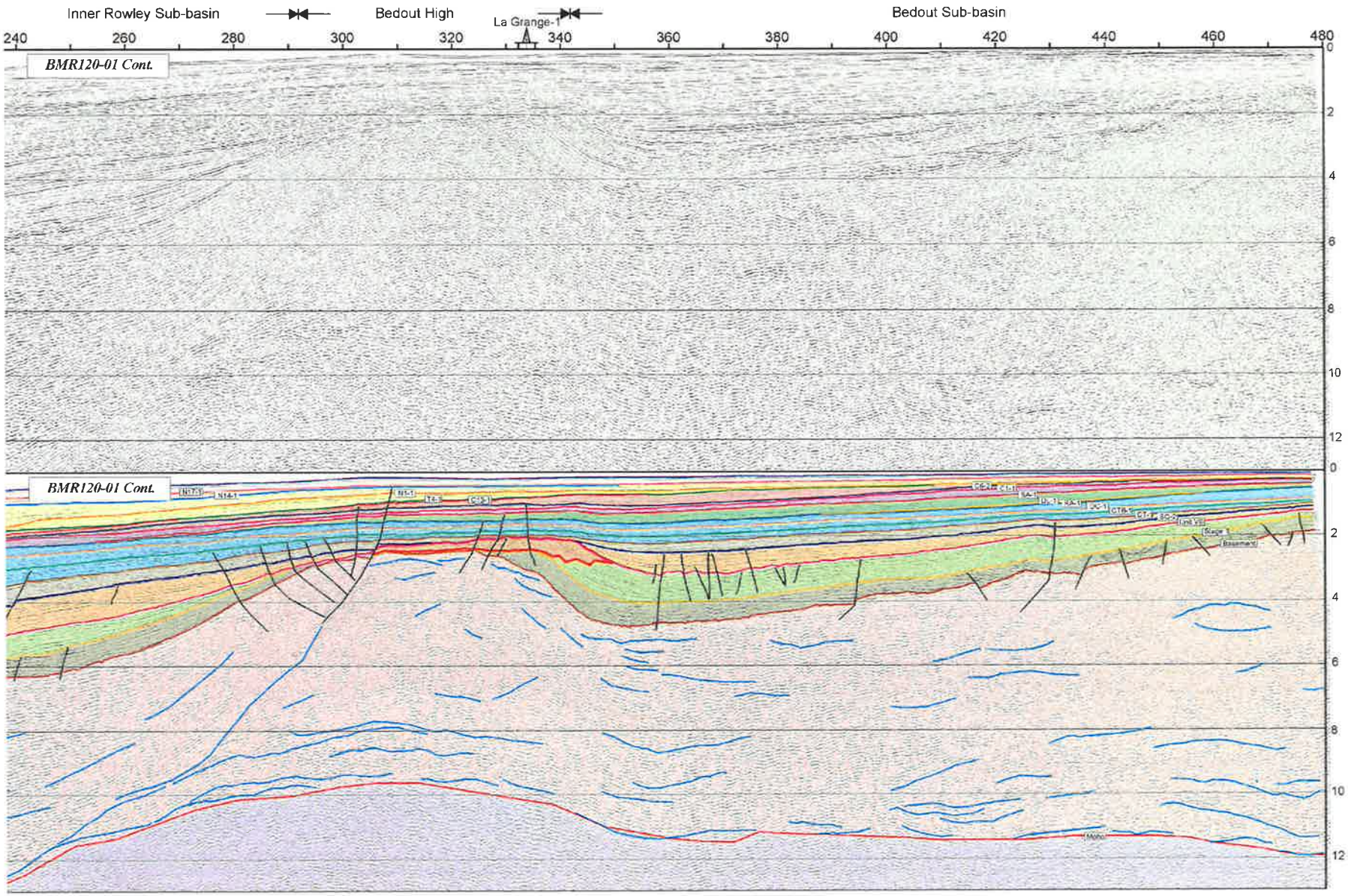

Figure A1.2 (con't)

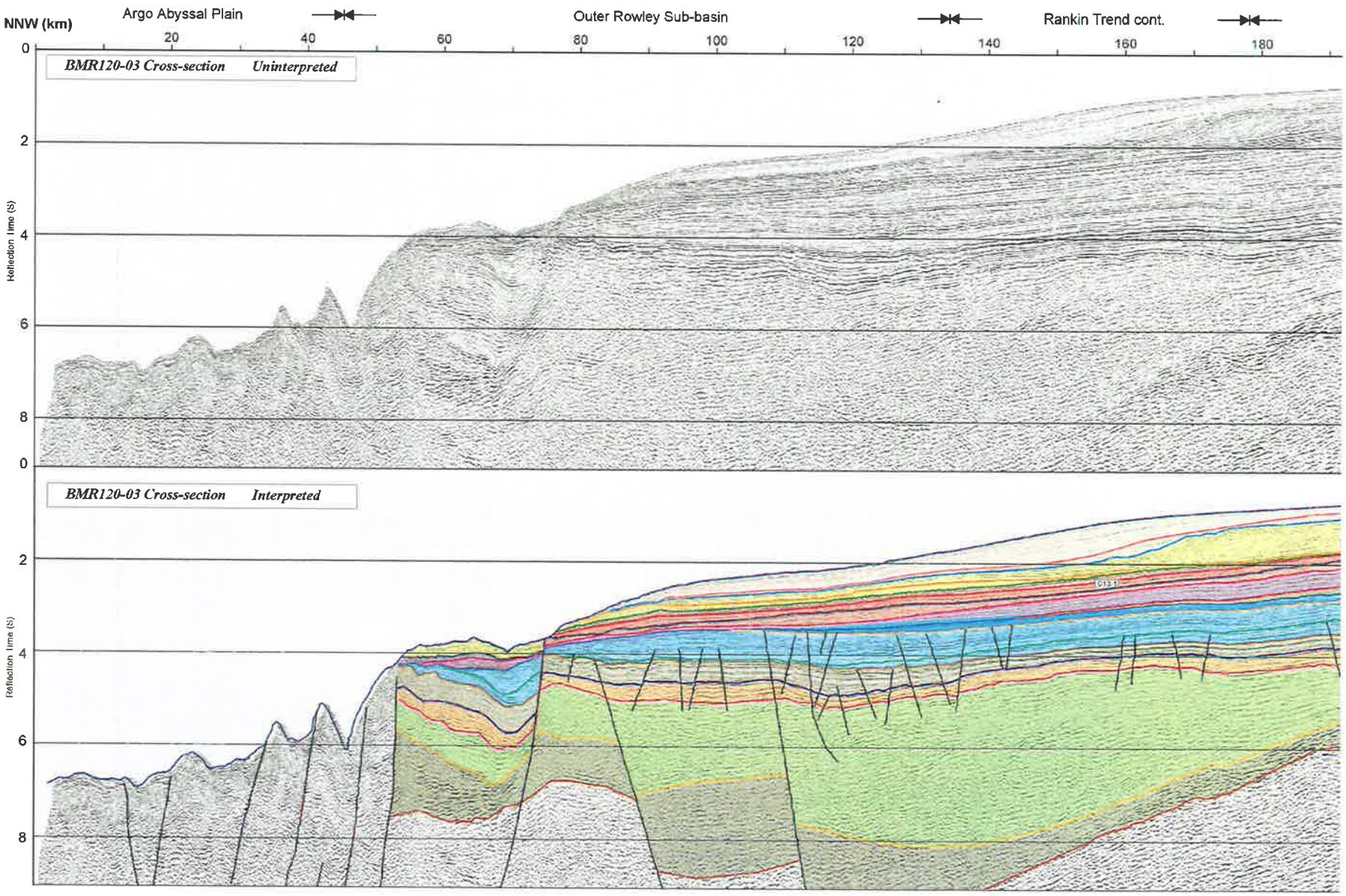

Figure A1.3 Interpreted and uninterpreted regional cross-section (seismic line BMR120-03). Continued over page.

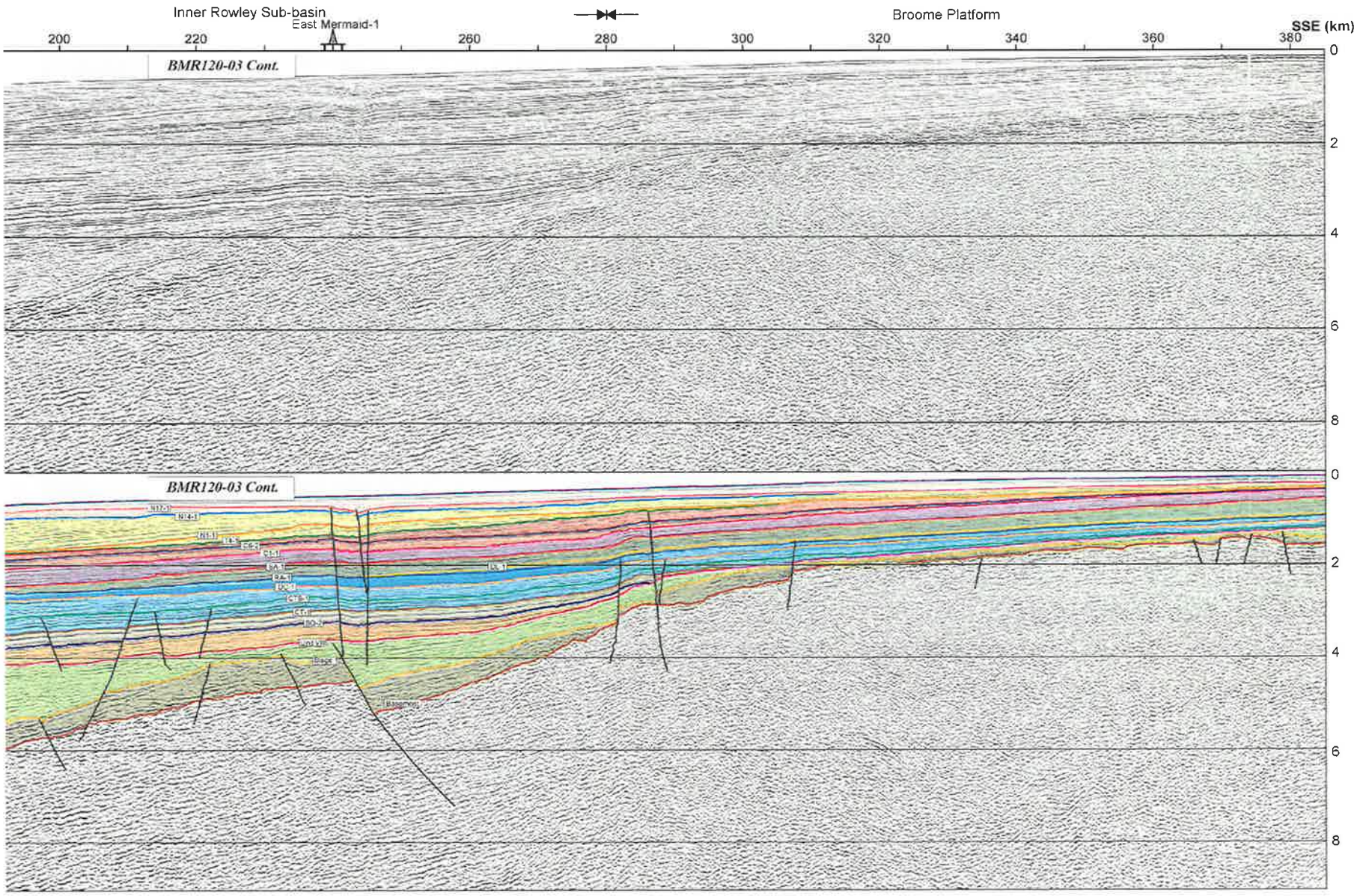

Figure A1.3 (con't)

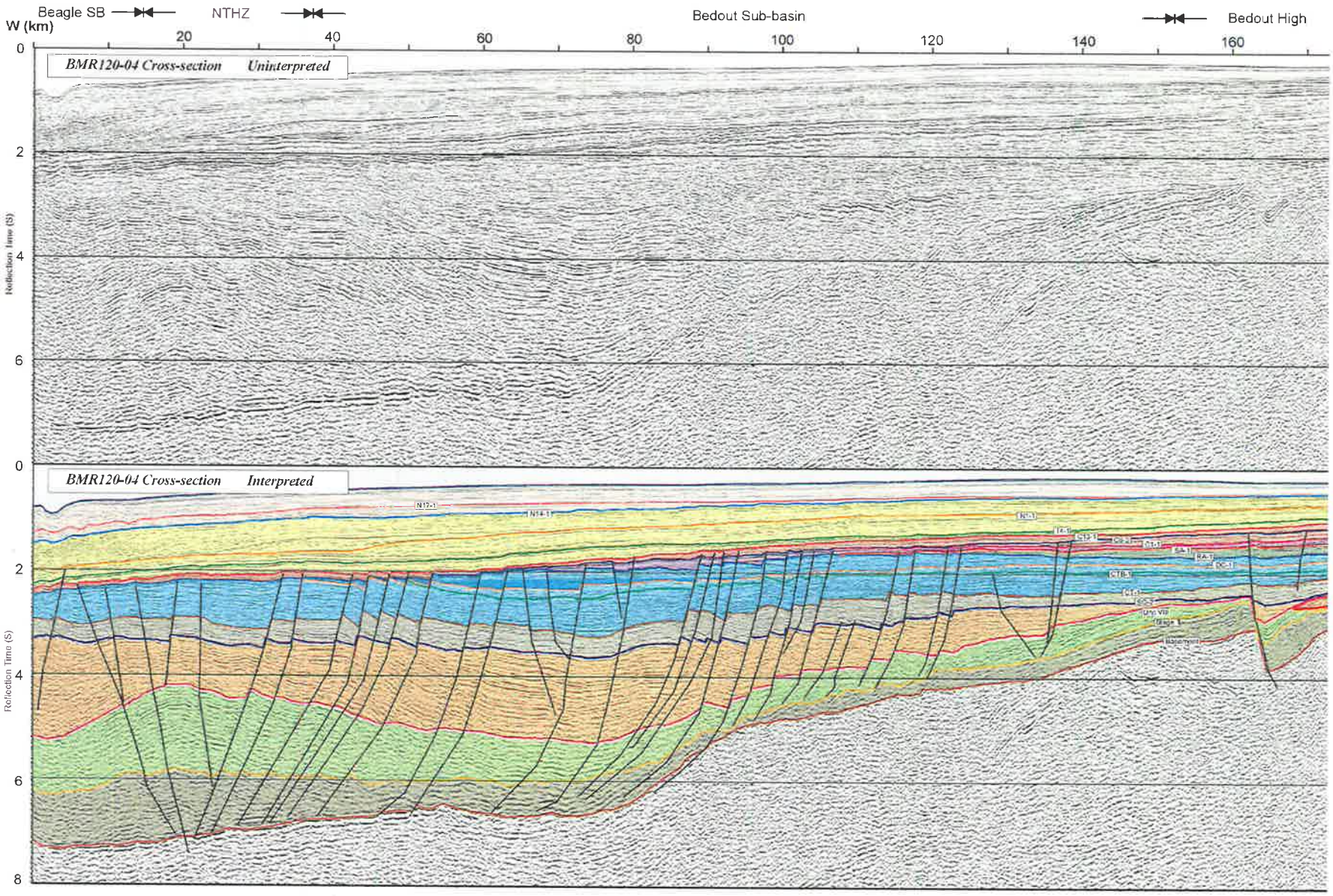

Figure A1.4 Interpreted and uninterpreted regional cross-section (seismic line BMR120-04). Continued over page.

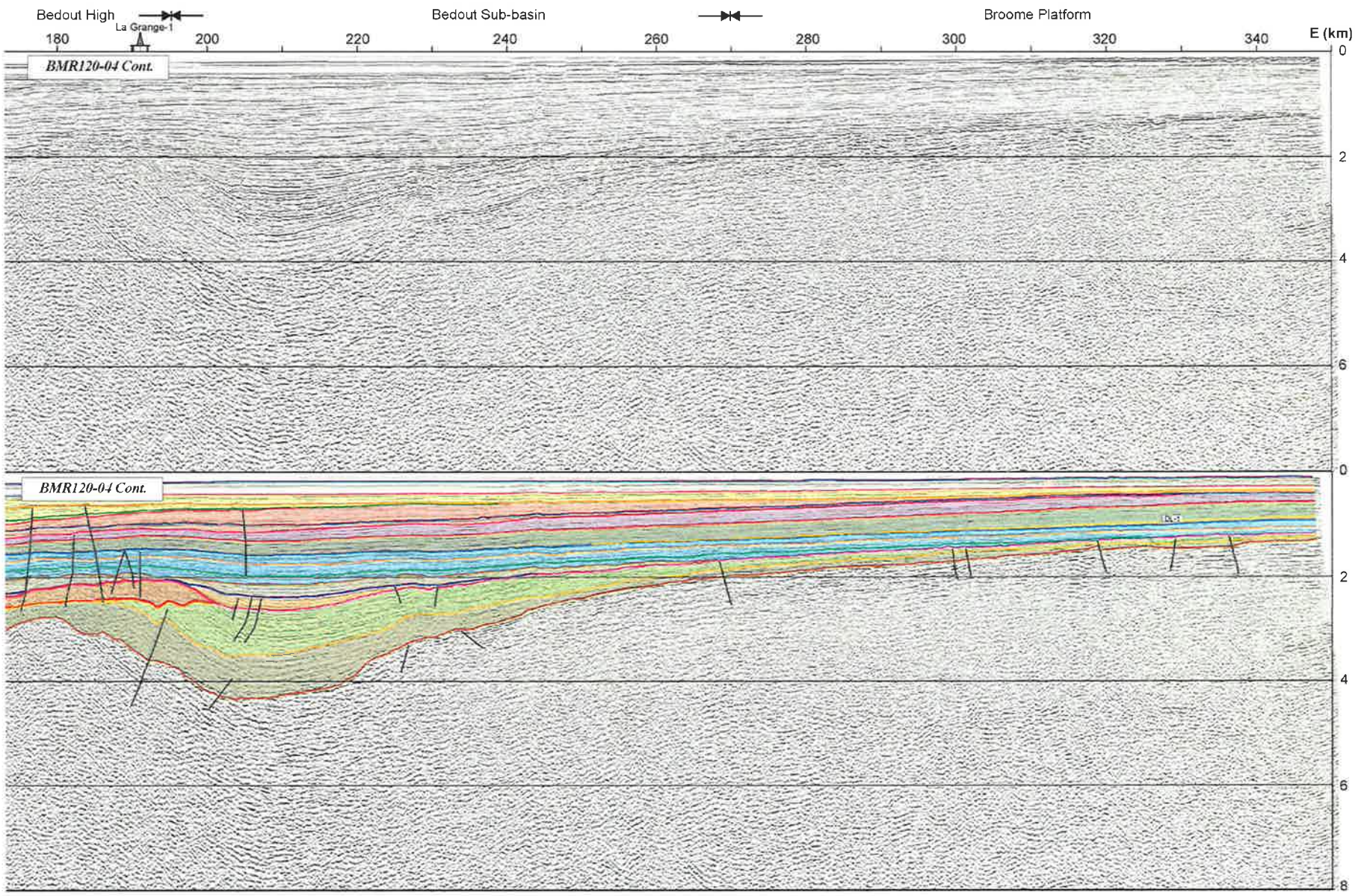

Figure A1.4 (con't)

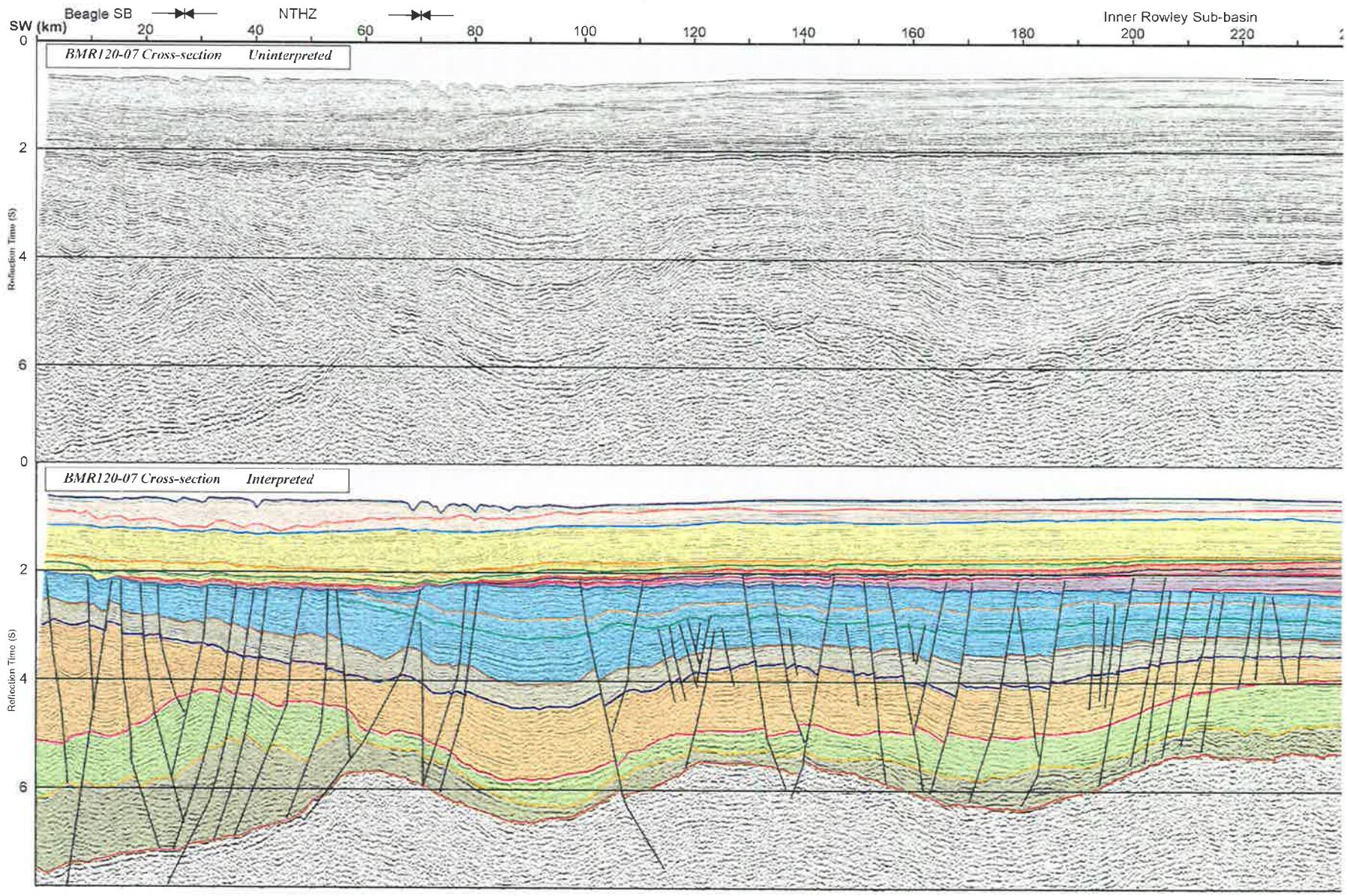

Figure A1.5 Interpreted and uninterpreted regional cross-section (seismic line BMR120-07).

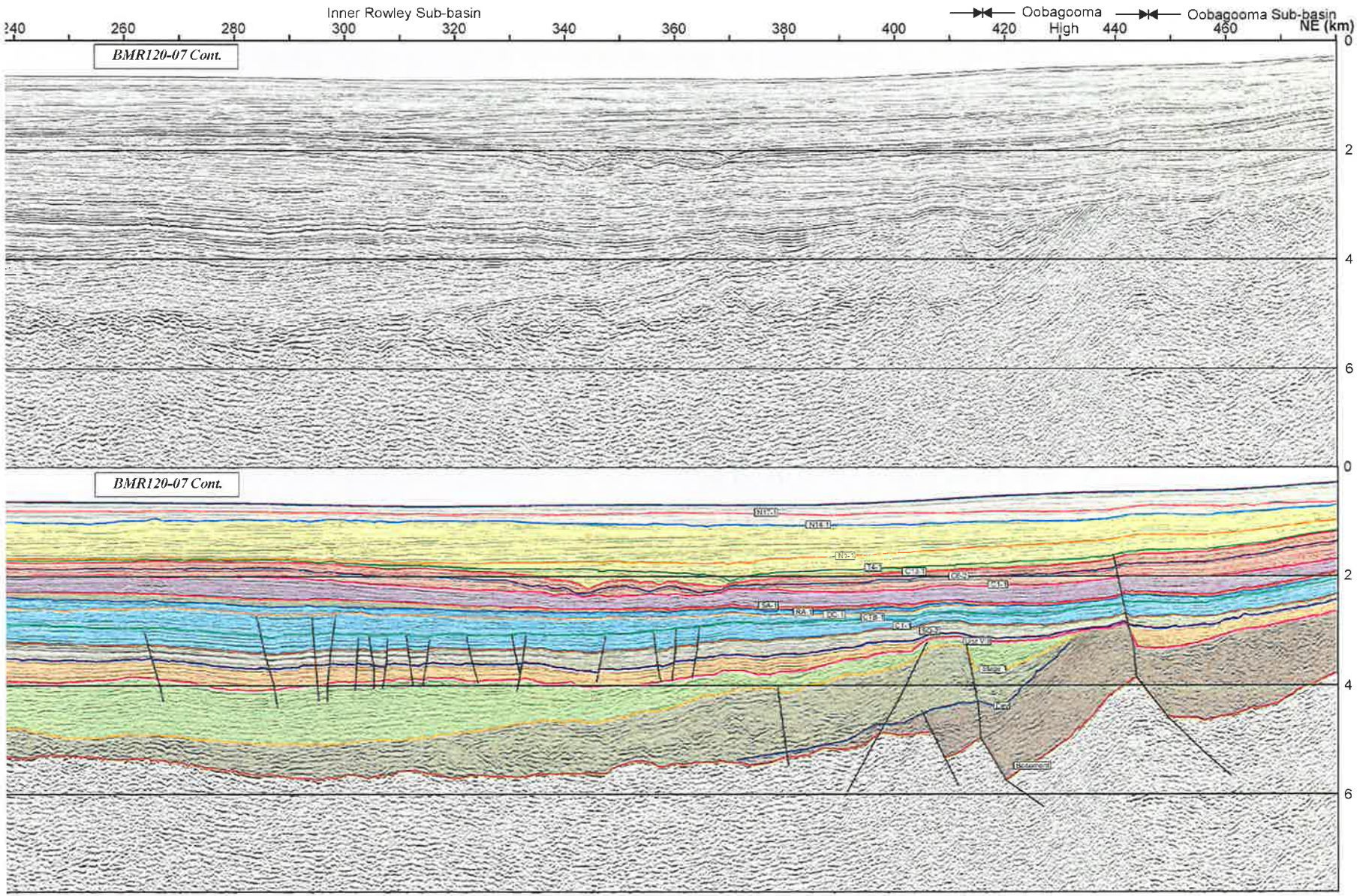

Figure A1.5 (con't)

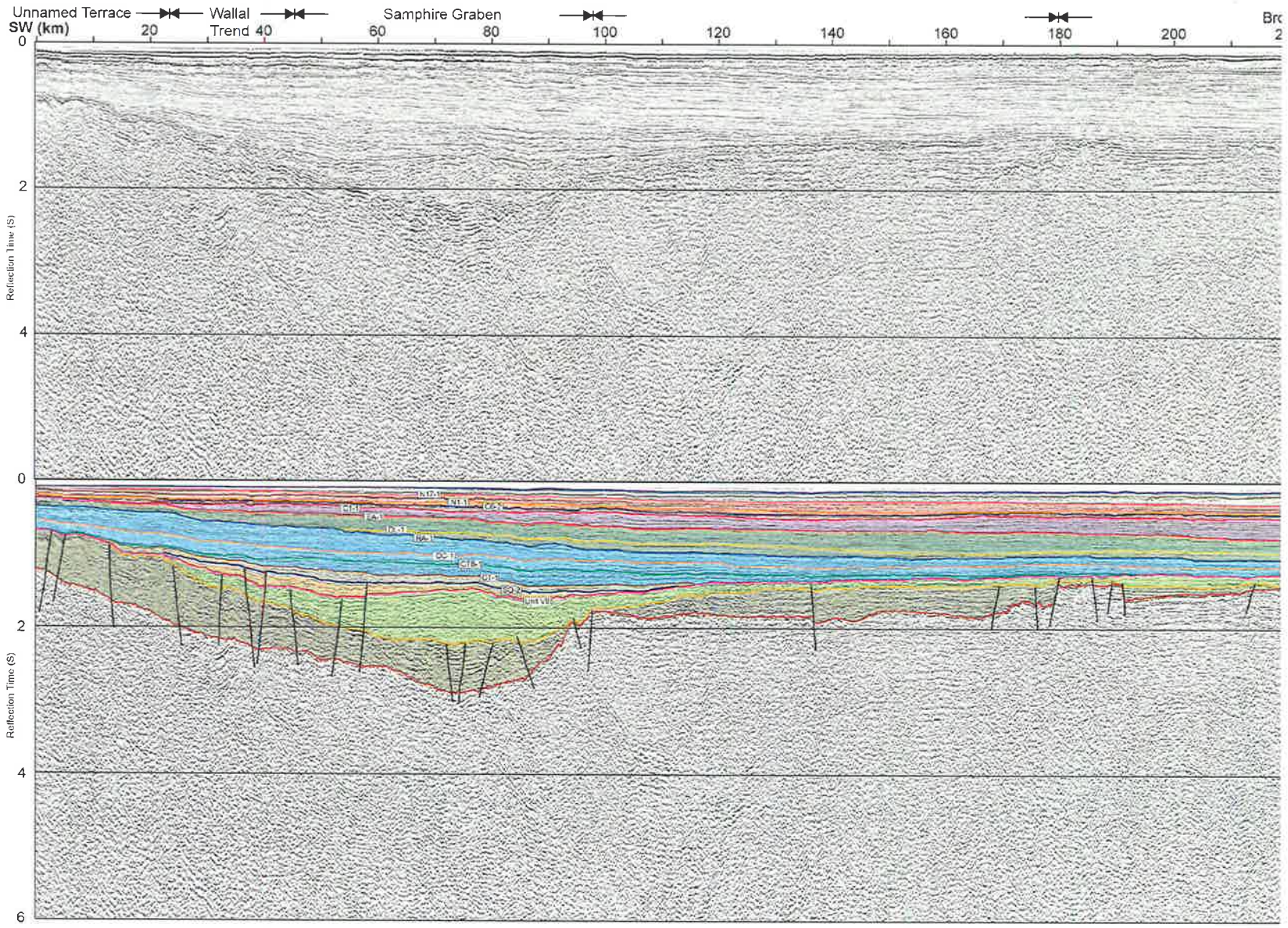

Figure A1.6 Interpreted and uninterpreted regional cross-section (seismic line BMR120-12). Continued over page.

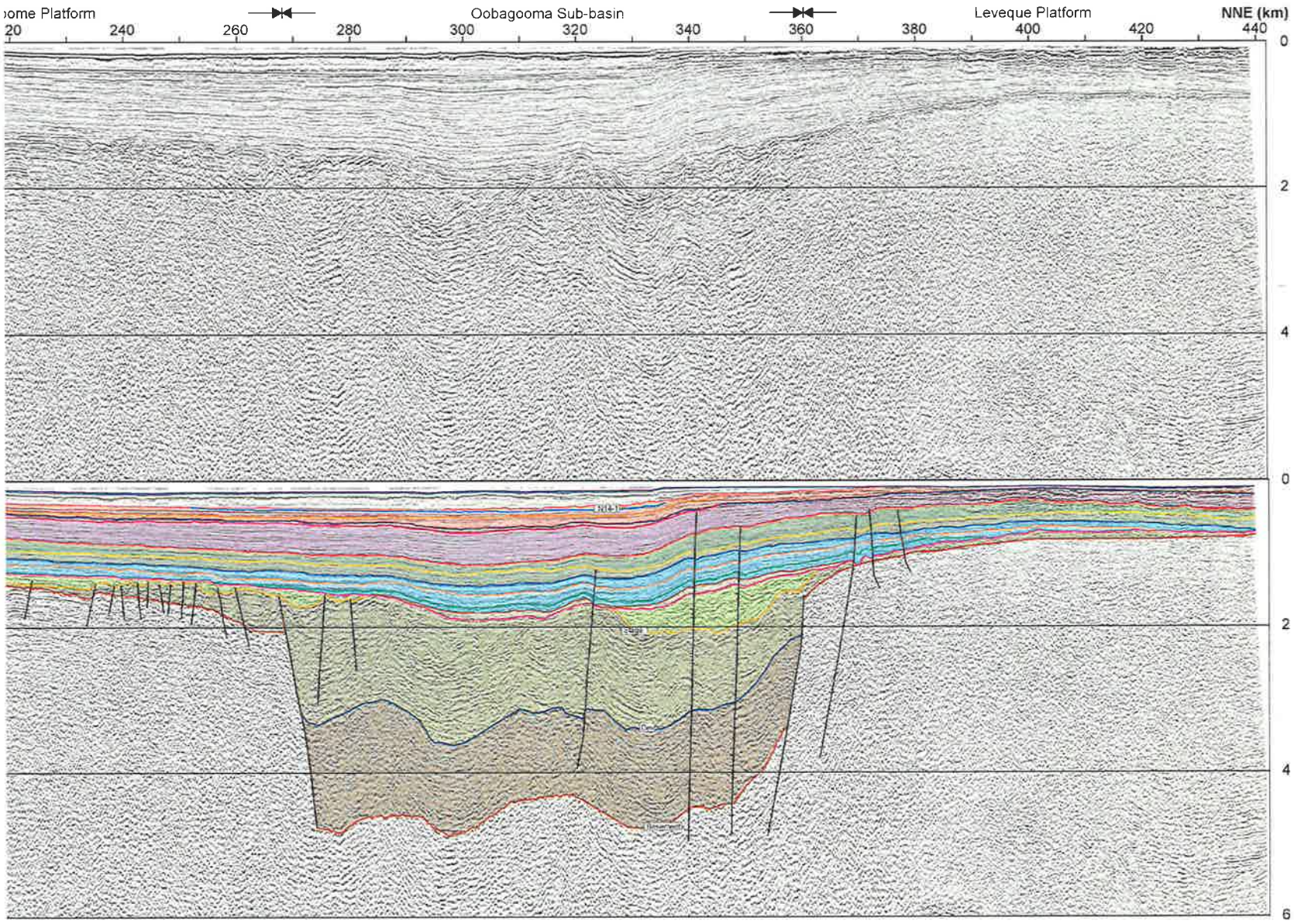

Figure A1.6 (con't)

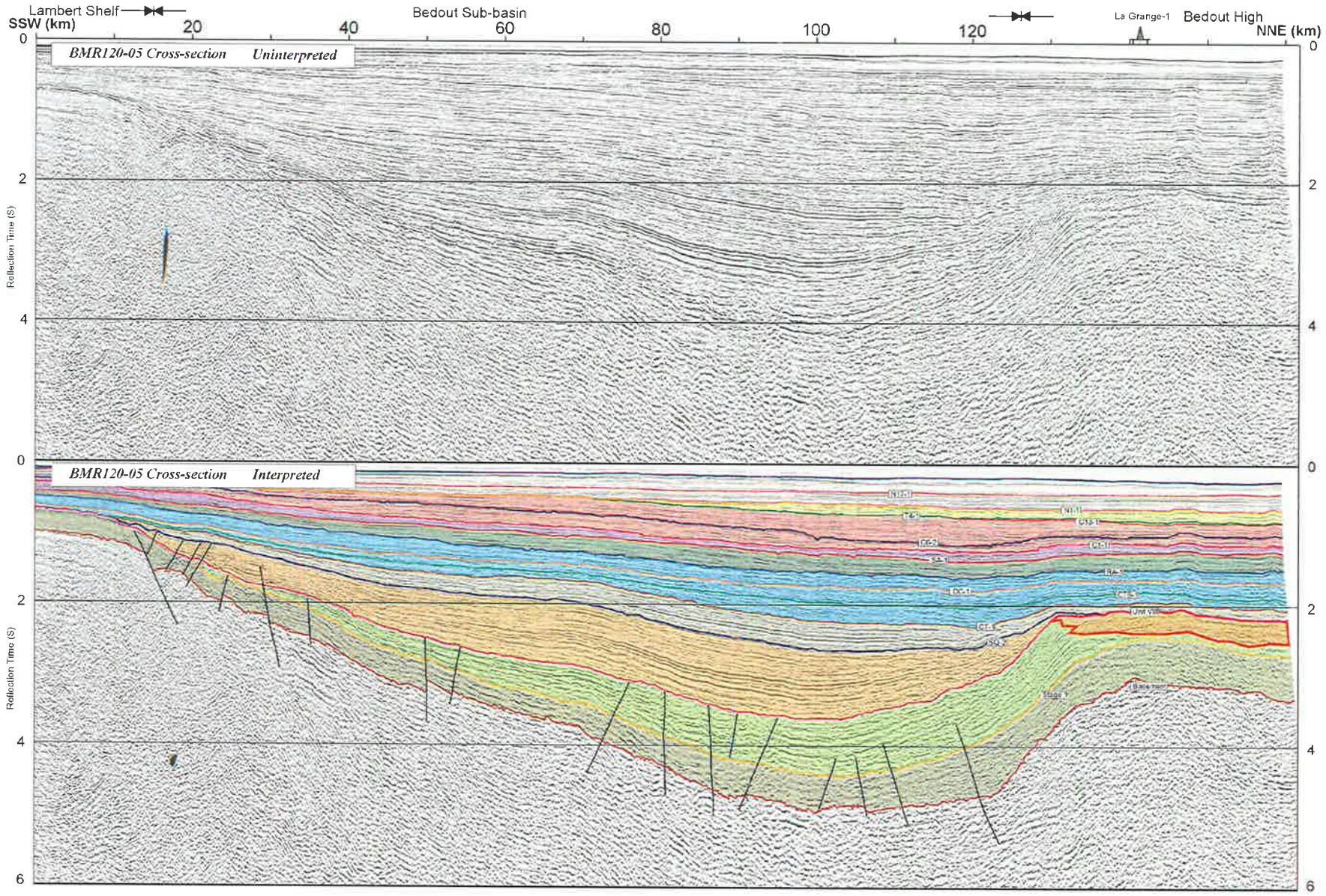

Figure A1.7 Interpreted and uninterpreted regional cross-section (seismic line BMR120-05).

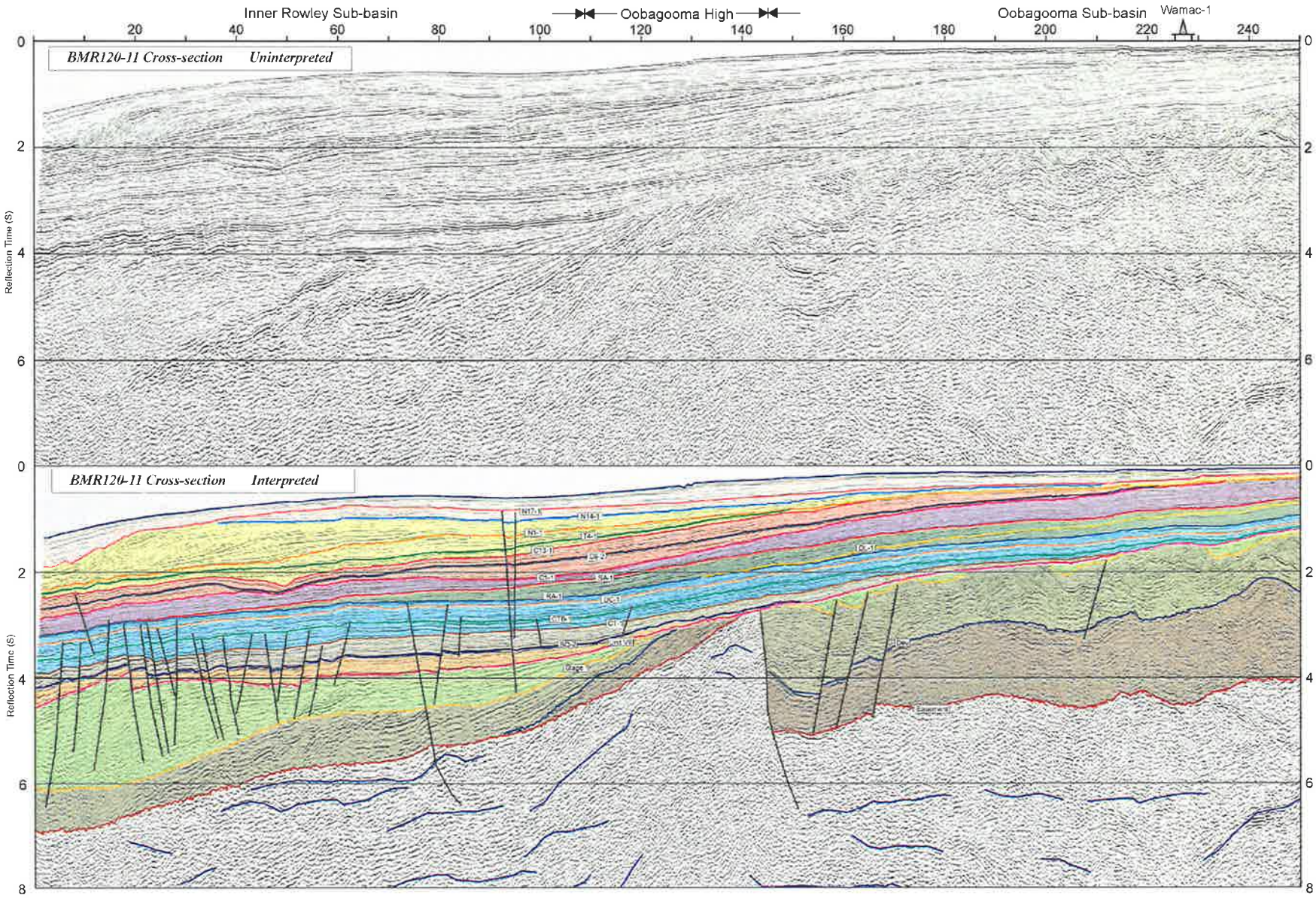

Figure A1.8 Interpreted and uninterpreted regional cross-section (seismic line BMR120-11).

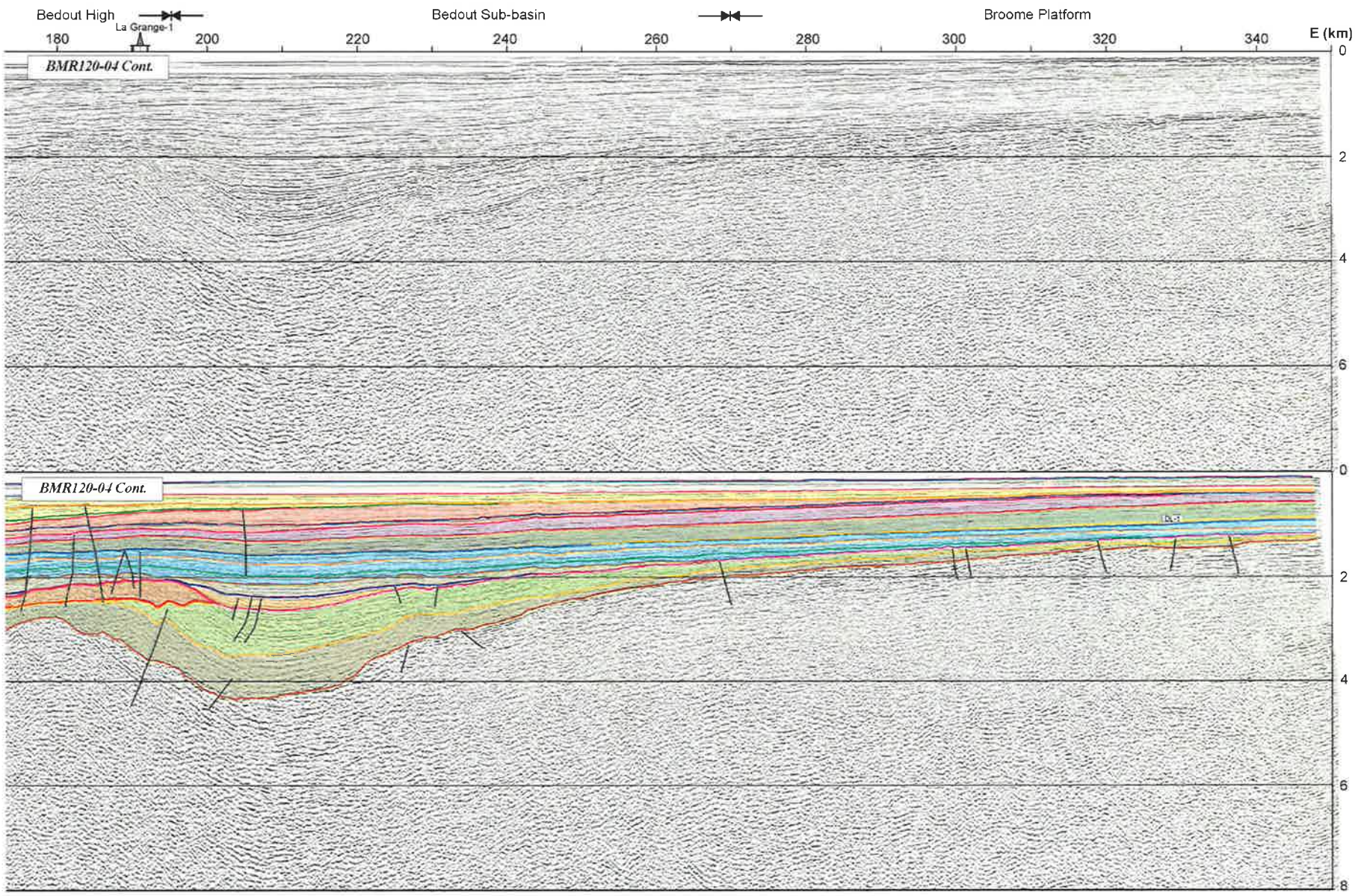

Figure A1.4 (con't)

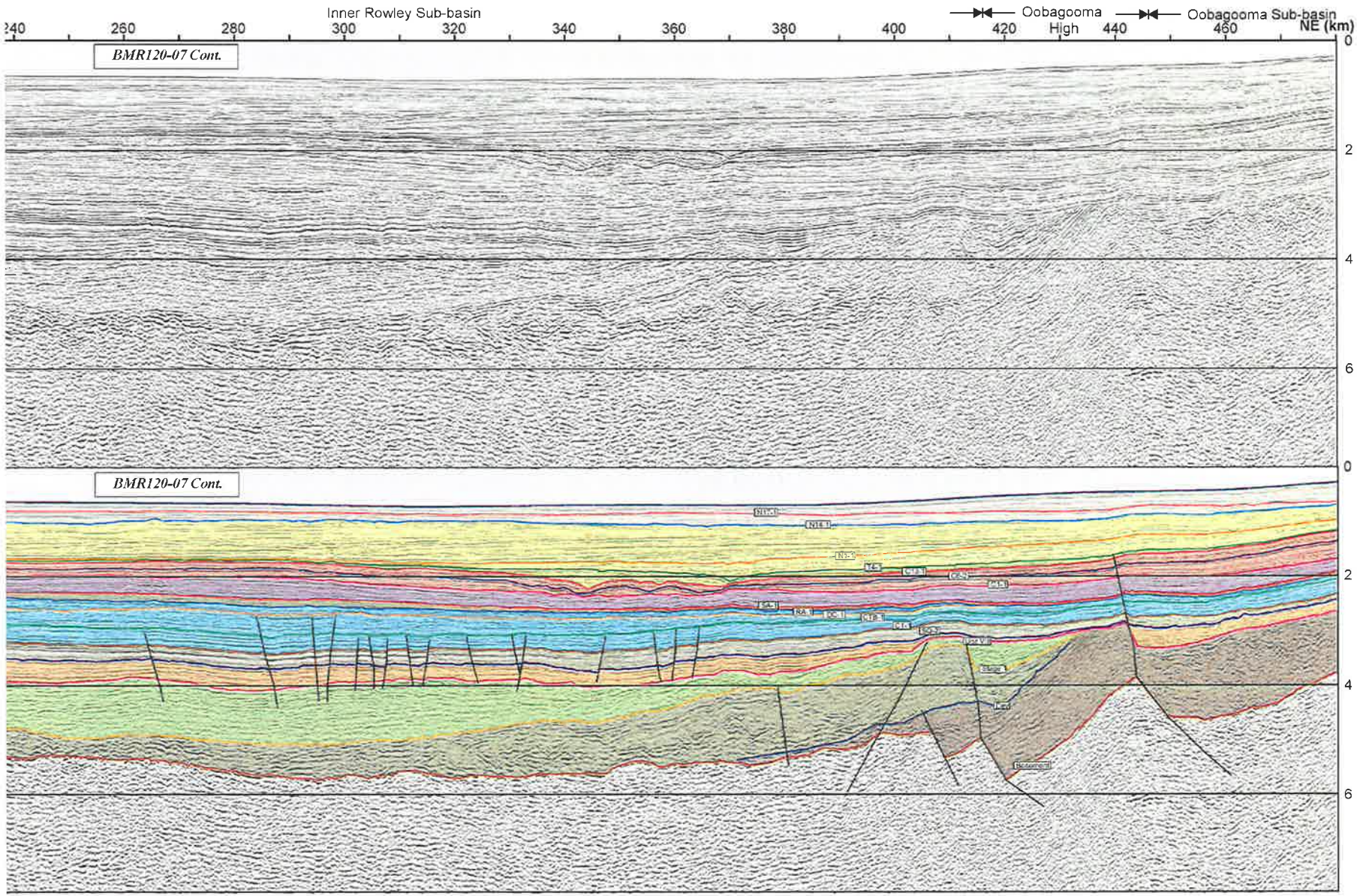

Figure A1.5 (con't)

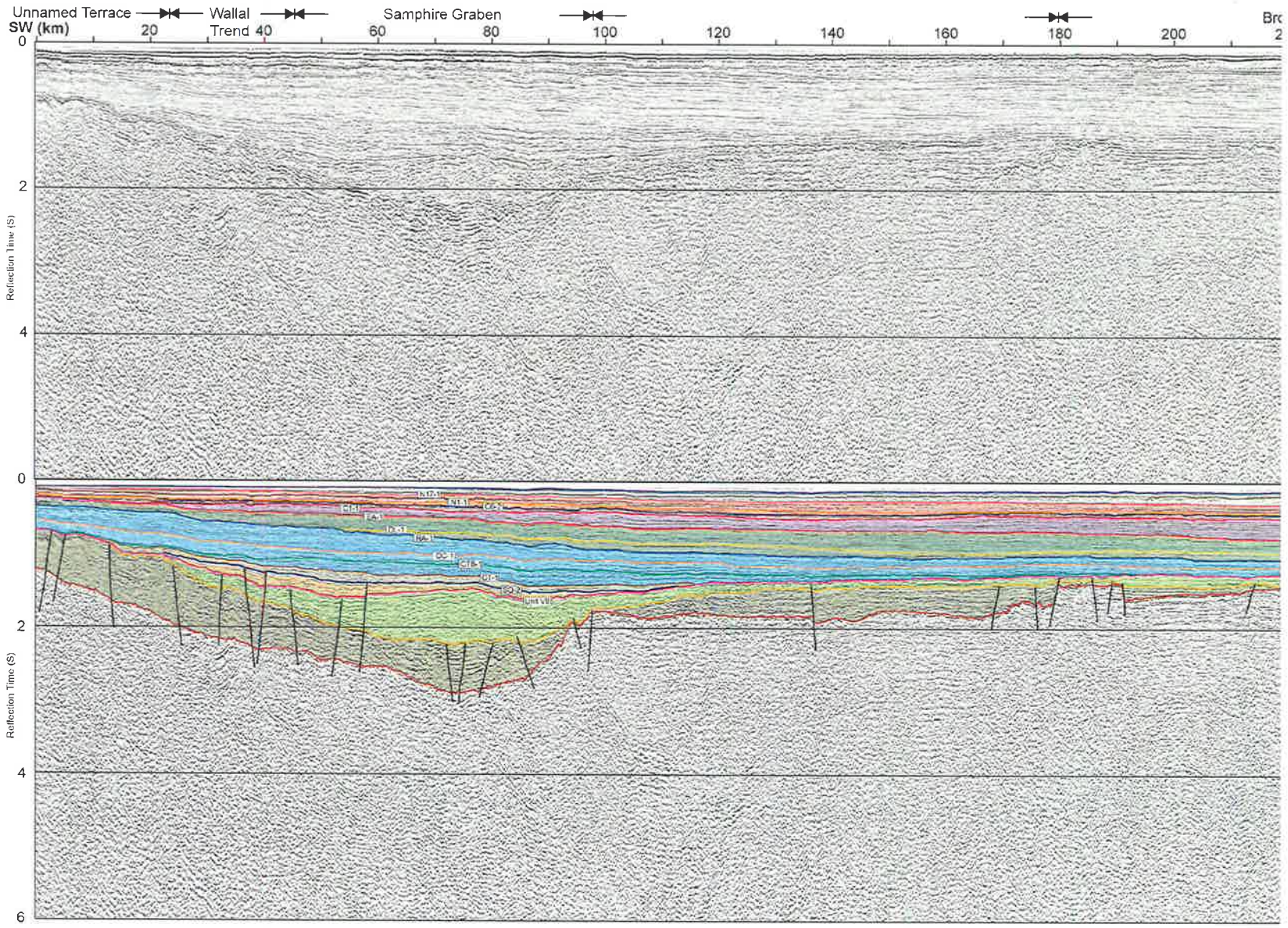

Figure A1.6 Interpreted and uninterpreted regional cross-section (seismic line BMR120-12). Continued over page.

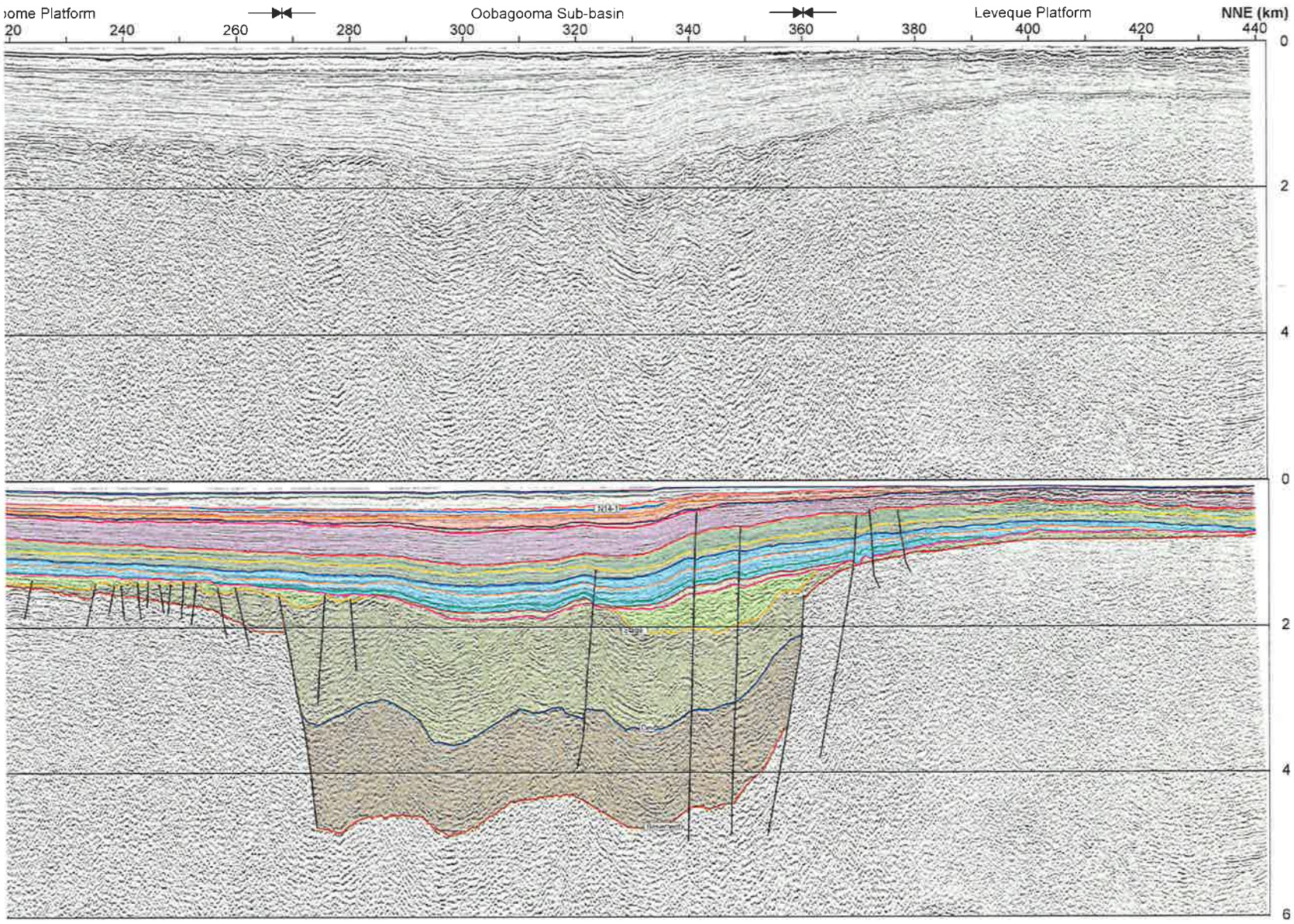

Figure A1.6 (con't)

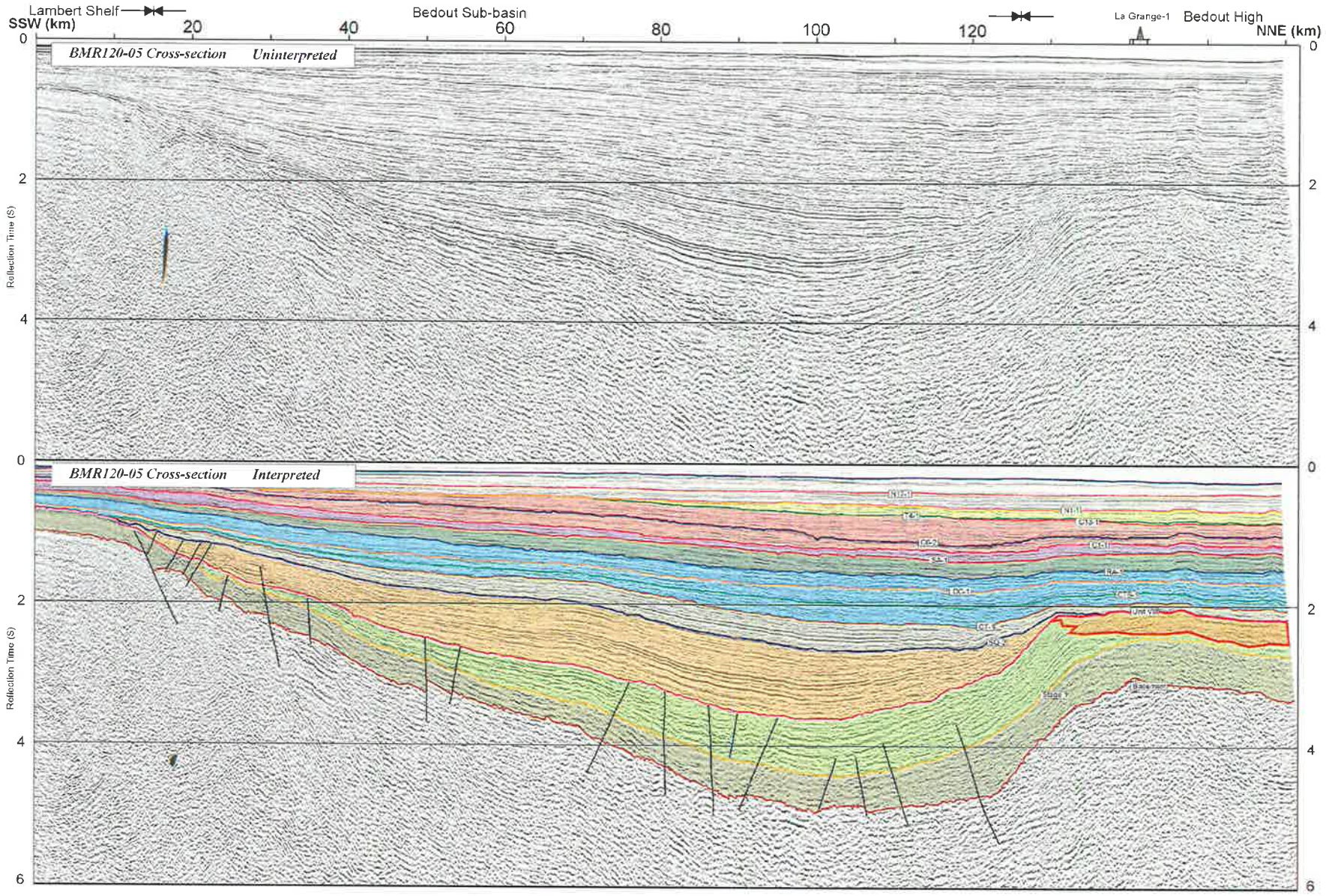

Figure A1.7 Interpreted and uninterpreted regional cross-section (seismic line BMR120-05).

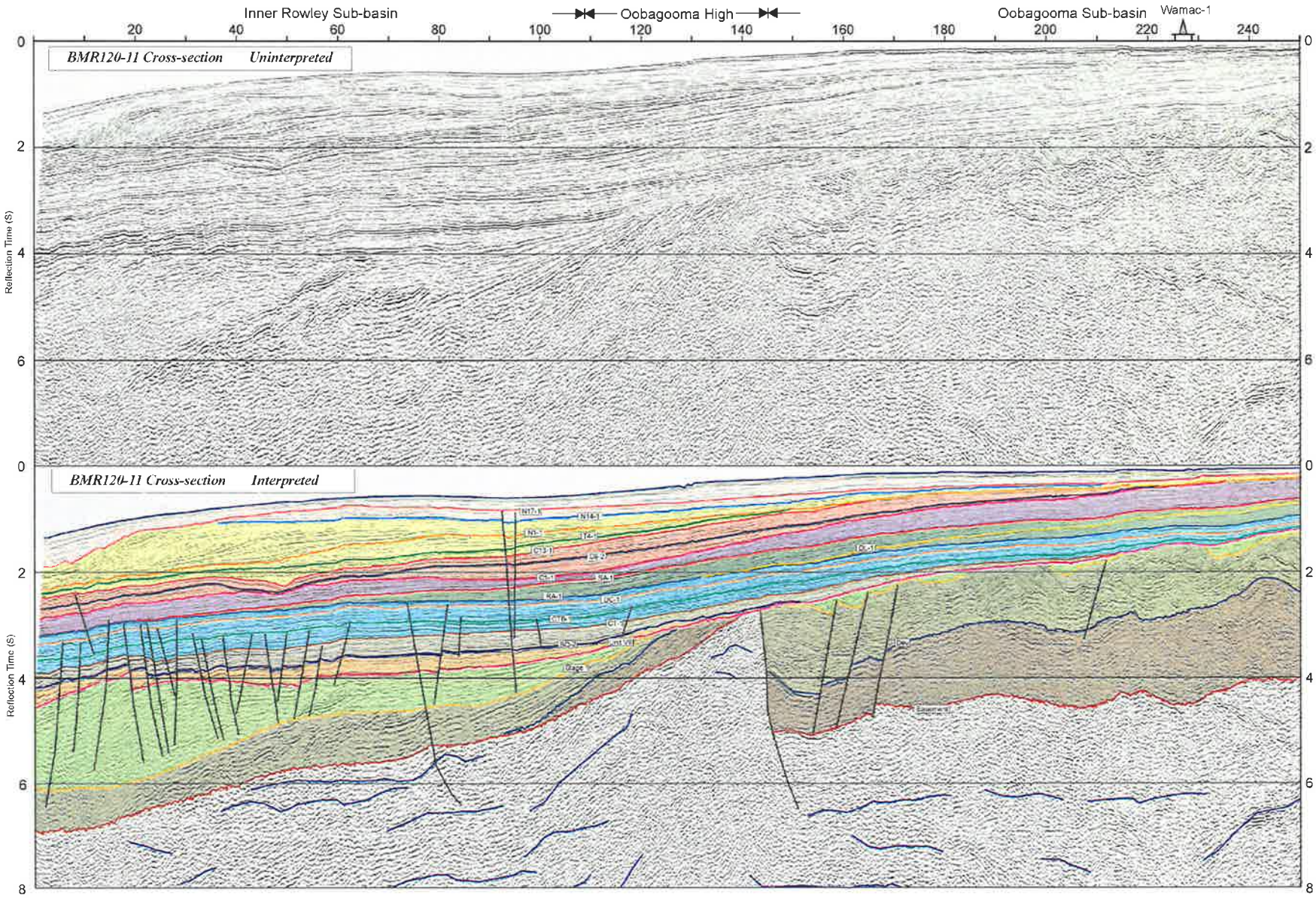

Figure A1.8 Interpreted and uninterpreted regional cross-section (seismic line BMR120-11).

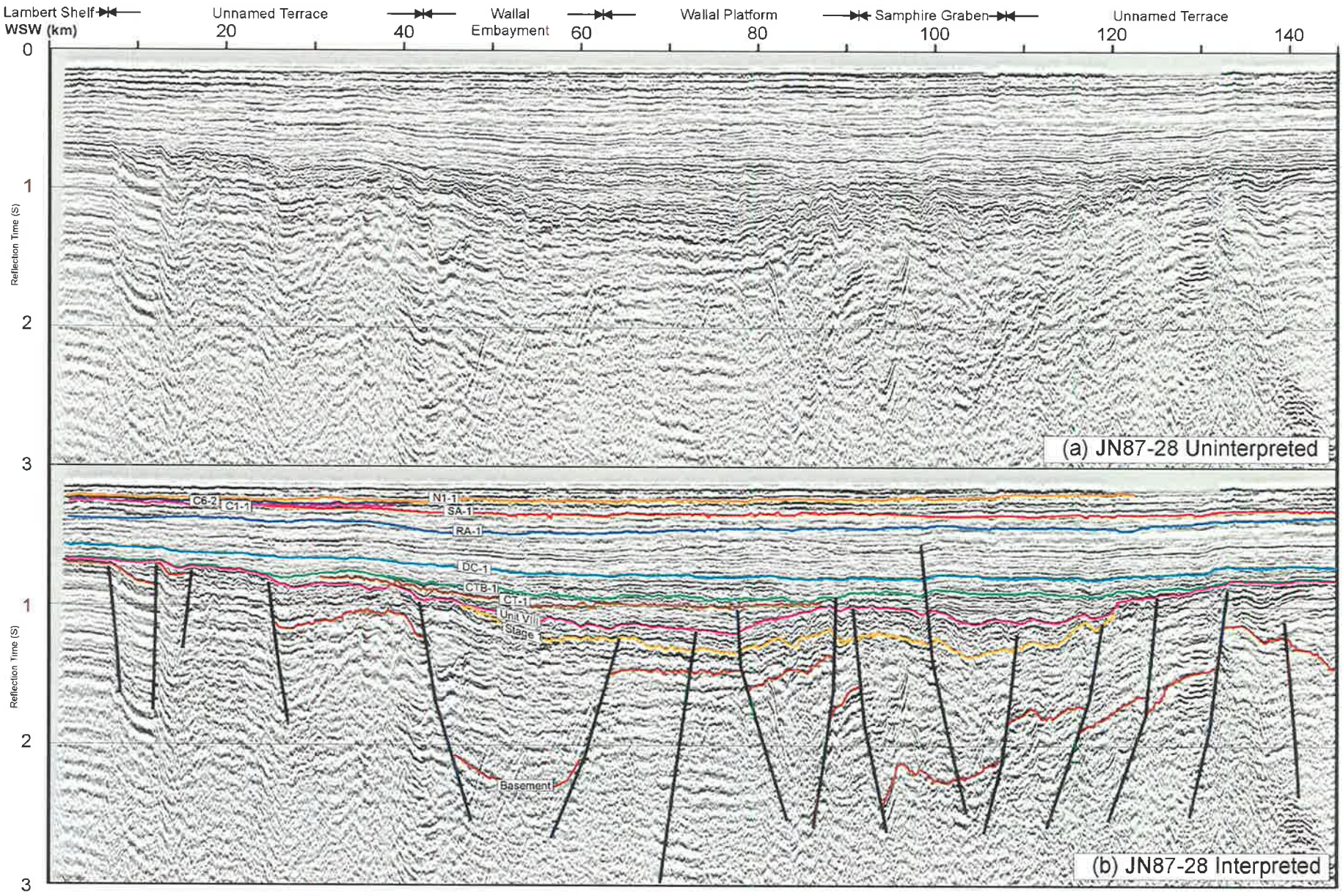

Figure A1.9 Interpreted and uninterpreted regional cross-section (seismic line JN87-28).

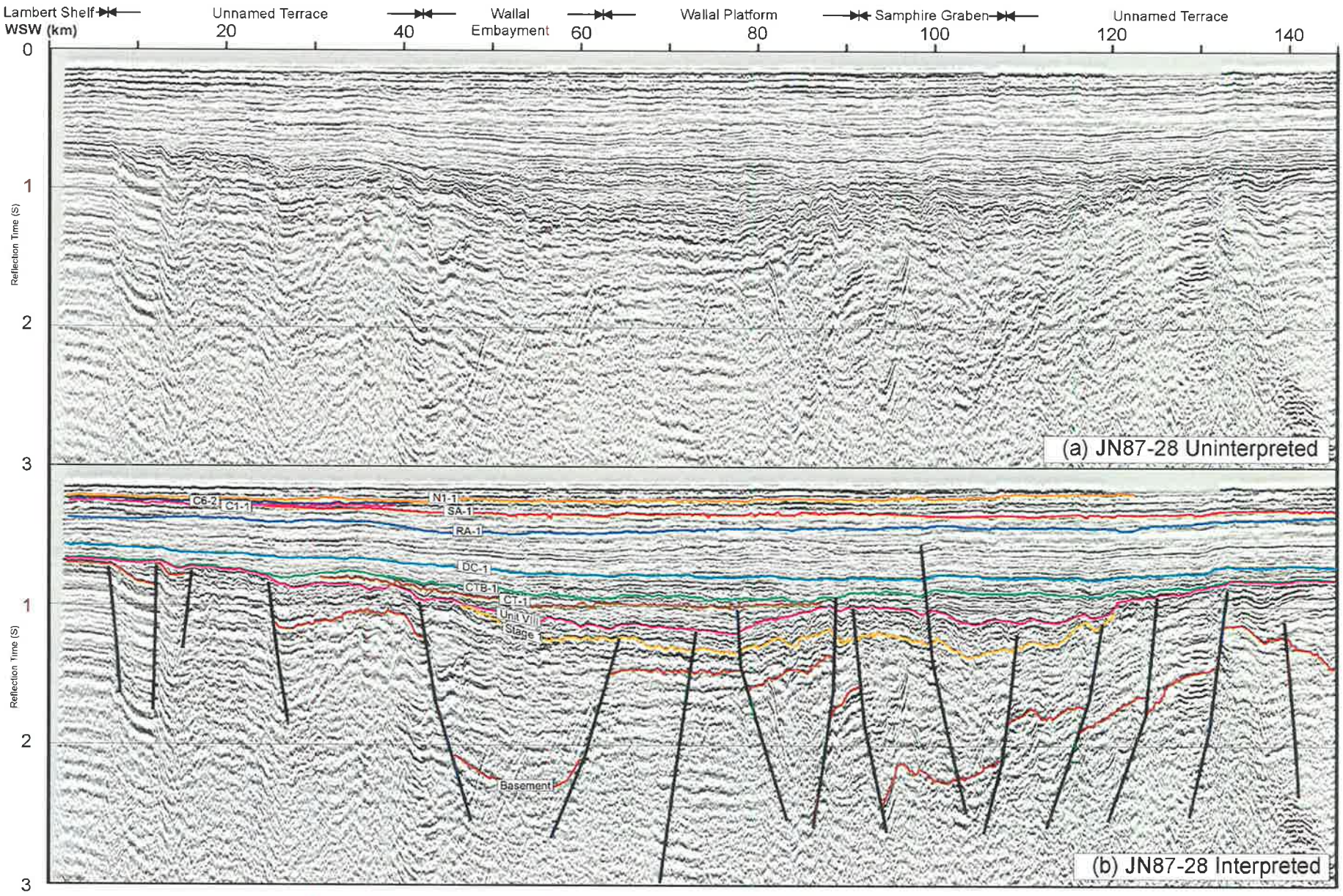

Figure A1.9 Interpreted and uninterpreted regional cross-section (seismic line JN87-28).

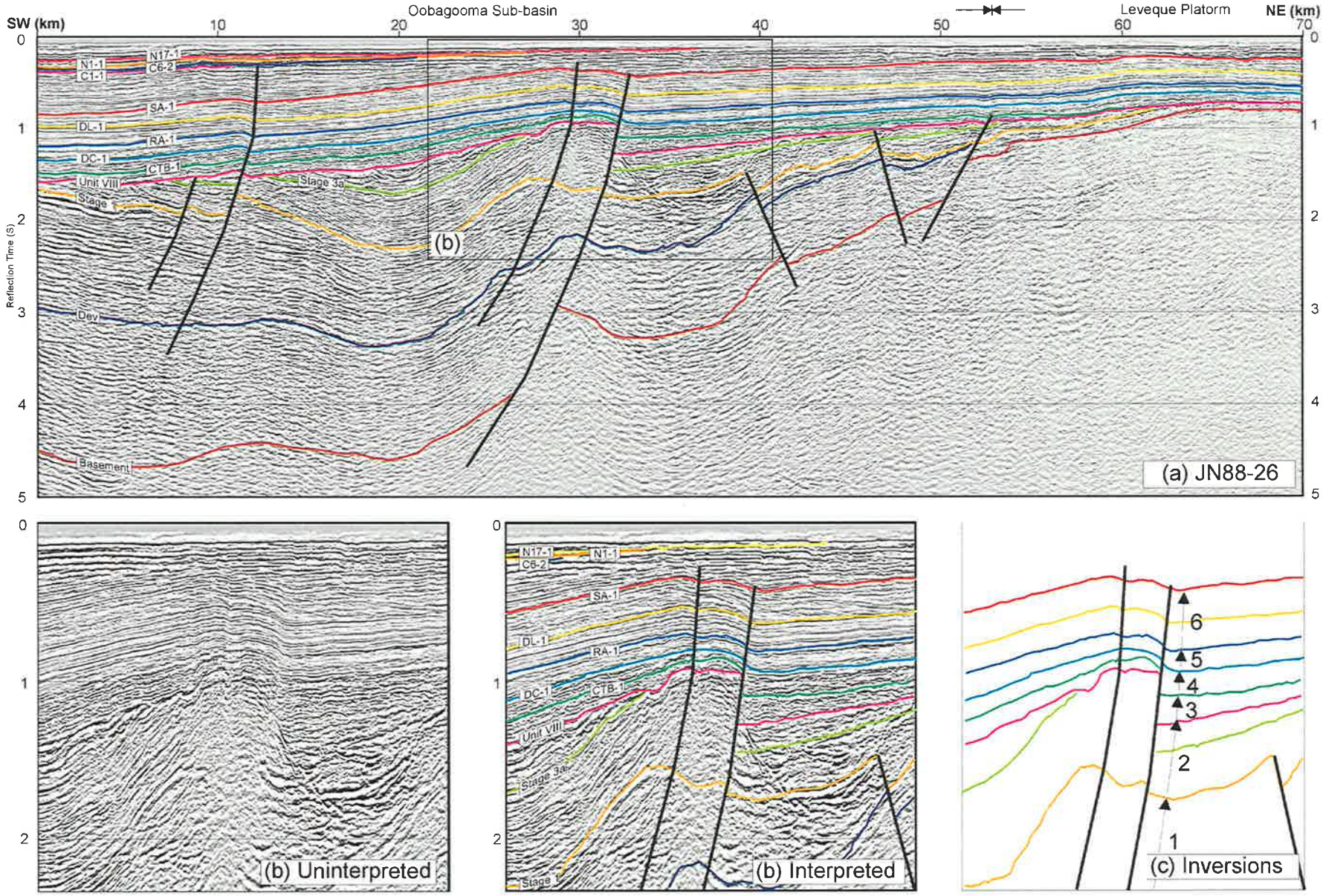

Figure A1.10 Interpreted regional cross-section (seismic line JN88-26).

APPENDIX 2

Two-Way-Time Structure Maps

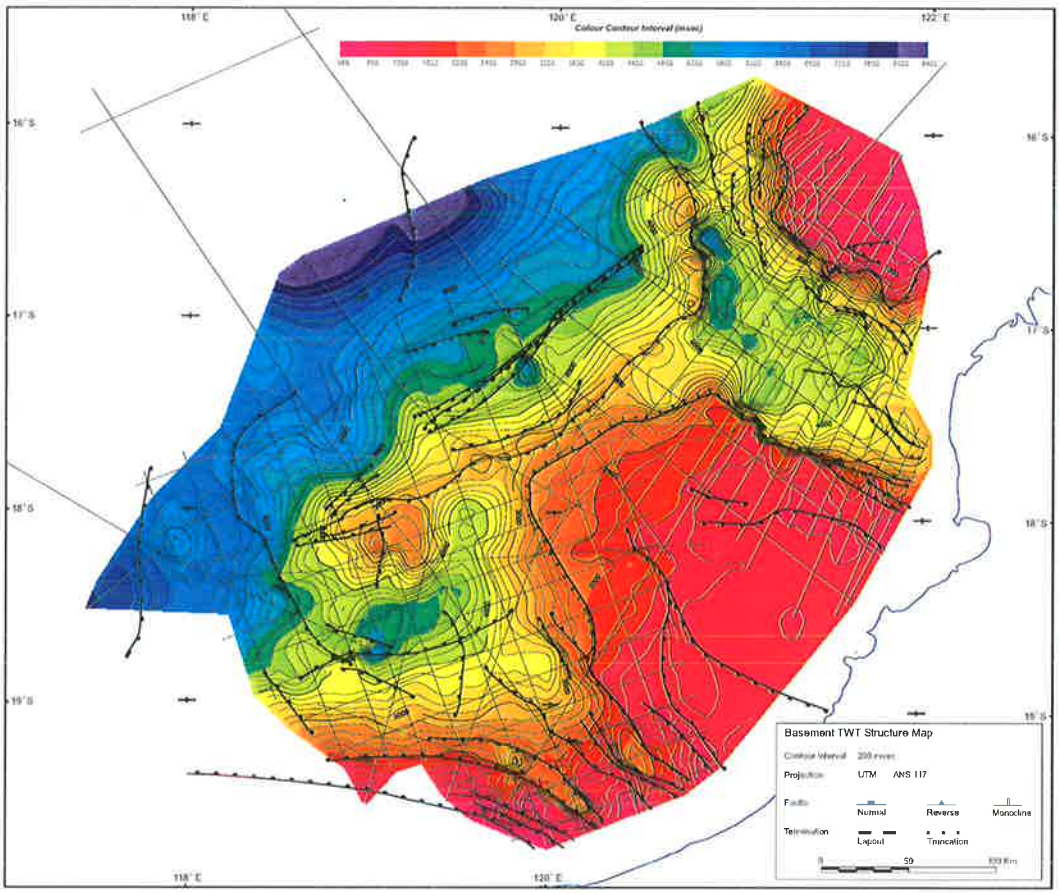

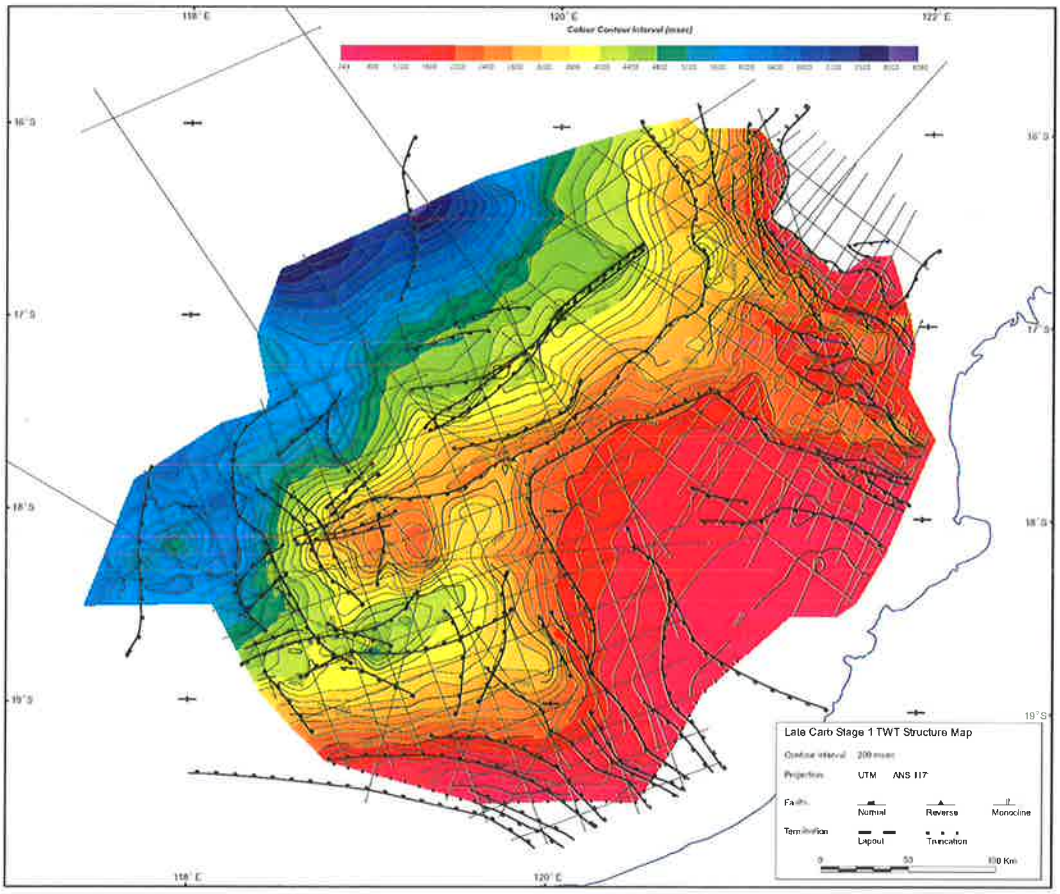

Figure A2.1 (Top) Basement TWT structure map.
Figure A2.2 (Bottom) Late Carboniferous Stage 1 TWT structure map.

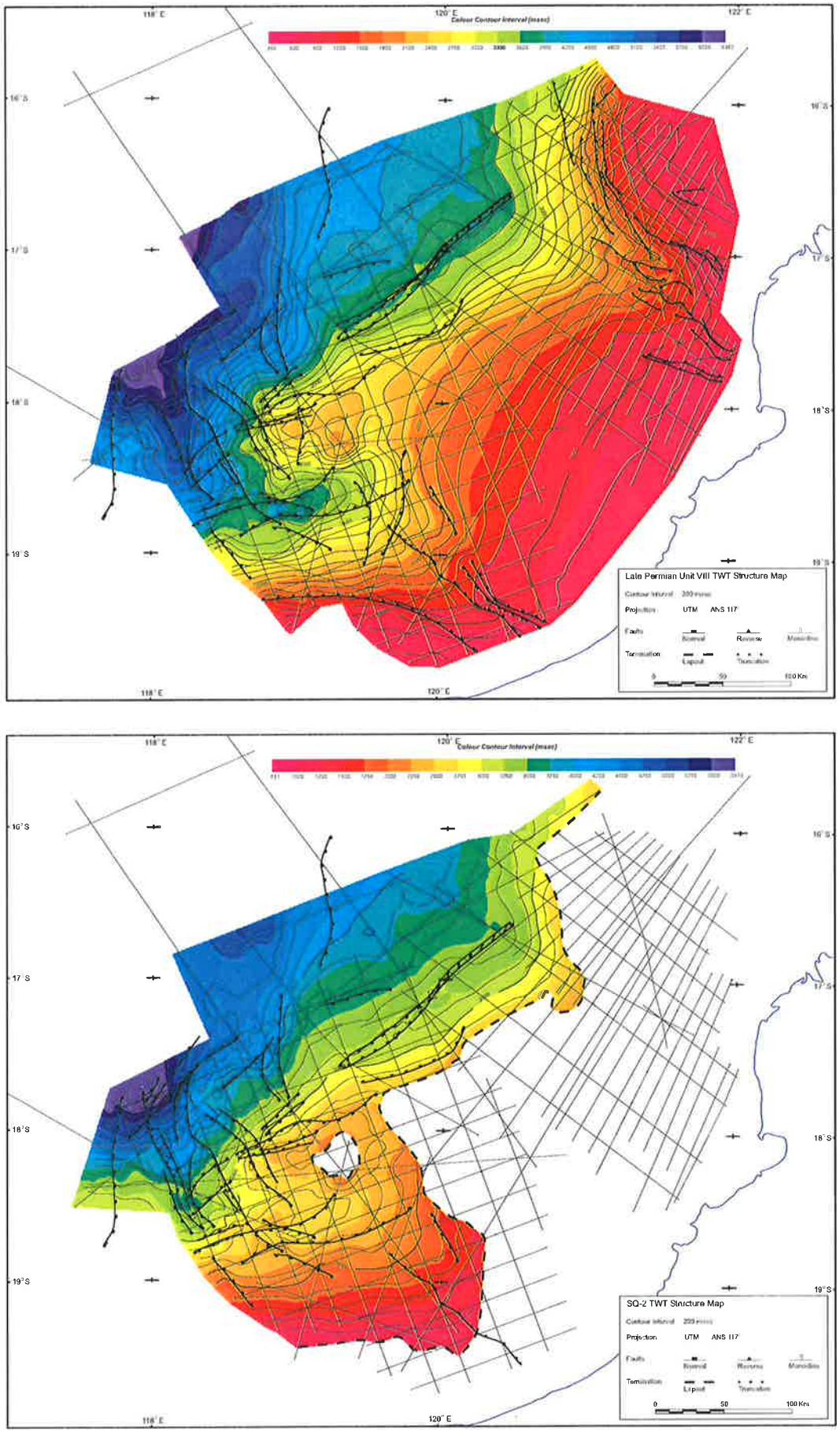

Figure A2.3 (Top) Late Permian Unit VIII TWT structure map.
Figure A2.4 (Bottom) Middle Triassic SQ-2 TWT structure map.

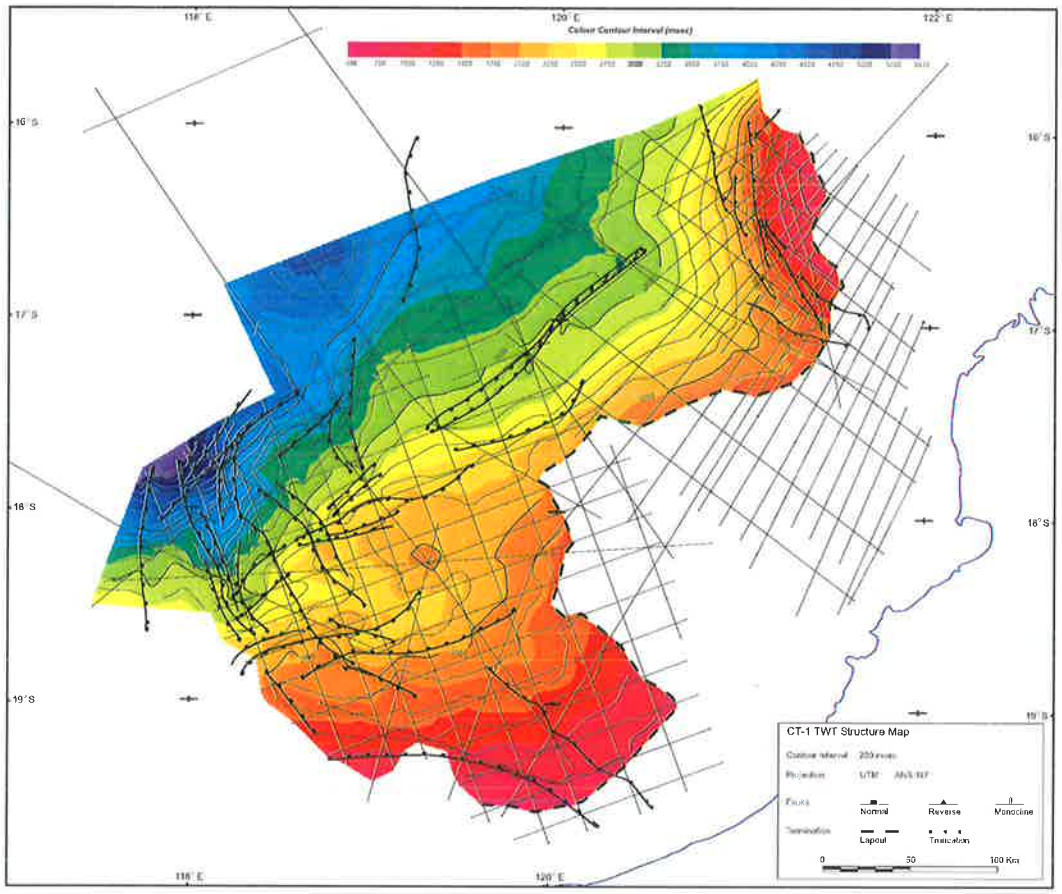

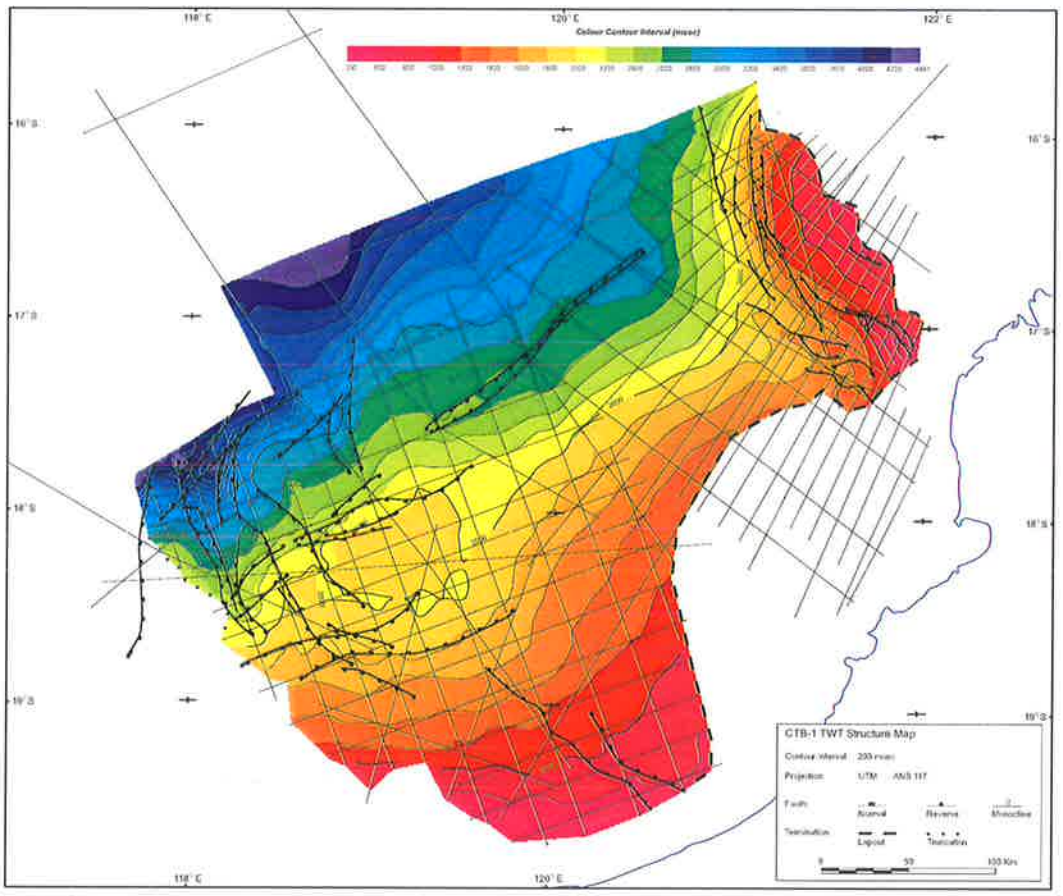

Figure A2.5 (Top) Early Jurassic CT-1 TWT structure map.
Figure A2.6 (Bottom) Middle Jurassic CTB-1 TWT structure map.

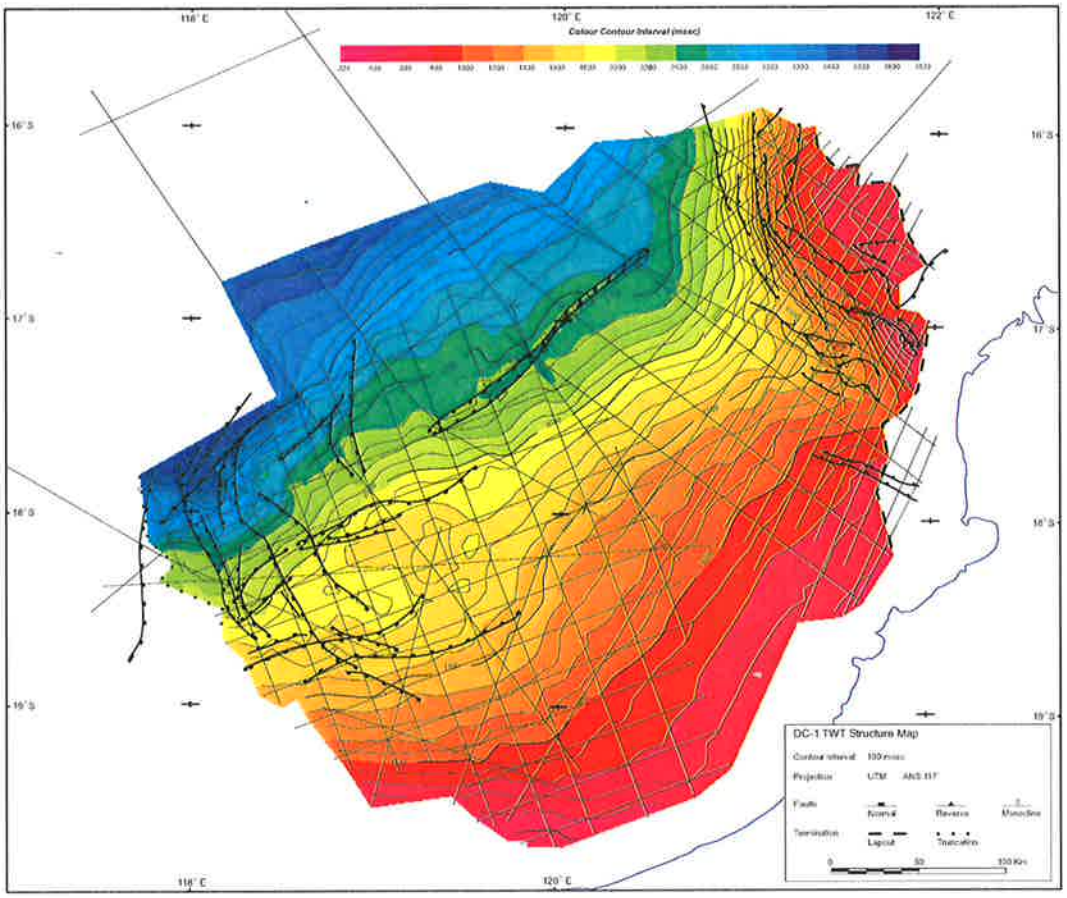

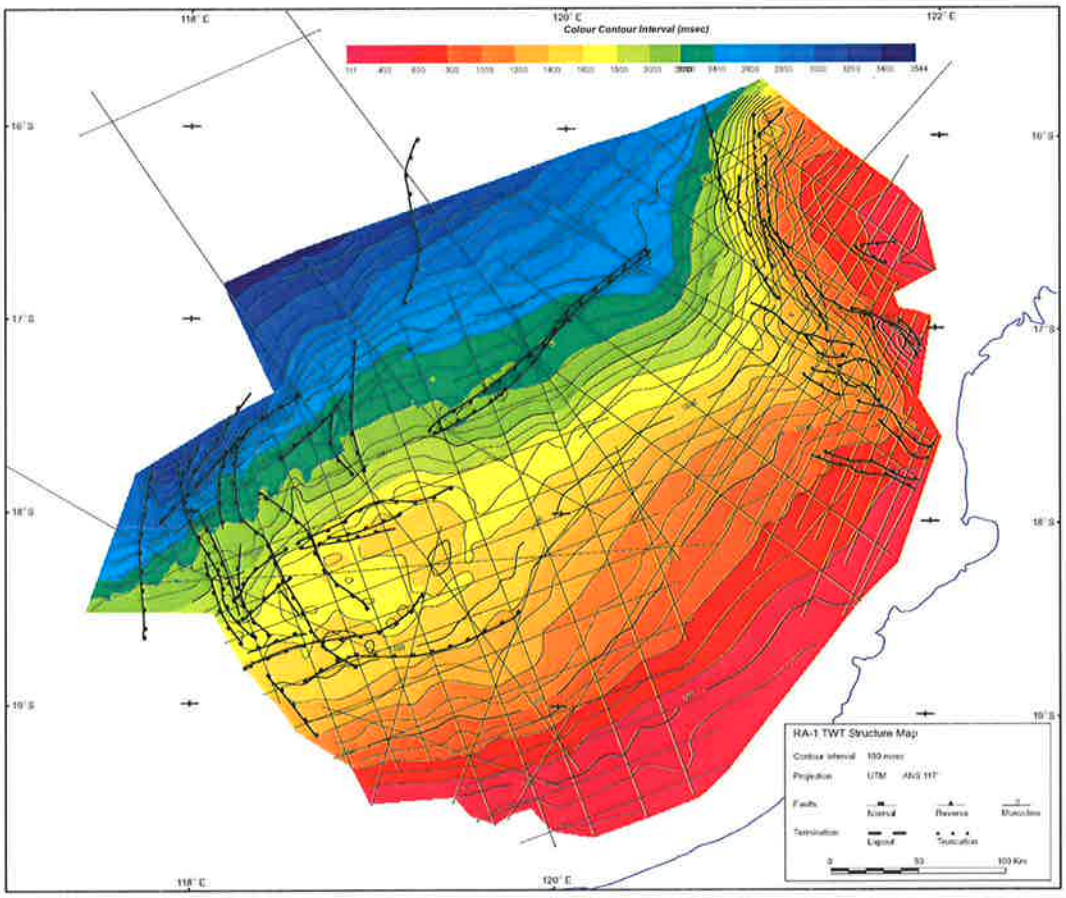

Figure A2.7 (Top) Middle Jurassic DC-1 TWT structure map.
Figure A2.8 (Bottom) Middle Jurassic RA-1 TWT structure map.

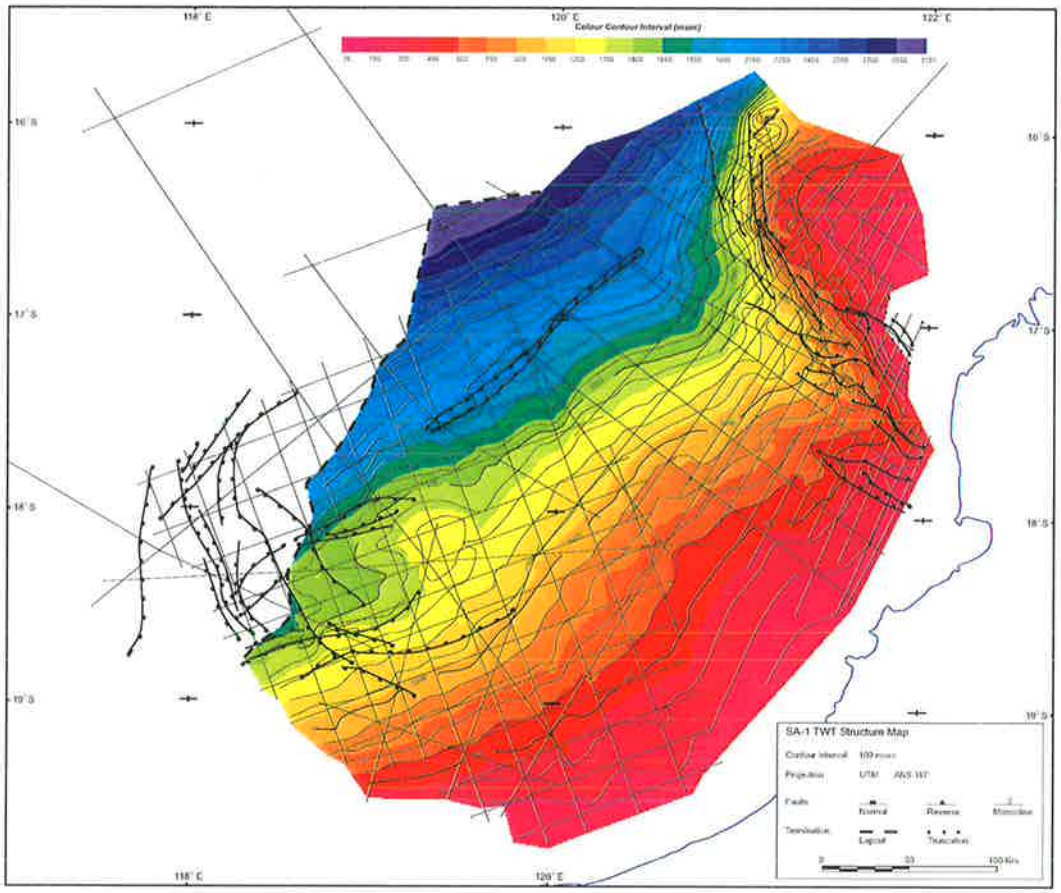

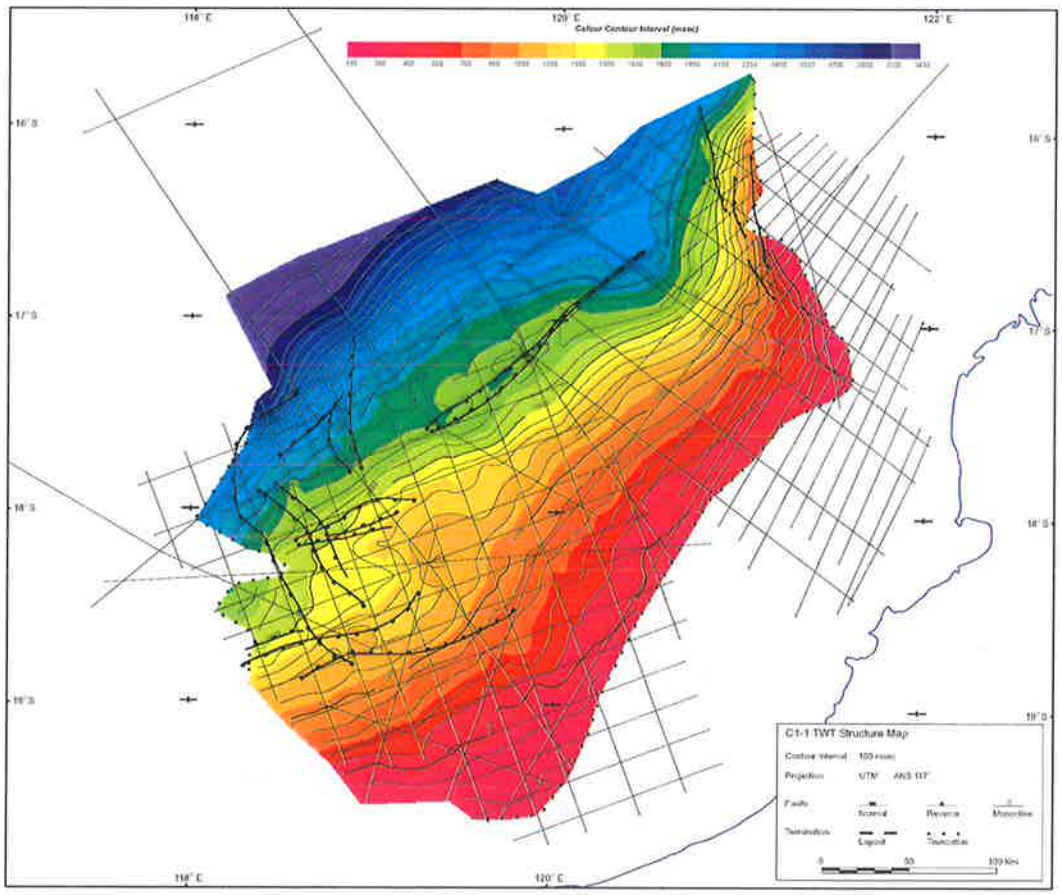

Figure A2.9 (Top) Early Cretaceous SA-1 TWT structure map.
Figure A2.10 (Bottom) Early Cretaceous C1-1 TWT structure map.

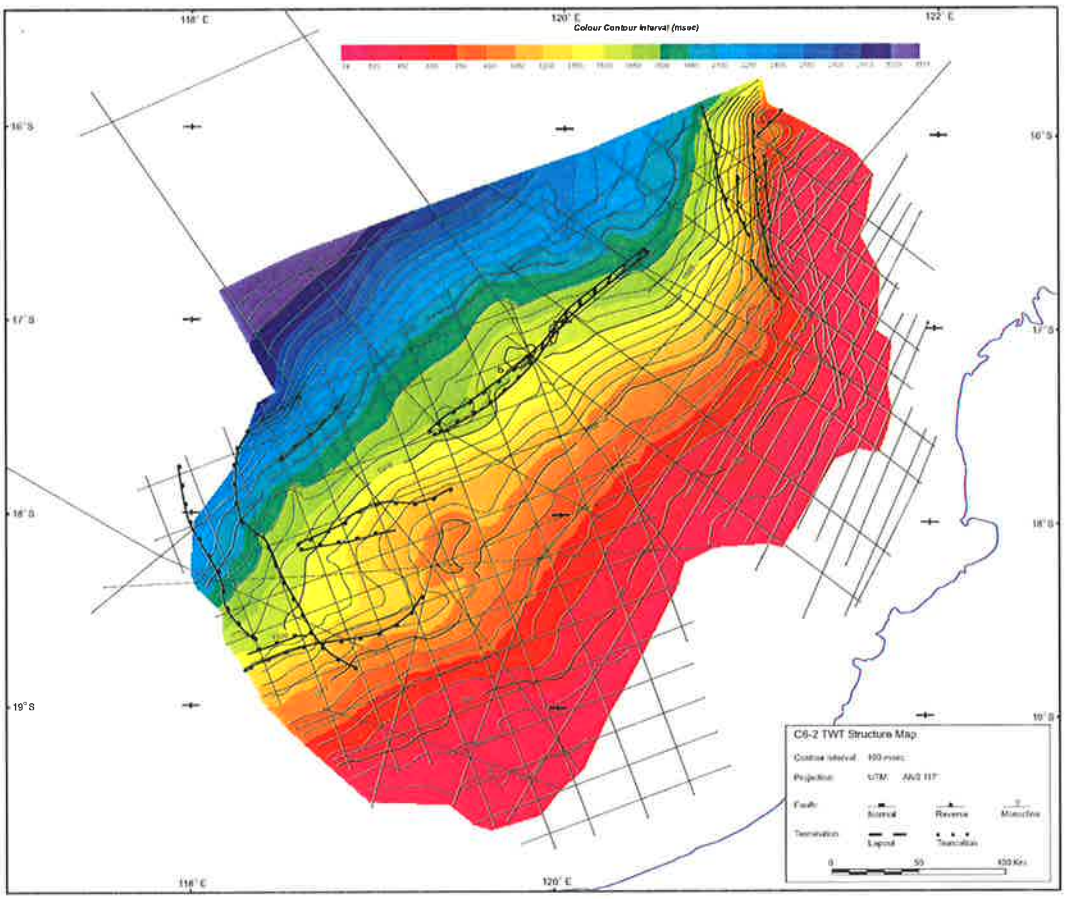

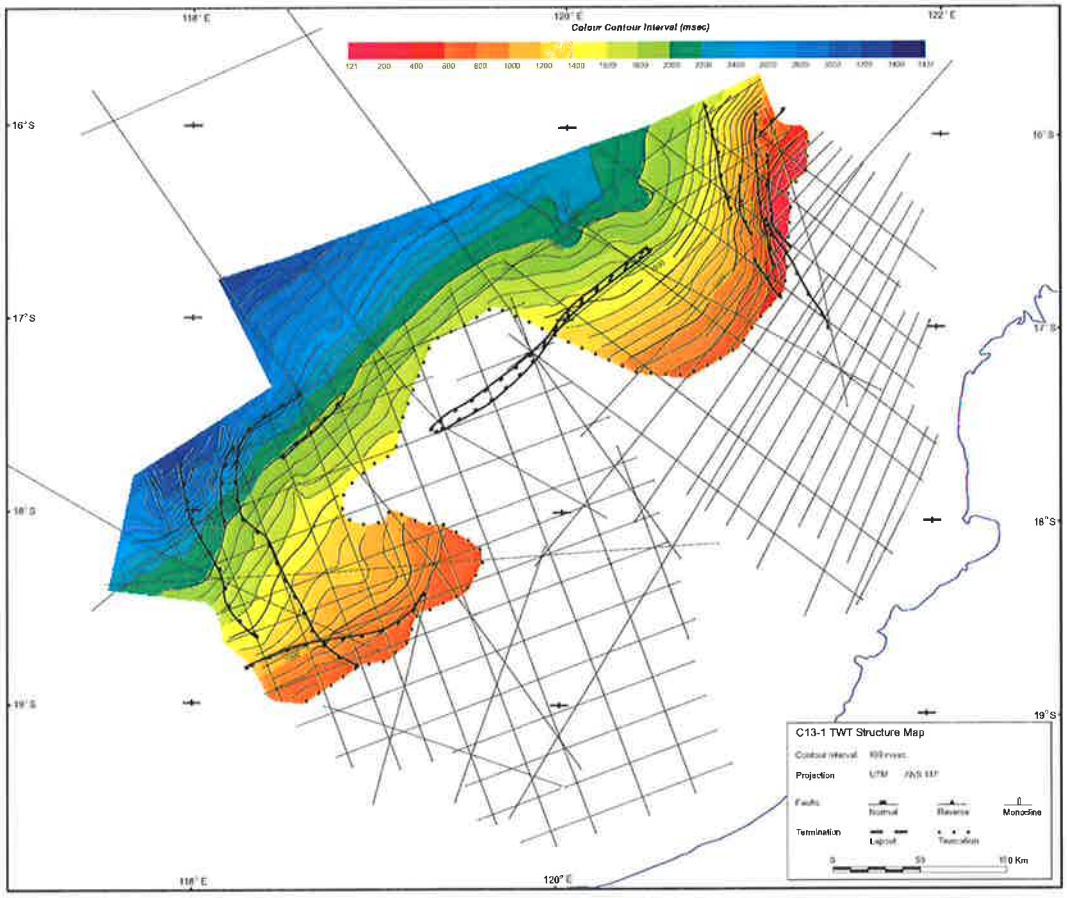

Figure A2.11 (Top) Late Cretaceous C6-2 TWT structure map.
Figure A2.12 (Bottom) Early Tertiary C13-1 TWT structure map.

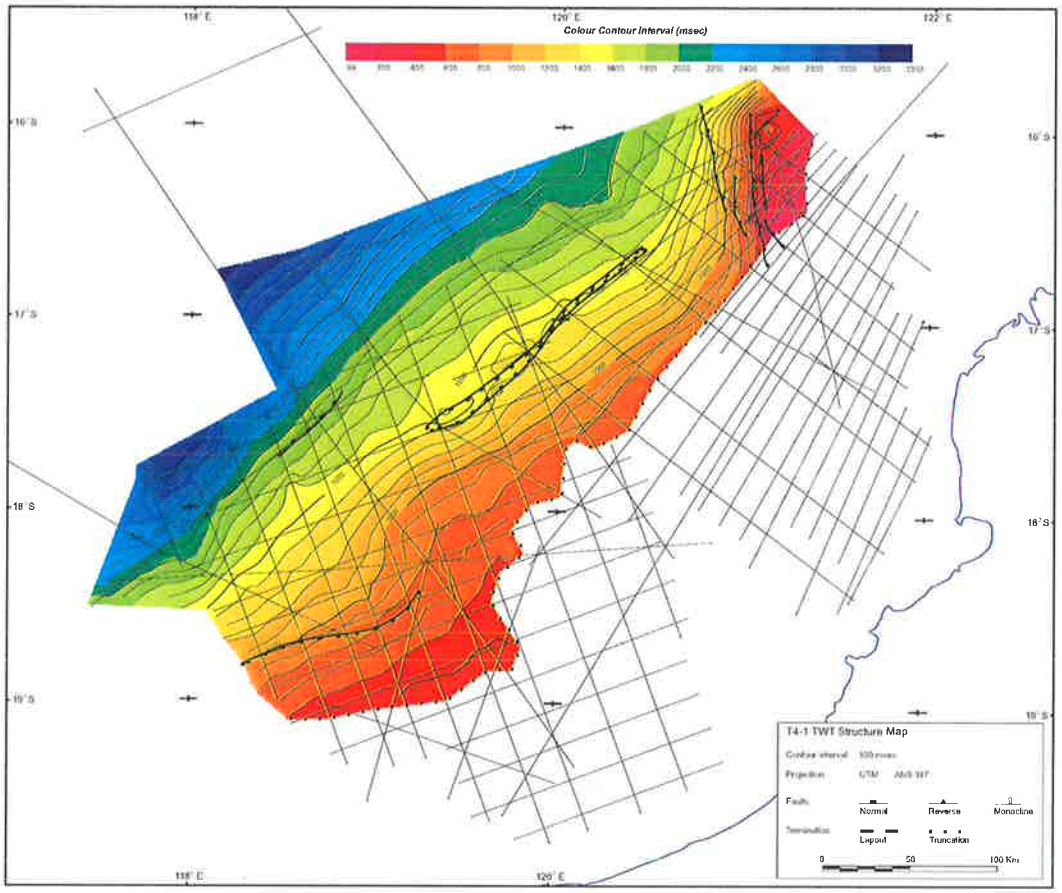

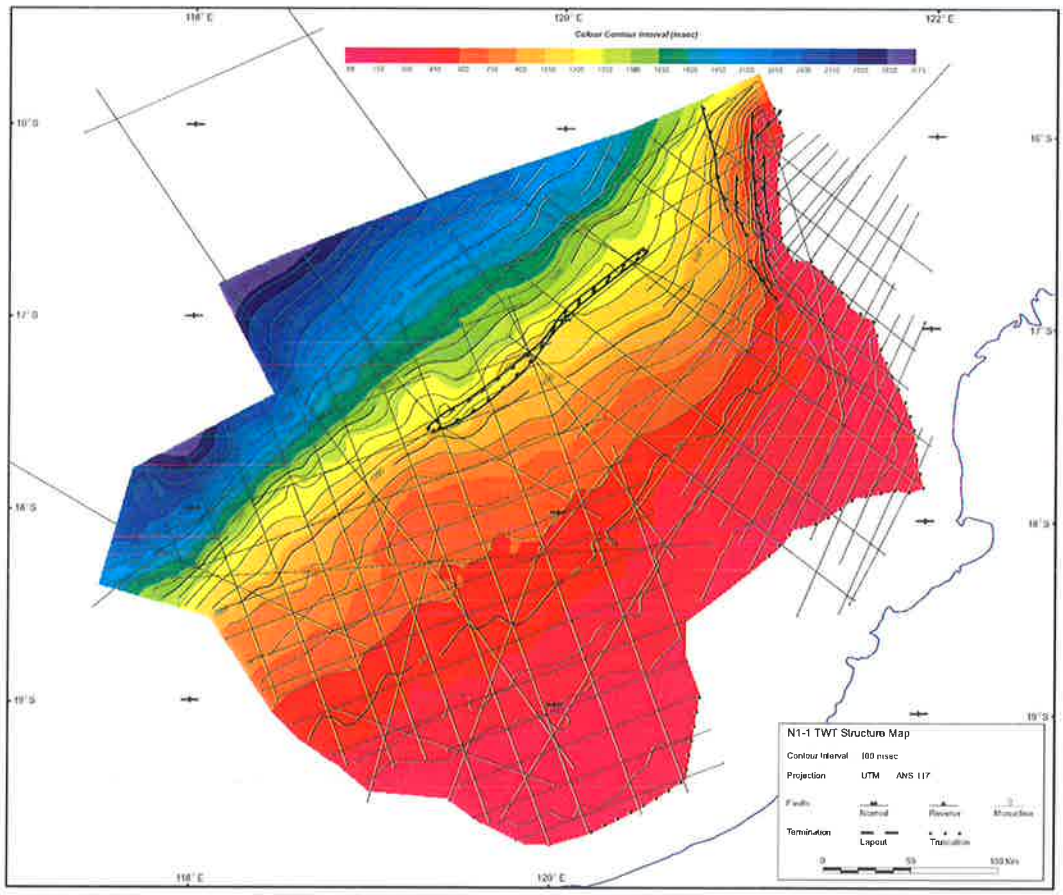

Figure A2.13 (Top) Early Tertiary T4-1 TWT structure map.
Figure A2.14 (Bottom) Late Tertiary N1-1 TWT structure map.

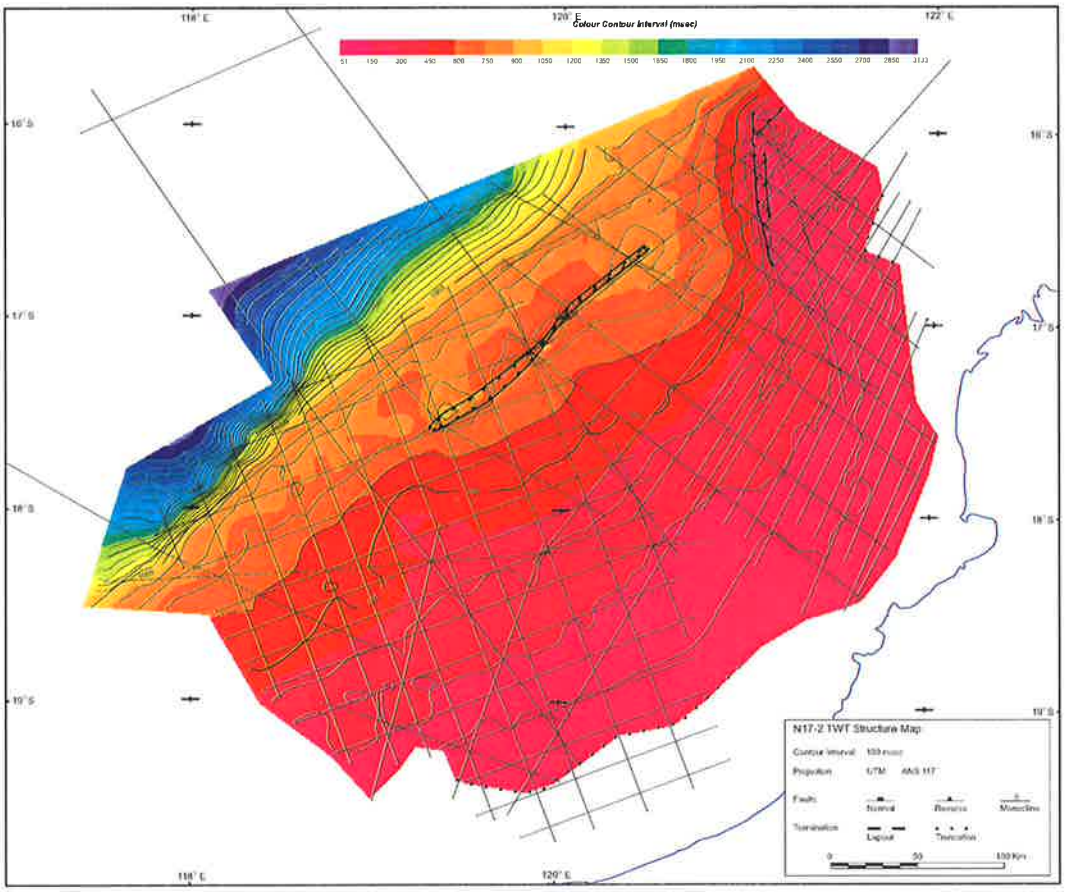

Figure A2.15 Late Tertiary N17-2 TWT structure map.

APPENDIX 3

Isopach Maps

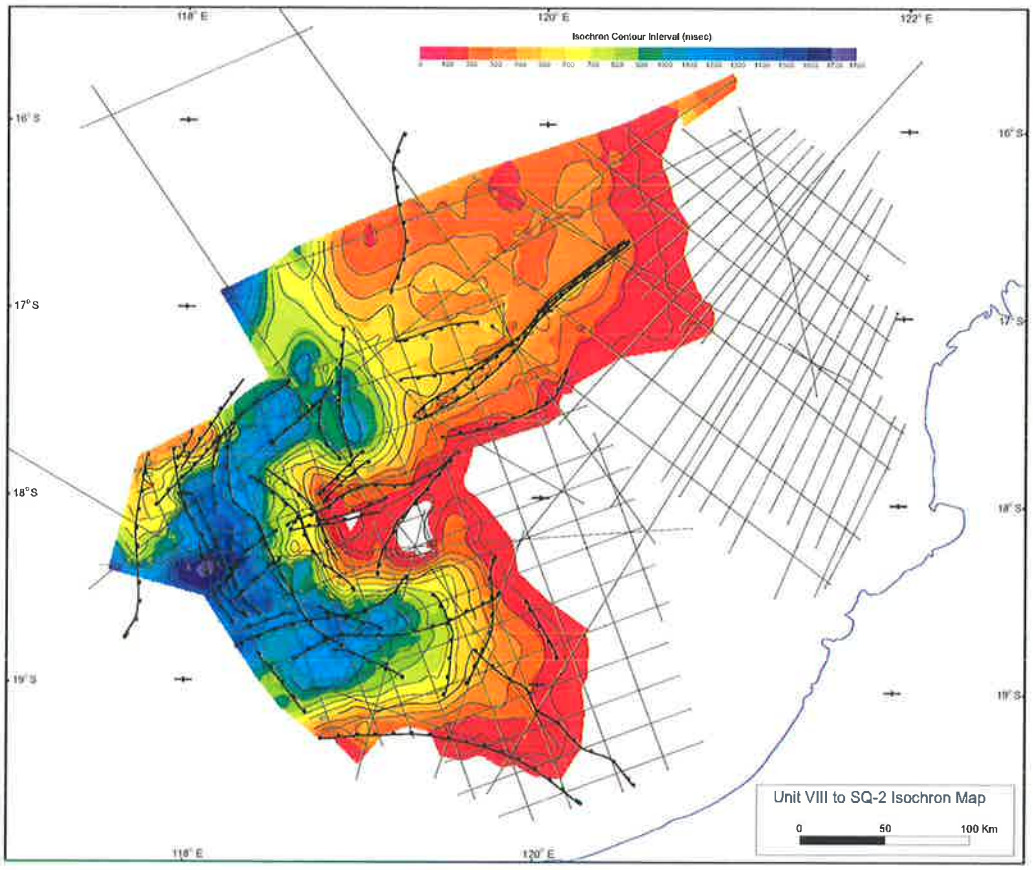

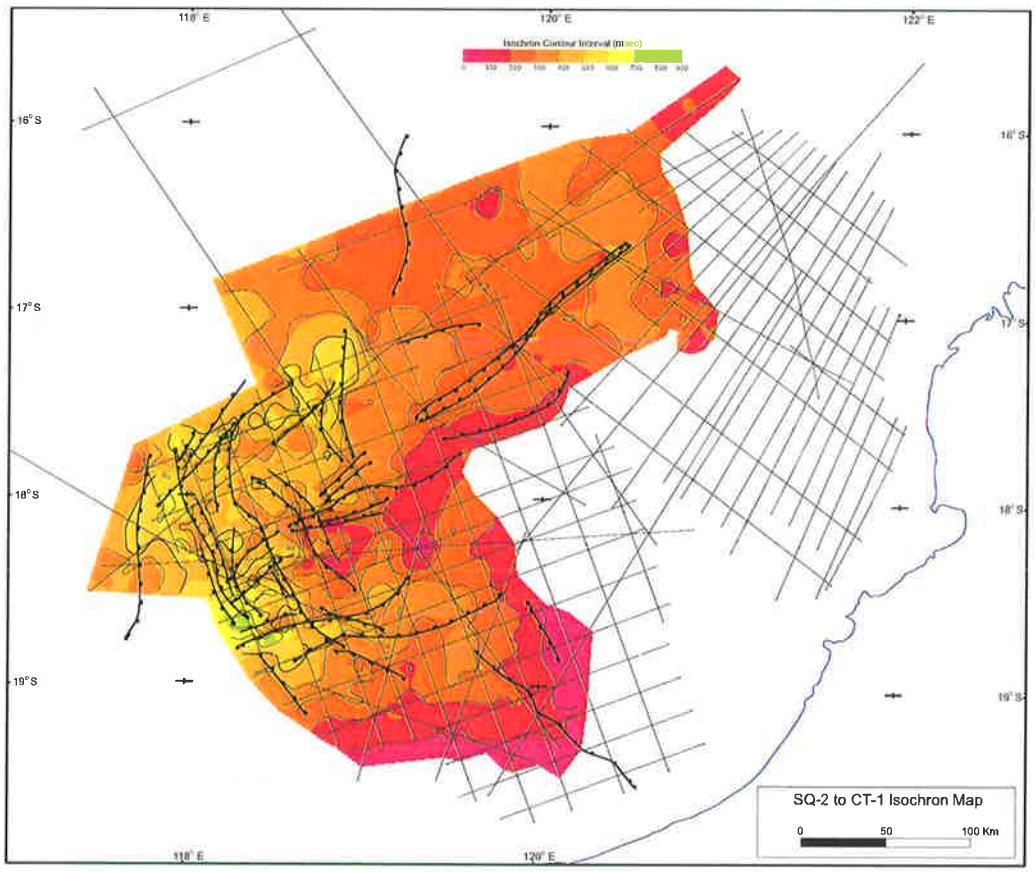

Figure A3.1 (Top) Late Permian Unit VIII to Middle Triassic SQ-2 isopach map.
Figure A3.2 (Bottom) Middle Triassic SQ-2 to Early Jurassic CT-1 isopach map.

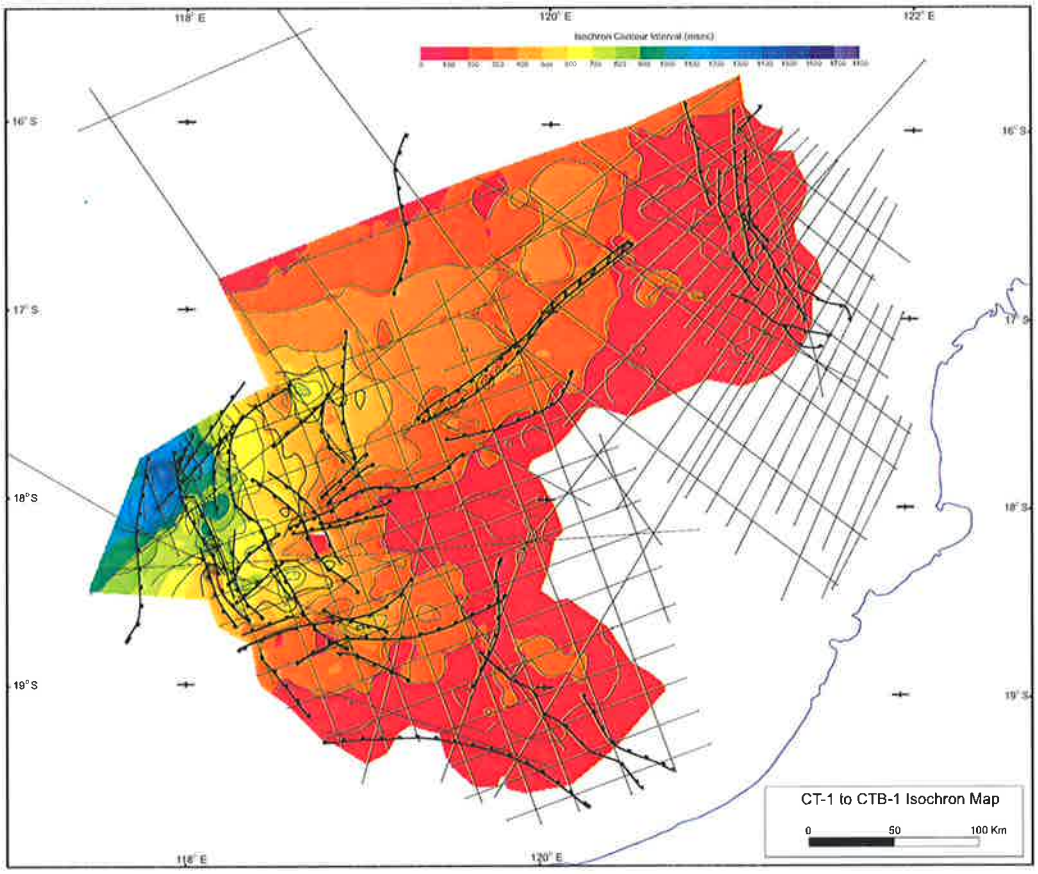

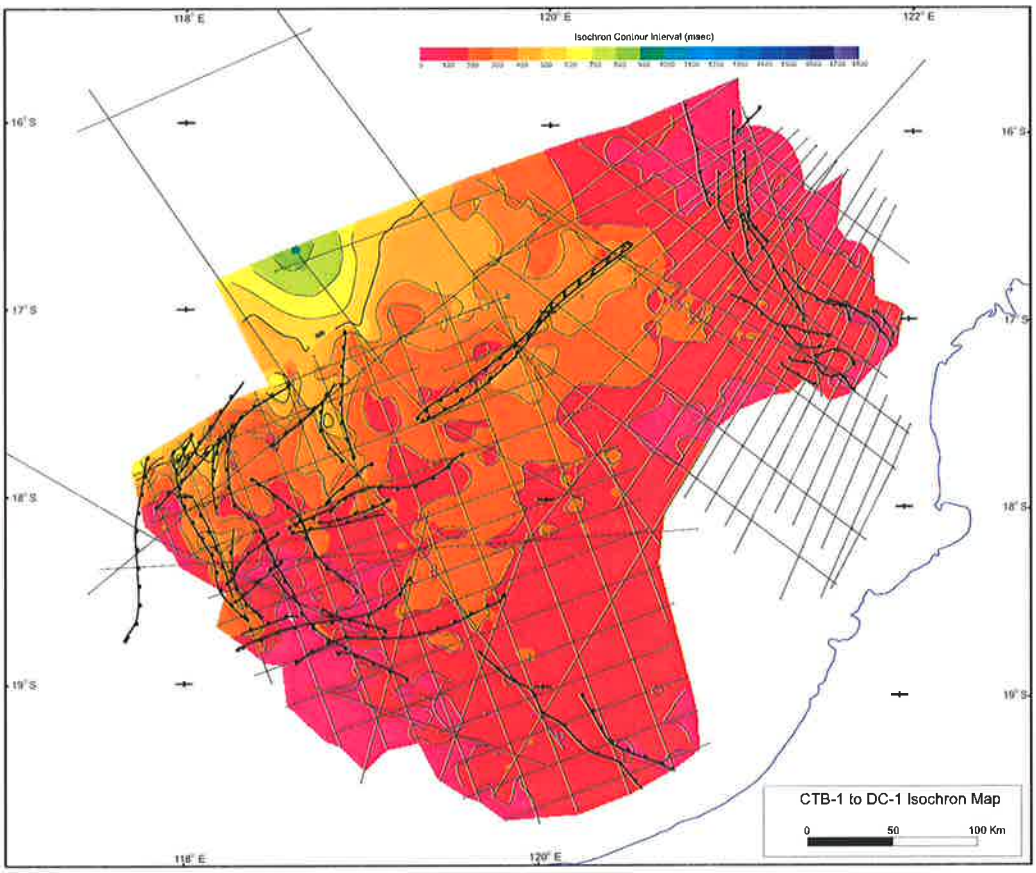

Figure A3.3 (Top) Early Jurassic CT-1 to Middle Jurassic CTB-1 isopach map.
Figure A3.4 (Bottom) Middle Jurassic CTB-1 to Middle Jurassic DC-1 isopach map.

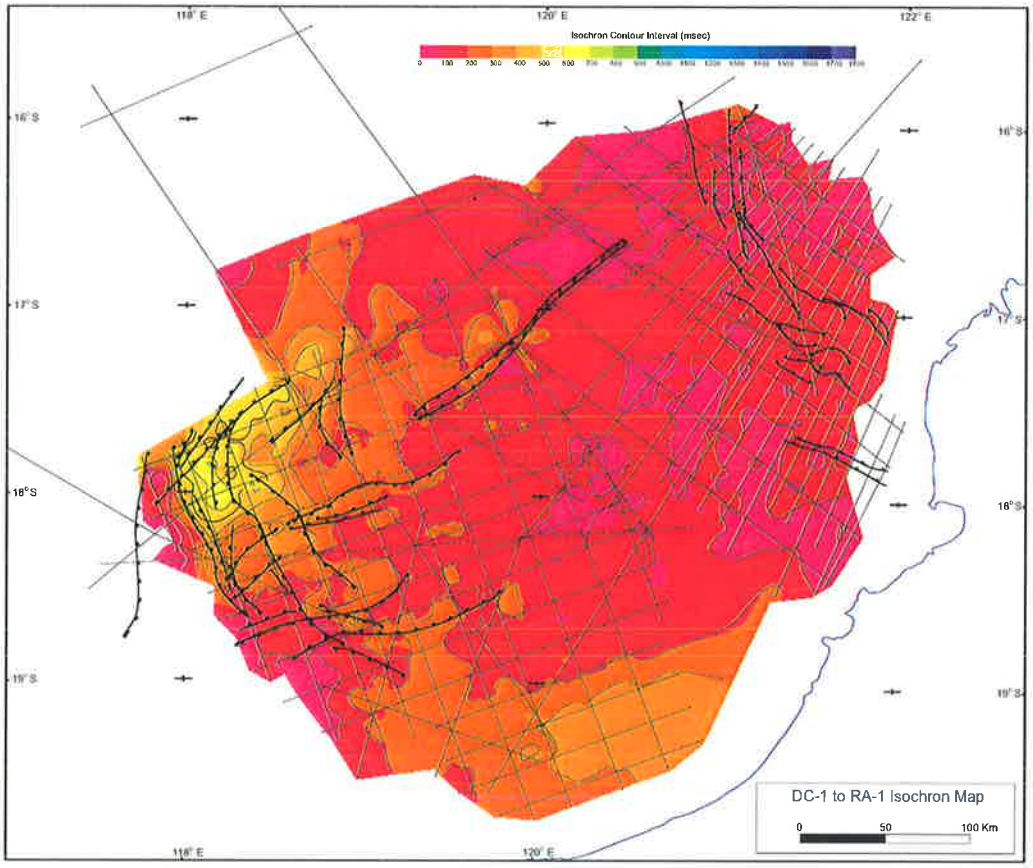

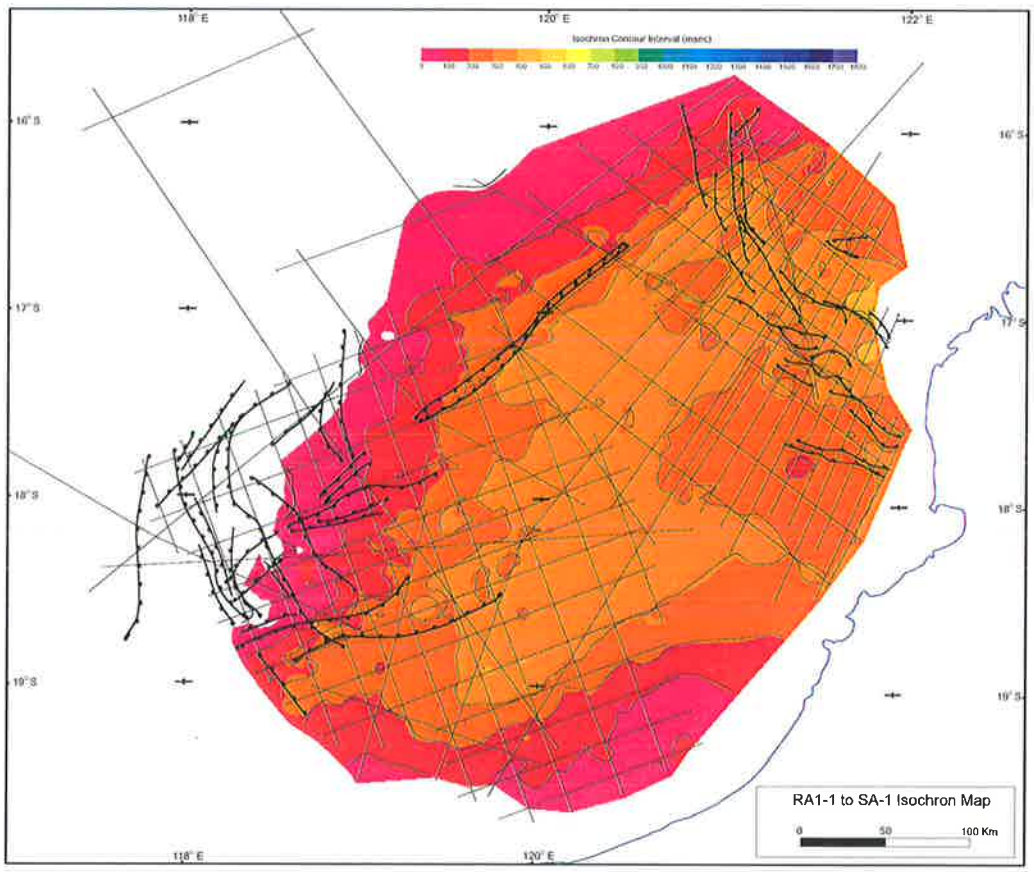

Figure A3.5 (Top) Middle Jurassic DC-1 to Middle Jurassic RA-1 isopach map.
Figure A3.6 (Bottom) Middle Jurassic RA-1 to Early Cretaceous SA-1 isopach map.

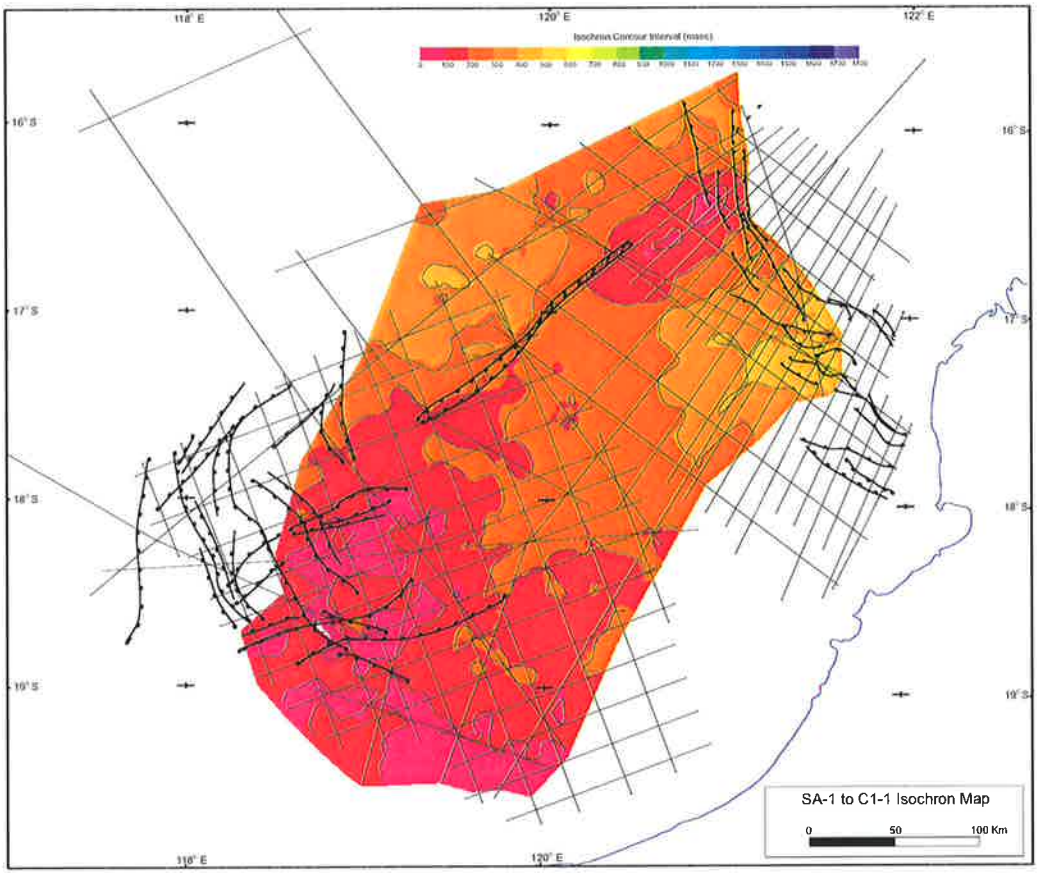

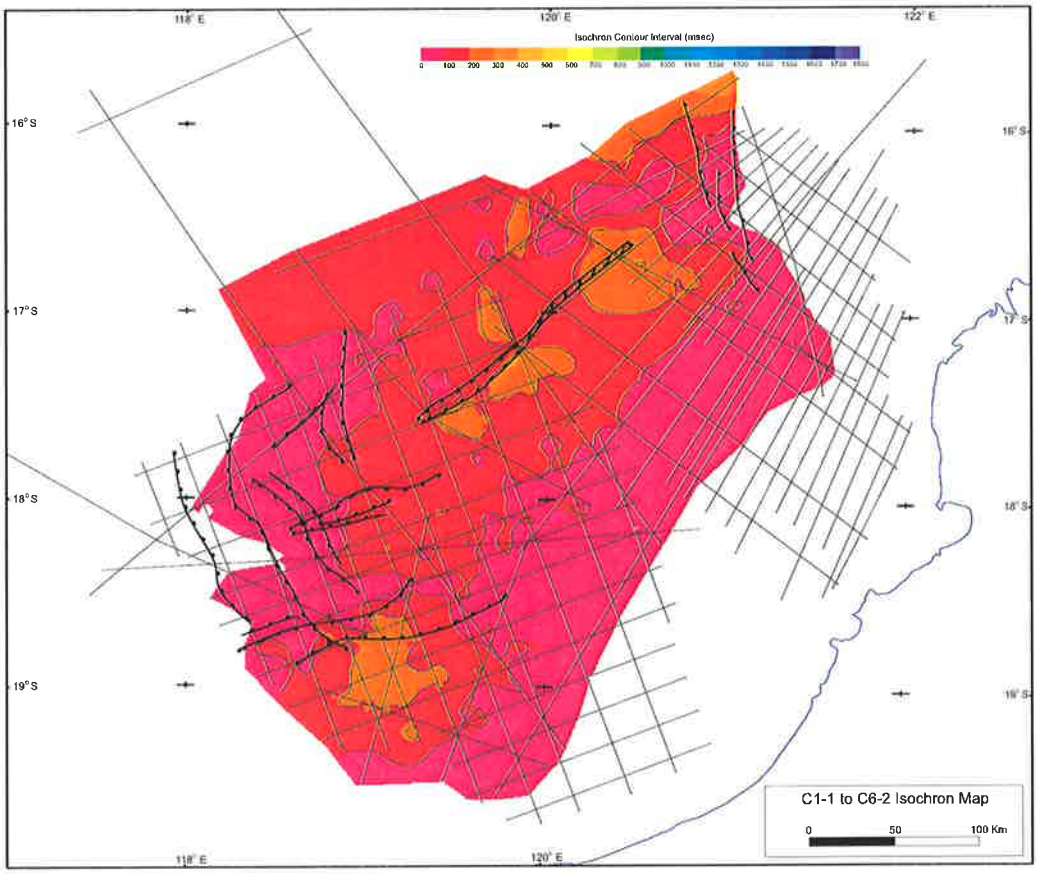

Figure A3.7 (Top) Early Cretaceous SA-1 to Early Cretaceous C1-1 isopach map.
Figure A3.8 (Bottom) Early Cretaceous C1-1 to Late Cretaceous C6-2 isopach map.

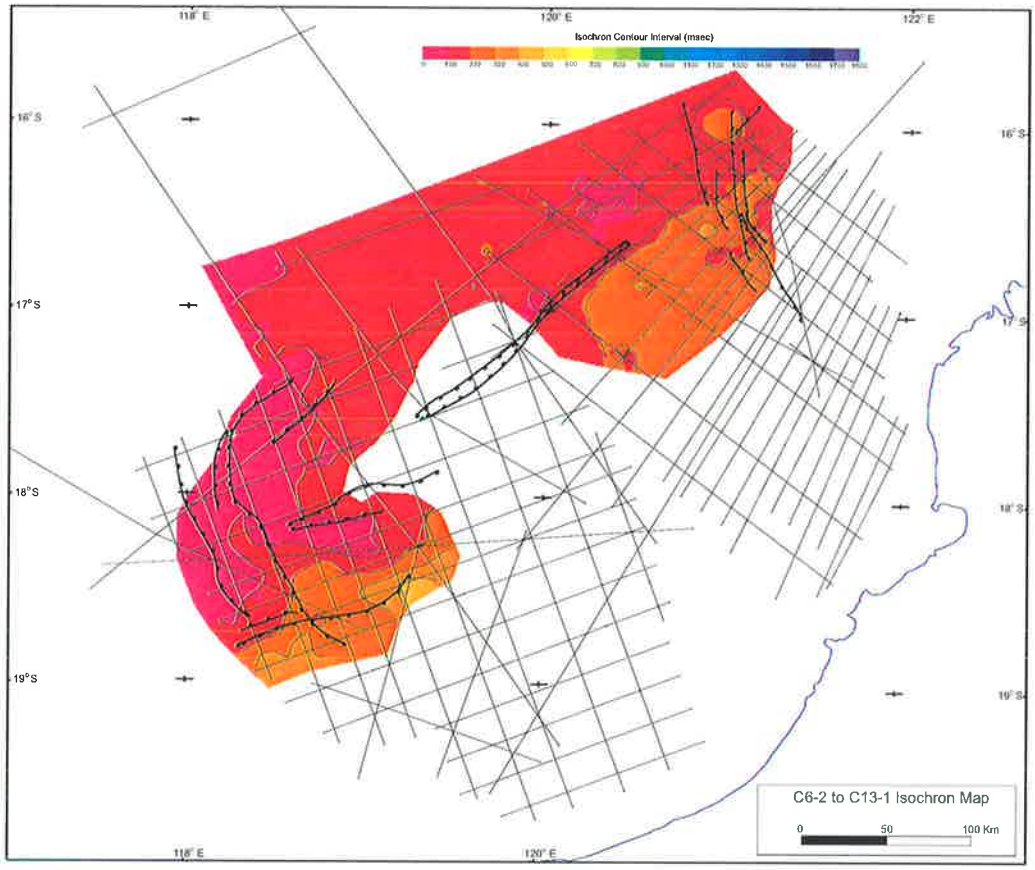

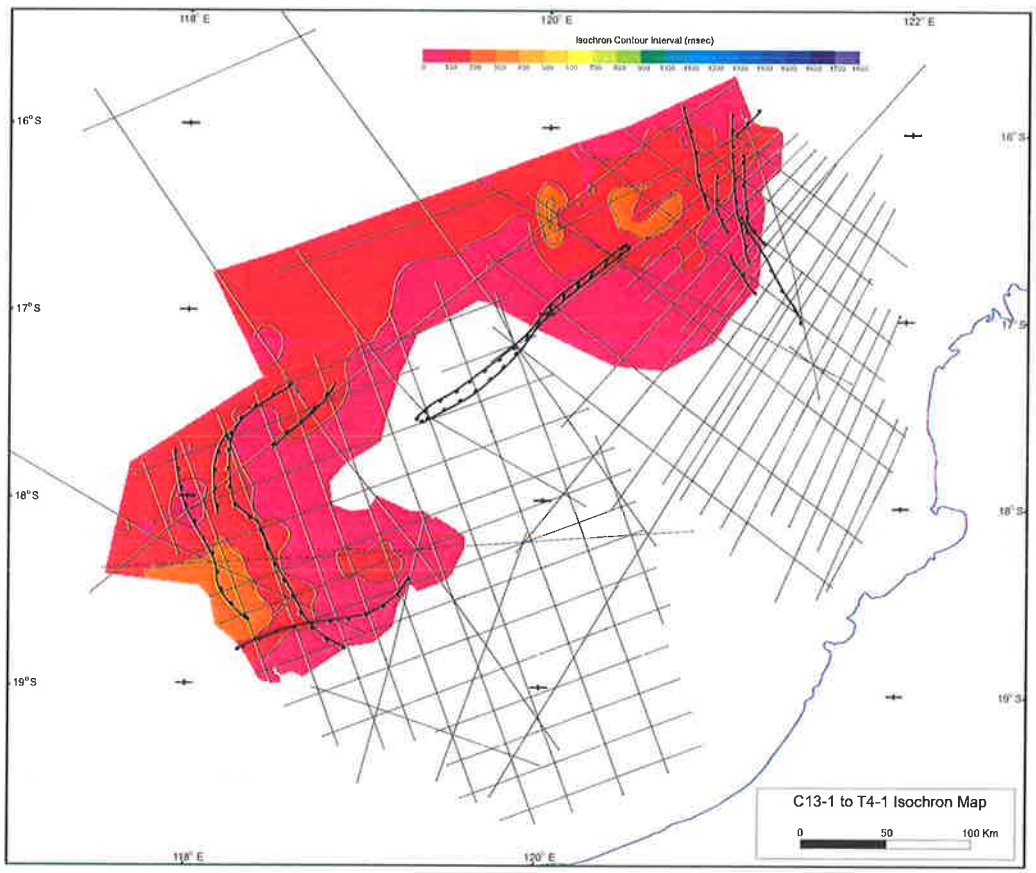

Figure A3.9 (Top) Late Cretaceous C6-2 to Early Tertiary C13-1 isopach map.
Figure A3.10 (Bottom) Early Tertiary C13-1 to Early Tertiary T4-1 isopach map.

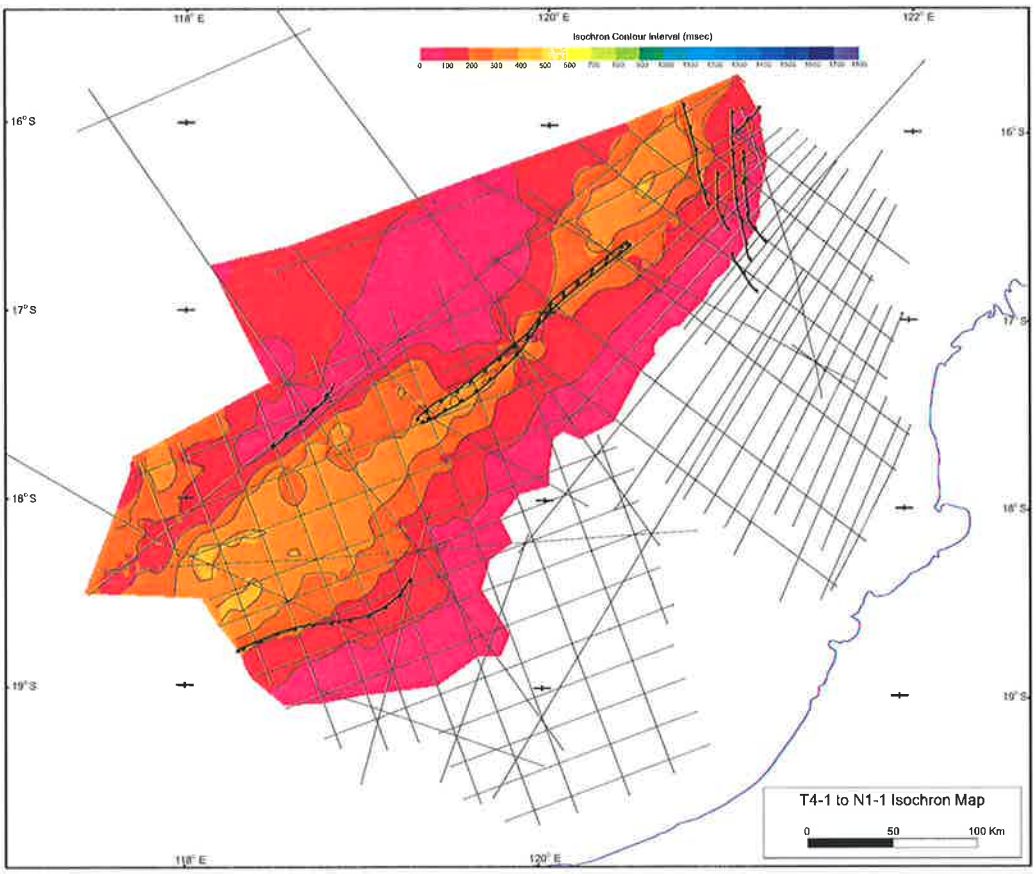

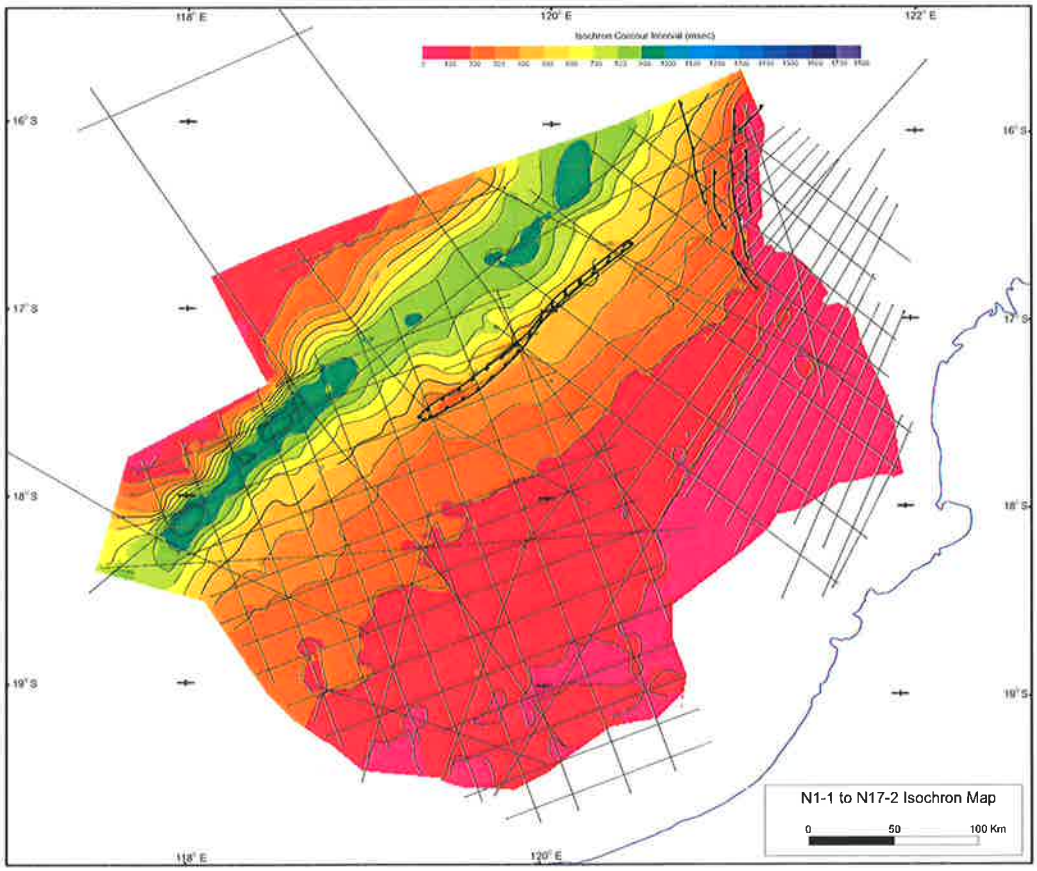

Figure A3.11 (Top) Early Tertiary T4-1 to Late Tertiary N1-1 isopach map.
Figure A3.12 (Bottom) Late Tertiary N1-1 to Late Tertiary N17-2 isopach map.

APPENDIX 4

Fault Movement Maps

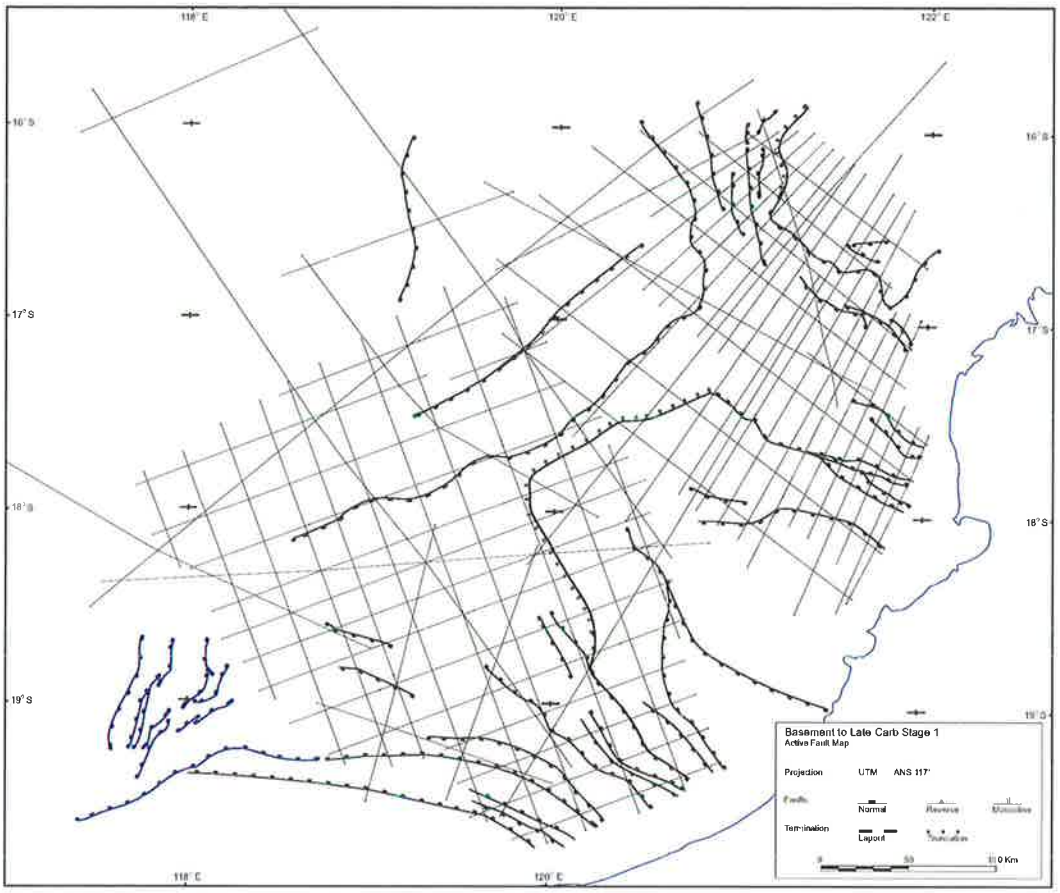

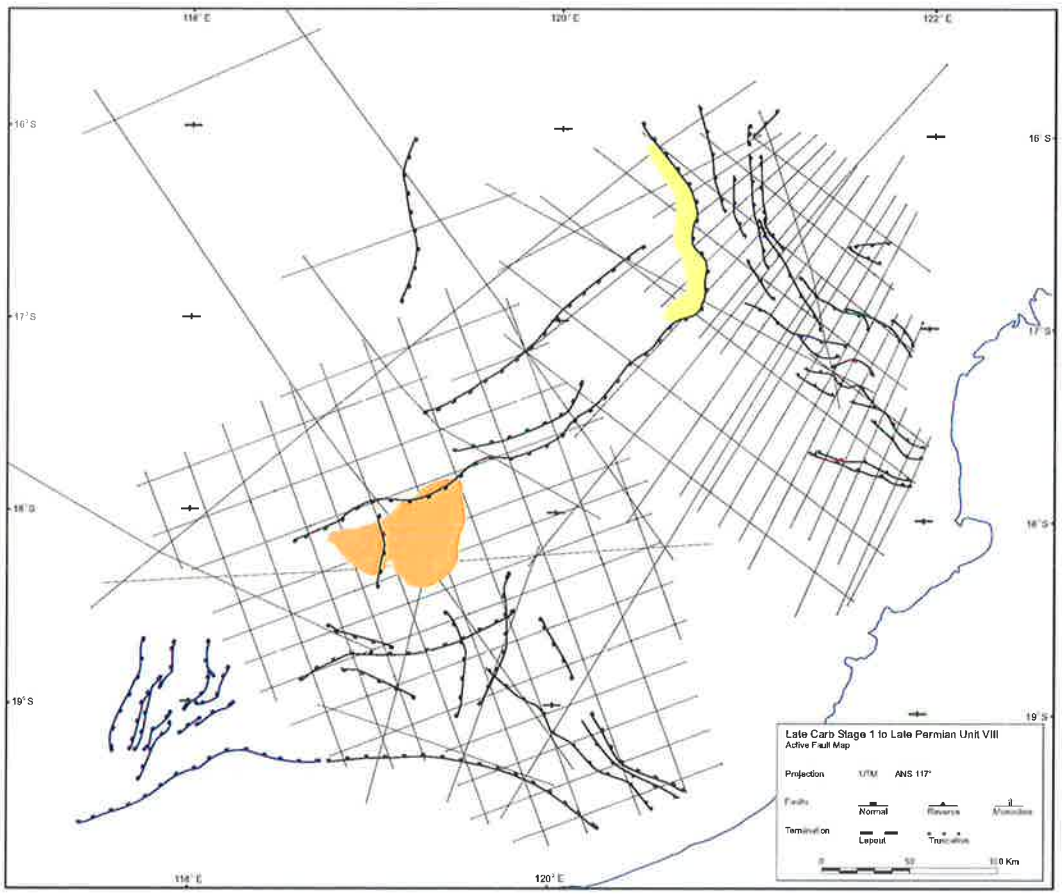

Figure A4.1 (Top) Basement to Late Carboniferous Stage 1 fault activity map.
Figure A4.2 (Bottom) Late Carb Stage 1 to Late Permian Unit VIII fault activity map.

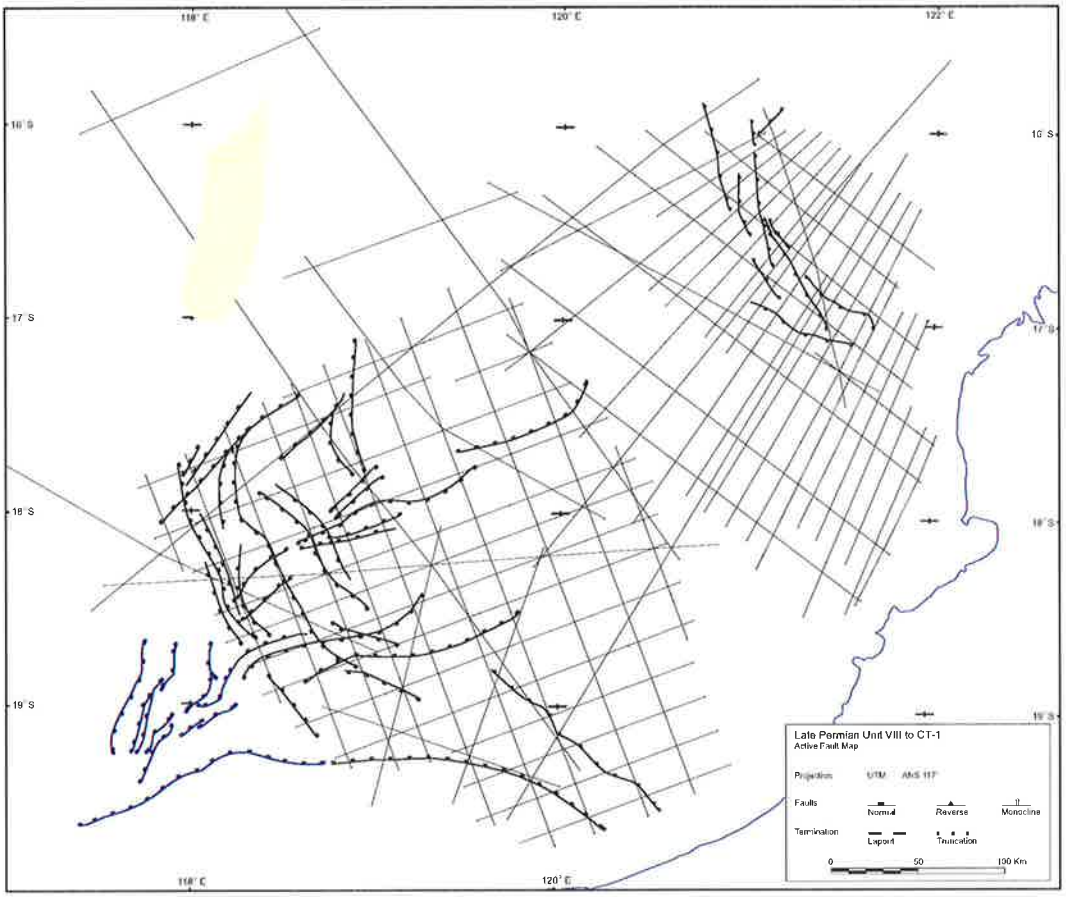

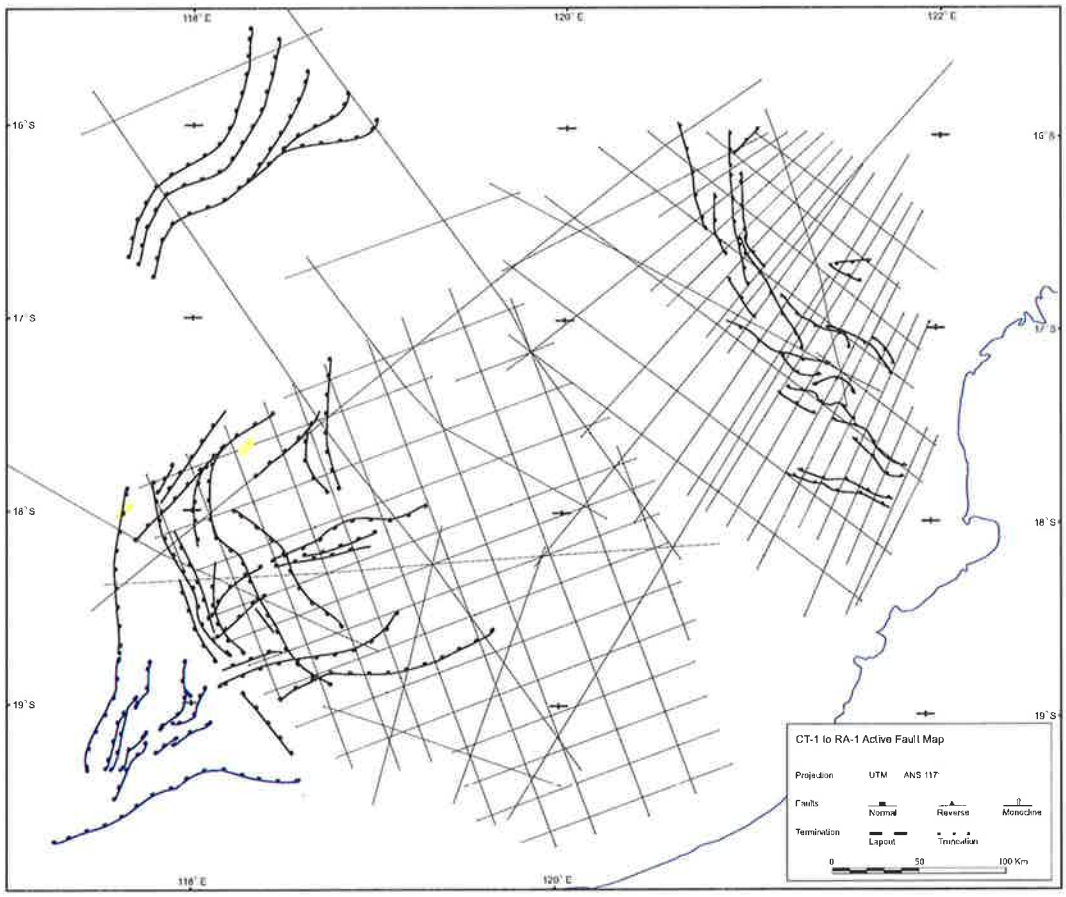

Figure A4.3 (Top) Late Permian Unit VIII to Early Jurassic CT-1 fault activity map.
Figure A4.4 (Bottom) Early Jurassic CT-1 to Middle Jurassic RA-1 fault activity map.

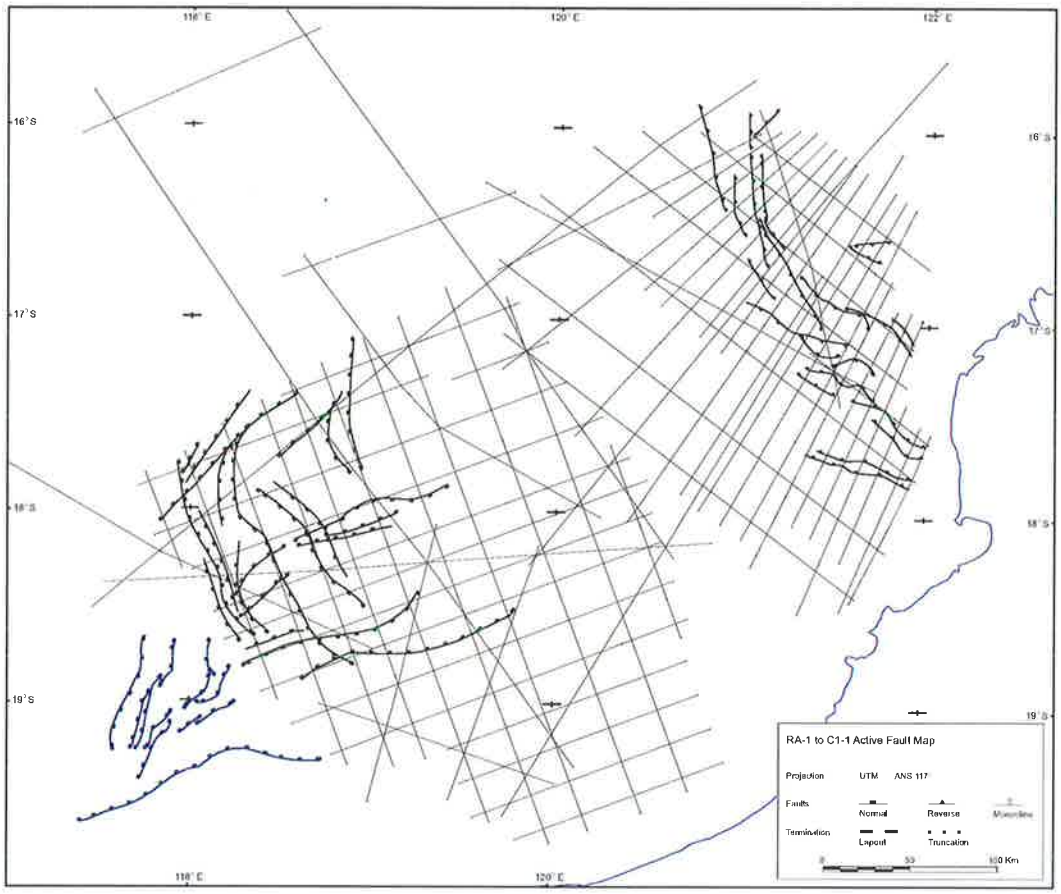

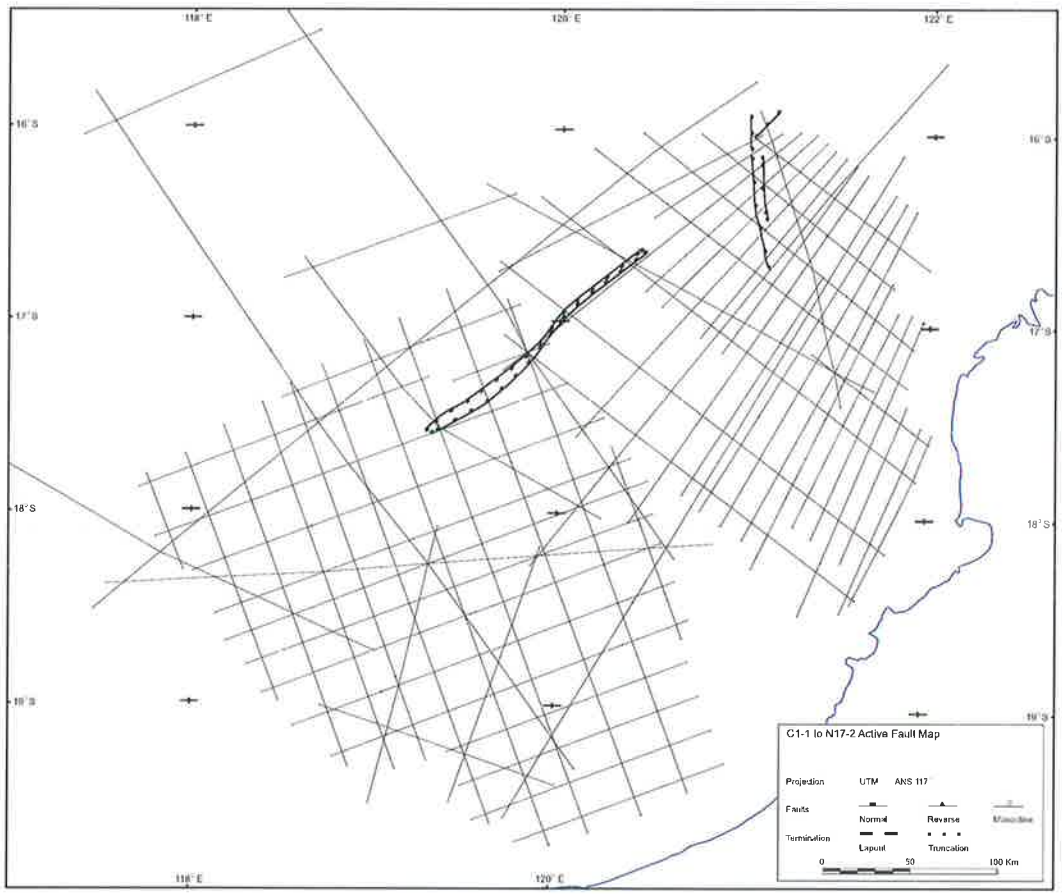

Figure A4.5 (Top) Early Jurassic RA-1 to Early Jurassic C1-1 fault activity map.
Figure A4.6 (Bottom) Early Jurassic C1-1 to Late Tertiary N17-2 fault activity map.